Selective effects of Liver X Receptor activation in host-bacteria interaction

Estibaliz Glaría Percaz

UNIVERSITAT DE BARCELONA

Selective effects of Liver X Receptor activation in host–bacteria interaction

Doctoral programme in Biomedicine

Cell Biology, Physiology, and Immunology Department

Faculty of Biology

Thesis submitted by **Estibaliz Glaría Percaz**
for the degree of Doctor
by the University of Barcelona

Barcelona, April 2021

Ph.D. candidate:

Estibaliz Glaría Percaz

Director and tutor:

Dr. Annabel Valledor Fernández

This work was supported by the following grants:

- Spanish Ministry of Economy and Competitivity (MINECO) grant SAF2017-89510-R to A. Valledor
- Spanish Ministry of Economy and Competitivity (MINECO) grant SAF2014-57856-P to A. Valledor
- Spanish Ministry of Economy and Competitivity (MINECO) grant SAF2017-90604-REDT to the NuRCaMeIn network
- Spanish Ministry of Economy and Competitivity (MINECO) grant SAF2015-71878-REDT to the NuRCaMeIn network
- Fundació La Marató de TV3 grant 201605-31 to A. Valledor
- European Cooperation in Science and Technology (COST) Action BM1404 to the Mye-EUNITER network
- Estibaliz Glaría received a pre-doctoral fellowship from the University of Barcelona (APIF)
- Estibaliz Glaría received an European Federation of Immunological Societies (EFIS)-Immunology Letters (IL) Short-Term Fellowship to conduct research during three months in the Institute for Medical Microbiology, Virology and Hygiene, University Medical Center Eppendorf, Hamburg, Germany

ABSTRACT

Macrophages exert potent microbicidal functions against pathogens; however, some intracellular bacteria have developed strategies to survive within intracellular phagolysosomes and use macrophages as a preferential niche to replicate. Liver X receptors (LXRs) are ligand-activated transcription factors of the nuclear receptor superfamily that regulate metabolic and immune functions. In this study, we explored the impact of LXR activation on host–bacteria interactions and its consequences on infection. In a murine model of orally-acquired salmonellosis, the pharmacological activation of LXRs reduced extraintestinal bacterial dissemination and attenuated the clinical signs of infection. The beneficial effects of LXR activation in the control of infection required the expression of the multifunctional protein CD38 in bone marrow-derived cells. We had previously described CD38 as a new LXR target gene that is synergistically induced by the combination of LXR agonists and inflammatory stimuli in macrophages. Here, we have identified the transcription factor C/EBPβ as an essential mediator of *Cd38* induction by TNFα, IFNγ, or LPS, as well as by the combination of these inflammatory signals and an LXR agonist.

In murine macrophages, LXR activation reduced the internalisation of *Salmonella* Typhimurium, uropathogenic *E. coli*, and enteroinvasive *E. coli* (EIEC) but not of *Listeria monocytogenes*, *Staphylococcus aureus,* or latex microspheres. After analysing several LXR-mediated activities, we found that *S.* Typhimurium infection correlated with the abundance of free cholesterol in macrophages, indicating that the reduction in cellular cholesterol caused by LXR activation might mediate the inhibitory effect on bacterial entry. In primary human macrophages, LXR activation reduced the infection by *S*. Typhimurium but not by EIEC or *S. aureus*. Strikingly, LXR activation caused either no effect or a reduction in the internalisation of *L. monocytogenes* and latex microspheres depending on the donor. In conclusion, this work delves into the mechanisms by which LXRs modulate host interactions with bacteria. Given that the ability of many bacteria to invade host cells largely depends on initial surface contacts, modulating these events through LXR-targeting compounds opens new potential therapeutic opportunities for antibacterial drug development.

CONTENTS

ABBREVIATIONS

ABC: ATP-binding cassette transporter

ACC: acetyl coenzyme A carboxylase

ADP: adenosine diphosphate

ADPR: ADP ribose

AF: activation function

AP1: activator protein 1

APO: apolipoprotein

ASC: apoptosis-associated speck-like protein containing a CARD

ATF: activating transcription factor

ATP: adenosine triphosphate

Act: actin polymerisation protein

Arg1: arginase 1

Atg protein: autophagy-related protein

BCR: B-cell receptor

BMDM: bone marrow-derived macrophages

bZIP: basic leucine zipper

CARD: caspase recruitment domain

cADPR: cyclic ADPR

C/EBPβ: CCAAT-enhancer binding protein β

CCL: chemokine (C-C motif) ligand

CD5L: CD5 molecule-like

CFU: colony-forming unit

CLR: C-type lectin receptor

COX2: cyclooxygenase 2

CREB: cAMP-responsive element binding protein

CTL: cytotoxic T lymphocytes

CXCL: chemokine (C-X-C motif) ligand

ChREBP: carbohydrate-responsive element-binding protein

DAG: diacylglycerol

DAMP: danger-associated molecular pattern

DMSO: dimethyl sulfoxide

DNA: desoxyribonucleic acid

dsRNA: double-stranded RNA

E. coli: *Escherichia coli*

EEA: early endosome antigen

EIEC: enteroinvasive *E. coli*

ERK: extracellular signal-regulated kinase

FADD: Fas-associated death domain protein

FASN: fatty acid synthase

FITC: fluorescein isothiocyanate

GAP: GTPase-activating protein

GAS: genes containing an IFNγ activation site

GDP: guanosine diphosphate

GEF: guanine exchange factor

GLUT4: glucose transporter type 4

GM-CSF: granulocyte- and macrophage-colony-stimulating factor

GTP: guanosine triphosphate

HDL: high-density lipoprotein

HIV: human immunodeficiency virus

ICAM: intercellular adhesion molecule

IDOL: inducible degrader of LDL receptor

IFN: interferon

IFNGR: IFNγ receptor

IKK: IκB kinase

IL: interleukin

iNOS: inducible nitric oxide synthase

IRF: interferon regulatory factor

ISRE: IFN-stimulated response element

Ig: immunoglobulin

Inl: internalin

IκB: inhibitor of NF-κB

JNK: c-JUN N-terminal kinase

L. monocytogenes: *Listeria monocytogenes*

LAP: liver-enriched activator protein

LBP: LPS-binding protein

LC3: microtubule-associated 1A/1B-light chain 3

LDL: low-density lipoprotein

LIP: liver-enriched inhibitory protein

LPS: lipopolysaccharide

LRR: leucine-rich repeat

LTA: lipoteichoic acid

LUBAC: linear ubiquitin chain assembly complex

LXR: liver X receptor

LXRE: LXR response element

M cells: microfold cells

M-CSF: macrophage colony-stimulating factor

MAPK: mitogen-activated protein kinase

MAPKK: MAPK kinase

MAPKKK: MAPKK kinase

MARCO: macrophage receptor with collagenous structure

MAVS/VISA: Mitochondrial antiviral-signaling protein

MDA5: Melanoma Differentiation-Associated protein 5

MDP: muramyl dipeptide

MHC: Major histocompatibility complex

MLK: mixed-lineage protein kinase

MLKL: MLK domain-like protein

MOI: multiplicity of infection

MR: mannose receptor

mTORC: mammalian target of rapamycin complex

MYB: myeloblastosis oncogene

MyD88: myeloid differentiation primary response 88

NAD^+: nicotinamide adenine dinucleotide

$NADP^+$/NADPH: NAD^+ phosphate

NCoR: nuclear receptor co-repressor

NEMO: NF-κB essential modulator

NF-κB: nuclear factor kappa B

NK cells: Natural killer cells

NLR: NOD-like receptor

NLRC: NOD-LRR family with CARD

NLRP: NOD-, LRR- and pyrin domain-containing protein

NO: nitric oxide

NOD: nucleotide-binding oligomerisation domain

OMP: outer membrane protein

PAMP: pathogen-associated molecular pattern

PI3K: phosphatidylinositol 3 kinase

PIP3: phosphatidylinositol (3,4,5)-triphosphate

PKC: protein kinase C

PLC: phospholipase C

PPAR: peroxisome-proliferator-activated receptor

PRR: pattern recognition receptor

RFP: red fluorescent protein

RIG: retinoic acid-inducible gene

RLR: RIG-I-like receptor

RNA: ribonucleic acid

RNS: reactive nitrogen species

ROS: reactive oxygen species

RUNX: runt-related transcription factor

RXR: retinoid X receptor

***S*. Typhimurium**: *Salmonella* Typhimurium

SCD: stearoyl coenzyme A desaturase

SCV: *Salmonella*-containing vacuole

SLAM: signalling lymphocytic activation molecule

SMRT: silencing mediator of retinoic acid and thyroid hormone receptor

SOCS: suppressor of cytokine signalling

SPI: *Salmonella* pathogenicity island

SREBP: sterol regulatory element-binding protein

STAT: signal transducer and activator of transcription

sTNFα: soluble TNFα

SUMO: small ubiquitin-like modifier

T1317: T0901317 (LXR agonist)

T3SS: type three secretion system

TAB: TAK1-binding protein

TAK: TGFβ-activated kinase

TANK: TRAF-family member-associated NF-κB activator

TCR: T-cell receptor

TGF: transforming growth factor

TIR: toll/interleukin-1 receptor

TIRAP: TIR domain-containing adaptor protein

TLR: Toll-like receptor

tmTNFα: transmembrane TNFα

TNF: tumour necrosis factor

TNFR: TNF receptor

TRADD: TNFR1-associated death domain protein

TRAF: TNF receptor-associated factor

TRAM: TRIF-related adaptor molecule

TRIF: TIR domain-containing adaptor inducing IFNβ

Th cells: T helper cells

Treg: regulatory T cell

UPEC: uropathogenic *E. coli*

VLDL: very LDL

WASp: Wiskott-Aldrich Syndrome protein

WT: wild-type

INTRODUCTION

1. Basic principles of the immune response

The immune system consists of a coordinated network of cells and molecules that protect us from many infectious agents and other types of aggressions (Murphy, 2012). Despite the continuous exposure to microbes, we only occasionally get ill, a fact that illustrates how effective our protective mechanisms are to maintain us safe. The natural barriers of our bodies represent the first containment mechanism against infection. Covering epithelia separate our internal tissues from the external environment and, together with mucosae, hinder the access of microorganisms. Additionally, the antimicrobial molecules and normal microbiota in our surfaces build a hostile milieu for microbes. However, some pathogens use invasive factors to overcome our anatomical barriers and cause infections. Upon entering the body, microbes are rapidly detected by immune cells that constantly monitor the tissues looking for non-self entities. Immediately, these sentinels become activated and initiate a cascade of events to activate other cells and mount an appropriate response to eliminate the dangerous agent.

The immune response is divided into two main components, the innate and the adaptive immune systems, which act complementarily at different levels to combat pathogens. Innate immune cells possess a set of invariable receptors that recognise conserved motifs on microorganisms and rapidly initiate an inflammatory response (Murphy, 2012). Inflammation is characterised by increased vascular permeability and the infiltration of plasma proteins and white blood cells to the tissue following an insult such as injury or infection. Resident macrophages are the primary immune cells beneath mucosal epithelia, and they immediately respond to potential pathogens by the release of inflammatory molecules that affect the behaviour of other cells (cytokines) and attract more cells (chemokines). Subsequently, more immune cells—first neutrophils, and later monocytes and other immune cells—are recruited to the infection site. Macrophages and neutrophils are professional phagocytes (cells that internalise extracellular materials) that engulf pathogens to degrade them within specialised intracellular vesicles (phagolysosomes). Additionally, soluble proteins of the complement system bind to conserved structures on pathogens and either directly induce pathogen lysis or facilitate pathogen phagocytosis by macrophages. During infections caused by intracellular pathogens, natural killer (NK) cells have an important role in promoting the microbicidal activities of macrophages and inducing the death of infected cells. The sensing of pathogen structures also activates conventional dendritic cells, which form the bridge between the innate and adaptive immune responses. Dendritic cells constantly sample the environment by a process

known as macropinocytosis, which consists in the unspecific internalisation of large amounts of extracellular fluid. When they are activated by pathogen structures or altered self-molecules, dendritic cells expose small pieces of the threatening entity (antigens) in their surface and start producing cytokines. Then, dendritic cells undergo a maturation process that drives the migration to the draining lymph node and the stimulation of the adaptive immune response.

The two types of cells that mediate the adaptive immune response are T lymphocytes (T cells) and B lymphocytes (B cells). The detection of foreign agents provides stimulatory signals for both types of lymphocytes in secondary lymphoid organs, an event that instigates cell proliferation and differentiation to become fully functional effector cells. The set of lymphocytes that are activated by an antigen are the ones which express specific receptors that can bind it with enough affinity. Additionally, the type of soluble mediators present in the microenvironment during lymphocyte stimulation will determine their differentiation towards a certain effector phenotype.

T cells are subdivided into two functional groups, helper T cells (Th, $CD4^+$) and cytotoxic T cells (CTL, $CD8^+$), which either secrete cytokines that modulate the activities of other cells or directly kill target cells, respectively (Murphy, 2012). T-cell receptors (TCRs) detect antigenic peptides presented by the major histocompatibility complex (MHC) at the surface of other cells. MHC molecules are transmembrane glycoproteins that exhibit a repertoire of peptides obtained from intracellular proteins or from extracellular materials that have been taken up by the cell through phagocytosis. There are two types of MHC, namely, the class I MHC (MHC-I) and the class II MHC (MHC-II). MHC-I harbours peptides present in the cytosol, whereas MHC-II carries peptides from endosomal vesicles. Each of them is recognised by $CD8^+$ or $CD4^+$ T cells, respectively.

Following detection of pathogen- or danger-associated structures, conventional dendritic cells increase the expression of chemotactic receptors, MHC-II, and co-stimulatory molecules on their surface (Murphy, 2012). Mature dendritic cells migrate to the T cell area of the lymph nodes, where the MHC-II loaded with antigenic peptides on dendritic cells interacts with the TCR on unstimulated (naive) T cells. Simultaneously, other surface proteins expressed by mature dendritic cells, known as co-stimulatory molecules, bind their cognate receptors on T cells and provide a second stimulatory signal for activation. Additionally, the cytokines that are secreted by dendritic cells or by other cells during the MHC:TCR interactions shape the differentiation of T cells. As a result, helper T cells can differentiate into Th1, Th2, Th17, or regulatory T cells (Treg), which will determine the type of cytokines they will secrete afterwards. First, Th1 cells contribute to killing intracellular bacteria and viruses by infected cells. Th1 cell differentiation is

induced by interleukin (IL)-12 and gamma interferon (IFNγ), and these cells secrete IL2, IFNγ, and tumour necrosis factor (TNF)β. Second, Th2 cells participate in parasite killing. The cytokine IL4 determines their conversion to Th2 cells; afterwards, they secrete large amounts of IL4, IL5, and IL13. Third, Th17 cells aid in the elimination of extracellular bacteria and fungi. IL6 and IL23 induce $CD4^+$ T cell differentiation to Th17, which then secrete different forms of IL17. By contrast, Treg cells control immune responses by inhibiting the activities of other lymphocytes and myeloid cells. In the absence of infection, dendritic cells produce transforming growth factor (TGF) β, which promote Treg differentiation.

In contrast to T cells, B cells can directly detect antigens by surface receptors, named B-cell receptors (BCRs), and differentiate into antibody-producing plasma cells. However, most B-cell responses require a second stimulatory signal from T cells to function optimally. Upon antigen binding by the BCR, B cells internalise it and expose small peptides on the surface MHC-II. Then, a differentiated helper T cell with the same antigen specificity binds this MHC-II by the TCR and secretes cytokines that trigger the full proliferation and differentiation of B cells. In humans, there are five different types (isotypes) of antibodies (also known as immunoglobulins, Ig) classified according to their functional characteristics into IgA, IgD, IgE, IgG, and IgM. Together, the set of antibodies secreted by plasma cells compose the humoral adaptive response.

The adaptive immune response comes to action several days after the dangerous antigen is detected. If the pathogen persists once the adaptive response is ready, antibodies and effector T cells will infiltrate the inflamed tissue and specifically target the invading agent for effective elimination. Notably, each type of insult induces distinct immune responses that activate the most suitable mechanisms for resolution. For example, CD8+ T cells and NK cells play pivotal roles in viral infections because they detect intracellular infection and kill target cells. Some intracellular bacteria reside within macrophage phagosomes and activate Th1 cells that boost the macrophage killing machinery and cytotoxic T cell responses. Conversely, the infection by parasites requires extracellular killing mechanisms and is combated by mast cells, basophils, and eosinophils, all of which can interact with antibodies to accomplish pathogen eradication.

Finally, a pool of naïve lymphocytes stimulated in secondary lymphoid organs will differentiate into memory cells. These adaptive cells persist in our bodies after the infection has resolved to confer immunological memory, which ensures the rapid recognition and more efficient elimination of a specific pathogen upon second exposure.

2. Macrophages

2.1 Macrophage functional diversity and phenotypes

Macrophages are myeloid cells that display pleiotropic roles to maintain body homeostasis. To begin, macrophages are necessary for the correct patterning of tissues during developmental stages and to ensure tissue integrity throughout life (reviewed in Wynn et al., 2013). Indeed, many organs undergo alterations when macrophages or some of their functions are selectively eliminated. In addition, macrophages participate in the metabolic adaptation to the changing nutrient and microenvironmental conditions: they promote insulin tolerance and adaptive thermogenesis (reviewed in Hotamisligil, 2006). Macrophages are also required for erythrocyte clearance and iron metabolism (reviewed in Soares and Hamza, 2016). Through phagocytosis, macrophages remove apoptotic cells and cell debris from the tissues and suppress inflammation and autoimmunity (Henson and Hume, 2006). Similarly, they participate in the resolution phase of inflammation and promote tissue repair (reviewed in Wynn and Vannella, 2016). Tissue macrophages express an array of receptors by which they monitor the presence of strange entities (immune surveillance). Upon recognition of microbial ligands, they orchestrate the immune response against pathogens (reviewed in Davies et al., 2013).

Tissue-resident macrophages comprise a greatly diverse group of cells that present anatomical and functional specialization. They have various origins, including differentiation from yolk-sac or foetal liver during embryogenesis or maturation from circulating monocytes in adulthood (reviewed in Davies et al., 2013). During stress conditions such as infection, large amounts of monocytes arise from the bone marrow by emergency myelopoiesis. Among them, LY6C^{hi} monocytes are recruited to the inflammation site and differentiate into macrophages *in situ* (reviewed in Murray and Wynn, 2011). Moreover, tissue-resident macrophages can proliferate in some inflammatory contexts, although their contribution remains elusive.

Macrophages are extremely plastic cells that shift their phenotype to adapt to the microenvironmental conditions. Macrophage activation, has been defined as the “acquisition of competence to execute a complex function” (Adams, 1989). The study of macrophages in particular immunological contexts led to their functional classification as “classically” or “alternatively” activated cells, terms that are currently used by some authors as equivalent to M1 or M2 phenotypes, respectively (reviewed in Martinez and Gordon, 2014). Classically activated macrophages were described first. They perform activities linked to Th1 responses

such as the production of high amounts of pro-inflammatory cytokines (e.g., TNFα) and reactive oxygen species (ROS) to kill microbes. Later, the identification of the opposite phenotype, which was related to Th2 activities, led to the definition of alternatively activated or M2 macrophages. These macrophages have anti-inflammatory and immunoregulatory roles (reviewed in Shapouri-Moghaddam et al., 2018). M2 macrophages are involved in the immune response to parasites and are critical for tissue repair. This phenotype is characterised by high expression of IL10, TGFβ, arginase 1 (ARG1), chemokine (C-C motif) ligand (CCL) 17, CCL22, and CCL24 (reviewed in Shapouri-Moghaddam et al., 2018). However, as research continued it became evident that a continuum spectrum of macrophage phenotypes exists rather than two opposite polarization states. In fact, macrophage phenotypes in tissues are determined by the balance of interactions with multiple stimuli such as pathogen components, cytokines, and growth factors that define their transcriptional profile.

A terminology was suggested to classify macrophage subsets depending on the inductor stimuli and several markers (Mantovani et al., 2004), which has been updated later (Martinez and Gordon, 2014) (Figure 1). The M1 stimuli include IFNγ, toll-like receptor (TLR) ligands (mainly lipopolysaccharide, LPS), TNFα, and granulocyte- and macrophage-colony-stimulating factor (GM-CSF). On the other hand, the M2 macrophage phenotype comprises several subtypes. The M2a phenotype is promoted by the presence of IL4 and IL13; the differentiation to M2b macrophages is stimulated by immune complexes and TLR/IL.1R ligands, and; the M2c macrophage phenotype is determined by the presence of glucocorticoids or IL10. Macrophage colony-stimulating factor (M-CSF) has also been classified as an M2 stimulus. Nevertheless, it should be noted that the signalling pathways and transcriptional patterns induced by each stimulus within the same class of macrophage are distinct. Consequently, some concepts have been reassessed and a nomenclature guideline was published to standardise descriptions in experimental activation of macrophages (reviewed in Murray et al., 2014).

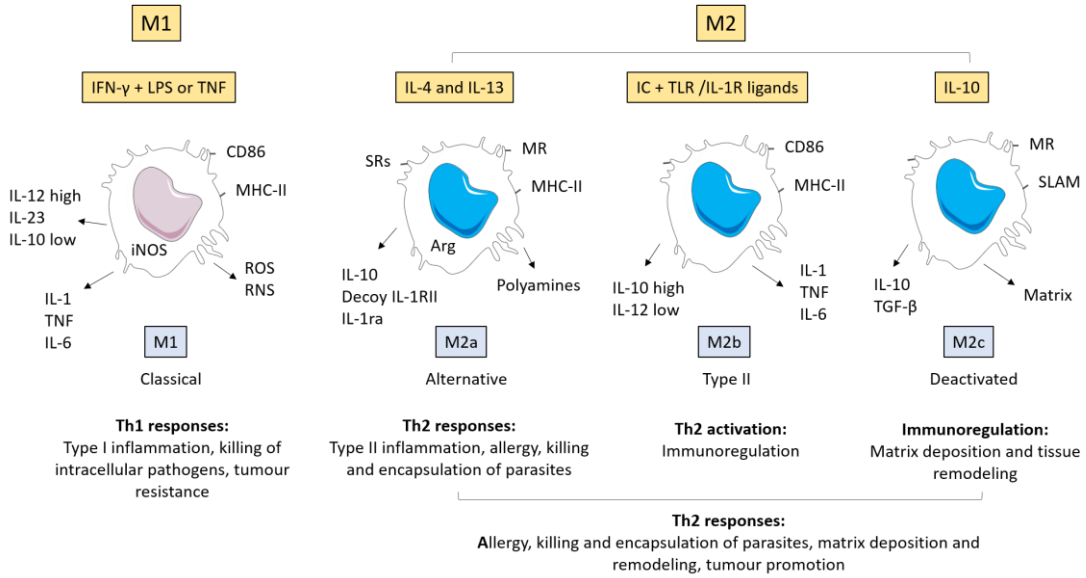

Figure 1. Model of M1-M2 macrophage polarisation proposed by Mantovani and colleagues (Mantovani et al., 2004). Macrophages polarise to the M1 phenotype upon stimulation with interferon-gamma (IFNγ) + LPS or TNF and exert potent microbicidal and antitumoral activities. The M2 phenotype is induced by IL4 (M2a), immune complexes + TLR ligands (M2b), or IL10 and glucocorticoids (M2c). M2 macrophages exert immunomodulatory and pro-tumoral activities, including type II responses, suppression of immune responses, and tissue remodelling. IC: immune complexes; iNOS: inducible nitric oxide synthase; MR: mannose receptor; PTX3: pentraxin 3; RNS: reactive nitrogen species; ROS: reactive oxygen species; SLAM: signalling lymphocytic activation molecule; SRs: scavenger receptors. Figure created based on the figure of (Mantovani et al., 2004).

2.2 Pattern recognition receptors

Professional phagocytes contain a set of germline-encoded receptors that detect microbial structures and aberrant endogenous molecules. These receptors, termed pattern recognition receptors (PRRs), bind pathogen-associated molecular patterns (PAMPs) or danger-associated molecular patterns (DAMPs), and initiate signalling cascades that result in the production of cytokines and microbicidal molecules (Murphy, 2012). Animals are often infected by microorganisms, i.e., bacteria, viruses, fungi, and protozoa. Some helminths are frequent causative agents for infections as well. To identify pathogens, PRRs detect conserved motifs or molecules that are not shared by mammal cells. PRRs localise to various subcellular compartments and recognise specific types of ligands present at each stage of infection. Some PRRs function as phagocytic receptors, whereas others are signalling receptors.

Phagocytic receptors are transmembrane proteins that upon binding microbial surfaces trigger phagocytosis. They are classified into opsonic or non-opsonic phagocytic receptors (Figure 2 A). Opsonins are host proteins that react with microbes and promote their ingestion by phagocytic cells containing the corresponding receptors. The main opsonic receptors are complement

receptors and Fcγ receptors (FcγR), which recognise proteins of the complement system or antibodies (IgG), respectively, associated with the particle to be phagocytosed. Non-opsonic receptors, instead, directly bind pathogen structures. This group comprises CD14, dectin-1, mannose receptor, scavenger receptor A, CD36, and macrophage receptor with collagenous structure (MARCO) (Rosales and Uribe-Querol, 2017).

A different set of PRRs comprises signalling receptors that lead to the transcriptional activation of cytokines, chemokines, and microbicidal proteins (Takeuchi, 2010). These signalling receptors belong to four main families, namely, membrane TLRs and C-type lectin receptors (CLRs), and cytoplasmic retinoic acid-inducible gene (RIG)-I-like receptors (RLRs) and nucleotide-binding oligomerisation domain (NOD)-like receptors (NLRs) (Figure 2 B). Among them, TLRs are the best characterised receptors. TLRs recognise microbes present at extracellular spaces or within endosomes and recruit adaptor proteins that signal through two main pathways. These pathways are mediated by toll/interleukin-1 receptor (TIR) domain-containing adaptor molecules, precisely, myeloid differentiation primary response 88 (MyD88) (MyD88-dependent pathway) or TIR domain-containing adaptor inducing IFNβ (TRIF) (MyD88-independent pathway). On the other hand, RLRs recognise viral nucleic acids in the cytoplasm. NLRs detect different microbial components in the cytoplasm, and they can initiate a caspase-1-dependent inflammatory type of programmed cell death. Following PRR engagement, the sequential activation of serine/threonine kinases and other intermediary proteins results in the activation of inflammatory transcription factors. Common downstream targets of PRRs include nuclear

A

Phagocytic receptor	Ligands
Pattern-recognition receptors	
Dectin-1	Polysaccharides of some yeasts
Mannose receptor	Mannan
CD14	Lipopolysaccharide-binding protein
Scavenger receptor A	Lipopolysaccharide, lipoteichoic acid
CD36	Plasmodium faciparum-infected erythrocytes
MARCO	Bacteria
Opsonic receptors	
FcγRI (CD64)	IgG1 – IgG3 > IgG4
FcγRIIa (CD32a)	IgG3 ≥IgG1 – IgG2
FcγRIIIa (CD16a)	IgG
CR 1 (CD35)	Mannan-binding lectin, C1q, C4b, C3b
CR 3 (CD11b/CD18, Mac-1)	iC3b
CR 4 (CD11c/CD18)	iC3b
Integrin α5β1	Fibronectin, vitronectin

B

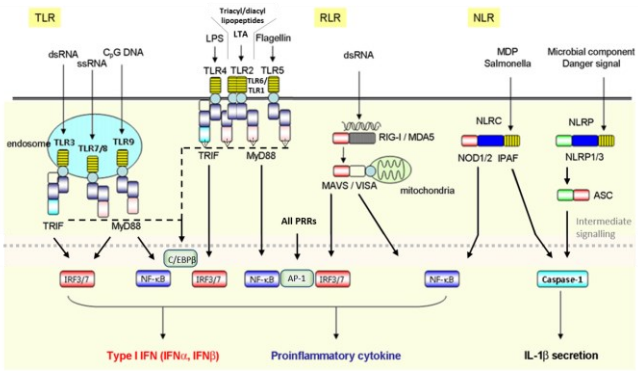

Figure 2. Pattern recognition receptors. A) List of selected phagocytic receptors and their ligands. B) Representation of the main members of the PRR families: TLRs, RLRs, and NLRs. C1q, C4b, C3b, and iC3b: complement proteins; LTA: lipoteichoic acid; dsRNA: double-stranded RNA; MDP: muramyl dipeptide: MDA5: Melanoma Differentiation-Associated protein 5; NLRC: NOD-leucine-rich repeat family with caspase recruitment domain (CARD); NLRP: NOD-, LRR- and pyrin domain-containing protein; ASC: apoptosis-associated speck-like protein containing a CARD; MAVS/VISA: Mitochondrial antiviral-signalling protein. Figure adapted from (Rosales and Uribe-Querol, 2017) (A) (Hong et al., 2011) (B).

factor kappa B (NF-κB), activator protein 1 (AP1), interferon regulatory factors (IRFs), and CCAAT-enhancer-binding protein β (C/EBPβ).

2.3 C/EBPβ

The transcription factor C/EBPβ is a master regulator of gene expression in monocytic cells (reviewed in Huber et al., 2012). C/EBPβ belongs to the C/EBP family of transcription factors, which are widely expressed and regulate multiple biological functions. The six members of the C/EBP family are characterised by a highly-conserved basic leucine zipper (bZIP) domain at the carboxy-terminus by which they dimerise and bind to the DNA, and an effector domain at the amino-terminus that mediates transactivation or repression (reviewed in Tsukada et al., 2011). To modulate transcription, C/EBPs bind to palindromic α-helical recognition sequences along the major groove of the DNA forming a *Y*-shaped structure (Glover and Harrison, 1995; Miller et al., 2003). C/EBPβ binds to the DNA as a homodimer or a heterodimer. To form a heterodimer, C/EBPβ can associate either with other members of the C/EBP family or with different bZIP transcription factors such as JUN/FOS proto-oncogenes (AP1 transcription factor subunits), cAMP-responsive element-binding protein (CREB)/activating transcription factor (ATF) family members, and MAF (Grigoryan et al., 2009; Newman and Keating, 2003). In addition, C/EBPβ can physically interact with some non-bZIP transcription factors, including the following: NF-κB (Diehl and Hannink, 1994; Dooher et al., 2011; Faggioli et al., 2004; Ruocco et al., 1996); the hematopoietic transcription factors myeloblastosis oncogene (MYB) (Tahirov et al., 2002), PU.1 (Listman et al., 2005) and runt-related transcription factor (RUNX) 1; and the nuclear receptors glucocorticoid receptor (reviewed in Roos and Nord, 2012), peroxisome-proliferator-activated receptors (PPAR) α (Mouthiers et al., 2005), and liver X receptor (LXR) (Tian et al., 2016). Some of these interactions are cooperative, whereas others have counteracting effects (reviewed in Pulido-Salgado et al., 2015).

C/EBPβ expression is regulated by proliferation- and differentiation-inducing extracellular factors as well as by inflammatory molecules (reviewed in Tsukada et al., 2011). It is upregulated during the differentiation of (pre)monocytes to macrophages (Natsuka et al., 1992) and controls monocytic cell proliferation and the orchestration of the innate immune response, including inflammatory gene expression and phagocytosis (Figure 3). In macrophages, C/EBPβ expression is induced by the presence of the cytokines TNF, IL1, IL6, and IFNγ as well as by PAMPs such as LPS (Goethe and Phi-van, 1997; Hsu et al., 1994; Hu et al., 2001; Natsuka et al., 1992; Sonoki et al., 1997; Tengku-Muhammad et al., 2000). Reciprocally, C/EBPβ binds to gene regulatory

regions of several cytokines (e.g., *Tnfa*, *Il1b*, *Il6, Il12*), chemokines (e.g., *Il8*, *Ccl3* (also named *Mip1a*) and *Ccl4* (also named *Mip1b*)), acute-phase proteins, and growth factor receptors (Akira et al., 1990). The relevance of C/EBPβ in the macrophage microbicidal activities is evidenced by the fact that C/EBPβ-deficient mice present increased susceptibility to infection by intracellular bacteria associated with an impaired bactericidal activity (Screpanti et al., 1995; Tanaka et al., 1995). Besides, C/EBPβ has been linked to M2-associated gene expression (e.g., *Arg1*, *Il10*) after being upregulated by CREB in response to IFNγ + LPS (Ruffell et al., 2009).

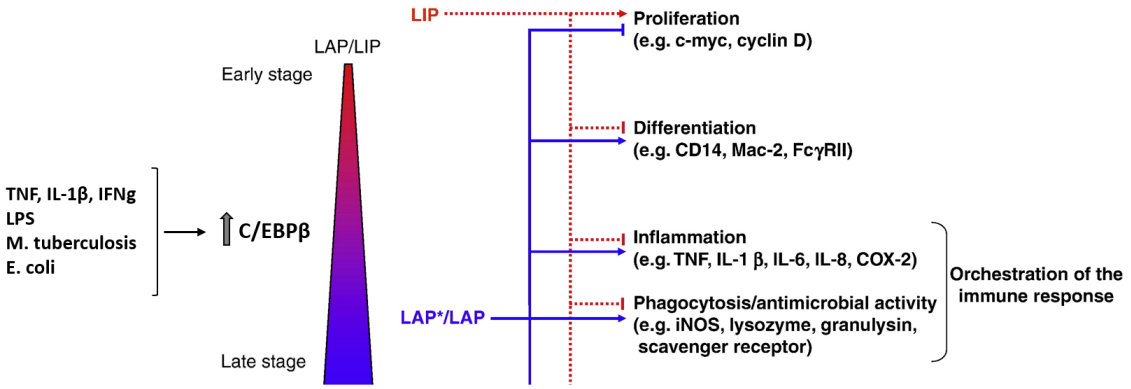

Figure 3. Roles of C/EBPβ in monocytic cells. Various inflammatory molecules and bacteria increase the protein levels of C/EBPβ. The LAP/LIP ratio is enhanced during the monocyte differentiation process. The positive and negative modulation of several biological processes by LAP* and LAP (blue line) or LIP (red dotted line) are shown. iNOS: inducible nitric oxide synthase; COX-2: cyclooxygenase 2. Figure adapted from (Huber et al., 2012).

C/EBPβ presents three different isoforms that arise from alternative translation initiation sites (reviewed in Huber et al., 2012). Two of the isoforms, the liver-enriched activating protein* (LAP*, the full length protein) and LAP, are transcriptional activators that differ slightly in length, whereas the liver-enriched inhibitory protein (LIP) is the smallest isoform, which lacks the transactivation domain and generally acts as a dominant-negative isoform. After protein synthesis, C/EBPβ rapidly translocates to the nucleus to regulate transcription (reviewed in Pulido-Salgado et al., 2015). Its activities are further regulated by post-translational modifications, which can be activating or inhibitory, and affect the protein stability, binding to DNA, interactions with other transcription factors, and transactivation capacity. While C/EBPβ phosphorylation is usually associated with an activating effect, the linkage of small ubiquitin-like modifier (SUMO) presumably induces inhibition, yet acetylation can have both positive and negative modulatory actions. In conclusion, C/EBPβ is a central mediator of the macrophage inflammatory response that can be modulated by diverse molecules through a plethora of mechanisms.

2.4 Roles of macrophages against bacterial infection

2.4.1 Bacterial sensing and intracellular signalling

Several TLRs detect conserved molecules on bacteria. Cell surface TLR1, TLR2, and TLR6 form heterodimers (TLR1/2 and TLR2/6) that bind lipoteichoic acid on Gram-positive bacteria or diacyl and triacyl lipoproteins on Gram-negative bacteria, among others. Flagellin in bacteria can be detected by surface TLR5. Additionally, TLR9, embedded in endosomal membranes of immune cells, recognises unmethylated CpG dinucleotides present in bacteria and viruses.

Gram-negative bacteria are rapidly recognised by phagocytic cells through TLR4, which binds to LPS, an integral component of the bacterial outer membrane (Murphy, 2012). Bacterial LPS, also known as endotoxin, is a potent immunostimulatory molecule that polarises macrophages towards the prototypic M1 phenotype. During infection, LPS can dissociate from bacterial cell wall and be picked up by the soluble LPS-binding protein (LBP). Then, LBP transfers LPS to CD14 on the surface of phagocytes, where it finally interacts with TLR4 and its accessory protein MD-2 to induce TLR4 dimerization and signal transduction (Figure 4 A) (reviewed in Lu et al., 2008). In humans, TLR4 and MD-2 are predominantly expressed on monocytes, macrophages, and dendritic cells (reviewed in Vaure and Liu, 2014). Upon LPS binding, TLR4 recruits adaptor proteins containing TIR domains. Then, TLR4 initiates two separate signalling pathways: the MyD88 protein-dependent pathway and the MyD88-independent pathway (reviewed in Kagan et al., 2008). The MyD88-dependent pathway occurs during the first minutes after TLR4 engagement at the plasma membrane and mediates inflammatory gene expression (Figure 4 B). Interactions between TLR4 and TIR domain-containing adaptor protein (TIRAP) attract MyD88, which activates IL1 receptor-associated kinase-4 (IRAK4), and this, in turn, activates IRAK1 (reviewed in Lu et al., 2008). Subsequently, TNF receptor-associated factor (TRAF) 6 activates TGFβ-activated kinase 1 (TAK1), which results in the activation of the inhibitor of NF-κB (IκB) kinase (IKK) and mitogen-activated protein kinase (MAPK) pathways. On the one hand, the IKK complex induces the degradation of IκB, a protein that sequesters NF-κB, thereby releasing NF-κB and enabling transcriptional activation of its target genes. On the other hand, the sequential activation of MAPK proteins leads to the activation of the transcription factor AP1. Later on, TLR4 is endocytosed and initiates the MyD88-independent pathway by interacting with different adaptor molecules (Figure 4 C) (reviewed in Kagan et al., 2008). From the endosomal membrane, TLR4 recruits TRIF-related adaptor molecule (TRAM) and TRIF (reviewed in Lu et al., 2008). At this point, two divergent cascades are promoted by TRIF. On the one hand, RIP-1 activates IKK

and MAPKs. On the other hand, TRAF3 induces IRF3 activation. To activate IRF3, TRAF3 recruits a protein complex formed by TRAF family member-associated NF-κB activator (TANK), TANK binding kinase 1 (TBK1) and inducible IKK. Subsequently, IRF3 induces the expression of antimicrobial mediators such as IFNβ, chemokine (C-X-C motif) ligand (CXCL)-10, and TNFα. Furthermore, the secretion of IFNβ and TNFα in response to LPS amplifies the inflammatory response through the activation of their respective receptors and subsequent signalling cascades. Given the extreme inflammatory potential of LPS, negative regulators act at many different levels on the pathway to prevent excessive tissue damage. Additionally, after exposure to small amounts of LPS, the cells become transiently unresponsive to new challenges with this molecule. This phenomenon, termed endotoxin tolerance, further protects tissues from uncontrolled inflammation (reviewed in Biswas and Lopez-Collazo, 2009).

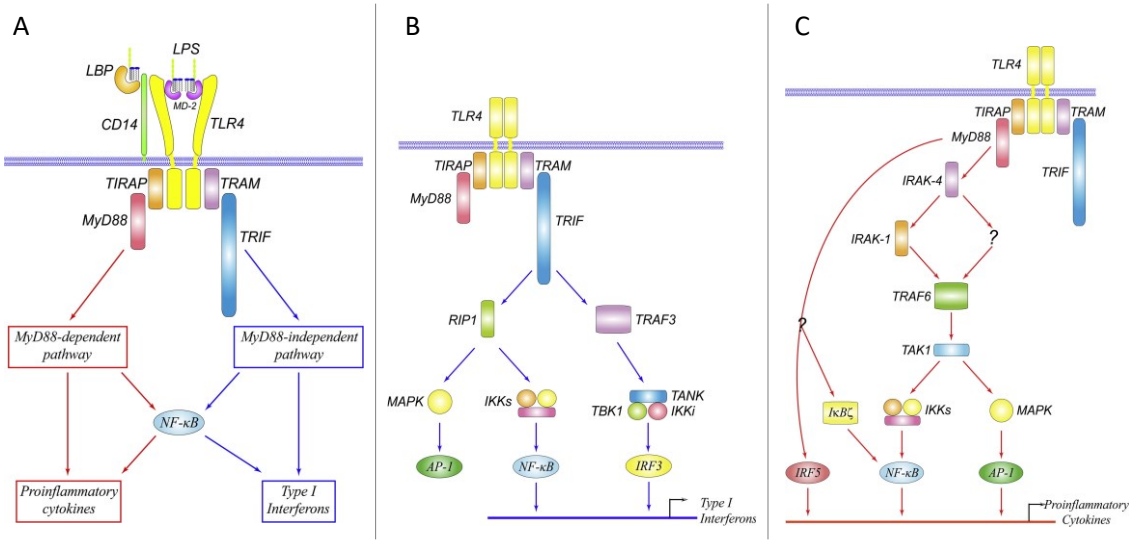

Figure 4. LPS/TLR4 signalling pathway. A) LPS signaling is mediated by the TLR4/MD-2 receptor complex and progresses through MyD88-dependent and MyD88-independent pathways, leading to the activation of pro-inflammatory cytokines and type I interferons. B) MyD88-independent pathway. TRIF recruits TRAF3 and RIP1, which activate downstream kinases that mediate the activation of the transcription factors AP1, NF-κB, and IRF3. C) MyD88-dependent pathway. IRAK proteins and TRAF6 activate other downstream proteins that lead to the activation of IRF5, NF-κB, and AP1. Figure adapted from (Lu et al., 2008).

A central signalling platform during macrophage activation is constituted by the MAPK family of proteins. MAPKs are serine/threonine kinases that couple extracellular signals with numerous intracellular responses, including gene expression, metabolism, proliferation, survival, differentiation, and stress response. (reviewed in Cargnello and Roux, 2011; reviewed in Plotnikov et al., 2011). There are three main MAPK categories that become sequentially activated by phosphorylation (Figure 5). Generally, a MAPK kinase kinase (MAPKKK) is activated by a small guanosine-5'-triphosphate hydrolase (GTPase) or protein kinase downstream of a

surface receptor. Next, this MAPKKK phosphorylates a MAPK kinase (MAPKK), which in turn, phosphorylates a MAPK. Then, the final MAPK phosphorylates diverse substrates to regulate biological activities (reviewed in Morrison, 2012).

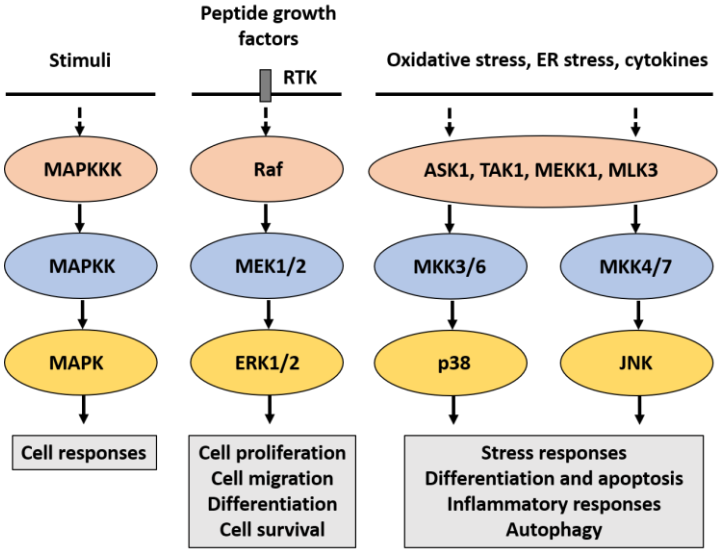

Figure 5. MAPK signalling pathways. Multiple extracellular and intracellular signals stimulate MAPK pathways. Each signalling pathway consists of sequentially-activated MAPKKKs, MAPKKs, and MAPKs. Activated MAPKs phosphorylate diverse target molecules, including transcription factors such as c-JUN, c-MYC, and ATF2, which mediate diverse cellular responses (e.g., proliferation, migration, differentiation, survival or apoptosis, autophagy, and inflammatory reactions). ASK1: apoptosis signal-regulating kinase 1; MEKK and MKK are MAPKKs; JNK: c-Jun NH2-terminal kinase; ERK: extracellular signal-regulated. MEK: MAPK/ERK kinase; RTK: receptor tyrosine kinase. Figure created based on the figure from (Kim and Choi, 2015).

Microbial ligands of PRRs and several cytokines, indeed, trigger signalling cascades that activate MAPK pathways in innate immune cells (reviewed in Arthur and Ley, 2013). In mammals, the most studied MAPKs are extracellular signal-regulated kinase (ERK) 1 and ERK 2, p38, and c-JUN N-terminal kinase (JNK) 1 (JNK 1) and JNK 2. JNK 1/2 and ERK 1/2 participate in the macrophage inflammatory response elicited by M1 stimuli such as LPS. Of the two p38 isoforms, only p38α seems to participate in pro-inflammatory cytokine synthesis downstream of TLR signalling (Kang et al., 2008; O'Keefe et al., 2007).

Macrophage activation by PAMPs/DAMPs or cytokines is accompanied by metabolic shifts that support their functions (reviewed in Vergadi, 2017). The phosphatidylinositol 3 kinase (PI3K)/AKT pathway is at the crossroads of metabolic and immune adaptation of macrophages and enables phenotypic specialisation. AKT is a serine/threonine kinase that controls not only macrophage survival, proliferation, and migration, but also metabolism and immune activities (reviewed in Song et al., 2005). AKT is activated by nutrient availability (reviewed in Dibble and Manning, 2013) and inflammatory molecules, including TLR ligands, cytokines and chemokines,

and FcγRs (Figure 6) (reviewed in: Covarrubias et al., 2015; Troutman et al., 2012). All these stimuli lead to PI3K activation, which generates phosphatidylinositol (3,4,5)-triphosphate (PIP3) at the plasma membrane that subsequently recruits mammalian target of rapamycin complex (mTORC) 2 to activate AKT. Then, AKT activates mTORC1 and mediates diverse biologic functions. In general, AKT activation by TLRs or cytokines restricts inflammation and promotes M2 polarisation (Beharka et al., 2005; Gong et al., 2012a; Lopez-Pelaez et al., 2011; Rocher and Singla, 2013; Weisser et al., 2011). However, different PI3K and AKT isoforms have shown variable effects on M1 or M2 polarisation (reviewed in Vergadi, 2017). On the other hand, AKT fosters phagocytosis of apoptotic bodies (Murakami et al., 2014) and IgG-coated particles (Ganesan et al., 2004; Shiratsuchi and Basson, 2007), but it inhibits autophagy (Ito et al., 2015b; Owen et al., 2014; Park et al., 2011). Additionally, AKT prevents apoptosis (Fernandez-Hernando et al., 2007; Larson-Casey et al., 2016). Therefore, the AKT pathway integrates metabolic and immune signals driving phenotypic activation of macrophages towards M1 or M2, and regulates biological processes to meet their energetic and immune requirements.

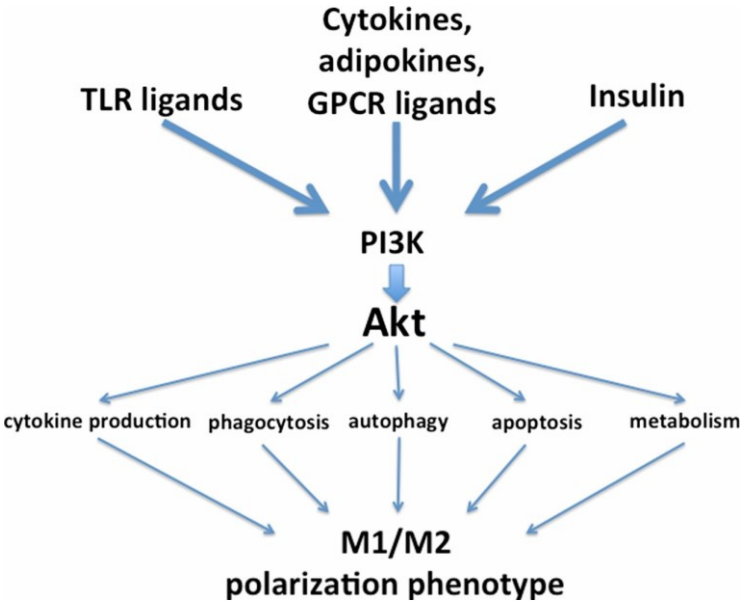

Figure 6. The AKT pathway regulates diverse biological activities and contributes to the macrophages polarisation towards the M1 or M2 phenotype. Multiple extracellular stimuli induce signalling events that activate the PI3K/AKT pathway, which subsequently modulates various cellular processes that help determine the macrophage polarisation towards an M1 or M2 phenotype. Figure obtained from (Vergadi, 2017).

2.4.2 Secretion of inflammatory mediators

Upon microbial recognition and cell activation, macrophages start producing cytokines. The main cytokines secreted by macrophages against bacterial infections belong to the IL1 family (IL1β and IL18), hematopoietin family (IL6), IL12 family (IL12), and TNF family (TNFα) (Murphy,

2012; reviewed in Vignali and Kuchroo, 2012). Together, these cytokines set up the milieu to exploit innate immune mechanisms and stimulate adaptive immune responses.

Locally, IL1β and TNFα increase the vascular permeability to allow the influx of effector cells and molecules (Murphy, 2012). IL18 is a chemoattractant that recruits more immune cells to the infection site. Moreover, IL1β, TNFα, and IL6 act systemically to induce fever and stimulate the production of acute-phase proteins by the liver. Acute-phase proteins bind conserved structures on bacterial surfaces and serve as opsonins that can activate the complement cascade.

TNFα, mainly produced by macrophages and T cells, is a key pro-inflammatory mediator during inflammation (reviewed in Zelova and Hosek, 2013). Its production is stimulated by PAMPs, especially LPS, as well as by cytokines, including IL1 and IFNγ, or TNFα itself in an autocrine manner. Numerous events taking place during inflammation are directly or indirectly mediated by TNFα. So far, it is involved in vasodilation, leukocyte adhesion to the endothelium, edema (increased accumulation of fluid in the tissue), blood coagulation at the injury site, ROS production, and fever. TNFα exists in transmembrane (tmTNFα) and soluble (sTNFα) forms, both active as homotrimers, but with different consequences due to unequal spatial range and receptor binding characteristics. The biological effects of TNFα are mediated by its interaction with the TNF receptor (TNFR) 1 and TNFR2, which can also be cleaved and become soluble receptors. TNFR1 is ubiquitously expressed and can bind tmTNFα and sTNFα. In contrast, TNFR2 exclusively binds sTNFα and its expression is restricted to immune cells, endothelial cells, and neurons. The functional impact of TNFα depends on which signalling complexes are activated downstream of TNFR. There are four different signalling complexes, precisely, complex I, IIa, IIb, and IIc (Figure 7A,B) (reviewed in Kalliolias and Ivashkiv, 2016). First, the signalling complex I is activated by TNFR1 or TNFR2 and promotes pro-inflammatory and anti-apoptotic activities (Figure 7 C). It is composed of TNFR type 1-associated death domain protein (TRADD), receptor-interacting protein-1 (RIP1), TRAF2, cellular inhibitor of apoptosis protein 1 (cIAP1) or cIAP2, and linear ubiquitin chain assembly complex (LUBAC). After ubiquitination, complex I signals through two separate pathways. On the one hand, signalling through the IKK complex leads to NF-κB activation. On the other hand, the TAK1 complex activates two MAPK pathways, namely JNK and p38 pathways. Then, JNK translocates to the nucleus, where it activates AP1. Noteworthy, the magnitude and kinetics of TNF signalling complex I are finely controlled by negative modulators. Second, the signalling complex II functions exclusively downstream of TNFR1 and leads to cell death. Complex IIa and IIb assemble at the cell cytoplasm with TRADD and Fas-associated death domain protein (FADD), which trigger subsequent steps in the signalling cascade to activate the

pro-apoptotic caspase 8 (reviewed in Kalliolias and Ivashkiv, 2016). Complex IIc, instead, induces cell death by necroptosis through the activation of mixed lineage kinase (MLK) domain-like protein (MLKL) in a RIP-3-dependent mechanism.

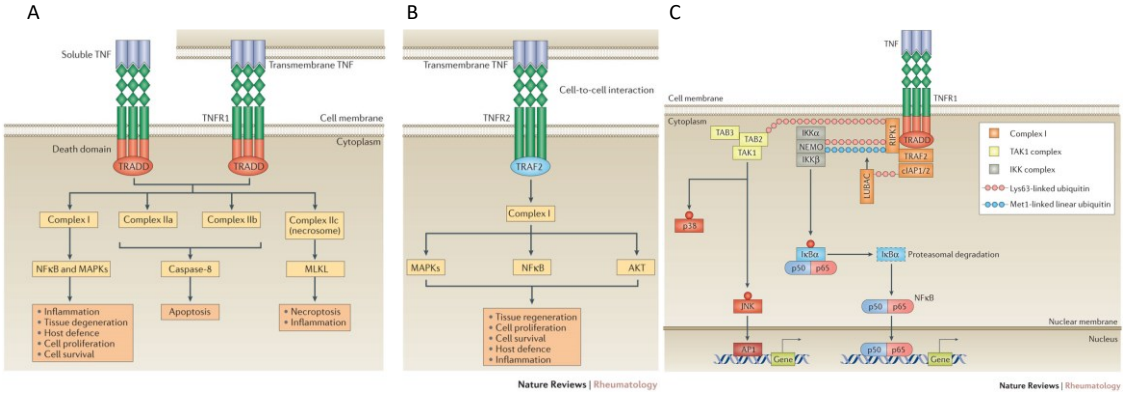

Figure 7. TNF signalling pathway. A) Signalling complexes activated by TNFR1. Soluble and transmembrane TNF activate TNFR1, which recruits the adaptor protein TRADD to mediate the assembly of different signalling complexes. First, TNFR1 initiates the signalling through complex I, resulting in activities involved in the immune defence against pathogens. Later, TNF might assemble the complexes IIa and IIb or IIc to induce either programmed cell death or necroptosis and inflammation, respectively. B) TNFR2 induces the assembly of complex I. C) Signalling pathway activated by the complex I. Assembly of complex I causes the activation of subsequent proteic complexes that lead to p38 and JNK activation and the transcription of target genes of AP1 and NF-κB. cIAP: cellular inhibitor of apoptosis protein; NEMO: NFκB essential modulator; TAB: TAK1-binding protein**.** Figure adapted from (Kalliolias and Ivashkiv, 2016).

Macrophages activated by the detection of bacteria also secrete IL12, which stimulates the activities of NK cells and Th1 lymphocytes. Reciprocally, NK cells and Th1 cells potentiate the microbicidal functions of macrophages through IFNγ secretion. Some pathogens can persist within macrophages for some time, but following exposure to IFNγ, macrophages boost their microbicidal capacity and effectively eliminate them. IL12 and IL18 are the main inducers of IFNγ production by NK cells, innate lymphoid cells, Th1 cells, and CTLs (reviewed in Schroder et al., 2004). NK cells are the first IFNγ producers before the adaptive immunity takes part. However, the complete activator effect of IFNγ on macrophages is only achieved after sensitisation induced by pathogen-specific Th1 cells. Th1 cells interact with infected macrophages by specific TCR:MHC-II interactions and provide the sensitising signal through the binding of CD40 ligand to CD40 on macrophages. The functional consequences of activation by IFNγ include higher production of TNFα; increased expression of CD40, TNFR, and MHC-II, and; enhanced intraphagosomal microbial degradation by reactive oxygen and nitrogen species (reviewed in Murphy, 2012).

A dimer of IFNγ binds to the IFNγ receptor (IFNGR), composed of two IFNGR1 and two IFNGR2 chains, to initiate the intracellular signalling cascade (Figure 8) (reviewed in Hu and Ivashkiv,

2009; reviewed in Majoros et al., 2017; reviewed in Schroder et al., 2004). IFNGR1 chains interact with intracellular Janus tyrosine kinase (JAK) 1 and signal transducer and activator of transcription (STAT) 1. IFNGR2 chains, instead, bind JAK2. The binding of IFNγ to its receptor causes JAK2 autophosphorylation, JAK1 phosphorylation by JAK2, and IFNGR1 phosphorylation by JAK1. Successively, a STAT1 homodimer is recruited to the receptor and becomes phosphorylated. Next, the phosphorylated STAT1 dimer dissociates from IFNGR-JAK1-JAK2 complex to enter the nucleus and regulate the transcription of genes containing an IFNγ activation site (GAS). Noteworthy, many of the STAT1 target genes are transcription factors, for example, IRF1 is directly induced by STAT1 and drives the second wave of transcriptional activation upon binding to IFN-stimulated response elements (ISRE). Non-canonical signalling pathways for IFNγ have also been described (reviewed in Majoros et al., 2017). Several negative regulators of the JAK-STAT pathway limit the extent and duration of IFNγ signalling, for example, the protein suppressor of cytokine signalling 1 (SOCS1) (reviewed in Schroder et al., 2004).

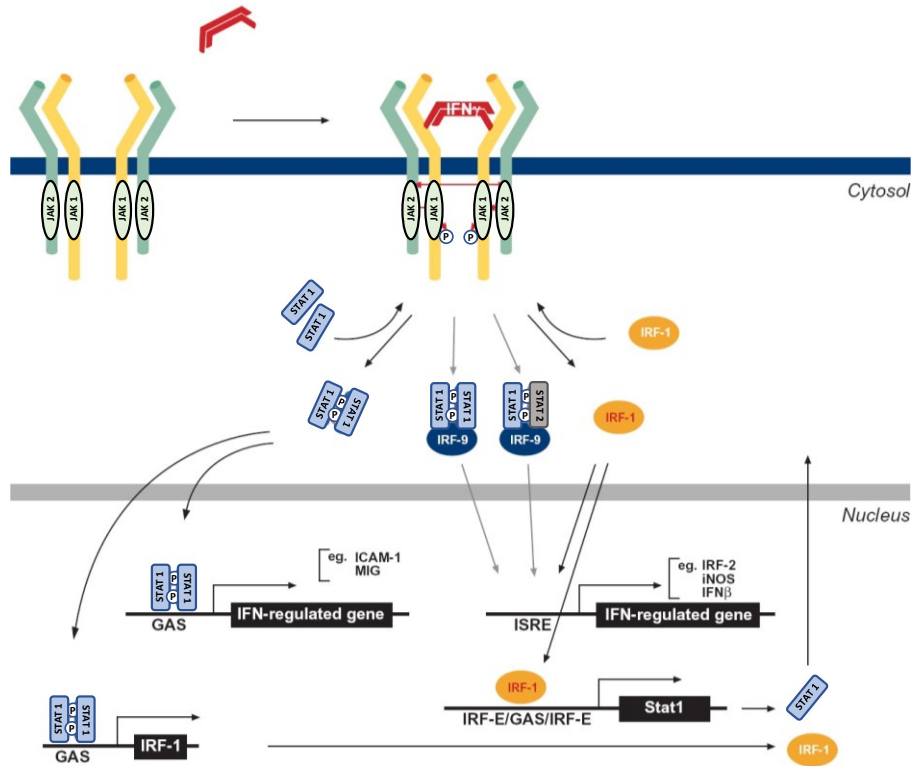

Figure 8. Signalling pathway mediated by IFNγ. Binding of FNγ to the IFNγR (IFNGR1, yellow; IFNGR2, green), induces a sequence of phosphorylation events in the receptor chains and JAK proteins that generate docking sites for STAT1. STAT-1 homodimers are subsequently phosphorylated and migrate to the nucleus, where they bind GAS elements to modulate the transcription of target genes. Many of the STAT1 target genes are in fact transcription factors that cause the second wave of transcription. This is the case of IRF1. To a lesser extent, IFNγ signalling induces the formation of STAT1:STAT1:IRF9 and STAT1:STAT2:IRF9 complexes. Those complexes and IRF-1 can bind to ISRE regions on target genes to regulate transcription. IRF-1 can also induce STAT1 expression through an unusual ISRE site (IRF-E/GAS/IRF-E). ICAM-1: intercellular adhesion molecule-1; MIG: monokine induced by IFNγ; iNOS: inducible nitric oxide synthase. Figure adapted from (Schroder et al., 2004).

2.4.3 Phagocytosis

Phagocytosis is defined as the ingestion of particles bigger than 0.5µm by cells (reviewed in Rosales and Uribe-Querol, 2017). It is a complex process that requires the activation of cell membrane receptors that initiate intracellular signalling cascades to induce the reorganisation of the actin cytoskeleton. Macrophages are professional phagocytes that exert homeostatic and immune functions by removing apoptotic cells and microbes. Indeed, the phagocytosis of pathogens is an essential step for an early contention of infection, and it stimulates antigen presentation by antigen-presenting cells.

Phagocytic receptors couple target particle recognition to phagocytosis. Besides triggering phagocytosis, some of them have broader effects such as the induction of cytokine production (Murphy, 2012). To be activated, phagocytic receptors need to aggregate (crosslink), a dynamic event that depends on the lateral diffusion of receptors (reviewed in Rosales and Uribe-Querol, 2017). Noteworthy, TLRs are not phagocytic receptors but they cooperate with non-opsonic phagocytic receptors to prepare (prime) phagocytosis. In fact, the activation of some TLRs reduces the spatial confinement of receptors in the plasma membrane by modulating the actin cytoskeleton (Figure 9 A) (reviewed in Freeman and Grinstein, 2014). Additionally, TLR engagement induces inside-out activation of integrins, which adopt a conformation with enhanced capability of ligand binding (reviewed in Rosales and Uribe-Querol, 2017). Phagocytosis mediated by CR and FcγR has been the focus of many studies. In contrast, the phagocytosis pathway mediated by non-opsonic receptors remains largely unknown. Therefore, the general steps mediating opsonic receptor-driven phagocytosis will be taken as a model to explain the process. First, membrane-bound cortical actin present during the macrophage resting state is disrupted (Figure 9 B) (reviewed in Rosales and Uribe-Querol, 2017). Initially, coronins debranch the actin meshwork and release linear filaments as substrates for cofilin and gelsolin, which dissociate them into actin monomers. The disruption of cortical actin also facilitates the diffusion of receptors through the plasma membrane. Second, actin polymerises, and the cell extends pseudopods to cover the particle to be phagocytosed. Various sequential steps mediate this event. Ligand binding to CR or FcγR activates intracellular kinases and phosphatases that recruit more proteins and generate second messengers and certain phosphoinositide forms. The changes in membrane lipid composition and the formation of signalling complexes activate downstream pathways. The small GTPases of the Rho family are core targets of this signalling cascade (reviewed in Rosales and Uribe-Querol, 2017). Small Rho

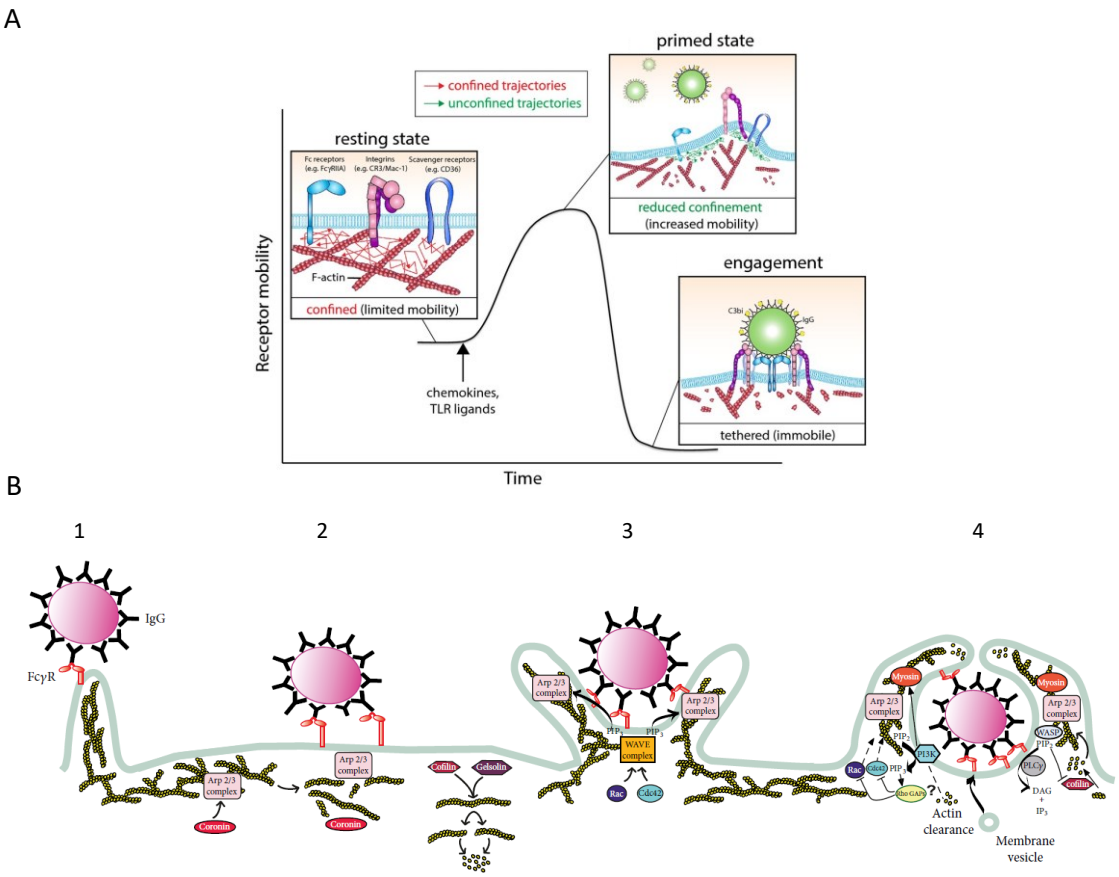

Figure 9. Steps for phagocytosis: receptor priming and actin cytoskeleton remodelling. A) Control of receptor mobility by the actin cytoskeleton. In the resting state, membrane receptors such as FcγRs, integrins, and scavenger receptors are confined by pickets attached to an F-actin meshwork. The interaction of chemokines or TLR ligands with their surface receptors induces actin remodelling, which leads to membrane ruffling and the formation of more branched and dynamic cortical actin filaments. Consequently, membrane receptors can diffuse more freely through the membrane and encounter ligands (primed state). The engagement of phagocytic receptors by target particles retains the receptors tethered to the ligand and, in some cases, anchored to the actin cytoskeleton, rendering them immobile (Freeman and Grinstein, 2014). B) Changes in the cytoskeleton during phagocytosis. Resting phagocytes project membrane extensions to sense their environment. These membrane extensions are primarily formed by linear actin fibres. Following recognition of the target particle, the actin cytoskeleton is disrupted at the phagocytic cup, and the cells start extending pseudopodia, which consist of branched actin filaments. The formation of these new actin filaments at the phagocytic cup is promoted by the coordinated actions of small GTPases, nucleation-promoting factors, and actin nucleator proteins. Finally, actin filaments at the base of the nascent phagosome depolymerise and the phagosome closes. Figures adapted from (Freeman and Grinstein, 2014) (A) and (Rosales and Uribe-Querol, 2017) (B).

GTPases are molecular switchers that alternate between the active (guanosine triphosphate (GTP)-bound) and inactive (guanosine diphosphate (GDP)-bound) forms to regulate the activity of effector proteins. The shifts from one state to the other are mediated by guanine exchange factors (GEF) and GTPase-activating proteins (GAPs). As a result of phagocytic receptor engagement, the small GTPases Rho, Rac, or Cdc42 (their use differs depending on the inducing phagocytic receptor) become activated. Next, they activate nucleation promoting factors (e.g., Wiskott-Aldrich Syndrome protein [WASp] or Scar/WAVE), which subsequently activate the

actin nucleating protein Arp2/3 to ultimately mediate pseudopod extension. Last, actin depolymerisation occurs at the base of the nascent phagosome and the phagocytic cup closes. The activities of PI3K and phospholipase C (PLC) generate PIP3 and diacylglycerol (DAG), respectively, which inactivate Rho family GTPases and, consequently, impair Arp2/3 activity. The activity of cofilin also contributes to actin depolymerisation. Once the phagosome is closed, it will follow the phagolysosomal degradative pathway to become an effective microbicidal compartment.

2.4.4 Macrophage bactericidal mechanisms

Macrophages deploy an arsenal of mechanisms to kill pathogens. For example, bacteria that are internalised through phagocytosis become entrapped within phagosomes, which become increasingly microbicidal compartments (reviewed in Flannagan et al., 2009). There, the bacterial replication is inhibited by restricting their access to essential metabolites, extreme acidification of the medium, and exposure to antimicrobial proteins such as reactive nitrogen and oxygen species. Alternatively, macrophages can initiate a type of programmed cell death known as pyroptosis to restrict infection (reviewed in Bergsbaken et al., 2009).

Bacteria that are taken up by phagocytosis remain entrapped within a phagosome that undergoes maturation by successive fusion and fission with vesicles from the endocytic pathway (Figure 10) (reviewed in Rosales and Uribe-Querol, 2017). The resulting remodelling of the phagosomal membrane and internal contents engender a hostile environment for pathogen survival. To begin, the GTPase Rab5 recruits early endosome antigen 1 (EEA1) to the membrane of the early phagosome, which promotes the fusion with recycling endosomes. Constantly during the maturation process, V-adenosine triphosphatases (V-ATPases) on the phagosomal membrane translocate protons into the lumen, leading to the gradual acidification of the compartment. At the stage of the intermediate phagosome, intraluminal vesicles emerge, which bear membrane-associated proteins that are targeted for degradation. Progressively, Rab5 is substituted by Rab7, which recruits new proteins and converts the vesicle into a late phagosome. Then, the late phagosome establishes contacts with microtubules that guide its centripetal movement. The microbicidal capacity of late phagosomes is enhanced by the acquisition of lysosomal-associated membrane proteins and luminal proteases from late endosomes or from vesicles originated in the Golgi complex. Finally, the late phagosome fuses with lysosomes to give rise to the phagolysosome. This ultimate vesicle is very acidic and concentrates numerous

microbicidal components such as hydrolytic enzymes, scavenger molecules, and nicotinamide adenine dinucleotide (NAD^+) phosphate (NADPH) oxidases.

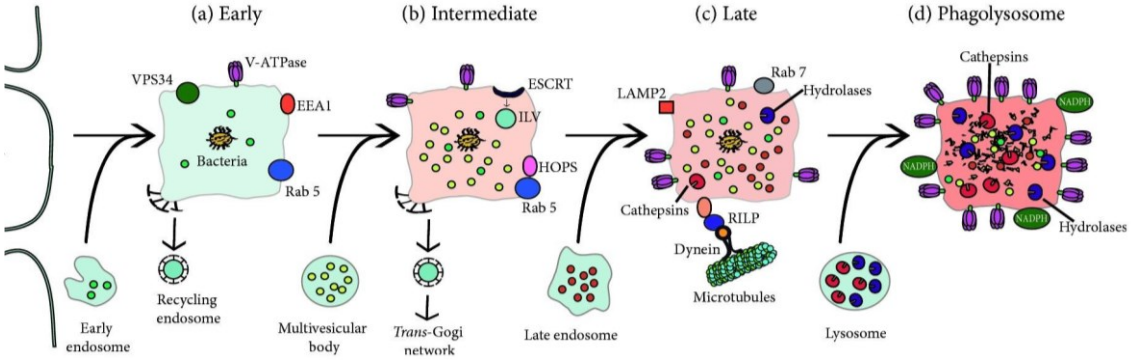

Figure 10. Steps of phagosomal maturation. Following phagocytosis, the phagosome matures by fusing with vesicles of the endocytic pathway and becomes a highly microbicidal compartment. The phagosome gradually acidifies by the action of a proton-pumping V-ATPases and it also acquires various degradative enzymes. The composition of the membrane changes through the acquisition of molecules that control membrane fusion such as the GTPases Rab. ESCRT: endosomal-sorting complex required for transport; HOPS: homotypic protein sorting; ILV: intraluminal vesicle; LAMP: lysosomal-associated membrane protein; RILP: Rab-interacting lysosomal protein; vPS34: vacuolar protein-sorting 34. Figure obtained from (Rosales and Uribe-Querol, 2017).

A different mechanism used by cells to degrade unwanted or damaged intracellular components is macroautophagy (from now on referred to as autophagy) (reviewed in Gong et al., 2012b). Autophagy is a process in which cytosolic materials are encapsulated in a double-membrane vacuole, the autophagosome, that fuses with lysosomes to give rise to the autophagolysosome, a potent degradative compartment. Xenophagy is a type of selective autophagy with antimicrobial functions. This process is highly regulated by multiple signalling pathways and coordinated by autophagy-related (Atg) proteins. Cytosolic sensors detect bacterial components or damaged phagosomes and provide an “eat me” signal that recruits autophagic receptors to induce subsequent microtubule-associated protein 1A/1B-light chain 3 (LC3)-dependent autophagy. Besides, some proteins of the autophagic machinery mediate non-canonical functions in a process named LC3-associated phagocytosis (reviewed in Heckmann and Green, 2019). LC3-associated phagocytosis is activated by the engagement of surface receptors by phagocytic cargos such as pathogens present in the extracellular space. For instance, the ligation of TLRs (TLR1-TLR2, TLR2-TLR6, and TLR4) or the C-type lectin dectin-1 can initiate this type of phagocytosis. Then, LC3 is recruited to the single-membrane phagosome and stimulates its maturation through fusion with endosomes and lysosomes to promote bacterial killing.

Macrophage pyroptosis can be induced by different conditions, including the infection by intracellular bacteria, as a host cell protective response (reviewed in Bergsbaken et al., 2009).

This type of cell death is characterised by the rapid lysis of the cell and the release of intracellular inflammatory contents. The binding of some NLRs to their cognate ligands in the cytosol induces the formation of a multiproteic complex known as the inflammasome. This complex activates caspase-1, which induces cellular DNA cleavage and plasma membrane pore formation. In addition, caspase-1 activates IL1β and IL18 that will be released to the extracellular medium after cell lysis. The inflammatory cytokines released by macrophages during this process attract and activate neutrophils to phagocytose and kill the ejected pathogens and cell debris. In that way, macrophages avoid the establishment of an intracellular bacterial niche within them.

2.5 The macrophage paradox

Despite the multiple antimicrobial mechanisms of macrophages, they represent, paradoxically, a preferential niche for the establishment of many intracellular bacteria (reviewed in Price and Vance, 2014). These intracellular bacteria have developed mechanisms to alter macrophage biology for their benefit (Figure 11) (reviewed in Sarantis and Grinstein, 2012). By different mechanisms, bacteria avoid being targeted for destruction and create the necessary conditions to sustain their replication. For example, some bacteria activate specific regulatory host cell receptors to alter the normal receptor crosstalk that would lead to bactericidal immune responses (reviewed in Hajishengallis and Lambris, 2011). The interference with the activation of critical protein kinases and phosphatases is another mechanism shared by many bacteria to inhibit macrophage activation. Typically inhibited targets include the JAK-STAT pathway, MAPK proteins, protein kinase C (PKC), PI3K, and TLR-induced activation of NF-κB (reviewed in Thi et al., 2012).

Macrophage phagocytosis is co-opted by numerous intracellular bacteria to gain access to their intracellular niche (reviewed in Sarantis and Grinstein, 2012). Indeed, bacteria that take profit from macrophage infection often possess their own invasive mechanisms to enter both phagocytic and non-phagocytic cells. Invasive bacteria contain virulence factors that manipulate critical steps of particle engulfment either by the engagement of host cell phagocytic receptors or by injection of bacterial effector molecules into the host cell cytosol. On the one hand, bacteria can supply ligands for macrophage cadherins and integrins that promote engulfment. On the other hand, some pathogens mimic the phagocytic receptor-driven signalling by providing intermediary molecules of the pathway. To transport their invasion factors, bacteria use specialised structures named secretion systems. These systems consist of a needle-like complex that injects proteins across the plasma membrane into the host cell cytosol. For

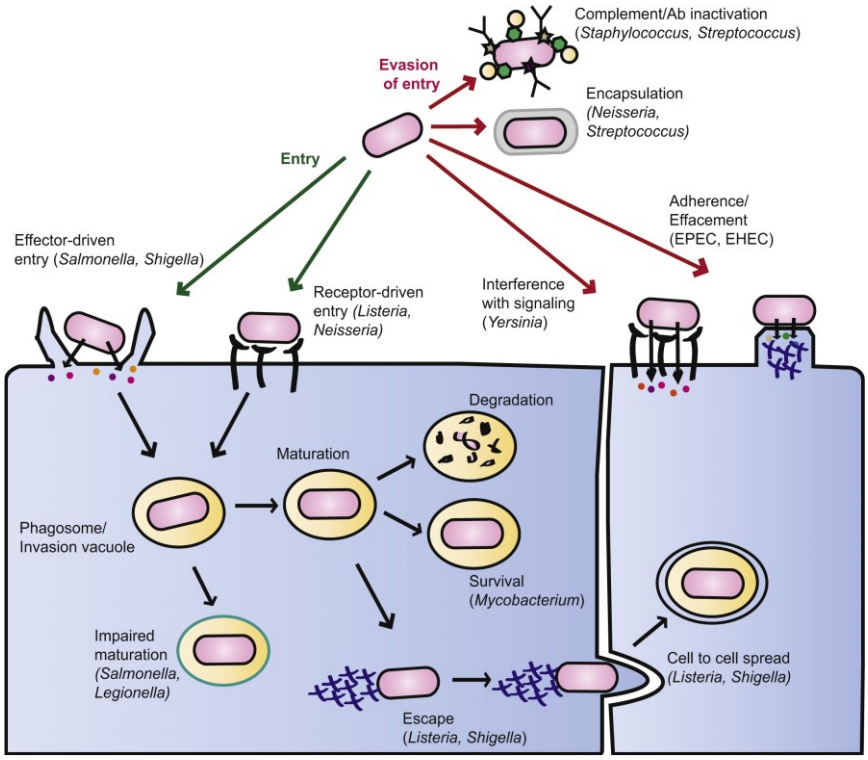

Figure 11. Strategies used by pathogens to subvert or evade phagocytosis. Pathogens can co-opt cellular receptors or inject effector proteins to promote their engulfment by host cells. Once inside the phagosome, pathogens can use different systems to escape from the phagosome into the cytoplasm, avoid phagosomal maturation, or survive to the hostile environment present in phagolysosomes. Other pathogens, instead, inhibit their recognition by host cells. Figure obtained from in (Sarantis and Grinstein, 2012).

instance, many bacteria induce their internalisation by macrophages through the signalling events promoted by phosphoinositides, either by injecting molecules that activate phosphatidylinositol kinases and phosphatases to generate phosphoinositides or by directly delivering their own signalling phosphoinositides into the host cell cytosol. Then, the conversion of specific phosphoinositides into second messengers by host cell enzymes recruits proteins that will coordinate phagocytosis to the nascent phagosome. Some bacteria can also produce their own GEFs and GAPs to control the activity of the Rho family small GTPases and induce actin reorganisation. Other bacteria inject actin nucleating proteins into the host cell to guide actin filament polymerisation.

In addition, early after being internalised by macrophages, intracellular bacteria start manipulating the phagosome to counteract its microbicidal activities. Commonly, these bacteria alter the phagosomal maturation or escape from the compartment to reach the cytosol (reviewed in Mitchell et al., 2016; reviewed in Thi et al., 2012). Intravacuolar bacteria modify the composition of the phagosomal membrane to prevent the acquisition of proteins involved in its maturation. As a result, intravacuolar bacteria can arrest phagosomal maturation or delay it until

they have adapted to survive within phagolysosomes. Even though phagosomes are devoid of nutrients to avoid microbial growth, intravacuolar bacteria express molecules that allow them to acquire the essential nutrients and co-factors, especially divalent cations and iron. Furthermore, some bacteria overcome the oxidative burst and generation of reactive nitrogen species. To accomplish so, they inhibit the assembly of NADPH oxidase at the phagosomal membrane or use deactivating enzymes that neutralise the reactive species. In contrast, cytosolic bacteria rapidly translocate virulence factors across the phagosomal membrane to leak out of the compartment. Once in the cytosol, these bacteria find a favourable nutrient-rich environment; however, they need to downregulate or modify the PAMPs to delay the recognition by cytoplasmic NLRs. Finally, bacteria that survive inside macrophages employ mechanisms to disseminate to other cells. For example, *Listeria* spreads using an actin-driven cell-to-cell invasion system that avoids extracellular exposure, whereas *Salmonella* induces pyroptosis and is released to the extracellular medium, from where it can infect other cells. In conclusion, each pathogen harbours a set of molecules that manipulate different host factors to fulfil its specific requirements and build a replication permissive intracellular niche.

3. CD38

CD38 is a multifunctional protein that is widely expressed in immune cells (reviewed in Malavasi et al., 2008). It is located in the plasma membrane and intracellular compartments as a transmembrane protein, or it can also be secreted as a soluble molecule. Transmembrane CD38 functions as a receptor, signalling mediator, and enzyme. As a receptor, it binds platelet endothelial cell adhesion molecule-1 (PECAM-1 or CD31) expressed by the cells within the vascular system, including endothelial cells (Deaglio et al., 1998). CD38 also participates in signalling events related to immune cell activation by laterally associating with other proteins or complexes. For example, it co-localises with the TCR, BCR, and MHC-II on the surface of T cells, B cells, and monocytes, respectively (Dianzani et al., 1995; Funaro et al., 1993; Zilber et al., 2005). On the other hand, CD38 is an enzyme that uses NAD^+ to generate calcium-mobilizing second messengers (reviewed in Hogan et al., 2019). At neutral pH, CD38 produces adenosine diphosphate (ADP) ribose (ADPR), cyclic ADPR (cADPR), and nicotinamide. These enzymatic activities require a large amount of NAD^+, consequently, its consumption by CD38 drastically impacts the intracellular NAD^+ levels. At acidic pH, CD38 converts $NADP^+$ into nicotinic acid adenine dinucleotide phosphate. CD38 can be placed in two opposite orientations in the membrane, each containing the catalytic domain at one side (Zhao et al., 2012). As a result, CD38 controls the levels of its substrate and products, mainly NAD^+ and ADPR, at the extracellular space, cytoplasm, and the lumen of the organelles.

The levels of CD38 expression by leukocytes are modulated by their activation or maturation state (reviewed in Glaría and Valledor, 2020). In macrophages, CD38 expression is induced by several inflammatory cytokines and the bacterial component LPS (Amici et al., 2018; Iqbal and Zaidi, 2006; Lee et al., 2012a; Lischke et al., 2013; Musso et al., 2001). Dendritic cells also upregulate CD38 expression during maturation (Beceiro et al., 2018; Fedele et al., 2004). In both types of leukocytes, CD38 expression is linked to the classical activation phenotype and the production of inflammatory cytokines. Some studies suggest that CD38 might modulate phagocytosis by macrophages, although the outcome of CD38 expression varies depending on the particle to be phagocytosed (Kang et al., 2012; Lucke et al., 2018; Matalonga et al., 2017). Additionally, CD38 participates in the migration of leukocytes through chemotaxis. For instance, CD38 is involved in neutrophil infiltration to the inflammation site and dendritic cell migration to the draining lymph nodes (Beceiro et al., 2018; Estrada-Figueroa et al., 2011; Frasca et al., 2006; Partida-Sanchez et al., 2001; Partida-Sanchez et al., 2007; Partida-Sanchez et al., 2004).

The mobilisation of calcium by the enzymatic products of CD38 contributes to the chemotactic events in neutrophils and dendritic cells, and, in the case of dendritic cells, the interactions between CD38 and CD31 have also a role in migration. Regarding the adaptive immune response, CD38 expression has been used as a lymphocyte activation marker in humans (reviewed in Glaría and Valledor, 2020). Besides, CD38 might participate in lymphocyte maturation and activation at different stages.

Finally, CD38 modulates the outcome of infection by different pathogens. *In vivo* models using CD38-deficient mice showed increased susceptibility to infection by *L. monocytogenes*, *Mycobacterium avium*, and *Streptococcus pneumoniae* (Lischke et al., 2013; Partida-Sanchez et al., 2001; Partida-Sanchez et al., 2003; Viegas et al., 2007). In contrast, in adult patients infected by the human immunodeficiency virus (HIV), CD38 expression is associated with the progression to acquired immunodeficiency syndrome and with poor prognosis (Benito et al., 1997; Giorgi et al., 1999; Liu et al., 1996; Mocroft et al., 1997). Various studies have analysed the role of CD38 during sepsis, a dangerous clinical condition characterised by exacerbated inflammation that can lead to organ dysfunction and death (van der Poll et al., 2017). Although the expression or enzymatic activities of CD38 had an impact in the pathology of sepsis, divergent outcomes were found among studies (Bahri et al., 2012; Patton et al., 2011; Shu et al., 2018) and further research would be required to elucidate the function of CD38 in sepsis.

To sum up, the body of evidence indicates that CD38 is modulated by different clinical conditions and it is involved in various immune cell functions. Monoclonal antibodies against CD38 have been approved for therapeutic use in multiple myeloma (reviewed in Morandi et al., 2018). Further research might determine whether targeting CD38 could be therapeutically exploited in other pathologies.

4. Features of pathogenic bacteria in humans

Bacteria are ubiquitous microorganisms present in the nature and in animal hosts. After birth, the body surfaces of humans that are exposed to the environment acquire microorganisms that persist as commensal bacteria (reviewed in Bhunia, 2018). Microbiota plays essential roles in human health, for instance, it regulates the nutrient absorbance and metabolism, protects us from invading microorganisms, and modulates the immune system. However, several microbes have acquired virulence factors that allow them to overcome the protective barriers of the organism and cause damage to host cells. As a result, pathogenic bacteria provoke host morbidity and/or mortality.

Bacteria can be classified according to many features. According to their pathogenicity, bacteria are defined as commensal (non-pathogenic), primary pathogens (regularly cause disease) or opportunistic (only cause disease in immunocompromised people or other risk populations) (reviewed in Bhunia, 2018). Regarding oxygen requirements, aerobic bacteria need oxygen, facultative anaerobic bacteria tolerate small amounts of oxygen, and strict anaerobic bacteria cannot withstand oxygen. Another important criterion for classification is the structure of the bacterial cell wall and Gram staining characteristics. Gram-positive bacteria consist of a rigid outer peptidoglycan layer and an inner cytoplasmatic membrane formed by a lipid bilayer (Figure 12 A). The outer peptidoglycan layer makes Gram-positive bacteria susceptible to the digestion by lysozyme. Besides, peptidoglycan potently stimulates the cytosolic NOD receptors in phagocytes. The cell wall of Gram-positive bacteria also contains teichoic acid, teichuronic acid, lipoteichoic acid, lipoglycan, and polysaccharide. The variety of lipoteichoic acid that stands above the bacterial cell wall determines the serotype (O antigen) of Gram-positive bacteria. On the other hand, Gram-negative bacteria have two lipid bilayers, the outer and the inner membranes, which are separated by a thin peptidoglycan layer and the periplasmatic space (Figure 12 B). The outer membrane consists of phospholipids, proteins, and LPS. The LPS molecule is formed by an outer O side chain, a core oligosaccharide, and lipid A, by which it anchors to the membrane. The O antigen serotyping profile of Gram-negative bacteria is determined by the O side chain of LPS. The proteins present in the outer membrane of Gram-negative bacteria are known as outer membrane proteins (OMPs) and participate in the nutrient and ion transport, enzymatic activities, and the adhesion to mammalian cells. Porins, which transport small molecules, are the most common OMPs, and they are potent immunostimulators.

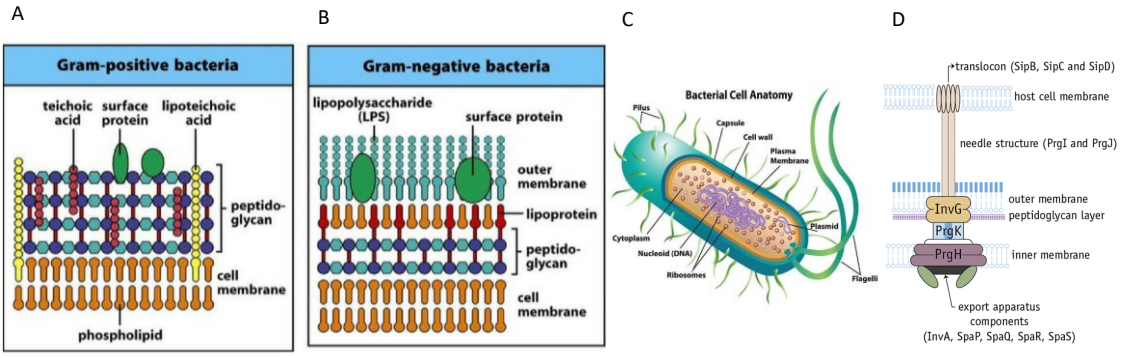

Figure 12. Bacterial components and accessory structures. A, B) Composition of the cell wall in Gram-positive (A) and Gram-negative (B) bacteria. C) Bacterial components and accessory structures. D) Structure of the T3SS. Figures adapted from: https://www.thesciencenotes.com/distinction-between-gram-positive-and-gram-negative-bacteria/ (A, B); https://biologydictionary.net/eubacteria/ (C); and (Dos Santos et al., 2019) (D).

Bacteria use extracellular accessory structures to accomplish diverse functions (Figure 12 C). (reviewed in Bhunia, 2018). Fimbriae or pili are long appendages that contribute to bacterial adhesion to surfaces or host cells, to bacterial motility, and to inter-bacterial exchange of genetic material. Most commonly, fimbriae are present in Gram-negative bacteria. On the other hand, flagella are filamentous structures that participate in bacterial locomotion, adhesion, and invasion. Depending on the number of flagella contained by bacteria and the flagellar arrangement throughout the cell, bacteria are categorised as monotrichous (a single flagellum), amphitrichous (one flagellum on each pole), lophotrichous (multiple flagella in each pole), or peritrichous (many flagella all around the cell). Various bacteria use adhesins to bind to molecules on host cells and promote invasion. The capsule is a layer of polysaccharides that surrounds the bacterial envelope and facilitates the adhesion to host cells. The capsule also serves to mask bacteria, thus hindering the recognition by phagocytic cells. Additionally, some bacteria bear nanomachine channels called secretion systems that enable the transport of proteins, DNA, and virulence factors across the bacterial envelope (Figure 12 D). For example, the type three secretion system (T3SS) is generally found in pathogenic bacteria and acts as a syringe to inject virulence factors into the eukaryotic cell cytoplasm. Conversely, Gram-positive bacteria frequently use the Sec pathway to translocate precursors of virulence proteins and enzymes that undergo proper folding after secretion.

The following section describes relevant characteristics of the bacterial pathogens studied in the present thesis. Selected features of these bacteria are listed in Table 1 at the end of the section.

4.1 *Salmonella enterica*

In humans, *Salmonella enterica* serovar Typhimurium (*S.* Typhimurium) is typically acquired by ingestion of contaminated food or water and causes self-limiting gastroenteritis in healthy individuals (reviewed in Malik-Kale et al., 2011). However, it can cause systemic infection in immunocompromised people (reviewed in Gordon, 2008).

Salmonella spp belong to the *Enterobacteriaceae* family. They are Gram-negative, non-spore-forming motile bacilli. They express peritrichous flagella and are facultative anaerobes (reviewed in Bhunia, 2018).

Intestinal phagocytic microfold cells (M cells) or CD18-expressing phagocytes transport ingested *S.* Typhimurium from the intestinal lumen to the submucosa (reviewed in Malik-Kale et al., 2011). Alternatively, *Salmonella* can traverse the intestinal epithelial barrier through transcytosis across enterocytes or paracellular movement between disrupted interepithelial junctions. Then, some bacteria are phagocytosed by resident immune cells whereas others invade enterocytes at the basolateral side (reviewed in Haraga et al., 2008). In epithelial cells, *Salmonella* elicits IL8 secretion, which recruits polymorphonuclear cells that release cytotoxic granules. Host cell invasion by *Salmonella* can be mediated by T3SS-dependent and T3SS-independent factors (reviewed in Velge et al., 2012). On the one hand, *Salmonella* uses the OMPs Rck and PagN as T3SS-independent mechanisms to bind host cell receptors and induce a receptor-driven "zipper" entry (Figure 13 A). This type of entry takes place through discrete actin rearrangements. *Salmonella* can also use different adhesins that promote its entry into host cells. On the other hand, for the T3SS-dependent invasion, bacteria inject effector proteins across the host cell plasma membrane that induce massive actin rearrangements and membrane ruffling (Figure 13 B). This type of invasion is known as "trigger" entry. The effector proteins mediating the engulfment of bacteria by host cells as well as the subsequent modifications in the vacuolar membrane are injected by two needle-like T3SSs. The type I T3SS (T3SS-1), encoded by the *Salmonella* pathogenicity island I (SPI1), is especially relevant for the induction of bacterial internalisation. The effector proteins translocated by the T3SS-1 are SipA, SipC, SopB, SopE, and SopE2. Through different activities these effectors induce the production of signalling phosphoinositides, activate or mimic mammalian GEFs (that subsequently activate Rac1 and Cdc42), and bind cellular actin to induce the drastic remodelling of the cytoskeleton. The type II T3SS (T3SS-2), encoded by the SPI2, translocates proteins across the phagosomal membrane to promote the intracellular survival and replication of bacteria. Both T3SSs sculpt

the *Salmonella*-containing vacuole (SCV), a spacious intracellular vesicle with an altered membrane composition that avoids microbicidal mechanisms (Figure 13 C) (reviewed in Malik-Kale et al., 2011). The SCV travels along microtubules towards a juxtanuclear position, where *Salmonella* can reach the necessary nutrients and start replicating. Bacterial replication occurs inside a dynamic tubular network that extends from the surface of the SCV known as *Salmonella*-induced filaments.

Macrophages represent a preferential niche for *Salmonella* replication and their migration through the reticuloendothelial system is responsible for bacterial dissemination to other organs and systemic infection (reviewed in Gogoi et al., 2019). Macrophages can detect extracellular *Salmonella* through TLR2 (diacyl and triacyl lipopeptides), TLR4 (LPS), and TLR5 (flagellin) (Arpaia et al., 2011). Early invasion by *Salmonella* induces MAPK signalling and the activation of AP1 and NF-kB, together with a boost of microbicidal activities (Hobbie et al., 1997; Patel and Galan, 2006; Vitiello et al., 2004). After phagocytosis, *Salmonella* undergoes an extensive remodelling of surface molecules, including the modification of LPS structure and the repression of T3SS-1 and flagellin expression (Ernst et al., 2001; Gibbons et al., 2005; reviewed in Haraga et al., 2008; Heithoff et al., 1999). Besides, the modulation of effector protein expression at different stages of infection allows *Salmonella* to interact with and manipulate various host inflammatory and cell death pathways such as pyroptosis, necroptosis, and apoptosis (reviewed in Wemyss and Pearson, 2019). However, macrophages can detect the presence of bacterial effector proteins or bacteria in the cytosol through NLRs, which trigger the formation of the inflammasome complex and macrophage pyroptosis, finally releasing *S.* Typhimurium to the extracellular space (Gogoi et al., 2019). Subsequently, the inflammation caused by pyroptosis recruits neutrophils that exert a key role in eliminating bacteria through ROS production (Miao et al., 2010).

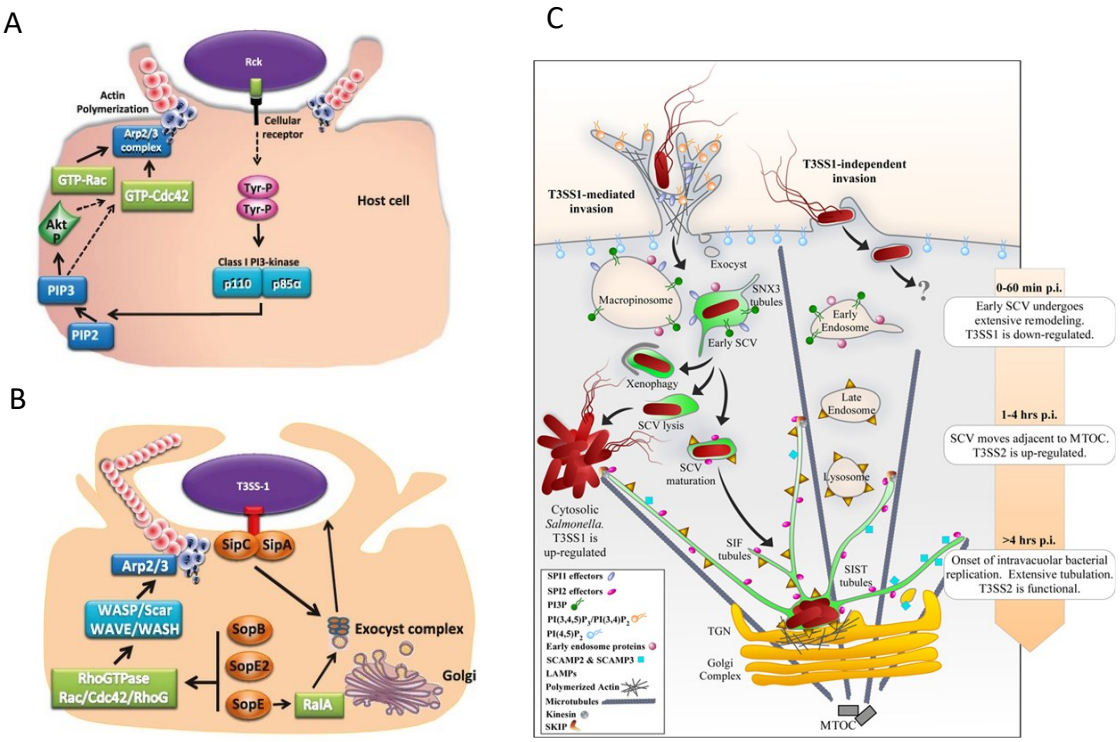

Figure 13. Strategies used by *Salmonella* to invade host cells and sustain intracellular replication. A) Zipper mechanism of *Salmonella* invasion. The receptor-driven entry of *Salmonella* into host cells activates different tyrosine kinases and the PI3K/AKT pathway. Then, small GTPases are activated and promote actin polymerisation by Arp2/3 to mediate bacterial engulfment. B) Trigger mechanism of *Salmonella* invasion. *Salmonella* injects bacterial effectors (SipA, SipC, SopB, SopE, SopE2) into the host cell cytoplasm. By different mechanisms, these effectors activate small GTPases and induce actin polymerisation at bacterial contact sites. The resulting membrane ruffling mediates *Salmonella* internalization. C) Intracellular fate of *Salmonella*. *Salmonella* can enter the host cell by T3SS-dependent or T3SS-independent pathways. Once internalised, *Salmonella* uses the T3SS-1 and T3SS-2 effector proteins to remodel the membrane of the vesicle and create the *Salmonella*-containing vacuole. Progressively, *Salmonella* acquires endosomal markers and migrates to a juxtanuclear position, where it encounters the necessary conditions to sustain replication. Bacterial replication occurs in *Salmonella*-induced filaments (SIFs). In some cases, *Salmonella* escapes from the SCV or is targeted by xenophagy. SNX3: sorting nexins; PI(3,4)P2: phosphatidylinositol (4,5)-bisphosphate; LAMPs: Lysosomal-associated membrane protein 1; MTOC: microtubule-organising centre. Figure adapted from (Velge et al., 2012) (A,B) and (Malik-Kale et al., 2011) (C).

4.2 *Escherichia coli*

Escherichia coli (*E. coli*) is a species of the *Escherichia* genus that belongs to the *Enterobacteriaceae* family (reviewed in Bhunia, 2018). *E. coli* is a Gram-negative rod-shaped bacterium that typically contains peritrichous flagella and fimbriae. It comprises diverse isolates that can be distinguished attending to the O antigen (somatic), H antigen (flagellar), or K antigen (capsular).

E. coli is a predominantly harmless bacterium that colonises the intestines of humans and animals early after birth, becoming part of the gut microbiota (reviewed in Bhunia, 2018). However, adapted pathogenic variants of *E. coli* have emerged by horizontal transfer of mobile genetic elements encoding virulence factors (reviewed in Croxen and Finlay, 2010). In contrast to commensal bacteria, *E. coli* pathovars often carry large virulence gene clusters, known as pathogenicity islands, in a plasmid or inserted into their chromosome. Pathogenic *E. coli* isolates share several virulence traits. For example, they modulate their internalisation by host cells using adhesins or proteins that manipulate signalling pathways. Besides, pathogenic *E. coli* strains often use strategies to evade host immune responses. Depending on the colonisation site, *E. coli* pathovars are divided into diarrhoeagenic or extraintestinal.

4.2.1 Enteroinvasive *E. coli*

Enteroinvasive *E. coli* (EIEC) is a gastroenteritis-causing isolate highly similar to *Shigella* (reviewed in Croxen and Finlay, 2010). Both EIEC and *Shigella* cause a disease that ranges from diarrhoea to severe bacillary dysentery. Their pathogenicity mechanisms are identical and are mediated by proteins encoded in the pINV plasmid. EIEC is a facultative intracellular pathogen (reviewed in Schroeder and Hilbi, 2008) that has unique features compared to other pathogenic *E. coli* isolates, as it does not express adherence factors or flagella. In addition, most of the EIEC serotypes are non-motile, although there are a few motile (for example, the O124:H30 serotype used in the present study) (Silva et al., 1980). The virulence factors of EIEC rely on a T3SS that mediates the invasion of host cells, bacterial survival, and the induction of macrophage apoptosis. After ingestion of contaminated food or water, EIEC traverses the epithelial barrier of the colon through transcytosis across intestinal M cells. Then, bacteria are taken up by macrophages and activate virulence factors to subvert the macrophage microbicidal activities. EIEC can escape from the phagosome and induce macrophage apoptosis. Concomitantly, it is released to the submucosa, where it invades colonocytes at the basolateral side. To enter colonocytes, EIEC uses invasion proteins that induce local actin reorganization. Afterwards, EIEC modulates signalling pathways, evades immune recognition, replicates in the host cell cytoplasm, and manipulates actin to be propelled for cell-to-cell dissemination.

4.2.2 Uropathogenic *E. coli*

Uropathogenic *E. coli* (UPEC) is the most common cause of community-acquired urinary tract infections (reviewed in Terlizzi et al., 2017). First, UPEC colonises the urethra, then, ascends to the bladder, and, finally, adheres to and invades epithelial cells. Within epithelial cells, UPEC can

establish intracellular bacterial communities that form reservoirs able to flux out to invade adjacent cells. To invade epithelial cells, UPEC uses fimbrial and non-fimbrial adhesins. For example, the fimbrial adhesin FimH induces Rho GTPase-dependent actin rearrangements in bladder epithelial cells. Other important virulence factors of UPEC include the polysaccharide capsule, flagella, outer membrane vesicles, OMPs, toxins, and iron acquisition systems. During infection, UPEC induces epithelial cell exfoliation and causes inflammation. The subsequent production of cytotoxic granules by the recruited neutrophils causes tissue damage.

4.3 *Listeria monocytogenes*

Listeria monocytogenes (*L. monocytogenes*) is a foodborne pathogen that causes gastroenteritis in healthy people, but can also originate a dangerous systemic disorder named Listeriosis in immunocompromised groups (reviewed in Bhunia, 2018). In pregnant women, infection by *Listeria* can cause abortion.

Listeria are Gram-positive, rod-shaped bacteria (reviewed in Bhunia, 2018). They contain peritrichous flagella, although their contribution to pathogenicity is unclear as their expression at body temperature (37°C) is low. Following ingestion of contaminated food, *Listeria* can traverse the intestinal epithelium passively through M cell- and dendritic cell-assisted pathways. Alternatively, these bacteria cross enterocytes by transcellular or paracellular pathways. To invade enterocytes, *L. monocytogenes* uses adhesion and invasion proteins that bind to surface receptors, initiating signalling cascades that promote local actin rearrangements and bacterial internalisation by host cells through a "zipper-like" entry. Important factors during adhesion and invasion include *Listeria* adhesion protein, internalin (Inl) A, InlB, and virulence invasion protein. Once inside the cell, *L. monocytogenes* escapes from the phagosome using a pore-forming haemolysin named Listeriolysin and a phosphatidylinositol-specific phospholipase that is transported by a type 2 secretion system known as Sec. In the cytoplasm, *Listeria* can access nutrients and replicate. Subsequently, the actin polymerisation protein (Act) A of *Listeria* recruits actin and drives actin polymerisation to mediate its cell-to-cell spread hidden from the extracellular defence mechanisms. The production of inflammatory mediators by enterocytes and resident immune cells in response to *Listeria* recruits more macrophages, dendritic cells, and neutrophils. The persistence of *Listeria* inside the cytoplasm of dendritic cells and macrophages facilitates systemic bacterial dissemination as they travel to the lymph nodes and other organs. Finally, the infection resolves mainly by the actions of cytotoxic T cells and macrophages.

4.4 *Staphylococcus aureus*

Staphylococcus aureus (*S. aureus*) is gaining attention because of the emergence of drug multiresistant strains that pose at risk the treatment of life-threatening infections (reviewed in Bhunia, 2018). Within the *Staphylococcus* genus, *S. aureus* is the most common disease-causing species in humans. It is an opportunistic bacterium that is present as commensal in human skin, nares, and respiratory and genital tracts. However, it can cause severe infections affecting many organs in susceptible populations.

S. aureus is a Gram-positive coccus-shaped bacterium that appears in clusters. Even though it is a non-motile bacterium, *S. aureus* contains virulence factors that promote infection, including adhesins, toxins, superantigens, pore-forming haemolysins, and proteases.

Table 1. Summary of the features of bacterial species used for our infection studies.

	Bacteria	Gram staining	Physical characteristics	Motility	Virulence factors	Disease	Host	Oxygen requirements	Life cycle
	***Salmonella enterica* serovar Typhimurium**	Gram-negative	• Peritrochous flagella, fimbriae • 1-2um, • Rod-shaped	Motile	T3SS, adhesins, OMPs	Gastroenteritis	Humans and other animals	Facultative anaerobe	Facultative intracellular
	Enteroinvasive *E. coli*	Gram-negative	• No flagella, no adherence factors • 1-2um • Rod-shaped	Majority non-motile. (Serotype O124:H30 motile)	T3SS	Diarrhoea, bacillary dysentery	Humans	Facultative anaerobe	Facultative intracellular
	**Uropathogenic *E. coli***	Gram-negative	• Peritrochous flagella, fimbriae • 1-2um • Rod-shaped	Motile	Adhesins, toxins	Cystitis, pyelonephritis, urosepsis syndrome	Humans	Facultative anaerobe	Facultative intracellular
	***Listeria monocytogenes***	Gram-positive	• Peritrichous flagella • 1-2um • Rod-shaped	Non-motile at 37ºC	Adhesins, invasins, Sec system, cell-to-cell spread	Diarrhoea, Listeriosis	Humans and ruminants	Facultative anaerobe	Facultative intracellular
	***Staphylococcus aureus***	Gram-positive	• 1um • Coccus	Non-motile	Adhesins, toxins (e.g., haemolysins), superantigens, proteases	Opportunistic (skin infections, endocarditis, osteomyelitis, toxic shock syndrome, sepsis, pneumonia)	Humans and other animals	Facultative anaerobe	Extracellular / facultative intracellular

5. Nuclear receptors

Nuclear receptors are a family of structurally conserved ligand-dependent transcription factors (reviewed in Glass and Ogawa, 2006). Their activity is controlled by hormones and other lipophilic molecules that drive adaptive responses to different physiological conditions. The structure of nuclear receptors is modular, consisting of an activation domain known as activation function 1, a DNA-binding domain, and a ligand-binding domain (Figure 14A). The ligand-binding domain contains an α-helical region known as activation function 2 (AF2), whose conformational changes modulate the interactions of nuclear receptors with transcriptional co-activators and co-repressors. To control transcription, LXRs bind to specific target sequences on DNA regulatory regions called response elements.

Nuclear receptors are divided into three categories: steroid and thyroid hormone receptors, orphan receptors, and adopted orphan receptors (reviewed in Glass and Ogawa, 2006). The first class of receptors includes the well-studied glucocorticoid- and oestrogen- receptors, as well as receptors for androgens, progesterone, and others. In contrast, orphan receptors have unknown physiological ligands. The discovery of physiological ligands for orphan receptors gave rise to the group of "adopted" orphan receptors. Among those, LXRs and PPARs have been characterised as important immunomodulators.

Liver X Receptors

Liver X Receptors are sterol sensors that control lipid and glucose metabolism, as well as innate and adaptive immune cell functions (reviewed in Schulman, 2017). They are activated by oxidised forms of cholesterol (e.g., 22(R)-, 24(S)-, 25-, and 27- hydroxycholesterol and 24(S)-, 25-epoxycholesterol) or the cholesterol precursor desmosterol. Highly specific synthetic LXR agonists have also been developed, such as T0901317 (T1317) and GW3965. The genes NR1H3 and NR1H2 encode two LXR isoforms, LXRα and LXRβ, respectively. While LXRβ is ubiquitously expressed in the body, LXRα is restricted to the tissues with high metabolic activity, i.e., the intestines, the liver, adipose tissue, adrenals, the kidney, and myeloid hematopoietic cells. The two LXR isoforms exert either overlapping or selective activities on gene expression (Ramon-Vazquez et al., 2019).

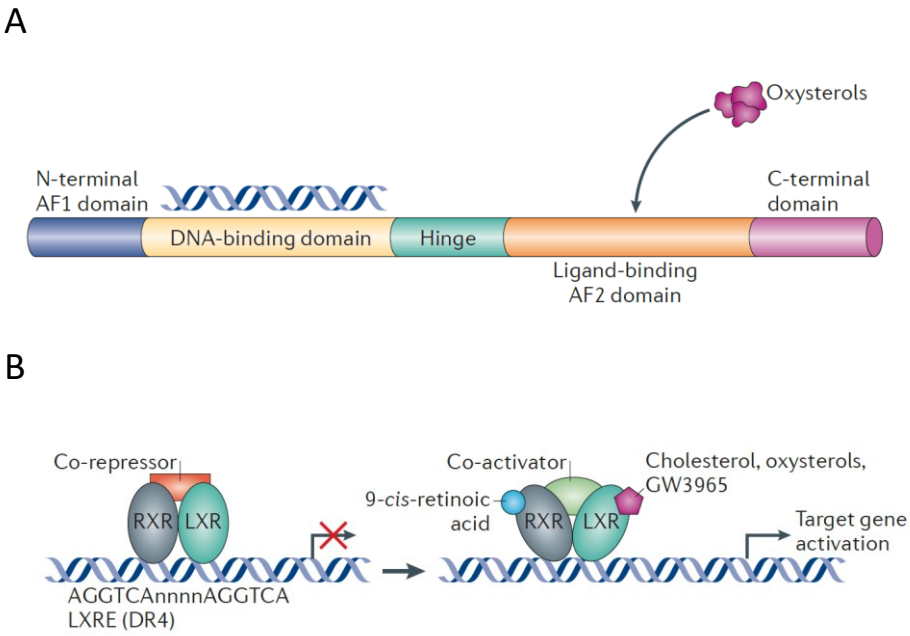

Figure 14. Secondary structure of LXRs and mechanism for ligand-dependent transcriptional activation. A) Secondary structure of LXRs. B) Ligand-dependent transcriptional activation by LXRs. In the absence of an LXR ligand, the RXR-LXR heterodimer is bound to the LXRE on target genes and represses gene expression. Upon ligand binding to any of the receptors, they undergo a conformational change that releases co-repressors and recruits co-activators to induce transcription. Figure adapted from (Calkin and Tontonoz, 2012).

To positively control transcription, LXRs form heterodimers with another nuclear receptor, the retinoid X receptor (RXR) (reviewed in Calkin and Tontonoz, 2012). The RXR-LXR heterodimer binds to LXR response elements (LXRE) on DNA, commonly composed of two direct repeat AGGTCA motifs separated by 4 nucleotides (Figure 14 B). Through different mechanisms, LXRs can positively or negatively modulate gene expression. In the absence of ligand, DNA-bound RXR-LXR dimers interact with co-repressors, mainly with nuclear receptor co-repressor (NCoR) and silencing mediator of retinoic acid and thyroid hormone receptor (SMRT), and repress gene transcription (Hu et al., 2003). In transgenic models, LXR-deficient cells express higher levels of some LXR target genes than their wild-type counterparts due to the release of basal repression, which is called de-repression (Wagner et al., 2003). The binding of an agonistic ligand to the ligand-binding domain of LXRs induces a conformational change in AF2 that promotes co-repressor release and attracts co-activators to induce gene transcription (Malini et al., 2008; Perissi et al., 2004; Svensson et al., 2003).

LXRs can also repress the expression following ligand binding. Several mechanisms have been proposed to explain this action, including transrepression, which is the repression of the activity of other transcription factors without direct binding of the nuclear receptor to DNA (Blaschke et al., 2006; Ghisletti et al., 2009; Ghisletti et al., 2007). Ligand-dependent transrepression has

been explored predominantly in macrophages because of its inhibitory effects on inflammatory stimulus-activated transcription factors such as NF-κB, STAT-1, and AP1 (reviewed in Glaría et al., 2020). To exert transrepression, LXRs undergo conjugation to small ubiquitin-related modifier (SUMO) and prevent co-repressor release from inflammatory gene promoters (Ghisletti et al., 2007; Lee et al., 2009; Nunomura et al., 2015; Venteclef et al., 2010).

LXRs regulate cholesterol, fatty acid, and glucose metabolism (Figure 15). To maintain systemic cholesterol homeostasis, LXRs control the expression of genes that modulate cholesterol absorption, excretion, efflux, transport, and conversion to bile acids in the liver (reviewed in Wang and Tontonoz, 2018). They promote reverse cholesterol transport from peripheral tissues to the liver by activating the transcription of various target genes. On the one hand, LXRs induce the expression of the ATP-binding cassette transporters (ABC) A1 (ABCA1) and G1 (ABCG1), which promote cholesterol efflux from peripheral cells such as macrophages. ABCA1 is located at the plasma membrane and exports cellular cholesterol and phospholipids to apolipoprotein (APO) A1 (APOA1) to form nascent high-density lipoproteins (HDL) in the plasma (Lee and Parks, 2005; Oram et al., 2000; Smith et al., 2004). It has recently been suggested that ABCA1 might access laterally transmembrane lipids for their export (Qian et al., 2017). In contrast, ABCG1 localises to endosomal membranes and stimulates cholesterol transport away from the endoplasmic reticulum (Tarling and Edwards, 2011). LXRs also induce the expression of different types of APOs, including APOE, which can be secreted by cells such as macrophages and facilitates cholesterol efflux (reviewed in Calkin and Tontonoz, 2012; Curtiss and Boisvert, 2000; Langer et al., 2000; Mazzone, 1996; Zhang et al., 1996). On the other hand, LXR activation inhibits the uptake of low-density lipoprotein (LDL) and very LDL (VLDL) by peripheral cells through augmented expression of the inducible degrader of LDL receptor (IDOL), thereby reducing cholesterol uptake by the cells (Zelcer et al., 2009). Additionally, LXRs increase ABCG5 and ABCG8 expression in the liver and the intestine, leading to cholesterol excretion and inhibition of dietary cholesterol absorption (reviewed in Wang and Tontonoz, 2018).

LXRs control fatty acid metabolism by directly binding to regulatory regions on lipogenic target genes or by inducing the expression of transcription factors that promote lipogenesis, namely, the sterol regulatory element-binding protein 1c (SREBP1c) and carbohydrate-responsive element-binding protein (ChREBP) (Cha and Repa, 2007; Repa et al., 2000a; reviewed in Wang and Tontonoz, 2018). Both SREBP1c and ChREBP promote the synthesis of fatty acids and triglycerides by transcriptional activation of genes such as acetyl coenzyme A carboxylase (ACC),

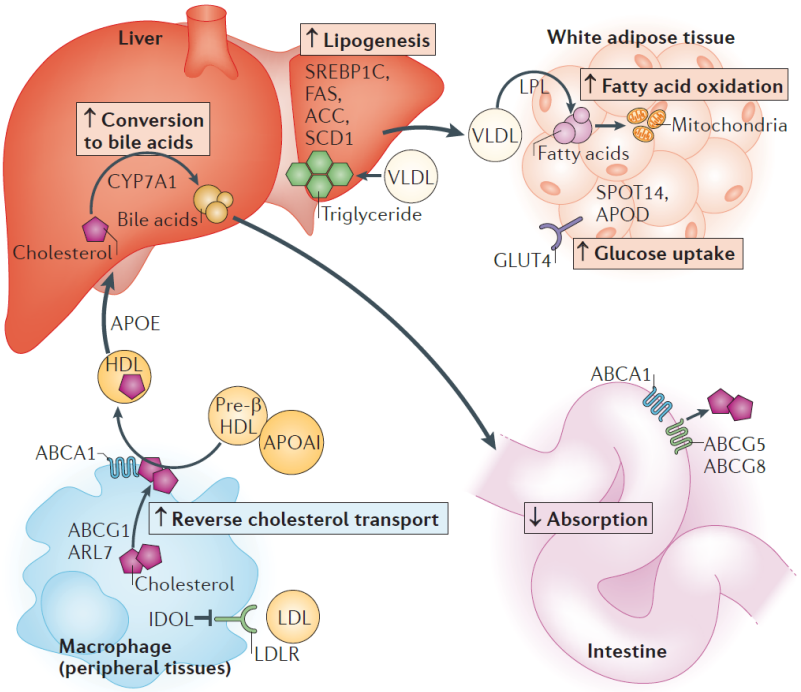

Figure 15. Metabolic activities of LXRs. In peripheral cells such as macrophages, LXRs stimulate cholesterol efflux and inhibit cholesterol uptake. As a result, the cholesterol transport to the liver by plasma HDL particles increases. In the liver, LXR promotes fatty acid synthesis and cholesterol conversion to bile acids. Then, the liver secretes triglycerides through VLDLs that reach peripheral tissues. The white adipose tissue captures fatty acids from VLDL and breaks them down through their β-oxidation stimulated by LXRs. LXR also promotes glucose uptake by adipocytes. ABC: ATP-binding cassette transporter; APO: apolipoprotein; ARL7: ADP-ribosylation factor-like 7 CYP7A1, LPL: lipoprotein lipase; SPOT14: thyroid hormone-responsive cytochrome P450 7A1. Figure adapted from (Calkin and Tontonoz, 2012).

stearoyl coenzyme A desaturase (SCD) 1, and fatty acid synthase (FASN) (reviewed in Wang et al., 2015). SREBP1c remains inactive in the membrane of the endoplasmic reticulum during normal cholesterol levels (reviewed in Goldstein et al., 2006). Upon cholesterol shortage, it is transported to the Golgi, where it undergoes proteolysis and is released from the membrane as an active transcription factor that will translocate to the nucleus. The transcription factor ChREBP is activated in response to elevated serum glucose levels through dephosphorylation mediated by the protein phosphatase 2. In addition to promoting lipogenesis, ChREBP induces the expression of genes involved in glucose metabolism such as liver pyruvate kinase, glucose-6-phosphate dehydrogenase, 6-phosphogluconate dehydrogenase, and the glucose transporter type 4 (GLUT4). LXRs can also directly activate the transcription of GLUT4, which is an insulin-stimulated glucose transporter that mediates glucose uptake by the adipose tissue and skeletal muscle (reviewed in Calkin and Tontonoz, 2012). Therefore, LXRs lower the cholesterol levels and promote glucose tolerance, facts that convert them into potentially powerful therapeutic targets for metabolic disorders (reviewed in Hong and Tontonoz, 2014). Besides, LXRs modulate the phospholipid composition of cell membranes through the induction of the target gene

lysophosphatidylcholine acyltransferase 3 (LPCAT3). LPCAT3 promotes the incorporation of polyunsaturated fatty acids into phospholipids, and the resulting changes in the membrane phospholipid composition confer protection against lipid stress (Demeure et al., 2011; Ishibashi et al., 2013; Rong et al., 2013).

Beyond metabolic regulation, LXRs exert immunomodulatory functions that contribute to the proper control of inflammatory responses (reviewed in Glaría et al., 2020). Remarkably, the expression of LXRs maintains a controlled anti-inflammatory state that preserves tissue homeostasis (Gonzalez et al., 2009). Macrophages initiate apoptotic cell clearance through signalling by MER tyrosine kinase (MERTK), a surface receptor that drives phagocytosis of apoptotic bodies (efferocytosis) (Rothlin et al., 2015). This event activates LXRs, which, in turn, increase the expression of MERTK, inhibit the synthesis of inflammatory mediators, and promote cholesterol efflux probably to compensate for the excess in the incorporation of lipids (Gonzalez et al., 2009).

LXR activation counter-regulates inflammatory gene expression stimulated by both TLR3/4 ligands and endogenous inflammatory cytokines (e.g., TNFα, IL1β, and IFNγ) in macrophages (Endo-Umeda et al., 2018; Ghisletti et al., 2007; Ito et al., 2015a; Joseph et al., 2003; Lee et al., 2009; Pascual-Garcia et al., 2013). One of the mechanisms mediating these effects is transrepression of inflammatory genes such as inducible nitric oxide synthase (iNOS), cyclooxygenase 2 (COX2), IL6, IL1β, and some chemokines (Figure 16). In addition, LXRs induce the expression of target genes that interfere with inflammation. For instance, ABCA1 causes plasma membrane alterations that impair inflammatory signalling downstream of TLRs (Ito et al., 2015a). More precisely, cholesterol efflux promoted by ABCA1 disturbs the organization of membrane microdomains that act as signalling platforms for TLRs. Those microdomains known as lipid rafts are dynamic assemblies of cholesterol, sphingolipids, and proteins that among other functions, modulate intracellular signalling in immune cells (Varshney et al., 2016). As a result of ABCA1-induced membrane modifications, the recruitment of TRAF6 and MyD88 to TLRs on lipid rafts is impaired and leads to lower MAPK and NF-kB activation. LXRs indirectly reduce inflammation-promoting polyunsaturated fatty acid synthesis through induction of the transcription factor SREBP1c and other lipogenic enzymes (Spann et al., 2012). Besides, LXRs increase IRF8 expression, which acts at various levels to inhibit the production and maturation of the cytokine IL18 (Pourcet et al., 2016). Complementarily, LXRs promote cell survival by inversely modulating anti- and pro-apoptotic genes (Joseph et al., 2004; Valledor et al., 2004). An important LXR target in that context is the CD5 molecule-like (CD5L) (also known as apoptosis

inhibitor of macrophages, AIM). CD5L is a scavenger receptor induced by LXRs that promotes cell survival (reviewed in Sanjurjo et al., 2015). Additionally, CD5L promotes an anti-inflammatory profile in macrophages and contributes to the resolution of inflammation. In conclusion, LXRs inhibit inflammation by multiple mechanisms. Reciprocally, IFNγ- and TLR3/4 ligands inhibit the ability of activated LXRs to induce the expression of target genes involved in metabolic homeostasis (Castrillo et al., 2003; Han et al., 2018; Pascual-Garcia et al., 2013).

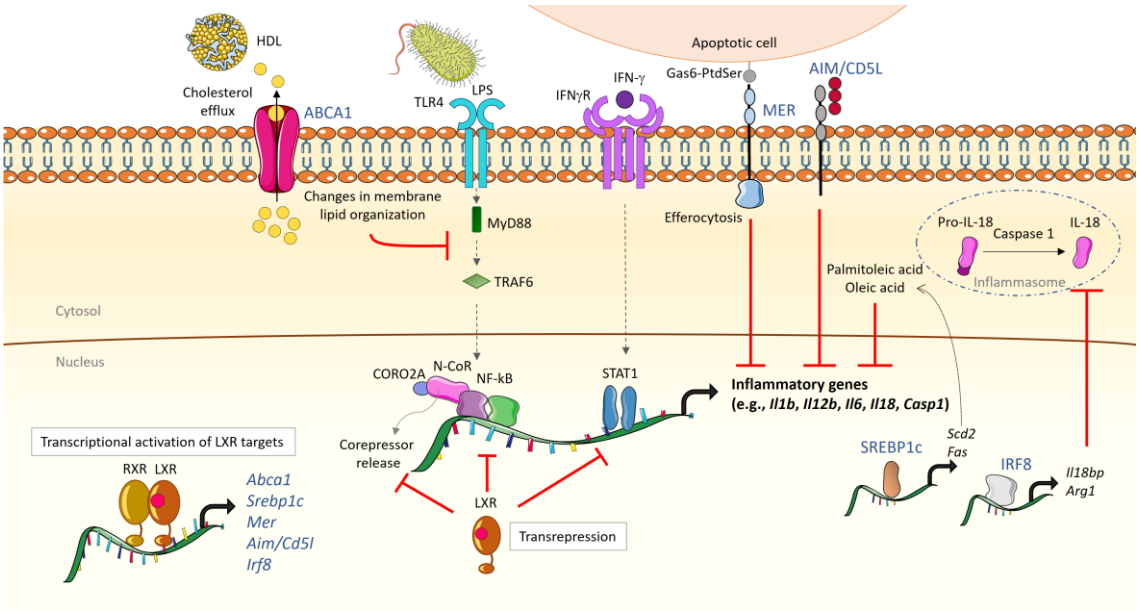

Figure 16. LXRs inhibit the inflammatory response in macrophages through multiple mechanisms. TLR signalling or IFNγ stimulation induce inflammatory gene expression. Agonist-bound LXRs mediate mechanisms of transrepression, which interfere with the release of corepressors or with the activity/recruitment of transcription factors (NF-κB, STAT1) required for inflammatory gene expression. In addition, LXRs inhibit inflammation indirectly through the transcriptional activation of LXR targets (in blue) involved in the modulation of metabolic and/or immune responses. The cholesterol efflux mediated by ABCA1 results in changes in the lipid composition of the membrane, which interferes with TLR signaling. SREBP1c induces the expression of enzymes involved in the generation of lipids with anti-inflammatory properties. MER couples efferocytosis (apoptotic cell phagocytosis) with the suppression of the inflammatory response. CD5L enhances the expression of molecules involved in the resolution of inflammation and promotes an anti-inflammatory profile. IRF8 induces the expression of IL18BP, which binds to secreted IL18 and inhibits its biological actions. Casp1: caspase 1. Figure obtained from (Glaría et al., 2020).

As mentioned in previous sections, some pathogens have developed strategies to escape from host defences (reviewed in: Hajishengallis and Lambris, 2011; Mitchell et al., 2016; Sarantis and Grinstein, 2012). Remarkably, both immune and metabolic pathways are targeted by different pathogens to establish successful infection (reviewed in: Glaría et al., 2020; Samanta et al., 2017). In line with this, pharmacological activation of LXRs impacts several bacterial, viral, and protozoan infections (Figure 17). LXR activation increases macrophage survival to infection by S. Typhimurium, L. monocytogenes, Bacillus anthracis, and E. coli (Joseph et al., 2004; Valledor et

al., 2004). In vivo, an LXR agonist reduces the bacterial burden of L. monocytogenes and Mycobacterium tuberculosis (M. tuberculosis) (Joseph et al., 2004; Korf et al., 2009). Moreover, LXR activation in macrophages infected by M. tuberculosis potentiates the synthesis of antimicrobial peptides (Ahsan et al., 2018). On the other hand, LXR activation impairs the entry of HIV, hepatitis C virus, and Newcastle disease virus into target cells through ABCA1-dependent mechanisms (Bocchetta et al., 2014; Hanley et al., 2010; Jiang et al., 2012; Morrow et al., 2010; Mujawar et al., 2006; Ramezani et al., 2015; Sheng et al., 2016). In contrast with the positive impact of LXRs in the previous settings, the activation of LXRs is detrimental for the resolution of Leishmania chagasi/infantum and Klebsiella pneumoniae infections due to a weakened inflammatory response or altered neutrophil infiltration to the inflammation site, respectively (Bruhn et al., 2010; Smoak et al., 2008).

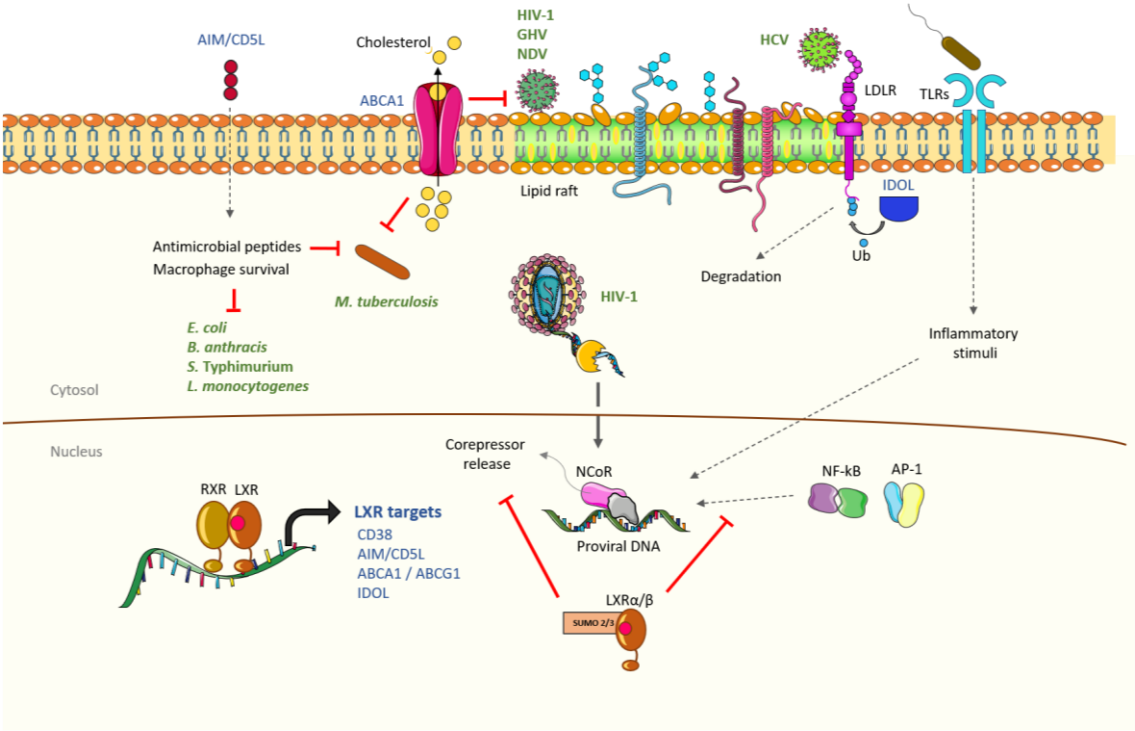

Figure 17. LXR activation induces protective mechanisms that limit viral and bacterial infection. LXR agonists upregulate the expression of LXR targets (in blue) that contribute in reducing the infection by several pathogens (names of pathogens in green). AIM/CD5L confers resistance to apoptosis and induces the synthesis of antimicrobial peptides. ABCA1 promotes cholesterol efflux. Consequently, the reduced intracellular cholesterol limits the growth of mycobacteria and, potentially, other bacterial strains that depend on intracellular cholesterol. In addition, changes in the cholesterol levels within lipid rafts may interfere with the entry of several viruses into host cells. IDOL, by virtue of its role in controlling the turnover of the LDLR, inhibits the capability of HCV to infect host cells. LXRs can also affect the intracellular replication of HIV-1 through mechanisms of transrepression, which affect corepressor release or transcription factor recruitment to the proviral DNA. Ub, ubiquitin: LDLR: LDL receptor. Figure adapted from (Glaría et al., 2020).

We identified CD38 as a new LXR target gene involved in the modulation of *Salmonella* infection in murine macrophages (Matalonga et al., 2017). The discovery revealed a previously unappreciated antibacterial circuit by which LXRs might protect from infection (Figure 18). Later studies corroborated the transcriptional control of CD38 by LXRs in dendritic cells, in which LXR-induced CD38 expression enhanced chemotaxis (Beceiro et al., 2018).

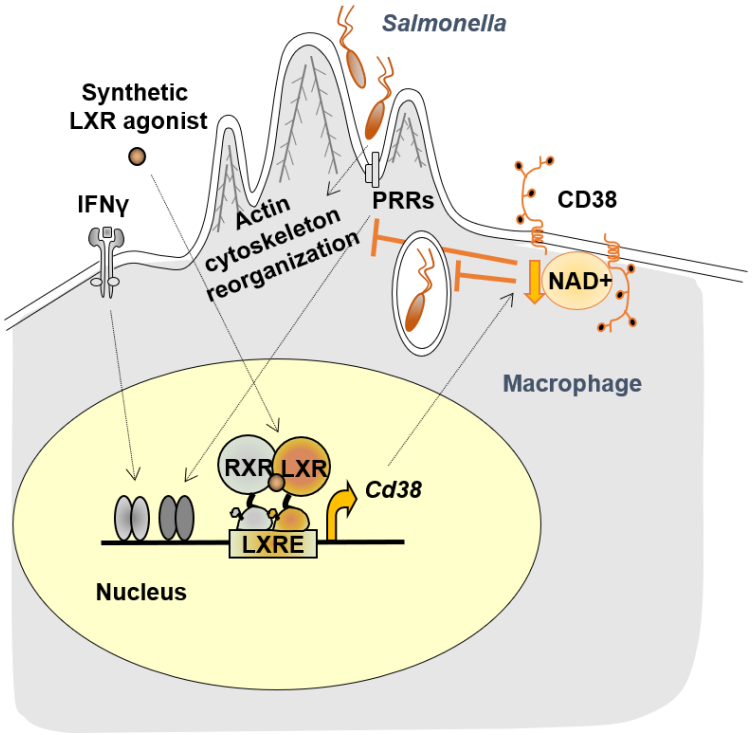

Figure 18. Working model. LXR activation limits macrophage infection by *Salmonella* through the transcriptional activation of CD38. Activation of LXRs by synthetic agonists increases the expression of CD38 and reduces the intracellular NAD+ levels. As a result, LXR-CD38 axis prevents the cytoskeletal changes associated with infection and limits bacterial entry into macrophages. Additionally, LXRs cooperate with inflammatory stimuli such as IFNγ or LPS to induce a stronger transcriptional activation of CD38 expression. Figure adapted from (Matalonga et al., 2017).

The activation of LXRs in macrophages increased the expression of the multifunctional protein CD38 and potentiated the intracellular NAD^+ glycohydrolase enzymatic activity in a CD38-dependent manner. As a result, macrophages exposed to *Salmonella* Typhimurium and treated with a synthetic LXR agonist failed to acquire the characteristic pancake-like morphology associated with bacterial infection. Specifically, LXR-induced CD38 expression and low NAD^+ levels reduced the dorsal F-actin in macrophages exposed to *Salmonella* and impaired the internalisation of non-opsonised bacteria. The products of the NAD^+ glycohydrolase activity of CD38 at neutral pH are calcium-mobilizing second messengers, namely ADPR, cADPR, and nicotinamide. Despite the fact that the production of these second messengers by CD38 may

have a physiological impact, this study suggested that the drop in intracellular NAD^+ as a consequence of consumption by CD38, rather than its enzymatic products mediated the inhibitory effects of LXRs on infection.

Going deeper into the mechanisms of LXR-mediated transcriptional control of *Cd38*, the study found an enhancer region containing an LXRE 2Kb upstream of the gene encoding for CD38 that was responsive to RXR-LXR agonists. Additionally, the activation of LXRs cooperated synergistically with LPS or the endogenous cytokines TNFα and IFNγ to induce transcriptional *Cd38* expression. Such collaborative action of LXRs and inflammatory mediators on *Cd38* expression contrast with the generalised reciprocal negative regulation of these pathways. These findings suggest that CD38 accomplishes relevant immune functions in contexts in which LXRs are activated, representing a potential point of convergence between immune and metabolic signals.

HYPOTHESIS

Based on the anti-inflammatory effects that LXR agonists exert in different models of inflammation and infection, initial predictions anticipated that LXR activation could impair the capability of immune cells to establish an aggressive response against pathogens. However, *in vivo* studies have shown increased susceptibility of LXR-deficient mice to infection by some bacterial species (Joseph et al., 2004; Korf et al., 2009). In addition, previous studies from our group indicated that LXR activation limits the infection of host macrophages by *Salmonella* Typhimurium. Based on these observations, we hypothesize that LXRs might modulate the interaction between host cells and different bacterial species in mice and humans. Therefore, in this work we have further investigated the consequences of LXR activation on the severity of the infection by *Salmonella* Typhimurium *in vivo* and we have analysed the impact of the LXR pathway—and the relevance of potential underlying mechanisms—on macrophage infection by different bacterial species in murine and human macrophages.

OBJECTIVES

1) To identify the transcriptional mechanisms by which LXRs and inflammatory stimuli control *Cd38* expression in murine macrophages.

2) To extend the knowledge of the scope of LXR-mediated antibacterial effects in mice:

    1.1) To determine the effect of pharmacological LXR activation on *S*. Typhimurium infection in vivo.

    1.2) To increase our understanding of the molecular mechanisms underlying LXR-induced limitation of *Salmonella* infection in macrophages.

    1.3) To elucidate the spectrum of bacteria that are susceptible to LXR-mediated inhibition of infection.

3) To define the impact of LXR activation in early events of bacterial infection in human macrophages.

MATERIALS AND METHODS

Reagents

A comprehensive list of the main reagents used in the present thesis is shown in Table 2.

Table 2. Laboratory products used in the studies of the present thesis.

Product	Manufacturer	Catalog number
Cell culture		
Accutase® solution	Sigma-Aldrich	A6964
Fetal Bovine Serum	Sigma-Aldrich	F7524
Ficoll-Paque™ PLUS	Cytiva	17-1440-02
Gentamicin sulfate salt	Sigma-Aldrich	G1264
Human Serum AB male HIV tested	biowest	S4190
HyClone Dulbecco's Modified Eagle Medium (DMEM) with high glucose	Cytiva	SH30022.01
HyClone RPMI 1640 media, with L-glutamine	Cytiva	SH30027.01
Phosphate Buffered Saline (PBS)	Cytiva	SH30028,02
Penicillin-Streptomycin	Sigma-Aldrich	P4333
Red blood cell lysing buffer 10X BD Pharm Lyse	BD Biosciencies	555899
Cytokines, growth factors and inflammatory mediators		
Lipopolysaccharides from E. Coli 0127:B8	Sigma-Aldrich	L3129
Phorbol 12-myristate 13-acetate (PMA)	Sigma-Aldrich	P8139
Recombinant Human M-CSF	Peprotech	300-25
Recombinant Murine IFN-γ	Peprotech	315-05
Recombinant Murine TNF-α	Peprotech	315-01A
Nuclear receptor agonists		
GW 3965 hydrochloride	Tocris bioscience	2474
LG268	URSA-PCB (IRBBarcelona)	-
T0901317 (T1317)	Cayman Chemical	71810
Stainings		
Alexa Fluor™ 488 Phalloidin	Thermo Fisher Scientific	A12379
bisBenzimide H 33342 trihydrochloride (Hoechst 33342)	Sigma-Aldrich	14533
Cholera Toxin Subunit B CF® 633 Dye Conjugate	biotium	00077
Crystal Violet	Sigma-Aldrich	C3886
Filipin complex, from *Streptomyces filipinensis*	Sigma-Aldrich	F9765
Fluorescein 5 (6)- isothiocyanate (FITC)	Sigma-Aldrich	F3651
Wheat Germ Agglutinin, Alexa Fluor™ 488 Conjugate	ThermoFisher	W11261
Wheat Germ Agglutinin, Alexa Fluor™ 555 Conjugate	Thermo Fisher Scientific	W32464
LIVE/DEAD Fixable Near-IR Dead Cell Stain Kit, for 633 or 635 nm	Thermo Fisher Scientific	L34975

Product	Manufacturer	Catalog number
cDNA synthesis and qPCR		
M-MLV Reverse Transcriptase, RNase H Minus, Point Mutant	Promega	M3682
oligo(dT)$_{15}$	Sigma-Aldrich	-
***Power* SYBR™ Green PCR Master Mix**	Applied Biosystems	4367659
PCR nucleotide mix (dATP, dCTP, dGTP, dTTP)	Promega	U1420
Western Blot		
Bio-Rad Protein Assay Dye Reagent Concentrate	Bio-Rad Laboratories	5000006
Clarity™ Western ECL Substrate	Bio-Rad Laboratories	1705060
Intercept® (TBS) Protein-Free Blocking Buffer	LI-COR	927-80001
UltraCruz® Protease Inhibitor Cocktail	Santa Cruz Biotechnology	sc-29130
Revert™ 700 Total Protein Stain for Western Blot Normalization	LI-COR	926-11011
Antibodies		
Akt1/2 antibody (N-19) (discontinued)	Santa Cruz Biotechnology	sc-1619
Anti-AKT1 (phospho S473) antibody	abcam	ab8932
Monoclonal anti-β-Actin antibody produced in mouse	Sigma-Aldrich	A5441
β-Tubulin antibody	Cell Signaling	2146
Purified rat anti-Mouse CD16/CD32 (Mouse BD Fc Block™)	BD Biosciences	553141
CD38 antibody (M-19) (discontinued)	Santa Cruz Biotechnology	sc-7049
C/EBP β antibody (C-19) (discontinued)	Santa Cruz Biotechnology	sc-150
ERK 2 antibody (D-2)	Santa Cruz Biotechnology	sc-1647
Phospho-p44/42 MAPK (Erk1/2) (Thr202/Tyr204) (D13.14.4E) XP® rabbit mAb	Cell Signaling	4370
FITC Rat anti-mouse CD38	BD Biosciences	558813
JNK1/3 antibody (C-17) (discontinued)	Santa Cruz Biotechnology	sc-474
Purified mouse anti-JNK/SAPK (pT183/pY185)	BD Biosciences	612541
p38 alpha/beta MAPK antibody (A-12)	Santa Cruz Biotechnology	sc-7972
Phospho-p38 MAPK (Thr180/Tyr182) antibody	Cell Signaling	9211s
Others		
Cholesterol-Water Soluble (Cholesterol–methyl-β-cyclodextrin)	Sigma-Aldrich	C4951
Firefly & Renilla Luciferase Single Tube Assay Kit	biotium	30081
Fluoresbrite® YG Microspheres 3.00µm	Polysciences	17155-2
Latrunculin A	Enzo	BML-T119
Methyl-β-cyclodextrin	Sigma-Aldrich	C4555
RhoA / Rac1 / Cdc42 G-LISA Activation Assay Bundle 3 Kits	Cytoskeleton	BK135 (BK124-S + BK127-S + BK128-S)
SuperFect Transfection Reagent	QIAGEN	301307

Animals

C57BL/6 mice were purchased from Harlan. For the *in vivo* infection study female adult mice were used, whereas either male or female mice were used as a source of bone-marrow derived macrophages for *in vitro* studies. LXRα-, LXRβ-, and LXRα/β-deficient mice were initially donated by Dr. David Mangelsdorf (UT Southwestern Medical Center, Dallas, TX)(Peet et al., 1998; Repa et al., 2000a) and backcrossed into C57BL/6 background for more than ten generations. These mice were raised as a colony in our animal facility under specific pathogen-free (SPF) conditions. STAT1-deficient mice were donated by Dr. Anna Planas (IDIBAPS, Barcelona, Spain) (Gorina et al., 2011) and raised as a colony under non-SPF conditions. CD38-deficient mice were raised as a colony under non-SPF conditions as part of a collaboration with Dr. Jaime Sancho (IPBLN-CSIC, Granada, Spain) (Cockayne et al., 1998). All the mice raised by our group were fed a regular chow diet and the protocols requiring animal manipulation have been approved by the Institutional Animal Care and Use Committees from the *Parc Científic de Barcelona* or *Universitat de Barcelona*. We obtained bone marrows from mice with myeloid C/EBPβ deficiency (LysMCre-C/EBP$\beta^{fl/fl}$) generated by Dr. Josep Saura (*Universitat de Barcelona* -IDIBAPS, Barcelona, Spain) (Pulido-Salgado et al., 2017). Bone marrows from CD38 catalytically-inactive (CI) "knock-in" mice were obtained in a collaboration with Dr. Eduardo N. Chini (Mayo Clinic College of Medicine, Rochester, USA) (Tarragó et al., 2018). Bone marrows from mice deficient for JNK1 or JNK2 were obtained from Dr. Carme Auladell (*Universitat de Barcelona*, Barcelona, Spain) (Dong et al., 1998; Yang et al., 1998). Bone marrows from IRF1-deficient mice were obtained from Dr. Lionel Apetoh (INSERM, Dijon, France) (Vegran et al., 2014).

Cell cultures

- **Murine bone marrow-derived macrophages**. Bone marrow-derived macrophages (BMDM) were obtained from femurs and tibiae of mice as described (Valledor et al., 2000). Bone marrow precursors were differentiated in Dulbecco's Modified Eagle Medium (DMEM) (Cytiva) supplemented with 20% heat-inactivated fetal bovine serum (FBS) and 30% L-cell conditioned medium as a source of M-CSF. After 6-9 days, macrophages were plated for subsequent experiments in DMEM supplemented with 10% heat-inactivated FBS.

- **RAW 264.7 murine macrophages** (ATCC TIB-71). Cultured in DMEM supplemented with 10% heat-inactivated FBS and 1% penicillin-streptomycin at 37°C, 5% CO_2.

- **COS-7 monkey fibroblast-like cells** (ATCC CRL-1651). Cultured in DMEM supplemented with 10% heat-inactivated FBS and 1% penicillin-streptomycin at 37°C, 5% CO_2.

- **L929 murine fibroblasts** (ATCC CCL-1). Cultured in DMEM supplemented with 10% heat-inactivated FBS at 37°C, 5% CO_2. After one week of cell culture, the supernatant containing M-CSF (L-cell) was collected and frozen in aliquots.

- **THP-1 human monocytes** (ATCC TIB-202) (donated by Dr. Maria Rosa Sarrias, IGTP, Barcelona, Spain). Cultured in Roswell Park Memorial Institute (RPMI)-1640 with 10% heat-inactivated FBS and 1% penicillin-streptomycin at 37°C, 5% CO_2. THP-1 monocytes were differentiated to macrophages by incubating them with 10 ng/ml of phorbol myristate acetate (PMA) for 96 h.

- **Primary human macrophages**. A fraction of leukocytes that had been separated from peripheral blood was obtained from healthy donors at the Blood and Tissue Bank (*Generalitat de Catalunya*). Peripheral blood mononuclear cells (PBMCs) were isolated by a Ficoll density gradient centrifugation and were subsequently washed 3 times with PBS. Erythrocytes were lysed for 10 min at room temperature. The cells were plated ($15x10^6$ cells/ml) in RPMI supplemented with 10% heat-inactivated human serum and incubated for 30 min at 37°C, 5% CO_2. Then, unadhered cells were eliminated by two washes with PBS and the monocytes that remained adhered to the plate were cultured for 6 days in RPMI with 10% heat-inactivated FBS and 50ng/ml recombinant human M-CSF. The culture medium was replaced after 3 days in culture. Once differentiated, the macrophages were either used directly (for RNA experiments) or detached in accutase for 45 min at 37°C and re-plated at the desired confluence (for infection studies). The culture medium of differentiated macrophages was not supplemented with M-CSF.

  Alternatively, primary human macrophages were obtained by a different protocol during a stay in the laboratory of Dr. Stefan Linder (Institute for Medical Microbiology, Virology and Hygiene, University Medical Center Eppendorf, Hamburg, Germany). This protocol has been previously described (Naj et al., 2013). The most remarkable differences from the protocol used by our group (described above) are that the monocytes from buffy coats are selected using magnetic beads coupled to anti-CD14 antibodies and that monocyte differentiation to macrophages is carried out in culture medium supplemented with 20% autologous human serum in the absence of exogenous recombinant M-CSF.

In vitro treatments

In most experiments, macrophages were treated with vehicle (dimethyl sulfoxide, DMSO), an LXR agonist (T1317 or GW3965) and/or an RXR agonist (LG268) at 1μM in culture medium complemented with 10% heat-inactivated FBS for different periods.

In studies on gene and protein expression induced by inflammatory signals, BMDMs were stimulated with IFNγ (5ng/ml), TNFα (20ng/ml) or LPS (100ng/ml) in DMEM-10% heat-inactivated FBS for different periods.

To deplete membrane cholesterol, the cells were incubated in non-supplemented culture medium (DMEM or RPMI, without FBS) in the presence of methyl-β-cyclodextrin (MβCD) (Sigma) (0.1-10mM, 1 h). To overload the cells with cholesterol, macrophages were incubated in non-supplemented culture medium in the presence of cholesterol-complexed MβCD (Chol-MβCD) (Sigma) (100μM, 2 h). Immediately after the incubation with either of these compounds, macrophages were washed with PBS and exposed to bacteria in non-supplemented culture medium (in MβCD-treated cells) or culture medium supplemented with 1% FBS (in Chol-MβCD-treated cells).

Bacterial strains and growth conditions

The following bacterial strains were used in these studies: *Salmonella enterica* serovar Typhimurium (*S.* Typhimurium) strain SV5015 (obtained from Dr. Antonio Juárez, *Universitat de Barcelona*, Barcelona, Spain) (*in vivo* study), *S.* Typhimurium strain SL1344 WT and invG (donated by Michael Hënsel, *Universität Osnabrück*, Osnabrück, Germany) (*in vitro* experiments), *Listeria monocytogenes* strain EDG-e (donated by Dr. Antonio Juárez, *Universitat de Barcelona*, Barcelona, Spain), enteroinvasive *E. coli* strain 0124:H30 (Dr. A. Juárez), *Staphylococcus aureus* subsp. *aureus* strain Rosenbach 1884 (Dr. A. Juárez), uropathogenic *E. coli* strain J96 (donated by Dr. Carlos Balsalobre, *Universitat de Barcelona*, Barcelona, Spain).

Gram-negative bacteria were transformed with a plasmid encoding red fluorescent protein (RFP) that also conferred resistance to ampicillin (pBR.RFP.1 plasmid) (Birmingham et al., 2006). For infection studies, bacteria were inoculated in 2xYT medium and grown overnight at 37°C and under agitation at 180 rpm (2xYT was supplemented with 100μg/ml ampicillin for the growth of transformed bacteria). Then, the bacterial culture was diluted 1:100 in 2xYT (± ampicillin) and bacteria were grown in the previously specified conditions until they reached the exponential

phase of growth (4 h approximately). The optical density of the culture was measured at 600 nm and the bacterial concentration was estimated based on a standard formula (Glaría et al., 2019). In experiments with Gram-positive bacteria, these bacteria were stained with 0.01% fluorescein isothiocyanate (FITC) in Na_2CO_3-$NaHCO_3$ buffer ($4x10^7$ CFU/ml) for 1 h at room temperature with agitation at about 50 rpm. The stained Gram-positive bacteria were washed three times with PBS before their use for infection.

In experiments of infection *in vivo*, *S.* Typhimurium was grown for 16 h in 2xYT supplemented with 100µg/ml ampicillin.

Infection and phagocytosis assays *in vitro*

Bacteria at the exponential phase of growth were added to macrophage cultures at the following multiplicity of infection (MOI): *S.* Typhimurium (MOI 3), UPEC (MOI 8), EIEC (MOI 15), *L. monocytogenes* (MOI 8), and *S. aureus* (MOI 5). Fluorescent microspheres (3-µm) were added at a ratio of 5 microspheres per macrophage. In initial experiments, controls of bacterial adhesion were performed by treating the macrophages with latrunculin A (1µM, 1 h) or by maintaining the cells at 4°C (starting 15 min before infection). To analyse infection or phagocytosis, macrophages were incubated with bacteria or microspheres (in culture medium supplemented with 10% heat-inactivated FBS, unless otherwise specified) for 30 min at 37°C, 5% CO_2. At the end, the cells were placed on ice and extracellular bacteria were eliminated by three washes with ice-cold PBS. Subsequently, the macrophages were processed as indicated in the next sections for each type of experiment.

In experiments evaluating the expression of inflammatory cytokines in response to infection (Figure 23), the macrophages were incubated with *S.* Typhimurium as described above, washed with PBS twice, and incubated in DMEM-10% heat-inactivated FBS complemented with gentamicin (10µg/ml) until 6 h after the onset of infection. Afterwards, the cells were lysed and processed for the analysis of RNA expression.

To corroborate the MOI in each experiment, the bacterial suspensions used for infection were subjected to 1:10 serial dilutions in 2xYT and were inoculated in Agar-LB dishes containing 100µg/ml ampicillin. Bacteria were allowed to grow at 37°C until colony forming units (CFUs) could be counted.

Analysis of infection by flow cytometry

After infection with bacteria, macrophages were detached from the plates either by scrapping (murine macrophages) or by incubation in accutase for 45 min at 37°C (human macrophages). Then, the cells were transferred to microtubes and pelleted by centrifugation. Subsequently, macrophages were fixed in 2% paraformaldehyde (PFA) (dissolved in PBS) for 20 min at room temperature. The fluorescence in the cells was analysed using a FacsAria I SORP sorter (Becton Dickinson). Eukaryotic cells were gated according to their forward *vs* side scatter and cell doublets were excluded in plots of forward scatter area (FSC-A) *vs* width (FSC-W). Excitation and emission wavelengths used with each marker are listed in Table 3. The fluorescence from bacteria or microspheres was plotted *vs* the general eukaryotic cell emission (autofluorescence) unless the employed fluorochromes overlapped with the channels used for the detection of autofluorescence; in that case, the fluorescence was plotted *vs* FSC-A. The bacterial index was calculated using the following formula (FL+ refers to fluorescent macrophages in the RFP or FITC channel depending on the use of Gram-negative or Gram-positive bacteria, respectively): bacterial index = (percentage of FL+ macrophages) x (mean fluorescence intensity in the FL+ population).

Table 3. Flow cytometry settings.

Fluorochrome	Excitation laser	Detection filter
Cholera Toxin Subunit B CF® 633 Dye Conjugate	Red (640nm)	780/60
Filipin complex, from *Streptomyces filipinensis*	Ultraviolet (355nm)	440/40
Fluoresbrite® YG Microspheres 3.00µm	Blue (488nm)	530/30
Fluorescein 5 (6)- isothiocyanate (FITC)	Blue (488nm)	530/30
Red Fluorescent Protein (in bacteria)	Green (561nm)	610/20
LIVE/DEAD Fixable Near-IR Dead Cell Stain Kit, for 633 or 635 nm	Red (640nm)	780/60

Analysis of cell viability by flow cytometry

Macrophages were stained with the LIVE/DEAD Fixable Near-IR Dead Cell Stain Kit for 633 or 635 nm (Thermo Fisher Scientific) at 1:1000 dilution in PBS for 30 min (on ice). Then, macrophages were fixed in 2% PFA (dissolved in PBS) for 20 min at room temperature. The cells were kept at 4°C until the analysis. The dead cells were detected by flow cytometry using the settings specified in Table 3.

Analysis of infection by confocal fluorescence microscopy

Macrophages were plated on glass coverslips that were placed inside culture plates and were infected as described above. The cells were washed with PBS three times and fixed in 2% PFA (in PBS) for 20 min at room temperature. The cell membrane was stained for 30 min with 2.5µg/ml Wheat Germ Agglutinin (WGA) Alexa Fluor™ 488- or 555- conjugated (Thermo Fisher Scientific) at room temperature. Cell nuclei were stained with Hoechst 33342 (Sigma) at 1µg/ml for 10 min at room temperature. The coverslips containing the sample were mounted on microscopy slides with Mowiol. Images were acquired using a *Carl Zeiss LSM 880* spectral confocal microscope with the 63x oil objective, zoom 0.6. In each sample, 5-7 fields were selected based on similar cell confluences to obtain at least 100 cells per sample. *S*erial 0.5µm z-axis optical images were acquired across the whole height of the cells. Intracellular bacteria were counted manually using the Fiji software. The cells in the image edges were excluded from the analysis.

Quantification of viable intracellular bacteria (CFU counting)

After infection, macrophages were lysed with 0.5% Triton X-100 (in PBS) on ice. The lysates were diluted in 2xYT and plated on agar-LB plates for subsequent growth at 37°C. Bacterial CFUs were counted once they were readily visible.

Crystal violet staining

Macrophages were washed with PBS and fixed with 10% formalin (Sigma) for 15 min. After washing again with PBS, the cells were stained with crystal violet solution (0.1% Crystal Violet, 0.2% ethanol in sterile water) for 10 min at room temperature. The wells were washed twice with sterile water and dried completely. Then, the cells were lysed in 2% sodium dodecyl sulphate (SDS) for 30 min. Crystal violet staining was quantified by absorbance at 590 nm in an Infinite M200 microplate reader (Tecan).

Analysis of lipid rafts and cholesterol by flow cytometry

Macrophages were scrapped off the plates, transferred to microtubes, and pelleted by centrifugation. Lipid rafts were stained with 2µg/ml Cholera Toxin Subunit B, CF633 conjugate (Biotium) in PBS-0.5% bovine serum albumin (BSA) for 30 min (on ice), followed by 3 washes with PBS-0.5% BSA. In some cases, the dead cells were stained as described before. Then, macrophages were fixed in 2% PFA (dissolved in PBS) for 20 min at room temperature.

Unesterified cholesterol was stained with Filipin complex (Sigma) at 50µg/ml in PBS-1% FBS for 2 h at room temperature.

The fluorescence in the cells was analysed using a FacsAria I SORP sorter (Becton Dickinson). Eukaryotic cells were gated according to their forward *vs* side scatter and cell doublets were excluded in plots of forward scatter area (FSC-A) *vs* width (FSC-W). Excitation and emission wavelengths used with each marker are listed in Table 3. The fluorescence from lipid rafts, cholesterol, and dead cells was analysed in plots of fluorescence *vs* FSC-A.

Analysis of human macrophage morphology and filamentous actin intensity by confocal fluorescence microscopy

This analysis was carried out during a three-month stay in the research group led by Dr. Stefan Linder (University Medical Center Eppendorf, Hamburg, Germany), with strong expertise in cytoskeletal regulation in vascular cells. During that period, we analysed the effects of LXR activation on the actin cytoskeleton of human macrophages incubated with *S.* Typhimurium.

Human macrophages were plated on glass coverslips, treated with the LXR agonist GW3965 (1µM, 24 h), and infected with *S.* Typhimurium as described in previous sections. Then, the cells were washed with PBS three times and fixed in 2% PFA (in PBS) for 20 min at room temperature. The actin cytoskeleton was stained with Alexa Fluor™ 488 Phalloidin (Thermo Fisher Scientific) at 4 units/ml for 45 min at 37°C. Cell nuclei were stained with Hoechst 33342 (Sigma) at 1µg/ml for 10 min at room temperature. The samples were mounted on microscopy slides with Mowiol. Images were acquired using a Leica TCS SP5 confocal microscope with the 40x oil objective. *S*erial 0.5µm z-axis optical images were acquired across the entire height of the cells. The parameters of interest were measured using the FIJI software. A macro was generated to automatise the analysis. Briefly, the 3D stack was "flattened" to obtain a 2D image that compiled the information across the entire height of the cells using the "Z-project" method. Then, several filters were applied to the image in the channel of filamentous actin (F-actin) and the brightness and contrast were set to defined values. The image was converted to binary, and the "adjustable watershed" plugin was used to segment the image into sections corresponding to each cell. The area occupied by each cell was established as a region of interest (ROI) and, in the cases in which the plugin generated inaccurate ROIs, we eliminated them and drew new ROIs manually. Afterwards, the area, circularity, and aspect ratio of the cell, as well as the intensity of F-actin were measured for each ROI using the commands "analyse particles" and "set measurements". The intensity of F-actin in each cell was measured using the "mean grey value" option (which

indicates the intensity corrected by the cell area) on images obtained using the average intensity "Z-project" method in FIJI.

In vivo infection by *Salmonella* Typhimurium

In experiments evaluating the clinical signs of infection, adult (3–5 months old) WT, LXR-deficient, or CD38-deficient female mice were administered 10% sodium bicarbonate by oral gavage and 10 min later the mice were infected by oral gavage with *S.* Typhimurium (10^7 CFU in 200 µL saline solution per animal). To evaluate the effects of LXR activation on morbidity, the animals were daily administered by intraperitoneal injection either vehicle (DMSO) or the LXR agonist T0901317 (T1317) (15 mg/kg animal) dissolved in physiologic saline, starting 24 h prior to infection. Each animal was daily monitored for weight changes and other parameters associated with infection-induced morbidity, and a clinical scoring system was defined according to the development of any of the following clinical signs (one point for each sign): >15% weight loss, severe hunched position, ruffled fur, watery eyes, or slow movement.

In some experiments, the mice were sacrificed at day 4 post-infection, and the infection index in the spleen was determined. In these assays, the spleens were disaggregated through a 100-mm cell strainer, and the erythrocytes were lysed using 1X Pharm Lyse lysing solution (BD Biosciences). The splenocytes were fixed in PBS 5% PFA, and the percentage of infected cells (containing RFP+ bacteria) was analysed by flow cytometry. Bacterial index was calculated for each animal by the following formula: bacterial index = (percentage of RFP+ splenocytes) x (mean fluorescence intensity in the RFP+ population). Spleen samples from non-infected mice were used as negative controls.

Mouse irradiation and bone marrow transfer

Eight-week-old C57BL/6 females were sub-lethally irradiated with two sessions of 4.5 Gy separated by 4 h. The animals were then injected with 3×10^6 bone marrow cells from either WT or CD38-deficient female donors. These procedures were carried out at the animal facility of *Parc de Recerca Biomèdica Barcelona* (PRBB). Two months after the bone marrow transfer, the mice were treated with an LXR agonist or vehicle and infected with *S.* Typhimurium as indicated above.

To analyse the efficiency of replacement of the hematopoietic system, we marked surface CD38 with fluorochrome-conjugated antibodies and detected its expression by flow cytometry. Cell suspensions were obtained from the blood, spleen, and bone marrow of non-infected mice. The

cells were centrifuged and resuspended in PBS-5 % FBS. To block unspecific binding of IgGs to Fcγ receptors on the cell surface of phagocytic cells, the cells were incubated with Fc-block (BD Biosciences) using the manufacturer's recommendations. CD38 surface expression was measured using anti-CD38-FITC conjugated antibodies (BD Biosciences). Flow cytometric determinations were carried out using a Cytomics FC500 MPL flow cytometer (Beckman Coulter).

RNA extraction and cDNA synthesis

Cells or tissues were lysed in TRIzol (Invitrogen) and the total RNA was extracted following the manufacturer's recommendations. Briefly, the lysates were passed several times through a 25G needle-syringe. Chloroform was added (1:6 dilution) and samples were vigorously agitated, followed by 3 min incubation at room temperature and centrifugation at 12,000 x*g* for 15 min at 4°C. The RNA from the upper aqueous phase was transferred to a different tube and 2-propanol (Sigma) (1:3 dilution) was added. Samples were frozen at -80°C until further processing. When the samples were recovered, the RNA was pelleted by centrifuging at 12,000 x*g* for 10 min at 4°C. RNA pellets were washed with 75% ethanol twice, centrifuged and the final pellet was dissolved in RNase free H2O-mQ. Total RNA was quantified by Nanodrop (Thermo Fisher Scientific).

cDNA synthesis was performed following the manufacturer's recommendations. Briefly, 0.5-1µg of total mRNA was subjected to reverse transcription using the following materials: 200 units of M-MLV reverse transcriptase RNase H Minus, Point Mutant (Promega); M-MLV reaction buffer; 4µM oligo$(dT)_{15}$ primer (Sigma), and; 0.5mM PCR nucleotide mix (Promega).

Quantitative real-time PCR analysis

Quantitative real-time PCR (qPCR) was performed using the Power SYBR Green Reagent Kit (Applied Biosystems) in a CFX384™ real-time system (Bio-Rad) at the following conditions: a denaturing step at 95°C for 10 min; 35 amplification cycles of 95°C, 60°C, and 72°C, 30 sec each; and a dissociation curve. Each sample was analysed in triplicates. Relative gene expression was calculated based on a standard formula for each gene and normalised by *L14* in murine samples or *GAPDH* in human samples. See the sequences of primers in Table 4.

Table 4. Sequences of the forward and reverse primers used for qPCR reactions.

Gene	Forward primer (5'-3')	Reverse primer (5'-3')
Murine		
Cd5l	GTTGGATCGTGTTTTTCAGA	TCCCACTAGCTGCACTTTGGT
Cd38	GCATGTTCAAGCTCCTCCTT	TCAGTCCAGGCTACAGGTGA
Cebpb	AAGCTGAGCGACGAGTACAAGA	TCAGCTCCAGCACCTTGTG
Cox2	ATTCTTTGCCCAGCACTTCA	GGGATACACCTCTCCACCAA
Il1b	TGGGCCTCAAAGGAAAGAAT	CAGGCTTGTGCTCTGCTTGT
Il6	CCAGAGATACAAAGAAATGATGG	ACTCCAGAAGACCAGAGGAAAT
Il12b	GGAAGCACGGCAGCAGAATA	AACTTGAGGGAGAAGTAGGAATGG
L14	TCCCAGGCTGTTAACGCGGT	GCGCTGGCTGAATGCTCTG
Mertk	GACTCCCTATCCCGGAGTTC	CTGCAGCCTCAACACAGAGA
Nos2	GCCACCAACAATGGCAACA	CGTACCGGATGAGCTGTGAATT
Tnfa	CCAGACCCTCACACTCAGATC	CACTTGGTGGTTTGCTACGAC
Human		
ABCA1	TGAGCTACCCACCCTATGAACA	CCCCTGAACCCAAGGAAGTG
ABCG1	GGTCGCTCCATCATTTGCAC	GCAGACTTTTCCCCGGTACA
CD38	TTGGGAACTCAGACCGTACC	GTTGCTGCAGTCCTTTCTCC
GAPDH	GTGAAGGTCGGAGTCAACGG	TTGAGGTCAATGAAGGGGTCA

Search of transcription factor binding sites

The DNA sequence of the *Cd38*enh was analysed in the AliBaba2 program, which predicts transcription factor binding sites in an unknown DNA sequence using the binding sites collected in TRANSFAC.

Reporter activity assays

A DNA fragment of 613bp located 2Kb upstream of the transcription initiation site of *Cd38 (Cd38*enh) was cloned into a pGL3 luciferase reporter vector (Promega). A variant of the *Cd38*enh construct with two point mutations in the LXRE (MUT) was generated by site-directed mutagenesis. To evaluate the transcriptional regulation on this region, we co-transfected RAW 264.7 macrophages or COS-7 fibroblasts with various plasmids: 500ng of pGL3-*Cd38*enh WT or MUT; 300ng of pBluescript (KS+) overexpression plasmid encoding murine C/EBPβ or empty pBluescript; 300ng of pcDNA3-LXRα or pcDNA3-LXRβ; 300ng pcDNA3-RXRα, and; 100ng of pRL-TK mammalian co-reporter vector (encoding renilla-luciferase). Transfections were carried out using the Superfect Transfection Reagent (Qiagen) following the manufacturer's instructions. Briefly, the cells were incubated with the transfection complexes (Superfect mixed with plasmids) for 2.5 h in regular growth conditions, followed by a wash with PBS and incubation

with vehicle (DMSO) or an LXR agonist for 24 h under regular culture conditions. Then, the cells were washed with PBS and lysed in 200µl of Passive Lysis buffer. Luciferase activity was assessed using the Firefly & Renilla Luciferase Single Tube Assay Kit (Biotium) following the manufacturer's recommendations. To measure luciferase activity, 20µl of lysate were placed inside a well of a 96-well plate, and the luminescence was measured after adding 100µl of Firefly luciferase working solution first and 100µl of Renilla luciferase working solution afterwards. Luciferase activity was detected in an Infinite M200 microplate reader (Tecan). The values obtained from Firefly luciferase activity were normalized by those of Renilla activity.

Protein extraction and Western blot analysis

The cells were placed on ice, washed with PBS, and lysed in RIPA lysis solution (50mM Tris-HCl pH 7.4, 1% Triton-X-100, 0.5% Na-deoxycholate, 0.1% SDS, 150mM NaCl, 2mM EDTA, 50mM NaF) supplemented with protease inhibitors (1mM phenylmethylsulfonyl fluoride, 0.2mM Na_3VO_4, and protease inhibitor cocktail (Santa Cruz Biotechnology)). Insoluble material was removed by centrifugation at 14,000 × *g* for 15 min at 4°C. Protein concentration in the lysates was determined by the Bradford assay.

Cell lysates (10–30 µg) were boiled for 5 min at 95°C in Laemmli SDS loading buffer. Proteins were separated by SDS-PAGE (10-12.5% acrylamide) electrophoresis and electrophoretically transferred to PVDF membranes (Immobilon-FL). The membranes were blocked in Odissey blocking buffer (Li-Cor) diluted 1:1 with TBS-0.05% Tween 20 (TBS-T) and later incubated with primary antibodies overnight at 4°C (the antibodies used in the study are listed in Table 2). Then, the membranes were washed three times in TBS-T and incubated for 1 h with peroxidase-conjugated secondary antibodies. After three washes with TBS-T, the membranes were incubated with enhanced chemiluminescence detection reagent (GE Healthcare) for 5 min and the chemiluminescence was measured in the Odyssey Fc Imaging System (Li-Cor). Protein band quantification was performed using the Image Studio ™ Lite software (Li-Cor). The protein expression in each sample was normalised by β-tubulin in most cases except for phosphorylated JNK, which overlapped with β-tubulin and was normalised by β-actin. In experiments evaluating total and activated forms of proteins (phosphorylated versus total, Akt or MAPKs), two electrophoretic gels and PVDF membranes were used in parallel under identical conditions except for the incubation with the specific primary and secondary antibodies.

Activity of Rho GTPases

Macrophages were treated for 24 h with vehicle (DMSO) or an LXR agonist in culture medium supplemented with 1% heat-inactivated FBS. Then, the cells were either directly processed or exposed to exponentially grown *Salmonella* at a MOI 3 (for Cdc42 detection) or 10 (for Rac1 detection) for different periods (between 1 and 10 min). The activation of small Rho family GTPases was assessed with the RhoA / Rac1 / Cdc42 G-LISA Activation Assay Bundle (Cytoskeleton) following the manufacturer's instructions. All the reagents and materials were cooled before their use and the samples were processed sequentially to minimise the degradation of GTP during sample processing. The cells were washed in PBS and lysed with the correspondent lysis buffer complemented with protease inhibitors. Cell lysates were harvested with a scraper and the insoluble material was removed by centrifugation at 14,000 × *g* for 1 min. The supernatants were immediately snap frozen in liquid nitrogen, except for a volume of 20µl that was used to measure the protein concentration in the lysate by the Protein Assay Reagent. The frozen lysates were stored at -80°C until the G-LISA protocol was performed in the following days. The samples were brought to the same concentrations (0.3-0.4µg/µl) and the protocol specified by the manufacturer for each of the Rho GTPases was used. Briefly, for Cdc42 and Rac1 detection, 50µl of lysate were directly added to each well on the strip (on ice), while for RhoA detection, the lysate was diluted 1:2 in binding buffer and 50µl of the diluted lysate were added. Simultaneously, 50µl of positive and negative control were used as specified in the protocol. The plate was placed in an orbital shaker at 240 rpm 4°C for 15 min (Cdc42) or 30 min (Rac1, RhoA). Then, the wells were washed twice with the Wash buffer provided by the manufacturer and incubated with antigen-presenting buffer for 2 min. The wells were washed again three times with the Wash buffer and incubated with the primary antibody on the orbital shaker at 240 rpm at room temperature for 30 min (Cdc42) or 45 min (Rac1, RhoA). Afterwards, the wells were washed three times with Wash buffer and incubated with the secondary antibody at the same conditions as with the primary antibody. Then, the wells were washed three times and incubated with the HRP detection reagent for 15 min at 37°C (Cdc42) or for 20 min at room temperature (Rac1, RhoA). At the end, the reaction was stopped by adding the HRP stop buffer. The colorimetric signal was measured at 490 nm in an Infinite M200 microplate reader (Tecan).

Data processing and statistical analysis

Raw data were recorded in a Microsoft Excel worksheet. To make data from different experiments comparable, in the indicated cases, the values were normalised by the ratio between the mean of all the experiments and the mean of each experiment. Data were then analysed using the GraphPad Prism 7.0 software. The normal distribution of the residues was

assessed by the Shapiro-Wilk test. Data following a Gaussian distribution were evaluated with parametric tests: T-test to detect differences between two groups, and either one-way or two-way ANOVA to detect differences among more than two groups according to one or two factors, respectively. When the ANOVA test indicated significant differences, one of the following *post-hoc* tests was used for multiple comparisons: Tukey's test, Sidak's test to compare selected groups, or Dunnet's test to compare all the conditions with the control. In Figure 32, the analysis was performed by multiple T-tests and the statistical significance was corrected by the Holm-Sidak's method. Differences in non-parametric data were evaluated by the Mann-Whitney U test (two groups) or Kruskal-Wallis + Dunn's test (more than two groups). The proportion of infected cells detected in confocal microscopy studies were registered as a contingency table and were analysed by the Fisher's exact test.

Statistical differences were considered significant at p-values < 0.05. The following signs are used to indicate the significant p-values in the figures: *p<0.05, **p<0.01, ***p<0.001, ****p<0.0001; $^{\#}$p<0.05, $^{\#\#}$p<0.01, $^{\#\#\#}$p<0.001, $^{\#\#\#\#}$p<0.0001; ^p<0.05, ^^p<0.01, ^^^p<0.001, ^^^^p<0.0001. Non-significant differences were indicated as "n.s.".

RESULTS

1. Pharmacological activation of LXRs ameliorates the clinical course of *Salmonella* Typhimurium infection *in vivo*

Upon ingestion of contaminated food, *S.* Typhimurium is able to cause infection by traversing the intestinal barrier and invading non-phagocytic epithelial cells and intestinal macrophages. Despite the microbicidal activities of macrophages, these cells represent a preferential niche for *Salmonella* replication and a means of transport for bacterial dissemination to other organs (Price and Vance, 2014). As described in the introduction, our previous data indicated that LXR activation restricts the entry of *S.* Typhimurium into murine macrophages (Matalonga et al., 2017). To evaluate whether pharmacological LXR activation results in a positive or negative outcome on infection by *S.* Typhimurium *in vivo*, we infected C57BL/6 female mice by oral gavage (*S.* Typhimurium, 10^7 CFU/mouse) and compared the progression of infection between vehicle- and LXR agonist-treated mice. The treatment with the LXR agonist (T1317) or the vehicle (DMSO) was initiated 24 h prior to the infection and was continued daily by intraperitoneal injection. Each day, the weight of mice was monitored as well as five clinical signs associated with infection: > 15% weight loss, severe hunched position, ruffled fur, watery eyes, and slow movement. A score was established for each animal based on the presence or absence of each of these clinical signs. The weight of mice was monitored daily as well. On day 4 post-infection, the differences in the clinical score and the body mass indicated an amelioration of the disease in mice treated with the LXR agonist compared to the vehicle-treated counterparts (Figure 19 A,B). Four days after the onset of infection, the levels of infected cells were measured in the spleen as an indicator of bacterial dissemination. In line with the amelioration of the clinical severity, the administration of the LXR agonist reduced the dissemination of *Salmonella* to the spleen (Figure 19 C). Likewise, LXRα/β-deficient ($LXR^{-/-}$) mice were challenged with *Salmonella* to evaluate the specificity of the LXR agonist. As expected, the LXR agonist did not ameliorate the clinical course of salmonellosis in $LXR^{-/-}$ mice (Figure 19 D,E). To assess the involvement of the LXR target CD38 in the protective effects of the LXR agonist, CD38-deficient ($CD38^{-/-}$) mice were also subjected to the infection *in vivo*. LXR activation in $CD38^{-/-}$ mice had no impact on the clinical indicators of disease or in the bacterial dissemination (Figure 19 F-H), suggesting that CD38 induction by LXRs plays a role in the protective effects against infection *in vivo*.

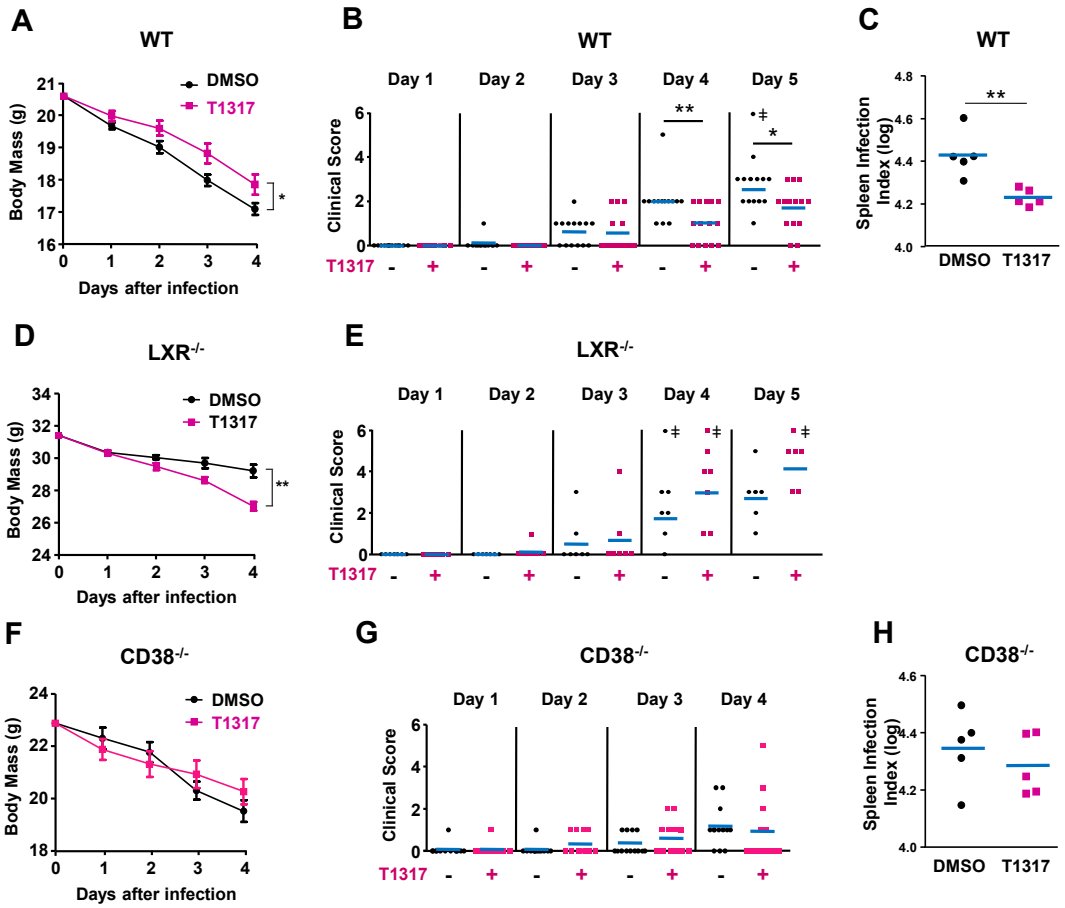

Figure 19. Pharmacological treatment with a synthetic LXR agonist ameliorates the clinical signs associated with *Salmonella* Infection in a CD38-dependent manner. Wild-type (WT) (A-C), LXR-deficient (LXR$^{-/-}$) (D, E), or CD38-deficient (CD38$^{-/-}$) (F-H) female mice were infected by oral gavage with *S.* Typhimurium (10^7 CFU per animal). The animals were daily administered by intraperitoneal injection either vehicle (DMSO in physiologic saline, black circles) or the LXR ligand T1317 (15 mg/kg animal dissolved in physiologic saline, magenta squares), starting 24 h before the infection. n = 14 (WT), n = 7 (LXR$^{-/-}$), and n = 13 (CD38$^{-/-}$) mice per group. (A, D, F) The weight of each mouse was measured daily starting before infection. The graphics represent estimated marginal means of mass ± standard error mean (SEM) during the first 4 days post-infection. The statistical analysis was performed using repeated-measures two-way ANCOVA after adjusting for mass at the time of infection. (B, E, G) Development of clinical signs during the first 4-5 days of infection. For each mouse, a score was calculated based on the presence of clinical signs (one point for each sign): >15% weight loss, severe hunched position, ruffled fur, watery eyes, or slow movement. Dead animals (‡) were assigned a score of 6. Horizontal bars represent mean values in the live population (Mann-Whitney U). (C, H) After 4 days, the infection index by RFP-expressing S. Typhimurium in splenocytes was determined by flow cytometry (log values). n=5 mice per group (T-test). $^{*}p < 0.05$, $^{**}p < 0.01$. These results were published in (Matalonga et al., 2017).

To further assess the involvement of CD38-expressing bone marrow-derived cells in the protective effects of LXR activation, wild-type (WT) mice were irradiated and transplanted with either WT or CD38$^{-/-}$ bone marrows. The efficiency of cell replacement after bone marrow transplantation was analysed through the detection of surface CD38 expression by flow cytometry (Figure 20 A). The proportion of CD38-expressing cells in mice transplanted with WT or CD38$^{-/-}$ bone marrow was: 48.4% *vs* 13.5% in the bone marrow, 50.9% *vs* 10.8% in the blood,

and 74.4% *vs* 9% in the spleen. Therefore, the cells derived from CD38$^{-/-}$ bone marrows largely replenished the cell populations in organs enriched in bone marrow-derived cells after transplantation. Pharmacological LXR activation improved the clinical profile and decreased the splenic bacterial load in mice that received WT bone marrows (Figure 20 B-D) but not in the ones

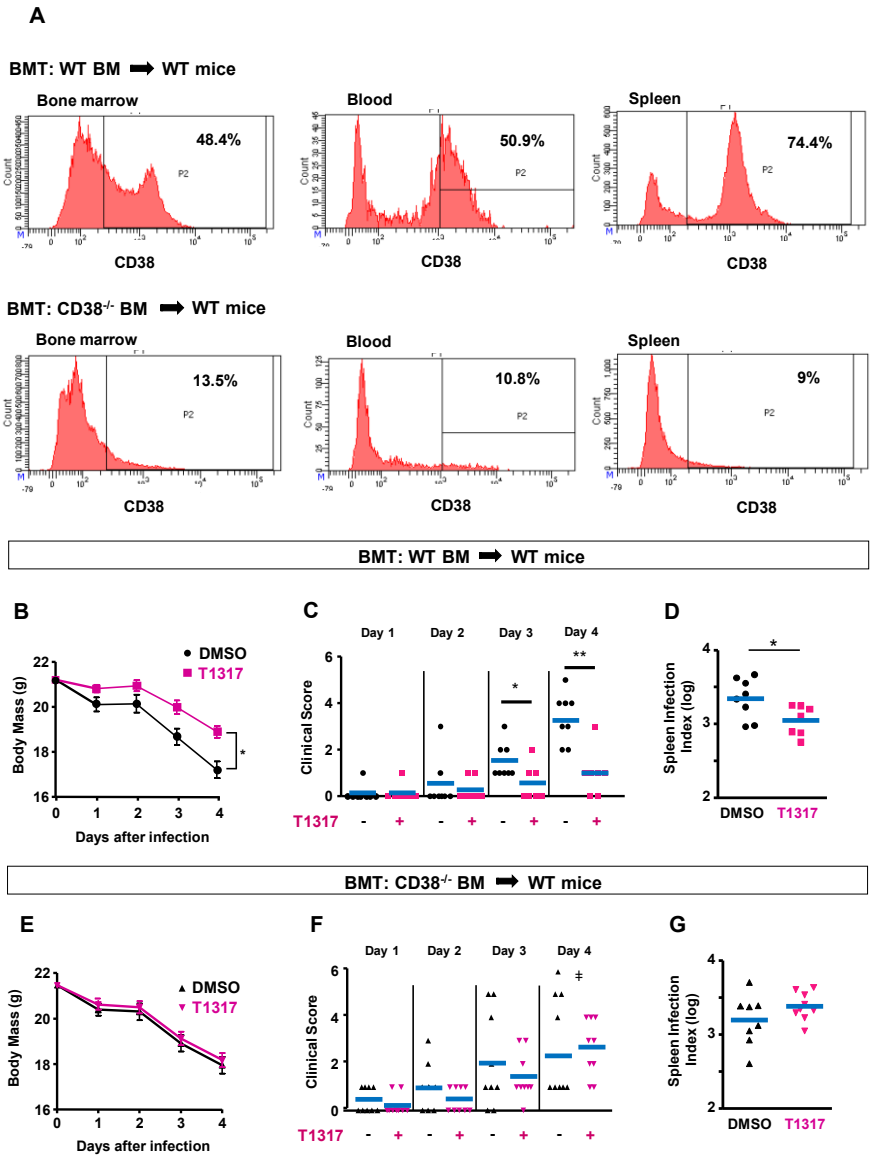

Figure 20. CD38 expression in bone marrow-derived cells contributes to the amelioration of *Salmonella* infection by pharmacological LXR activation. Sub-lethally irradiated WT female mice were subjected to bone marrow transplantation (3 × 10^6 bone marrow cells per animal) from either WT (A-D) or CD38-deficient (A, E-G) female donors. Two months after transplantation, the animals were infected with RFP-expressing *S.* Typhimurium (10^7 CFU/animal). Bacterial infection and administration of the LXR agonist T1317 or vehicle was performed as described in Figure 19. The efficacy of replacement of bone marrow-derived cells in the bone marrow, blood, and spleen was analysed by surface CD38 detection by flow cytometry (A). The body weight (B, E) and clinical score (C, F) were registered daily for 4 days after infection. (D, G) The infection index in splenocytes was evaluated by flow cytometry. n = 7–9 mice per group. Estimated marginal means of mass (± SEM) analysed by repeated-measures two-way ANCOVA after adjusting for mass at the time of infection (B, E), Mann-Whitney U (C, F), or t test (D, G). In C, D, F, and G the blue horizontal bars indicate mean values. $^*p < 0.05$; $^{**}p < 0.01$. These results were published in (Matalonga et al., 2017).

transplanted with CD38$^{-/-}$ bone marrows (Figure 20 E-G). These results indicate that CD38 expression by bone marrow-derived cells contributes to the beneficial effects of pharmacological LXR activation in *Salmonella* infection.

Besides evaluating pathological aspects associated with *Salmonella* infection, we explored the impact of LXR activation on the inflammatory status of the mice. After 4 days of infection, the expression of a group of classical inflammatory genes was measured by qPCR in the spleen and the liver: the main organs to which *S.* Typhimurium disseminates from the intestine. The infection by *Salmonella* potently increased the mRNA levels of *Il1b*, *Tnfa*, *Il6*, *Cox2*, and *Nos2* in vehicle-treated mice (Figure 21 A). Overall, WT mice treated with the LXR agonist expressed lower levels of these inflammatory molecules in both organs. Curiously, the LXR agonist did not

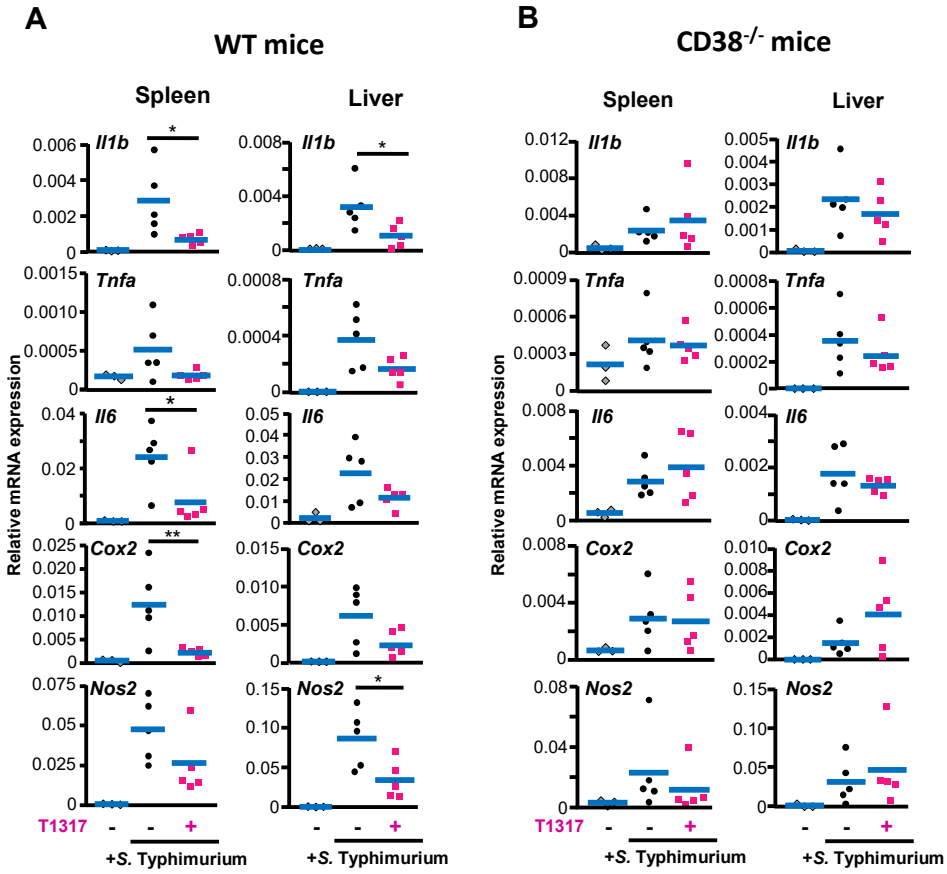

Figure 21. LXR activation inhibits inflammatory gene expression in spleens and livers from mice infected with *S.* Typhimurium. WT (A) or CD38-deficient (B) mice were infected by oral gavage with *S.* Typhimurium (10^7 CFU/animal). The animals were daily administered by intraperitoneal injection either vehicle (DMSO in physiologic saline) (black circles) or the LXR agonist T1317 (15 mg/kg animal dissolved in physiologic saline) (magenta squares), starting 24 h before the infection. The expression of inflammatory genes in the liver and the spleen was evaluated by real time qPCR four days after the onset of infection. Three non-infected animals from each genotype were used as negative controls (grey diamonds) without infection. The mRNA levels of each inflammatory gene were normalised by *L14* expression. n=5 mice/group. Blue bars represent mean values. *p < 0.05; **p < 0.01 (T-test comparing the two groups of infected mice, DMSO- vs T1317-treated animals). These results were published in (Matalonga et al., 2017).

inhibit significantly the expression of these inflammatory mediators in the liver and the spleen of CD38$^{-/-}$ mice (Figure 21 B). Similar effects were detected in the mice subjected to bone marrow transplantation: LXR activation diminished the expression of inflammatory mediators in mice that received a WT bone marrow, but it did not influence their levels in WT mice with CD38$^{-/-}$ bone marrow (Figure 22).

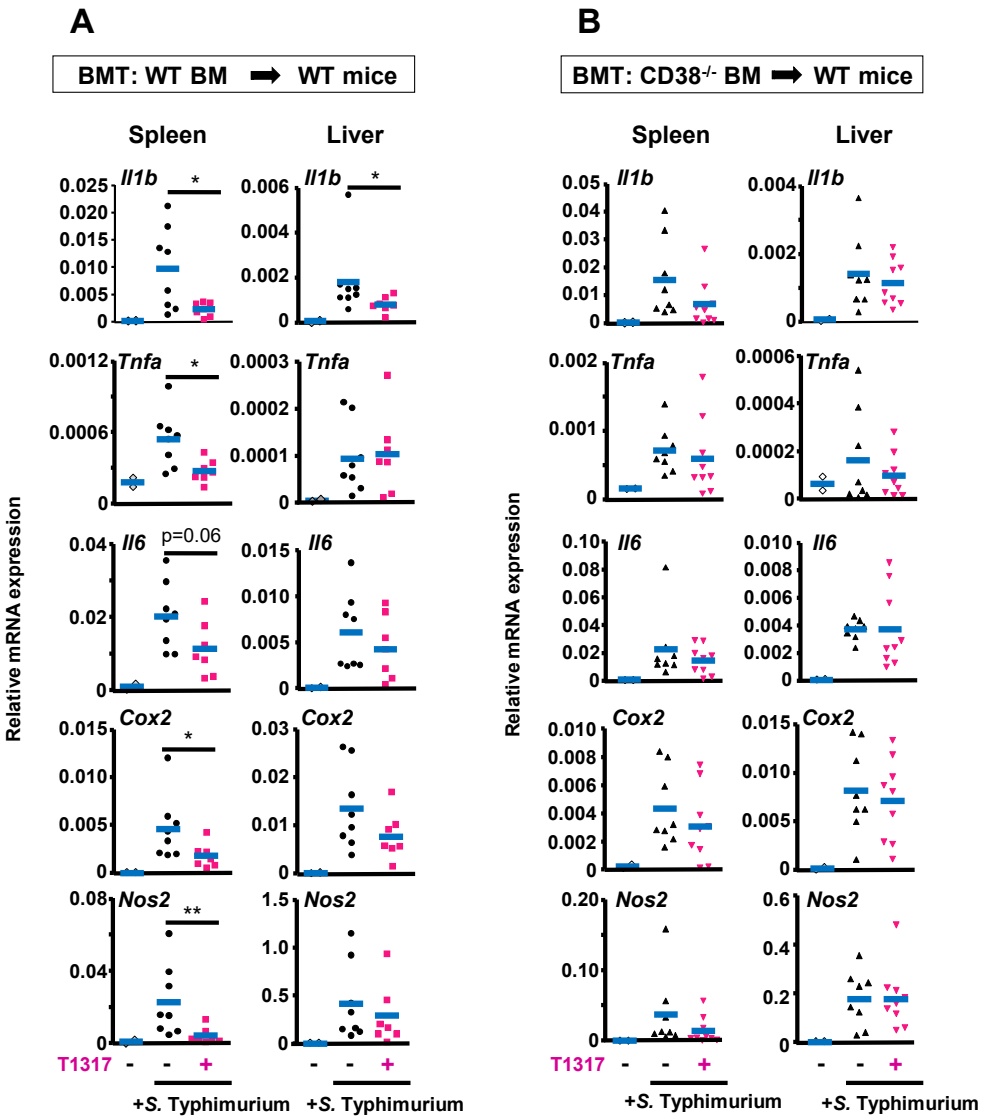

Figure 22. Effects of LXR activation on inflammatory gene expression after WT or CD38-deficient bone marrow transplantation and *S.* Typhimurium infection. Sub-lethally irradiated WT female mice were subjected to bone marrow transplantation (3x10^6 bone marrow cells/animal) from either WT or CD38-deficient female donors. Two months after transplantation the animals were infected with *S.* Typhimurium and treated with the LXR agonist/vehicle as described in Figure 21. The expression of inflammatory genes in the liver and the spleen was evaluated by real time qPCR four days after the onset of infection. The mRNA levels of each inflammatory gene were normalised by *L14* expression. In the groups subjected to infection, n=7-9 mice/group. Two non-infected animals from each bone marrow transfer group were used as negative controls (without infection). *p < 0.05 (T-test comparing the two groups subjected to infection, vehicle *vs* T1317-treated mice). These results were published in (Matalonga et al., 2017).

To evaluate whether CD38 contributes to the repressive actions of LXR agonists on inflammatory gene expression, we performed repression studies *in vitro* using bone marrow-derived macrophages (BMDM). Macrophages were treated with vehicle or the LXR agonist T1317 for 24 h and exposed to *S.* Typhimurium for 30 min or 1 h. After 6 h, the expression of inflammatory genes was evaluated by qPCR. In WT BMDM, the LXR agonist repressed the expression of all the analysed inflammatory mediators (Figure 23 A). Of note, the levels of induction of the cytokines *Il1b*, *Il6*, *Il12b*, and *Tnfa* were lower in CD38$^{-/-}$ macrophages. However, except for *Il6*, the LXR agonist inhibited inflammatory gene expression in these cells, suggesting that CD38 is not

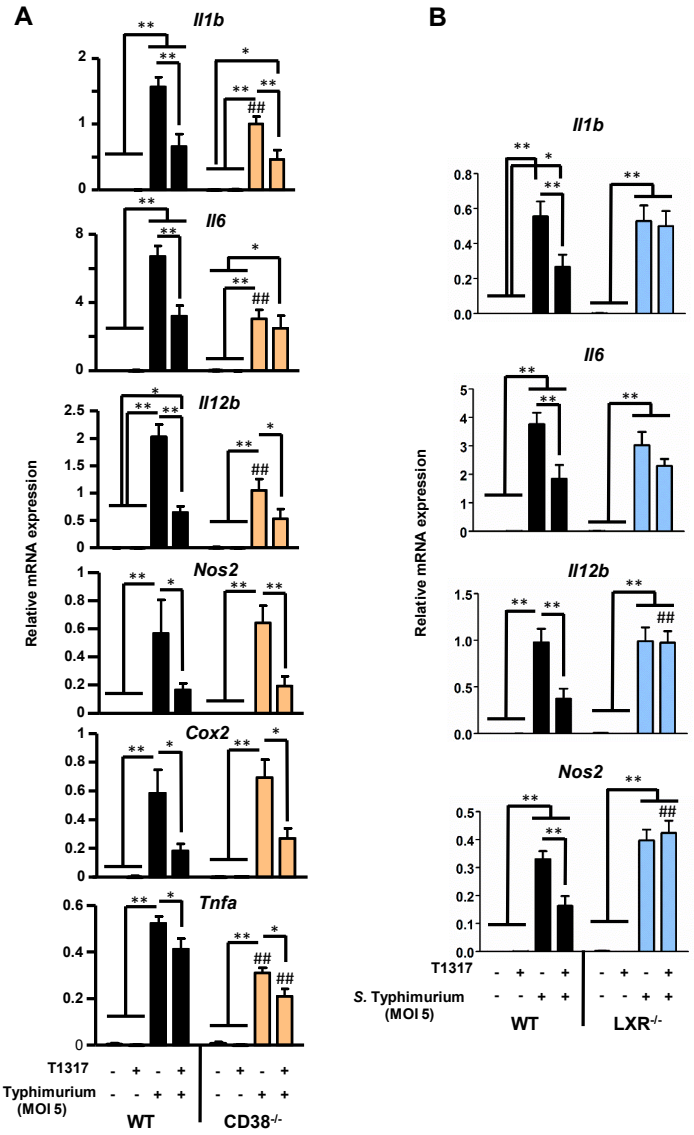

Figure 23. LXR activation represses *S.* Typhimurium-induced inflammatory gene expression in macrophages independently of CD38. WT, CD38$^{-/-}$ (A), or LXR$^{-/-}$ (B) BMDMs were pre-stimulated with T1317 (1µM) or vehicle (DMSO) for 24 h and exposed to *S.* Typhimurium (MOI 5) for 30 min (A) or 1 h (B). The cells were washed and incubated with gentamycin until 6 h post-infection. Data represent mean mRNA expression values quantified by qPCR and normalised by *L14* (± SEM). n=6 (A), n = 5 (B), two-way ANOVA Bonferroni. *p < 0.05; **p < 0.01. $^{\#\#}$p < 0.01 vs the same treatment in WT cells. These results were published in (Matalonga et al., 2017).

required for the anti-inflammatory actions of LXRs *in vitro*. These effects were specifically mediated by LXRs, as the agonist was not able to repress inflammatory gene expression in LXR$^{-/-}$ cells (Figure 23 B). Since CD38 did not participate in the LXR-mediated repression of inflammatory gene expression in infected macrophages *in vitro*, it is feasible that the reduced ability of the LXR agonist to suppress the expression of inflammatory mediators in CD38$^{-/-}$ mice during infection *in vivo*, is an indirect consequence of the lack of inhibition of bacterial dissemination by the LXR pathway in CD38$^{-/-}$ mice. The data shown in this section was incorporated in (Matalonga et al., 2017).

2. The transcription factor C/EBPβ mediates the cooperation between LXRs and inflammatory signals in the transcriptional control of *Cd38* expression

Accumulated evidence indicates the existence of reciprocal negative crosstalk between LXRs and inflammatory signals (Castrillo et al., 2003; Han et al., 2018; Pascual-Garcia et al., 2013). Through these actions, the activation of the LXR pathway represses the macrophage transcriptional response to inflammatory mediators (as shown in the previous section) and, reciprocally, pro-inflammatory signalling negatively affects the induction of several LXR target genes that play key roles in metabolism. In contrast with these general mutually opposing effects, LXRs and several inflammatory mediators (TNFα, IFNγ, and LPS) cooperate to synergistically increase the mRNA levels of *Cd38* (Matalonga et al., 2017). Moreover, the *in vivo* model of salmonellosis suggested that CD38 modulation during infection might play a role in the control of infection. Consequently, we next explored the molecular mechanisms that control *Cd38* induction by LXRs and inflammatory signals. In a study carried out by a Pulido-Salgado and co-workers (Pulido-Salgado et al., 2017), the RNA-sequencing analysis of microglial cells revealed that the induction of *Cd38* expression by LPS was impaired in C/EBPβ-deficient cells. This insight encouraged us to evaluate whether the transcription factor C/EBPβ contributes to *Cd38* expression in our experimental setting *in vitro*. BMDMs were obtained from mice with myeloid C/EBPβ deficiency or from WT mice. Surprisingly, the basal levels of *Cd38* were higher in C/EBPβ-deficient macrophages (hereafter referred to as C/EBPβ$^{-/-}$ macrophages) than in WT cells (Figure 24 A). As expected, the activation of LXRs with T1317 induced *Cd38* expression in WT cells; however, it reduced the levels of *Cd38* in C/EBPβ$^{-/-}$ macrophages. Afterwards, C/EBPβ$^{-/-}$ or WT macrophages were challenged with the inflammatory cytokines TNFα or IFNγ or the bacterial component LPS, either alone or in combination with the LXR agonist for 24 h. In WT macrophages, both TNFα

and IFNγ induced an upward tendency in *Cd38* expression, while LPS potently increased *Cd38* levels (Figure 24 B-D). The combination of each of these inflammatory signals with the LXR agonist synergistically stimulated *Cd38* expression. In C/EBPβ$^{-/-}$ cells, by contrast, none of the inflammatory signals stimulated *Cd38* expression, and the cooperativity with LXRs was either completely abolished in the case of TNFα and IFNγ or drastically impaired in the case of LPS. These results indicate that C/EBPβ participates in *Cd38* induction by at least some inflammatory mediators. In addition, its expression is required for the transcriptional cooperation between these inflammatory signals and LXRs in the activation of *Cd38*.

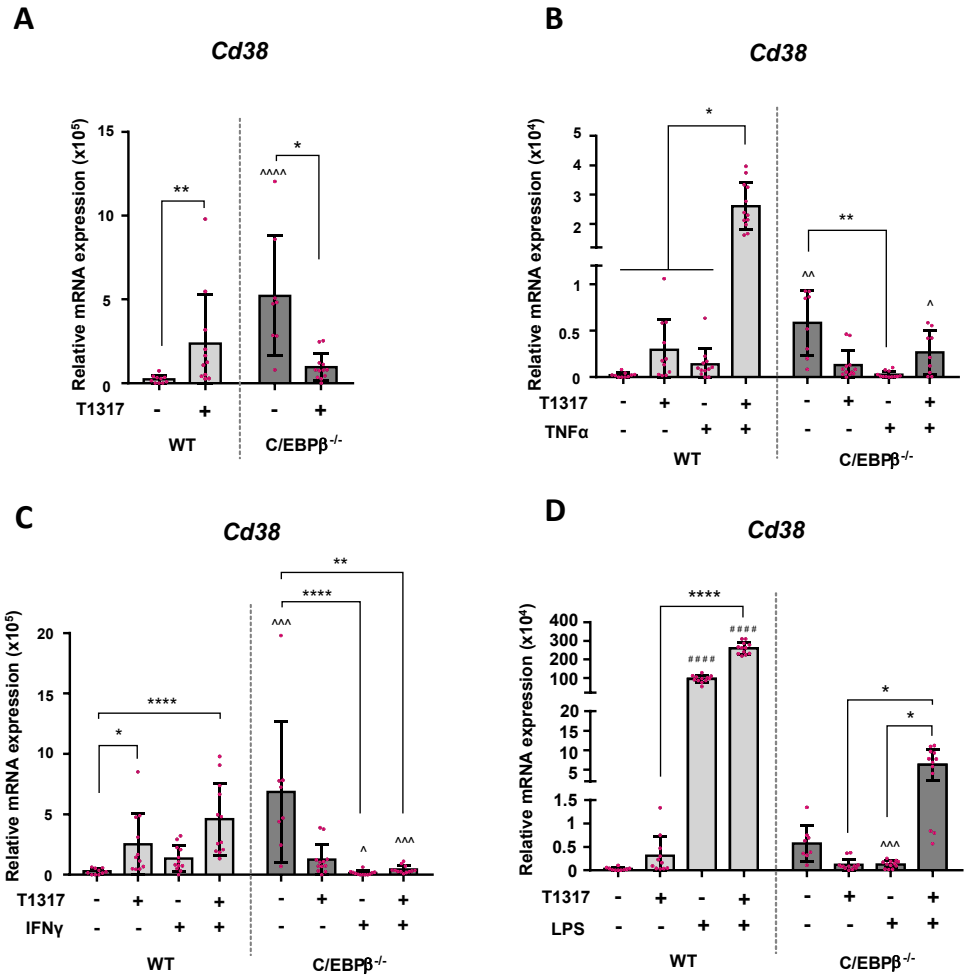

Figure 24. C/EBPβ mediates the cooperative effects of inflammatory signals and LXRs on *Cd38* induction. WT or C/EBPβ-deficient (C/EBPβ$^{-/-}$) BMDMs were treated with vehicle (DMSO) or an LXR agonist (T1317, 1 μM) and/or an inflammatory stimulus: TNFα (20 ng/ml) (B), IFNγ (5 ng/ml) (C) or LPS (100 ng/ml) (D) for 24 h. Gene expression was measured by qPCR and is represented as *Cd38* mRNA levels normalised by *L14* expression. Mean ± standard deviation (SD) of n=4 independent experiments performed with biological duplicates or triplicates. The pink dots indicate the values of each replicate. To make different experiments comparable, the statistical mean of all the conditions (including WT and C/EBPβ$^{-/-}$ cells) was calculated for each experiment and used to normalise data by the mean of all the experiments. Kruskal-Wallis test + Dunn's multiple comparisons. *p<0.05; **p < 0.01; ****p < 0.0001. ^p < 0.05; ^^p < 0.01; ^^^p < 0.001; ^^^^p < 0.0001 *vs* the same treatment in WT cells. ####p < 0.0001 *vs* the negative control.

Next, we explored how C/EBPβ is regulated by inflammatory signals. First, we measured the mRNA levels of *Cebpb* at different time points following macrophage stimulation with TNFα, IFNγ, or LPS, either in the presence or absence of the LXR agonist. Each inflammatory stimulus increased *Cebpb* levels, reaching a maximum between 3 and 6 h of stimulation (Figure 25). Interestingly, the induction of *Cebpb* by these stimuli was not altered by the LXR agonist, indicating that *Cebpb* expression is not targeted by LXR activation. In addition, using WT and LXR$^{-/-}$ macrophages we observed that the functional expression of LXRs was not required for *Cebpb* nor *Cd38* induction by these inflammatory molecules under the conditions used in these assays (Figure 26). Importantly, the dynamics of *Cd38* induction show that its levels raise early upon incubation with TNFα or IFNγ and drop by 14 h post-incubation. Instead, the induction by LPS appears more prolonged.

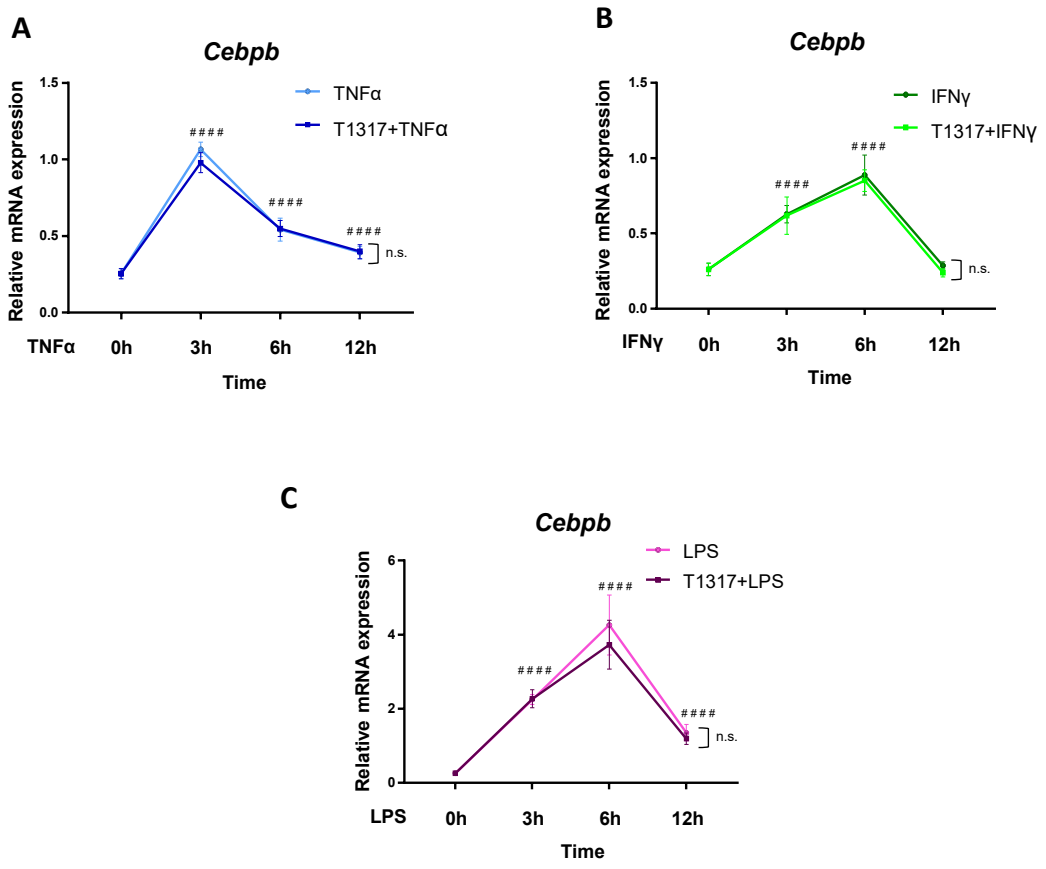

Figure 25. Inflammatory signals induce *Cebpb* expression. BMDMs were treated with vehicle (DMSO, represented as 0h in the graphic), an inflammatory stimulus [TNFα (20 ng/ml) (A), IFNγ (5 ng/ml) (B) or LPS (100 ng/ml) (C)] or an inflammatory stimulus together with the LXR agonist T1317 (1 μM) for 3, 6, or 12 h. Gene expression was measured by qPCR, and is represented as *Cebpb* mRNA levels normalised by *L14* expression. Mean ± SD of n=2 independent experiments performed with biological duplicates. To make different experiments comparable, the statistical mean of all the conditions was calculated for each experiment and used to normalise the data by the mean of all the experiments. Two-way ANOVA + Tukey's multiple comparisons among treatments in each time point. ####p < 0.0001 *vs* vehicle-treated. n.s.: non-significant statistical differences between treatments at the same time point.

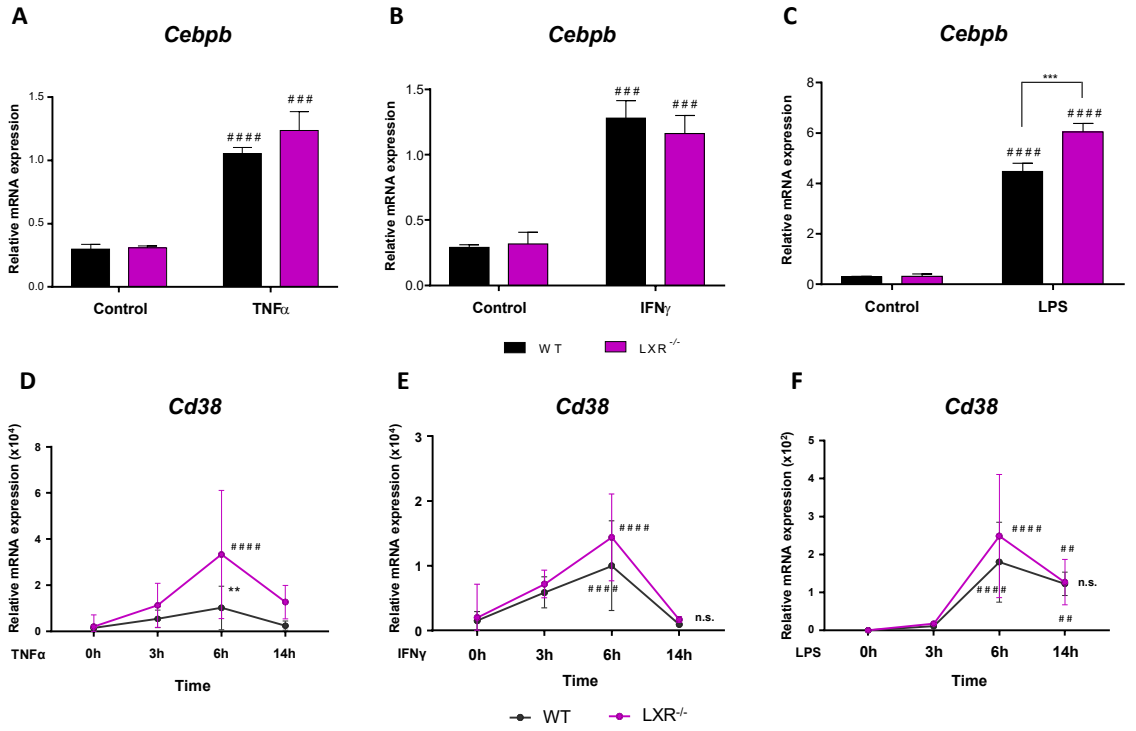

Figure 26. LXR expression is not required for *Cebpb* or *Cd38* induction by inflammatory signals in macrophages. WT or LXRα/β-deficient (LXR$^{-/-}$) BMDMs were treated with TNFα (20 ng/ml) (A, D), IFNγ (5 ng/ml) (B, E) or LPS (100 ng/ml) (C, F) for different periods: 3 h (A); 6 h (B, C); 3, 6, and 14h h (D-F). Gene expression was measured by qPCR, and is represented as *Cebpb* (A-C) or *Cd38* (D-E) mRNA levels normalised by *L14* expression. Mean ± SD of biological triplicates (A-C) or n=2-3 independent experiments with biological duplicates or triplicates (D-F). Two-way ANOVA + Sidak's test between treatments in each genotype (A, B); Two-way ANOVA + Tukey's test (C, D); Two-way ANOVA + Sidak's test between time points in each genotype (E-F). **p<0.01 in WT vs LXR$^{-/-}$ at 6h in (D). ***p < 0.001; ##p < 0.01; ###p < 0.001; ####p < 0.0001 *vs* control cells of the same genotype. n.s.: non-significant statistical differences between WT and LXR$^{-/-}$ BMDM at the same time point.

We also assessed the expression of C/EBPβ at the protein level. There are three C/EBPβ isoforms that arise from different initiation codons during translation (Huber et al., 2012). The isoforms LAP*, which is the full-length protein, and LAP, which is slightly shorter than LAP*, are transcriptional activators; instead, the third isoform, LIP, acts as an inhibitor. By immunoblotting, we detected that the activator isoform LAP is the most prominently expressed after macrophage stimulation with inflammatory mediators (Figure 27). In contrast, the isoform LAP* was not upregulated by the inflammatory signals used in this study. Although the expression of the inhibitory form LIP was lower than the expression of LAP, it was strongly stimulated by LPS after 12 h or weaklier by TNFα or IFNγ.

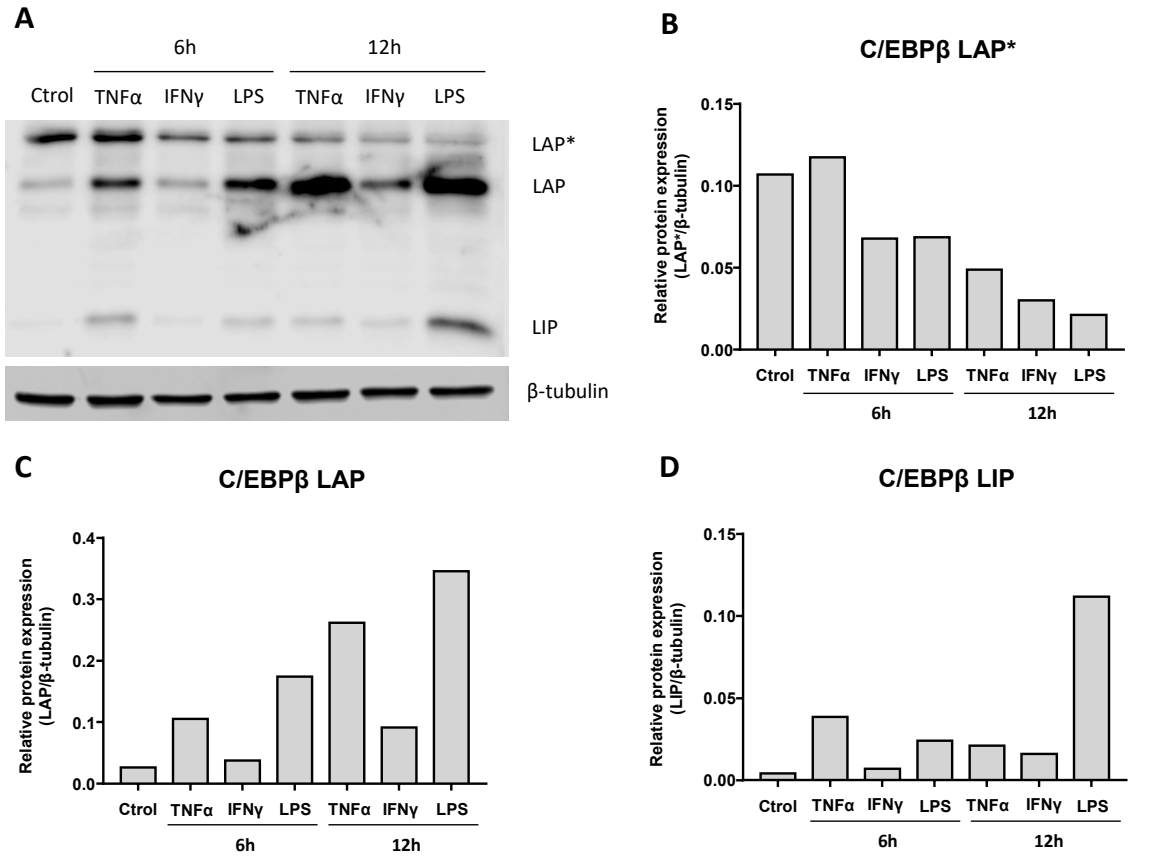

Figure 27. Inflammatory signals increase the expression of the isoform LAP of C/EBPβ. BMDMs were treated with TNFα (20 ng/ml), IFNγ (5 ng/ml), or LPS (100 ng/ml) for 6 or 12 h. Then, the cells were lysed and C/EBPβ protein isoforms were detected by Western Blot. (A) Representative immunoblot of 3 independent experiments that showed similar results. (B-D) Relative protein expression of each of the three C/EBPβ isoforms: LAP* (B) (38 kDa), LAP (C) (34 kDa), or LIP (D) (20 kDa). The protein expression of C/EBPβ isoforms was calculated using the Image Studio Lite software and was normalised to the values of β-tubulin expression. The results in B-D represent the quantification of the immunoblot shown in (A).

The transcription factors STAT1/STAT5 or CREB participate in the induction of *Cebpb* expression by IFNα (Yokota et al., 2019) or LPS+IFNγ (Ruffell et al., 2009), respectively, but the mechanism mediating *Cebpb* induction by IFNγ alone has not been described. Generally, the binding of IFNγ to its membrane receptor triggers STAT1 activation and the induction of its target genes, some of which are transcription factors such as IRF1 (reviewed in Schroder et al., 2004). Later, the second wave of transcriptional activation takes place, for example, by the actions of STAT1-induced IRF1. To assess whether STAT1 or IRF1 are involved in *Cebpb* expression in response to IFNγ, we analysed macrophages from STAT1 or IRF1 knockout mice. Interestingly, the induction of *Cebpb* by IFNγ was impaired in STAT1$^{-/-}$ macrophages but not in IRF1$^{-/-}$ cells (Figure 28). Therefore, STAT1 and not IRF1 mediates the induction of *Cebpb* by IFNγ in macrophages.

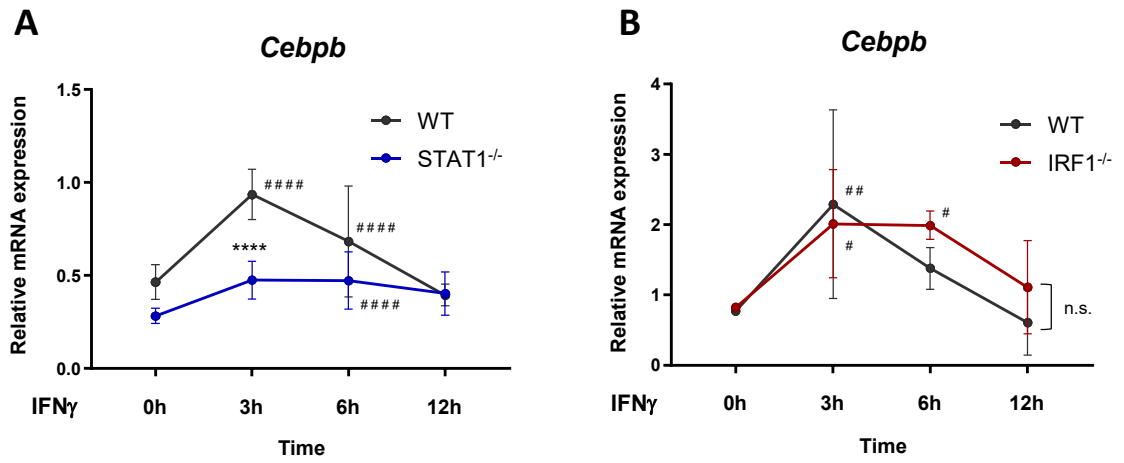

Figure 28. Role of STAT1 and IRF1 in the control of *Cebpb* induction by IFNγ. WT, STAT1-deficient (STAT1$^{-/-}$), or IRF1-deficient (IRF1$^{-/-}$) BMDMs were treated with IFNγ (5 ng/ml) for 3, 6, or 12 h. Gene expression was measured by qPCR and is represented as *Cebpb* mRNA levels normalised by *L14* expression. Mean ± SD of n=2-3 independent experiments performed in biological duplicates (A) or n=3 independent experiments (B). To make different experiments comparable, the basal (0h) expression in each genotype of each experiment was used to normalise the values by the basal expression mean of all the experiments. Two-way ANOVA + Tukey's test (A) or Two-way ANOVA + Sidak's test (B) among time-points in each genotype. ****p < 0.0001 in WT vs STAT1$^{-/-}$ at 3h. $^{\#}$p < 0.05; $^{\#\#}$p < 0.01; $^{\#\#\#\#}$p < 0.0001 *vs* control cells (0h) of the same genotype. n.s.: non-significant statistical differences between WT and IRF1$^{-/-}$ BMDM at the same time point.

To further evaluate the cooperative action of C/EBPβ and LXRs, we assessed the capability of these transcription factors to promote the transcription from an enhancer region containing an LXRE located 2 kb upstream of the transcription initiation site of *Cd38*. Our group had previously cloned a DNA fragment of 613 bp containing the LXRE (from now on referred to as *Cd38*enh) in a pGL3 luciferase reporter vector (Promega). Subsequent experiments showed increased enhancer activity in this region by RXR-LXR activation, thereby supporting its functionality as an LXRE (Matalonga et al., 2017). We then performed an *in-silico* analysis of the *Cd38*enh region to identify additional transcription factor binding sites using the Alibaba2.1 software. Eight potential binding sites for various C/EBP isoforms were found: five for C/EBPα, two for C/EBPβ, and one for C/EBPγ (Figure 29 A). To evaluate transcriptional modulation from this region, we transiently co-transfected two different cell types, specifically, COS-7 fibroblasts and RAW264.7 macrophages, with a plasmid containing the *Cd38*enh-luciferase construct and overexpression plasmids encoding *Lxra* or *Lxrb*, *Rxra*, and, in some cases, *Cebpb*. After optimising the conditions for transfection, we observed stronger promoter activity in the *Cd38*enh induced by the overexpression of LXRβ compared to LXRα (Figure 29 B). Consequently, we decided to continue the experiments with the overexpression plasmid encoding the LXRβ isoform. Thereafter, we performed the experiments using the original *Cd38*enh and a variant *Cd38*enh-luciferase construct that contained two point mutations in the LXRE (MUT LXRE) in parallel. In COS-7 cells,

the combination of C/EBPβ overexpression and the overexpression and activation (by GW3965) of LXRs moderately increased the promoter activity of the *Cd38*enh bearing either the WT or MUT LXRE (Figure 29 C). However, the transcriptional activation elicited by these conditions was much higher in the macrophage cell line RAW 264.7 (Figure 29 D). In these macrophages, the sole overexpression of C/EBPβ potently augmented the enhancer activity of the *Cd38*enh containing any of the LXRE variants. Of note, coupling C/EBPβ overexpression and LXR activation caused an upward trend in the promoter activity of the *Cd38*enh carrying the WT LXRE that was impaired when the mutant fragment was used. In conclusion, we have identified an enhancer region upstream of the gene encoding *Cd38* from which C/EBPβ and LXRβ cooperate to promote transcription. Whether this cooperation occurs by direct binding of C/EBPβ to the *Cd38*enh or through indirect actions needs to be determined.

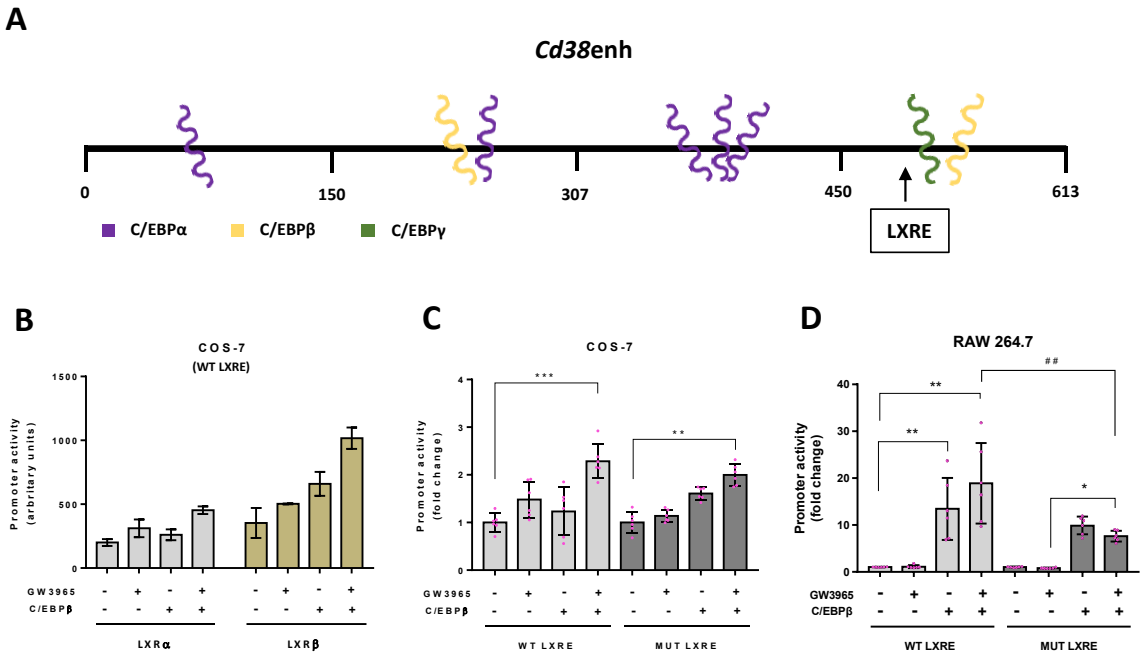

Figure 29. C/EBPβ cooperates with LXRs to induce transcriptional activity from an LXRE-containing enhancer upstream of the *Cd38* gene. (A) Representation of the predicted C/EBP binding sites in the *Cd38*enh by the software Alibaba 2.1. (B-D) Luciferase reporter assays. COS-7 fibroblasts (B, C) or RAW 264.7 macrophages (D) were transiently co-transfected with pGL3-*Cd38*enh containing either a WT LXRE or a mutated (MUT) LXRE (300ng, B; 500ng, C-D), pBluescript-C/EBPβ (or empty pBluescript) (300ng), pcDNA3-LXRβ (300ng, not added to the LXRα condition in B), pcDNA3-LXRα (300ng, only in the LXRα condition in B), pcDNA3-RXRα (300ng), and pRL-TK (100ng). Afterwards, the cells were treated with vehicle (DMSO) or an LXR agonist (GW3965, 1μM) for 24 h. The enhancer activity was quantified by luminescence detection in an Infinite 200 microplate reader (Tecan). Data are represented as luciferase activity normalised by renilla activity, either in absolute values (B) or as fold change to control cells transfected with the same *Cd38*enh fragment (WT or MUT LXRE) (C, D). Mean ± SD of biological duplicates (B) or n=3 independent experiments performed with biological duplicates (C, D). The pink dots indicate the values of each replicate. (C, D) Kruskal-Wallis + Dunn's multiple comparisons. *p < 0.05; **p < 0.01; ***p < 0.001. Selected conditions were also compared through a U Mann-Whitney test $^{\#\#}$p < 0.01.

We wondered if inflammatory stimuli might also collaborate with LXRs in the induction of other LXR target genes. We focused on two LXR target molecules with important immune functions in the inflammatory response: the protein CD5L, which promotes macrophage survival, bactericidal mechanisms, and autophagy (reviewed in Sanjurjo et al., 2015); and MERTK, which promotes the resolution of inflammation by stimulating macrophage-mediated efferocytosis and by inhibiting inflammatory pathways (reviewed in Rothlin et al., 2015). Incubation of macrophages with the LXR agonist T1317 induced the expression of both *Cd5l* and *Mertk* (Figure 30 A, E). Interestingly, TNFα or LPS repressed the expression of *Cd5l* and *Mertk*, whereas IFNγ decreased the expression of *Cd5l* but did not affect *Mertk* (Figure 30 B-H). The concomitant stimulation with the LXR agonist and each inflammatory signal did not result in a net increase in *Cd5l* or *Mertk* compared to the basal expression in most of the analysed conditions. Indeed, inflammatory signalling repressed the LXR-induced expression of *Cd5l* (Figure 30 B-D). Similar effects were observed for *Mertk* in response to LPS or TNFα but not in response to IFNγ (Figure 30 F-H). Of note, the deficiency in C/EBPβ expression did not affect the crosstalk between LXRs and inflammatory signals on *Cd5l* and *Mertk* expression. These findings suggest that the cooperative effects of C/EBPβ and LXRs are selective for *Cd38*.

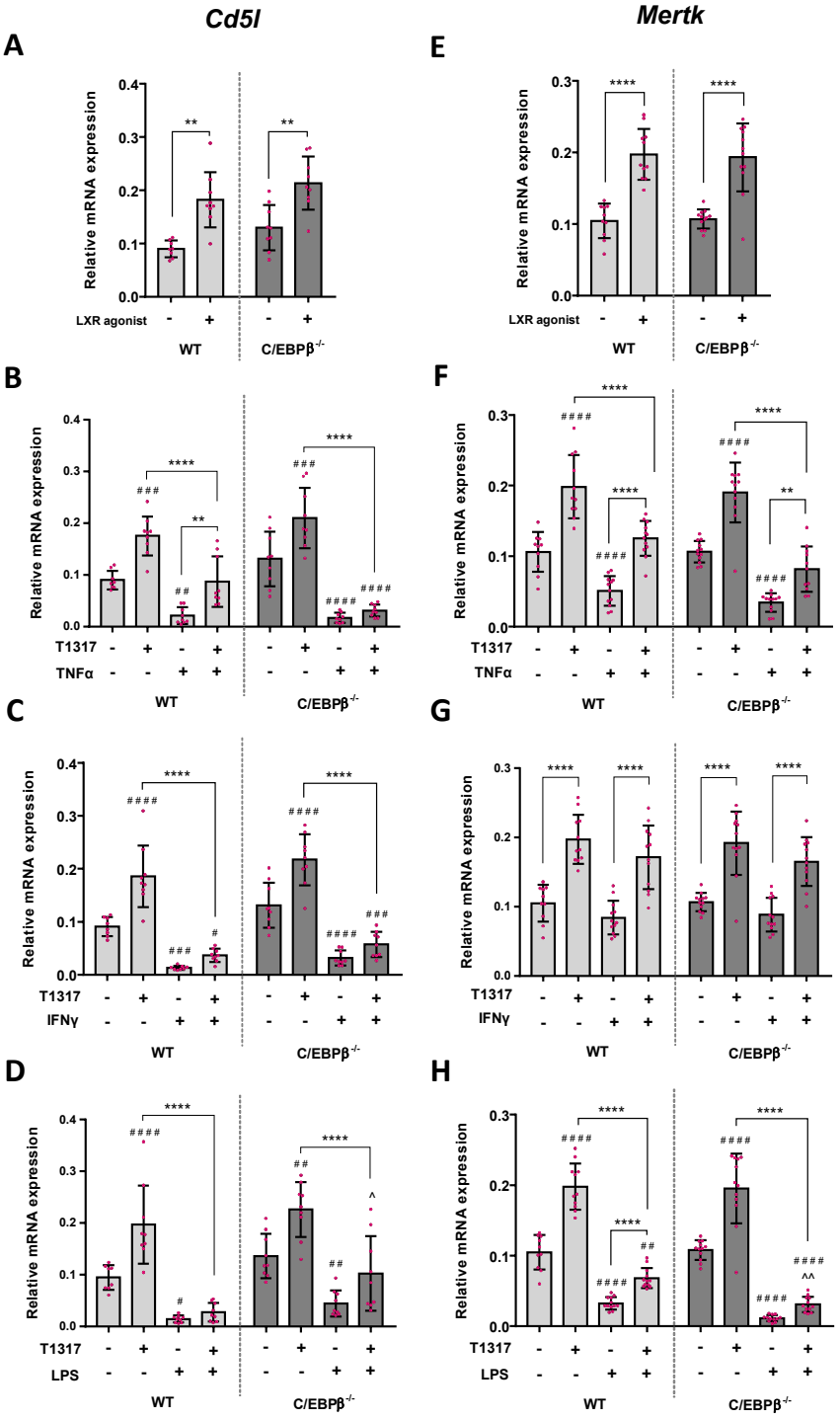

Figure 30. C/EBPβ is not involved in the crosstalk between LXRs and inflammatory signals on *Cd5l* and *Mertk* expression. WT or C/EBPβ-deficient (C/EBPβ$^{-/-}$) BMDMs were treated with vehicle (DMSO) or an LXR agonist (T1317, 1 μM) and/or an inflammatory stimulus: TNFα (20 ng/ml) (B, F), IFNγ (5 ng/ml) (C, G) or LPS (100 ng/ml) (D, H) for 24 h. Gene expression was measured by qPCR and is represented as *Cd5l* (A-D) or *Mertk* (E-H) mRNA levels normalised by *L14* expression. Mean ± SD of n=4 independent experiments performed with biological duplicates or triplicates. The pink dots indicate the values of each replicate. To make different experiments comparable, the statistical mean of all the conditions (including WT and C/EBPβ$^{-/-}$ cells) was calculated for each experiment and used to normalise data by the mean of all the experiments. Kruskal-Wallis test + Dunn's multiple comparisons. **p < 0.01; ****p < 0.0001. $^{\#}$p < 0.05; $^{\#\#}$p < 0.01; $^{\#\#\#}$p < 0.001; $^{\#\#\#\#}$p < 0.0001 *vs* the control of the same genotype. ^p < 0.05; ^^p < 0.01 *vs* the same treatment in WT cells.

3. The activation of LXRs selectively modulates bacterial entry into macrophages

Based on the inhibitory effects of LXR agonists (T1317 and GW3965) on the internalisation of *S.* Typhimurium, we extended the study to analyse the scope of LXR-mediated inhibitory effects on different bacterial species. We introduced some changes in the *in vitro* model of infection. On the one hand, bacteria were used at the exponential phase of growth, when they present the highest metabolic activity, instead of using bacteria in the stationary phase after the overnight culture. In addition, in the experiments with *S.* Typhimurium, we used the strain SL1344. Notably, in previous studies, we had used the strain SV5015, which was originated from the SL1344 strain by a minor modification that eliminated the histidine requirement (Vivero et al., 2008). On the other hand, we prescinded of L-cell (source of macrophage colony-stimulating factor) to avoid conditioning macrophages toward an M2-like phenotype. To estimate the internalisation of bacteria by macrophages we used flow cytometry in most of the studies, as it allows the rapid analysis of a large number of cells, thereby providing high statistical power. However, we are aware of the limitations of this method of analysis. For example, it does not discriminate between intracellular and adhered bacteria, making it necessary to include controls of cell attachment. In addition, the sensitivity might not be enough to detect macrophages infected by one or a few bacteria. Despite these limitations, it is an advantageous analysis technique for our studies and, when required, we used alternative approaches to corroborate the results and complement the information.

3.1 Studies in murine macrophages

3.1.1 LXR activation limits the internalisation of selective species of bacteria by macrophages

To determine whether LXR activation impacts macrophage interactions with different bacterial species, we selected representative Gram-negative and Gram-positive bacteria, precisely, UPEC, EIEC, *L. monocytogenes*, and *S. aureus*. To make bacteria fluorescent for the subsequent detection of infection, Gram-negative bacteria were transformed with a plasmid encoding RFP and Gram-positive bacteria were stained with FITC before each experiment. Murine bone marrow-derived macrophages were treated with vehicle (DMSO) or an LXR agonist (GW3965) for 24 h. Then, they were incubated with bacteria for 30 min at a multiplicity of infection (MOI) between 3 and 15 bacteria per macrophage depending on the bacterial species. Non-internalised bacteria were washed out and macrophages were processed for the quantification

of infection. The results obtained by flow cytometry are represented as the bacterial index, calculated by multiplying the proportion of infected macrophages by the mean intensity of infection in the infected population (determined by the number of bacteria that infect each cell). Interestingly, LXR activation reduced the levels of infection by UPEC and EIEC in addition to *S.* Typhimurium, whereas it did not affect the rates of *L. monocytogenes* or *S. aureus* infection (Figure 31).

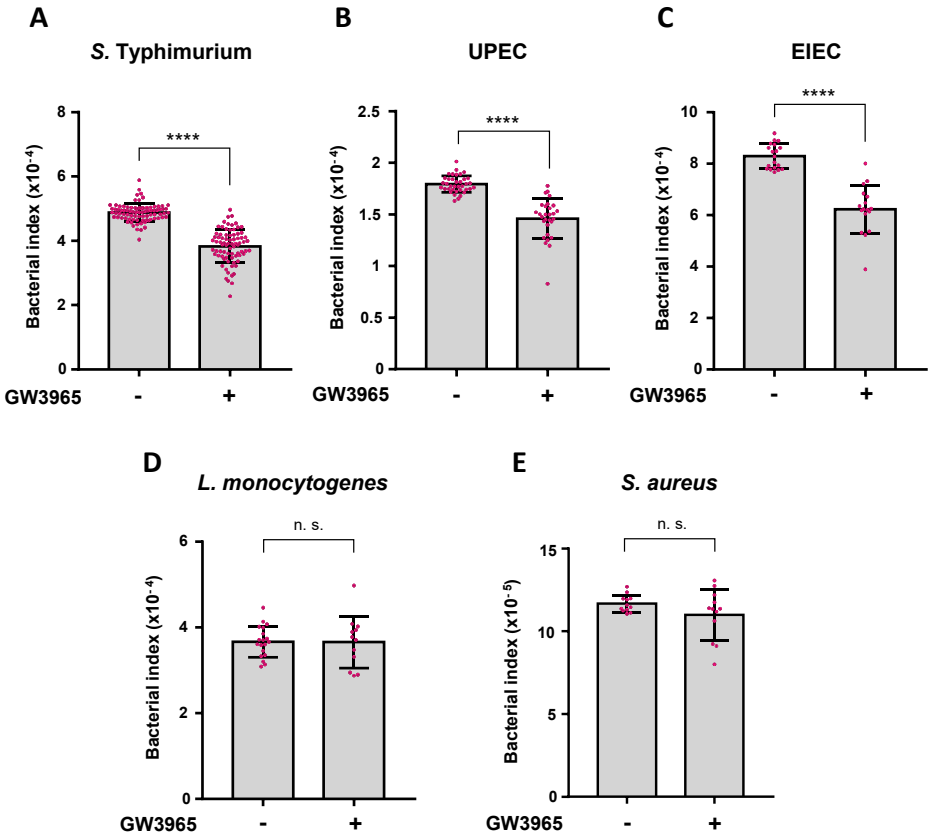

Figure 31. LXRs selectively reduce the internalisation of several bacterial strains by macrophages. BMDMs were treated with vehicle (DMSO) or an LXR agonist (GW3965, 1 µM) for 24 h and exposed for 30 min to the following exponentially grown bacteria: RFP⁺ *S.* Typhimurium (MOI 3) (A), RFP⁺ UPEC (MOI 8) (B), RFP⁺ EIEC (MOI 15) (C), FITC⁺ *L. monocytogenes* (MOI 8) (D), or FITC⁺ *S. aureus* (MOI 5) (E). The non-internalised bacteria were washed out with PBS. Macrophages containing fluorescent bacteria were detected by flow cytometry. The bacterial index in macrophages was obtained with the following formula: (% of bacteria-containing cells) x (mean fluorescence intensity of bacteria in bacteria-containing cells). Mean ± SD of n=28 (A), n=10 (B), n=6 (C), n=4 (D, E) independent experiments, all performed with biological triplicates. The pink dots indicate the values of each replicate. To make different experiments comparable, the statistical mean of the infection index in vehicle (DMSO)-treated cells was used to normalise the data in each experiment by the mean of all the experiments. T-test. ****p < 0.0001; n.s.: non-significant statistical differences.

To check if LXR activation caused differences in the number of macrophages remaining adhered to the plate after infection, we measured the cellularity by crystal violet staining. These assays were performed for those conditions in which LXR activation inhibited the internalisation of

bacteria. No differences were found between control- and LXR agonist-treated cells in any of the analysed conditions, suggesting that the detected differences in infection were not caused by alterations in macrophage viability (Figure 32).

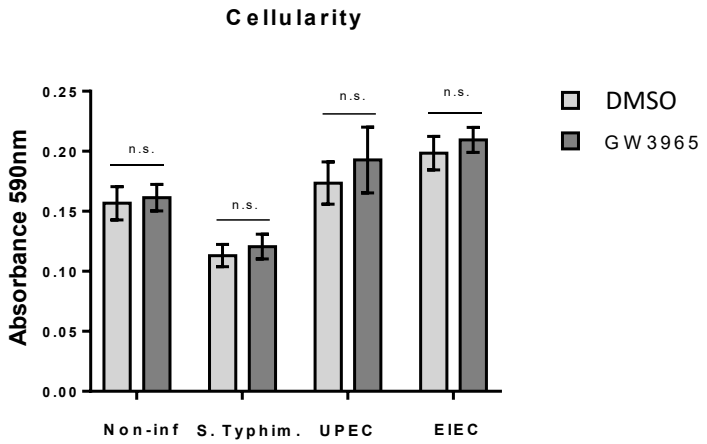

Figure 32. LXR activation does not affect macrophage density after bacterial infection. BMDMs were treated with vehicle (DMSO) or an LXR agonist (GW3965, 1 µM) for 24 h and exposed for 30 min to the following exponentially grown bacteria: *S.* Typhimurium (MOI 3), UPEC (MOI 8), or EIEC (MOI 15). The cells were then stained with crystal violet and the absorbance was measured at 590 nm in an Infinite 200 microplate reader (Tecan). Mean ± SD of n=2-3 independent experiments performed with biological triplicates. To make different experiments comparable, the statistical mean in non-infected cells (including DMSO- and GW3965-treated) was used to normalise the data in each experiment by the mean of all the experiments. Multiple T-tests between vehicle- and GW3965- treated non-infected or infected cells (statistical significance corrected by Holm-Sidak method). n.s.: non-significant statistical differences.

Given that the detection of bacterial fluorescence in macrophages through flow cytometry does not discriminate between intracellular and surface-adhered bacteria, we used an experimental approach to distinguish between these two possibilities. Macrophages were treated with latrunculin A (lat A), an inhibitor of the actin cytoskeleton that prevents phagocytosis (de Oliveira and Mantovani, 1988), or with vehicle. Subsequently, both types of samples were incubated with fluorescent bacteria using equivalent infection conditions and were processed for analysis by flow cytometry. As the bacterial fluorescence detected in lat A-treated macrophages reflected only bacterial adhesion (they were unable to internalise bacteria), we compared the rates of fluorescent cells in lat A-treated *vs* vehicle-treated macrophages. The percentage of bacteria-containing macrophages in vehicle-treated cells was established as 100%, and the proportion of macrophages with adhered bacteria in lat A-treated cells was calculated as the ratio to it: % macrophages containing adhered bacteria = [(lat A-treated % RFP+ macrophages) / (untreated % RFP+ macrophages) x 100] (Figure 33 A). The results showed that for all the bacteria analysed, the rate of fluorescent macrophages due to bacterial adhesion accounted for 5% - 15% of total fluorescent macrophages (containing internalised + adhered bacteria). That is,

most of the macrophages detected as positive for bacterial fluorescence contained successfully internalised bacteria. Importantly, the treatment with lat A did not affect cell viability (Figure 33 B).

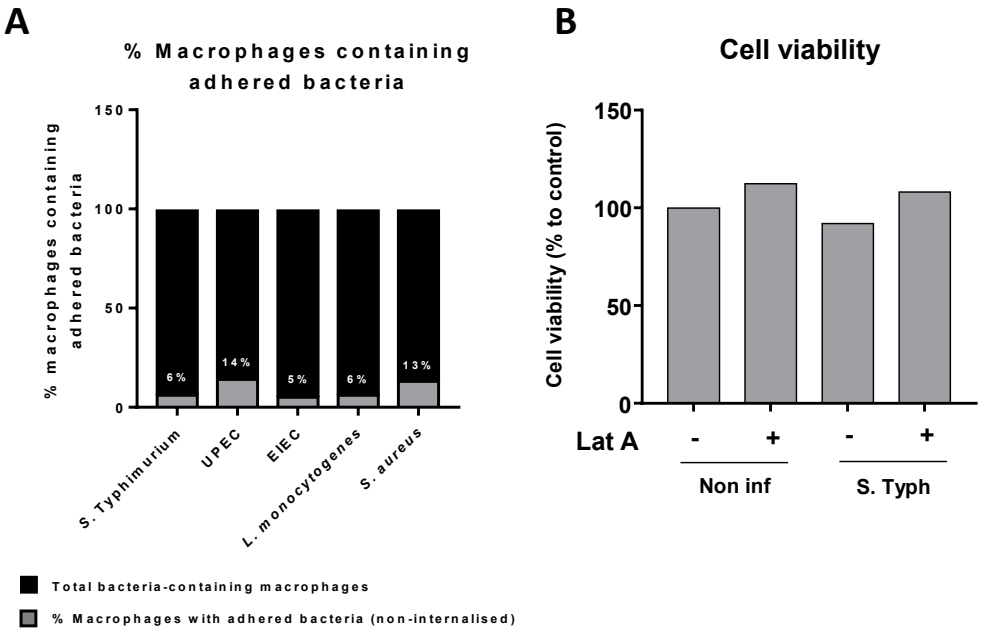

Figure 33. Most macrophages contain internalised bacteria upon infection. BMDMs were incubated with either latrunculin A (Lat A) (1µM) or vehicle (DMSO) for 1 h. Macrophages were then exposed for 30 min to exponentially grown bacteria: RFP$^+$ *S.* Typhimurium (MOI 3) (A, B), RFP$^+$ UPEC (MOI 8) (A), RFP$^+$ EIEC (MOI 15) (A), FITC$^+$ *L. monocytogenes* (MOI 8) (A), or FITC$^+$ *S. aureus* (MOI 5) (A). (A) Macrophages containing fluorescent bacteria were detected by flow cytometry. For each type of bacterium, the proportion of Lat A-treated macrophages exhibiting RFP fluorescence (grey bars), which cannot internalise bacteria and thus contain adhered bacteria, is represented respect to the total bacteria-containing vehicle-treated macrophages (black bars). Mean of n=1-2 independent experiments performed with biological duplicates or triplicates. (B) Non-infected or *S.* Typhimurium-infected cells (infected as described above) were stained with the LIVE/DEAD Fixable Near-IR Dead Cell Stain Kit for 633 or 635 nm (Thermo Fisher Scientific). Dead cells were detected by flow cytometry. The viable cells (non-stained) are represented as the proportion to the vehicle-treated non-infected cells. Bars represent the values obtained from one experiment.

We also evaluated the internalisation of bacteria by confocal microscopy (Figure 34). In line with the results obtained by flow cytometry, the counting of intracellular bacteria showed that LXRs selectively inhibited the entry of *S.* Typhimurium, UPEC, and EIEC into macrophages (Figure 35). In addition, we counted the number of viable intracellular bacteria after infecting the macrophages for 30 min and subsequently killing the extracellular bacteria by incubation with gentamycin for 1 h. The cells were then lysed and seeded for CFU counting. In line with the previous results, LXR activation diminished the load of *S.* Typhimurium, UPEC, and EIEC but not of *L. monocytogenes* or *S. aureus* (Figure 36). Surprisingly, the numbers of viable intracellular *S. aureus* increased upon LXR activation, a trend that was also perceptible in determination of intracellular bacteria by confocal microscopy.

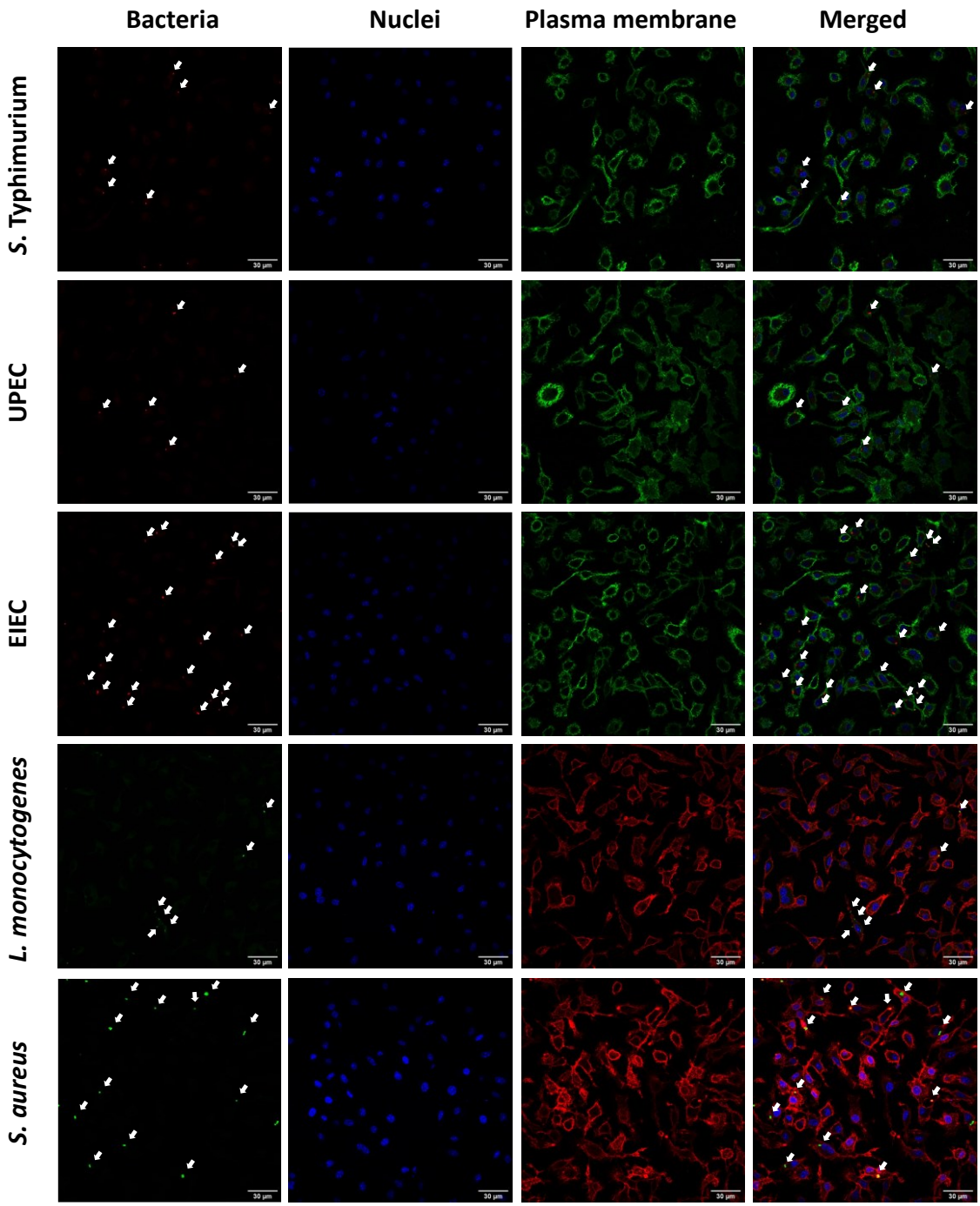

Figure 34. Confocal microscopy images from macrophages infected by different bacterial species. A representative section of vehicle-treated macrophages incubated with bacteria is shown (unique z position). BMDMs were incubated for 30 min with the following exponentially grown bacteria: RFP$^+$ *S*. Typhimurium (MOI 3), RFP$^+$ UPEC (MOI 8), RFP$^+$ EIEC (MOI 15), FITC$^+$ *L. monocytogenes* (MOI 8), or FITC$^+$ *S. aureus* (MOI 5). Cell membranes were stained with WGA-488 (in cells infected with *S*. Typhimurium, UPEC, and EIEC) (green) or WGA-555 (in cells infected *L. monocytogenes* and *S. aureus*) (red). Cell nuclei were stained with Hoechst 33342 (blue). Scale bars = 30µm.

A

Bacterial species	Treatment	Total non-infected macrophages	Total infected macrophages	p-value	Statistical significance
S. Typhimurium	DMSO	149	70	0,0002	***
	GW3965	147	27		
UPEC	DMSO	502	58	0,0003	***
	GW3965	569	28		
EIEC	DMSO	248	252	0,0408	*
	GW3965	271	211		
L. monocytogenes	DMSO	407	70	0,7151	n.s.
	GW3965	384	71		
S. aureus	DMSO	405	109	0,0639	n.s.
	GW3965	312	112		

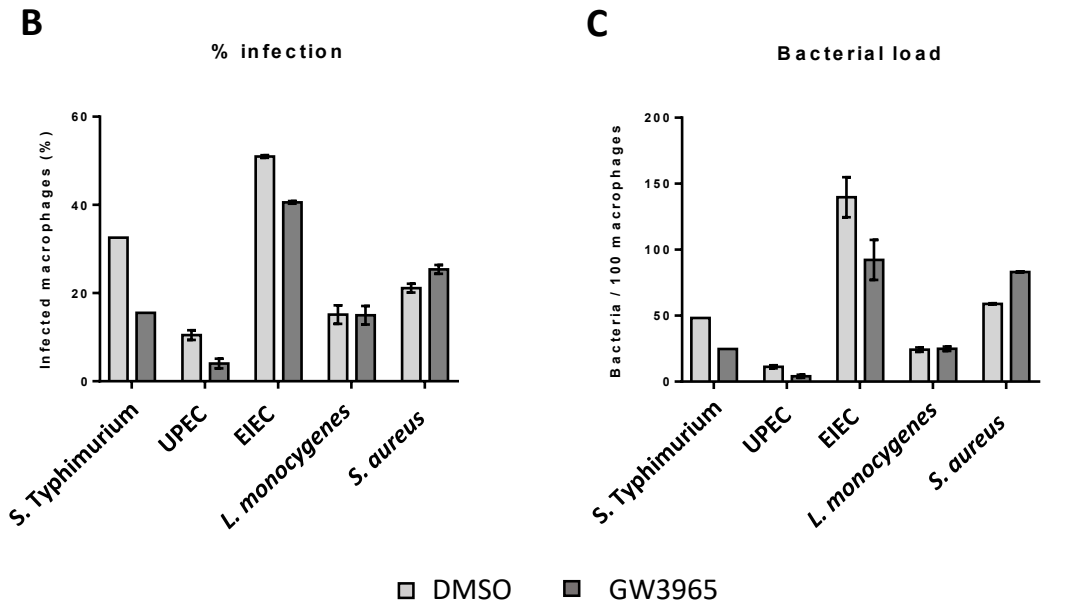

Figure 35. Selective inhibitory effects of LXR activation on bacterial internalisation by macrophages. BMDMs were treated with vehicle (DMSO) or an LXR agonist (GW3965, 1 µM) for 24 h and exposed for 30 min to the following exponentially grown bacteria: RFP^+ *S.* Typhimurium (MOI 3), RFP^+ UPEC (MOI 8), RFP^+ EIEC (MOI 15), $FITC^+$ *L. monocytogenes* (MOI 8), or $FITC^+$ *S. aureus* (MOI 5). Internalised fluorescent bacteria in macrophages were manually counted on images along the z-axis (one image every 0.5µm) obtained by confocal microscopy. The data represent the total number of macrophages obtained from 5-7 microscopy fields per sample from n=1 (*S*. Typhimurium) or n=2 (UPEC, EIEC, *L. monocytogenes*, and *S. aureus*) independent experiments. (A) The numbers of infected and non-infected macrophages were compared between vehicle- and GW3965-treated samples in a contingency table and analysed by the Fisher's exact test. (B, C) Mean ± SD of the percentage of infected cells (B) or the number of bacteria per 100 macrophages (C). To make different experiments comparable, the statistical mean of the experiment (including vehicle- and GW3965-treated cells) was used to normalise the data in each experiment by the mean of all the experiments. *$p < 0.05$; ***$p < 0.001$; n.s.: non-significant statistical differences.

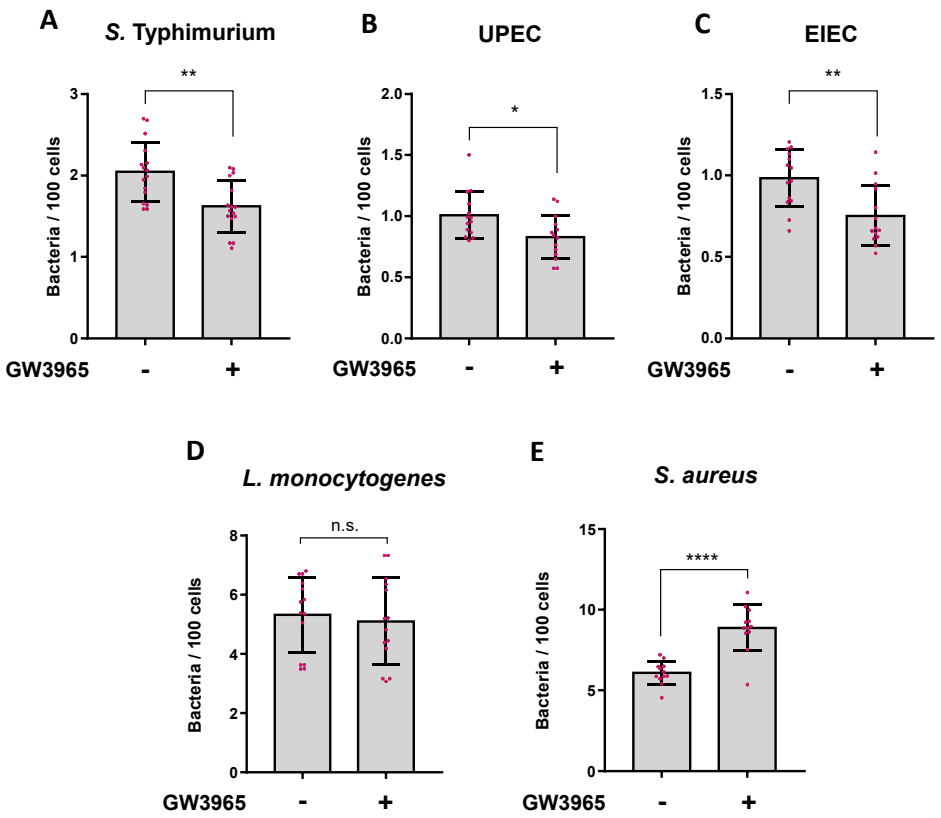

Figure 36. LXR activation selectively inhibits bacterial internalisation by macrophages. BMDMs were treated with vehicle (DMSO) or an LXR agonist (GW3965, 1 µM) for 24 h and exposed for 30 min to the following exponentially grown bacteria: *S*. Typhimurium (MOI 3) (A), UPEC (MOI 8) (B), EIEC (MOI 15) (C), *L. monocytogenes* (MOI 8) (D), or *S. aureus* (MOI 5) (E). Macrophages were lysed with 0.5% Triton X-100 and diluted in 2xYT before plating them on agar-LB plates for subsequent growth at 37°C. Viable intracellular bacteria per 100 cells were estimated from the count of CFUs in agar-LB plates corrected by the dilution factor and the number of macrophages per sample. Mean ± SD of n=8 (A), n=7 (B, C, D), or n=6 (E) independent experiments, all performed with biological duplicates. The pink dots indicate the values of each replicate. To make different experiments comparable, the statistical mean of the experiment (including vehicle- and GW3965-treated cells) was used to normalise data in each experiment by the mean of all the experiments. T-test. *p < 0.05; **p < 0.01; ****p < 0.0001; n.s.: non-significant statistical differences.

Next, we analysed the impact of LXR activation in the phagocytosis of latex microspheres of similar size to bacteria (3µm diameter). In this case, the LXR agonist did not affect the phagocytosis of latex microspheres (Figure 37 A). To evaluate if the changes induced by LXRs in macrophages to modulate selective particle internalisation can discriminate between two different target particles when found together, we incubated the cells simultaneously with *S.* Typhimurium and latex microspheres, either in the presence or absence of an LXR agonist. Interestingly, the combination of *Salmonella* and microspheres altered the internalisation of each other in opposite directions (Figure 37). Compared to the phagocytosis rate of each type of particle individually, the phagocytosis of microspheres increased in the presence of *Salmonella*, whereas the bacterial entry decreased in the presence of latex beads. Despite the

reciprocal impact of co-incubation of microspheres and *Salmonella*, the activation of LXRs reduced selectively the internalisation of bacteria and left the phagocytosis of microspheres unaffected. Collectively, these results suggest that LXRs alter specific mechanisms of internalisation or invasion activated by particular types of bacteria rather than affecting common aspects of phagocytosis.

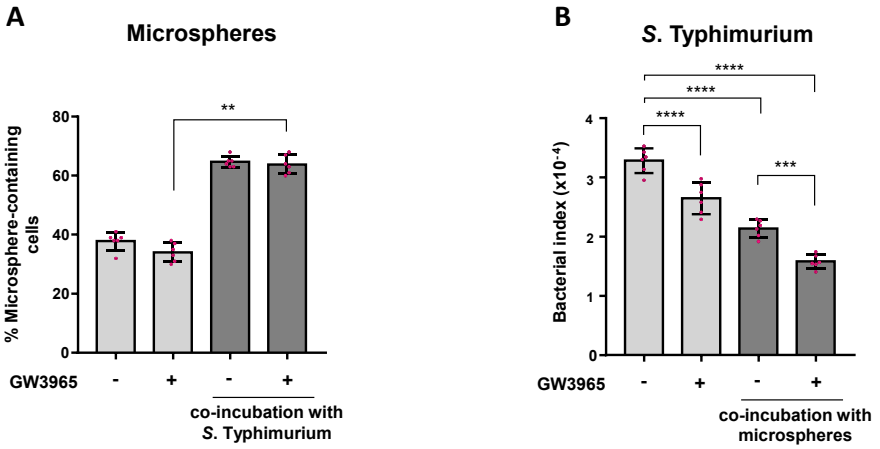

Figure 37. Activation of LXRs in macrophages selectively reduces the internalisation of *S.* Typhimurium but not of latex microspheres. BMDMs were treated with vehicle (DMSO) or an LXR agonist (GW3965, 1 µM) for 24 h and exposed during 30 min to exponentially grown S. Typhimurium (MOI 3), latex microspheres (5 microspheres per cell), or both. Internalised *S.* Typhimurium (RFP$^+$) and/or Fluoresbrite YG microspheres (Polysciences) were detected by flow cytometry. The graphs represent either the proportion of microsphere-containing cells (A) or of the bacterial index of *S.* Typhimurium (B) measured in the same experiment. Bacterial index = (% of bacteria-containing cells) x (mean fluorescence intensity of bacteria in bacteria-containing cells). Mean ± SD of n=3 independent experiments performed with biological duplicates. The pink dots indicate the values of each replicate. To make different experiments comparable, the statistical mean of all the conditions was calculated and used to normalise data in each experiment by the mean of all the experiments. (A) Kruskal-Wallis + Dunn's test. (B) One-way ANOVA + Sidak's test. **p < 0.01; ***p < 0.001; ****p < 0.0001.

3.1.2 Mechanisms mediating the restriction of *Salmonella* internalisation by LXRs

In this work, we have extended our studies to further decipher the molecular mechanisms responsible for LXR-mediated inhibition of bacterial entry. As explained above, our group discovered that LXR activation reduced the internalisation of *S.* Typhimurium by macrophages in a CD38-dependent manner and that the modulation of intracellular NAD^+ levels impacted bacterial entry (Matalonga et al., 2017). Therefore, our working model included the idea that the increased NAD^+ glycohydrolase (NADase) activity of CD38 and the resulting drop in intracellular NAD^+ levels would represent an important mechanism limiting the internalisation of bacteria upon LXR activation. To check this hypothesis, we compared the impact of LXR activation in WT BMDM and in BMDM from transgenic mice that contained an inactivating mutation in the catalytic site of the NADase activity of CD38 (hereafter named CD38 CI

macrophages) (Tarragó et al., 2018). To our surprise, LXR activation reduced *Salmonella* engulfment to a similar extent in CD38 CI and WT macrophages (Figure 38 A). In front of these results, we evaluated if CD38 expression was required for the inhibitory effect of LXRs on infection by exponentially grown bacteria. Unexpectedly, we found that, under these conditions, LXR activation reduced the uptake of *S.* Typhimurium similarly in WT and CD38$^{-/-}$ macrophages (Figure 38 B). In addition, LXRs also restrained UPEC and EIEC infection independently of CD38 (Figure 38 C,D). Therefore, even if CD38 expression contributed to limiting bacterial entry upon LXR activation in previous experiments using stationary phase bacteria, the mechanisms involved in the current experimental setting are independent of functional CD38 expression.

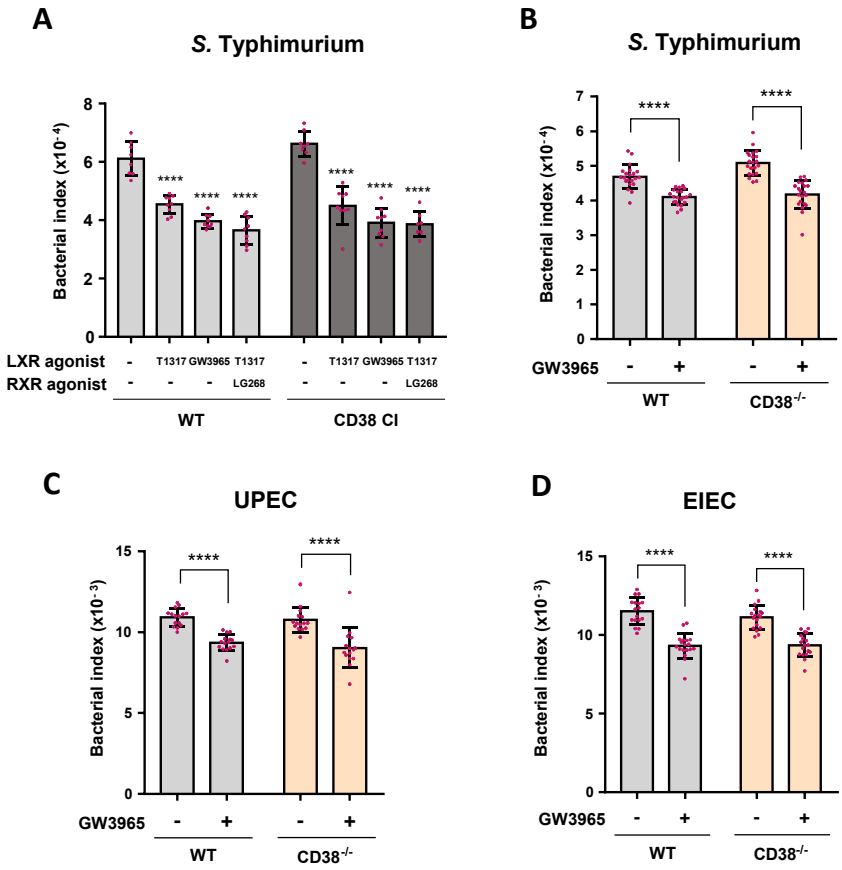

Figure 38. The inhibitory effect of LXR activation on the internalisation of exponentially grown *S.* Typhimurium by macrophages does not require the NADase activity or functional expression of CD38. WT, CD38 catalytically inactive (CD38 CI) (A), or CD38-deficient (CD38$^{-/-}$) (B-D) BMDMs were treated for 24 h with vehicle (DMSO) or an LXR agonist (T1317 or GW3965, 1 µM). In A, some samples were treated with a combination of an LXR agonist (T1317, 1µM) and an RXR agonist (LG268, 1µM) for 24 h. Macrophages were then exposed for 30 min to exponentially grown RFP^{+} *S.* Typhimurium (MOI 3) (A, B), RFP^{+} UPEC (MOI 8) (C), or RFP^{+} EIEC (MOI 15) (D) and the infection rate was measured by flow cytometry. Bacterial index = (% of bacteria-containing cells) x (mean fluorescence intensity of bacteria in bacteria-containing cells). Mean ± SD of n=3 (A), n=7 (B), n=5 (C), or n=6 (D) independent experiments, all performed with biological triplicates. The pink dots indicate the values of each replicate. To make different experiments comparable, the statistical mean of all the conditions in each genotype was calculated and used to normalise data by the genotype mean of all the experiments for that genotype. Two-way ANOVA + Sidak's test to compare treatments in each genotype. ****p < 0.0001 between the indicated conditions (B-D) or *vs* vehicle-treated cells (A).

Thereafter, we explored additional mechanisms by which LXRs could be selectively reducing bacterial internalisation. To start, we tested which LXR isoforms were involved in the inhibitory effects on infection. We differentiated macrophages from WT, LXRα-deficient (LXRα$^{-/-}$), LXRβ-deficient (LXRβ$^{-/-}$), or LXRα/β-deficient (LXR$^{-/-}$) murine bone marrows and incubated them with *S.* Typhimurium. The LXR agonist GW3965 decreased the infection in WT, LXRα$^{-/-}$, and LXRβ$^{-/-}$ macrophages (Figure 39). LXR activation inhibited bacterial entry at similar rates in WT and LXRα$^{-/-}$ macrophages (around 18% reduction), but it had a weaker effect in LXRβ$^{-/-}$ macrophages (12% reduction). Therefore, although both LXR isoforms can mediate the interference with bacterial internalisation, LXRβ seems to contribute more prominently to this effect. The unresponsiveness of LXR$^{-/-}$ macrophages to the LXR agonist corroborates that the effects described here are LXR-specific.

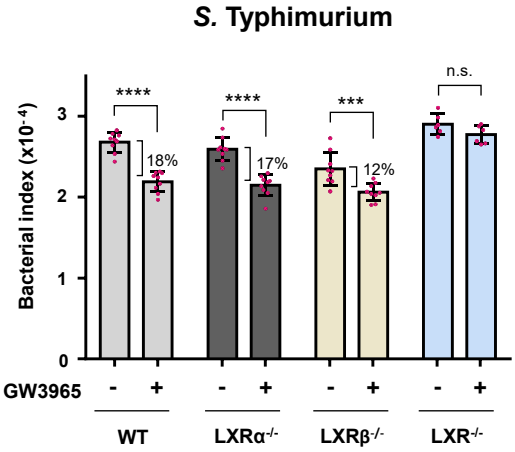

Figure 39. LXRα and LXRβ contribute to reduce bacterial internalisation by macrophages. WT, LXRα-deficient (LXRα$^{-/-}$), LXRβ-deficient (LXRβ$^{-/-}$), or LXRα/β-deficient (LXR$^{-/-}$) BMDMs were treated with vehicle (DMSO) or an LXR agonist (GW3965, 1 µM) for 24 h and exposed to exponentially grown *S.* Typhimurium for 30 min (MOI 3). Internalised RFP^{+} *S.* Typhimurium was detected by flow cytometry. Bacterial index = (% of bacteria-containing cells) x (mean fluorescence intensity of bacteria in bacteria-containing cells). Mean ± SD of n=2-3 independent experiments performed with biological triplicates. The pink dots indicate the values of each replicate. The percentage of reduction of bacterial infection by the LXR agonist is shown for each genotype. To make different experiments comparable, the statistical mean of the infection index in vehicle-treated cells of WT, LXRα$^{-/-}$, and LXRβ$^{-/-}$ cells was calculated and used to normalise the data in each experiment by the mean of all the experiments. Two-way ANOVA + Sidak's test between treatments of each genotype. ***p < 0.001; ****p < 0.0001; n.s.: non-significant statistical differences.

A study performed by Ito and colleagues (Ito et al., 2015a) revealed that the cholesterol efflux mediated by increased ABCA1 expression in LXR agonist-treated macrophages altered the properties of membrane microdomains in which TLRs are embedded, resulting in impaired downstream signalling upon TLR engagement. We hypothesised that cholesterol modulation by LXRs could also affect the properties of phagocytic or signalling receptors involved in bacterial phagocytosis or invasion. To begin, we examined whether there is a relation between the cellular cholesterol levels and the infection by *Salmonella*. In these assays, macrophages were

infected as described above and unesterified cholesterol in macrophages was stained with filipin. Subsequently, the infection by RFP$^+$ bacteria and the free cholesterol content in the cells were detected by flow cytometry. Using data obtained by flow cytometry, macrophages were segregated according to the infection levels into non-infected cells, infected cells, or highly infected cells (15% of cells with the highest RFP intensity from *Salmonella*) (Figure 40).

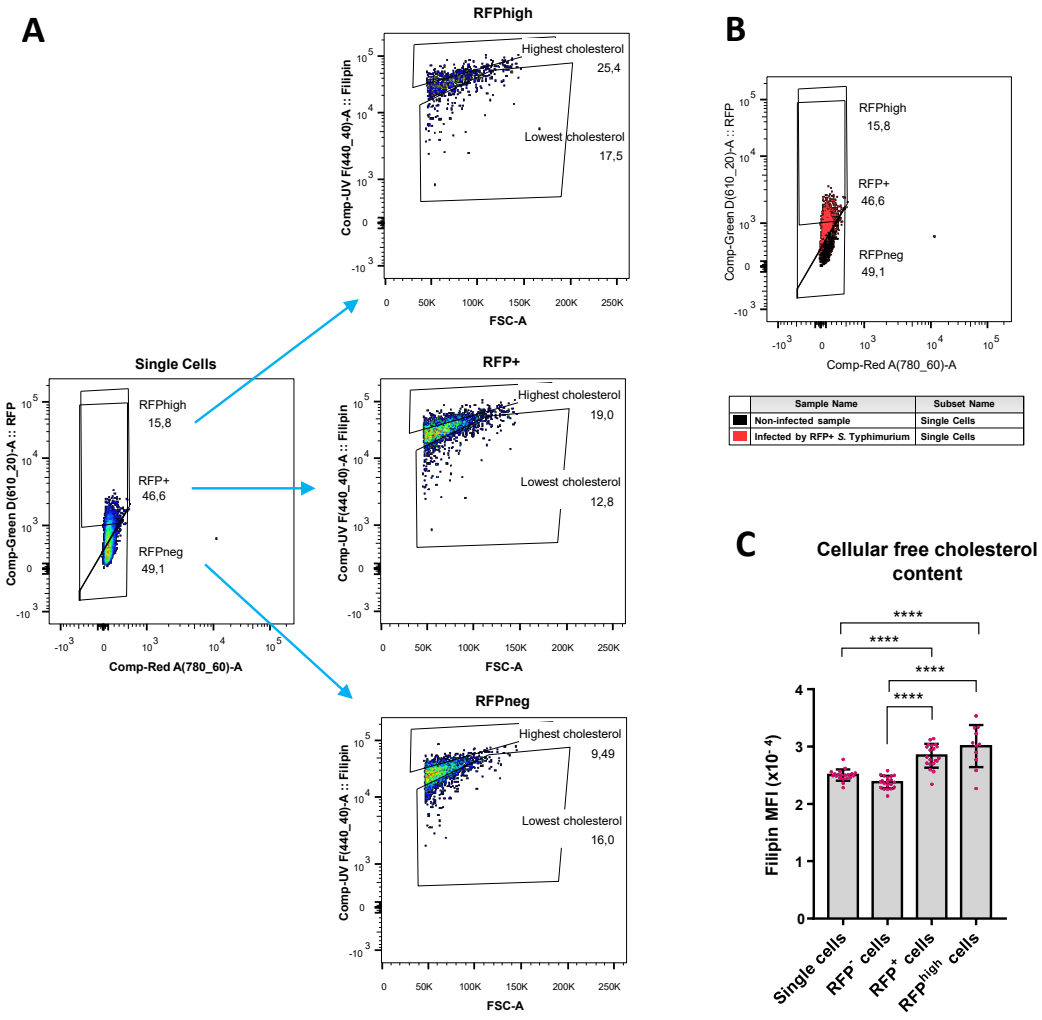

Figure 40. The extent of *S.* Typhimurium internalisation is associated with the cellular cholesterol levels. BMDMs were exposed to exponentially grown *S.* Typhimurium for 30 min (MOI 3). After cell fixation, the unesterified cholesterol in macrophages was stained with filipin. RFP$^+$ *S.* Typhimurium and filipin were detected by flow cytometry. (A) Gating strategy followed to segregate macrophage populations depending on bacterial infection: non-infected (RFP-neg), total infected (RFP+), and highly infected (RFPhigh) cells. To detect infected macrophages with the highest sensitivity, the RFP fluorescence from bacteria is plotted vs the general autofluorescence of eukaryotic cells in a non-overlapping channel. The mean fluorescence intensity (MFI) of filipin in each of these populations was used as an indicator of the cellular cholesterol content. The gates "highest cholesterol" and "lowest cholesterol" are just informative and were not further analysed. (B) Representative flow cytometry plot showing the superposition of a non-infected sample (black) and a sample incubated with S. Typhimurium (red). (C) The cellular cholesterol levels of each infection group are represented. Mean ± SD of n=7 independent experiments performed with biological duplicates or triplicates (n=4 in the RFPhigh group). The pink dots indicate the values of each replicate. The statistical mean of MFI in single cells was used to normalise the data in each experiment by the mean of all the experiments. One-way ANOVA + Tukey's test. ****p < 0.0001.

Interestingly, infected cells contained higher cholesterol levels than the non-infected ones, and even a greater upward tendency in cholesterol levels was observed in highly infected cells.

Then, we measured the content of free cholesterol in macrophages treated with the vehicle or an LXR agonist. In line with the role of LXRs promoting cholesterol efflux, the LXR agonist reduced the levels of free cholesterol in macrophages (Figure 41 A). We took a closer look at the impact of cellular cholesterol modulation on bacterial infection using cyclodextrins. To extract cholesterol from the plasma membrane, we used methyl-β-cyclodextrin (MβCD). The compound was added to the cell cultures prior to the incubation with bacteria in conditions that did not reduce the viability of macrophages (Figure 41 B). Treatment of macrophages with MβCD prominently reduced the free cholesterol levels in macrophages and led to an abrupt decrease in *Salmonella* infection, reaching a reduction of 75% compared to control cells (Figure 41 C,D). Moreover, the reduction of unesterified cholesterol and *Salmonella* internalisation caused by MβCD occurred in a dose-dependent manner (Figure 41 E,F). By contrast, cholesterol depletion did not alter latex microsphere phagocytosis, suggesting that changes in cholesterol do not affect unspecific phagocytosis (Figure 41 G). Inversely, loading the plasma membrane of macrophages with cholesterol using cholesterol complexed with MβCD (Chol-MβCD) resulted in higher bacterial load in concert with elevated cellular free cholesterol levels, supporting the notion that cholesterol modulates bacterial internalisation (Figure 41 H,I).

Lipid rafts are dynamic assemblies of cholesterol, sphingolipids, and proteins that, among other functions, modulate intracellular signalling from the plasma membrane of immune cells (reviewed in Varshney et al., 2016). The role of cholesterol in regulating bacterial entry into macrophages prompted us to analyse the abundance of lipid rafts in our infection model. We used a fluorochrome-conjugated cholera toxin B subunit that binds to monosialotetrahexosylganglioside (GM1) as a marker of lipid rafts (Holmgren, 1973). Lipid raft staining in LXR agonist-treated macrophages did not show differences compared to control cells (Figure 42 A). However, the categorisation of cells according to the levels of infection revealed that the infected cells displayed higher lipid raft staining than the non-infected cells, indicating a possible link between the abundance of lipid rafts and bacterial internalisation (Figure 42 B). Indeed, various types of bacteria preferentially interact with lipid rafts to mediate host cell invasion (Hartlova et al., 2010). In the case of *Salmonella*, some studies have suggested that this bacterium requires plasma membrane cholesterol to enter non-phagocytic cells and uses the type three secretion system 1 (T3SS-1) to accumulate membrane cholesterol at bacterial entry sites (Garner et al., 2002; Hayward et al., 2005). For this reason, we tested if LXRs exert their

inhibitory actions on bacterial entry by modifying the interactions between the T3SS-1 of

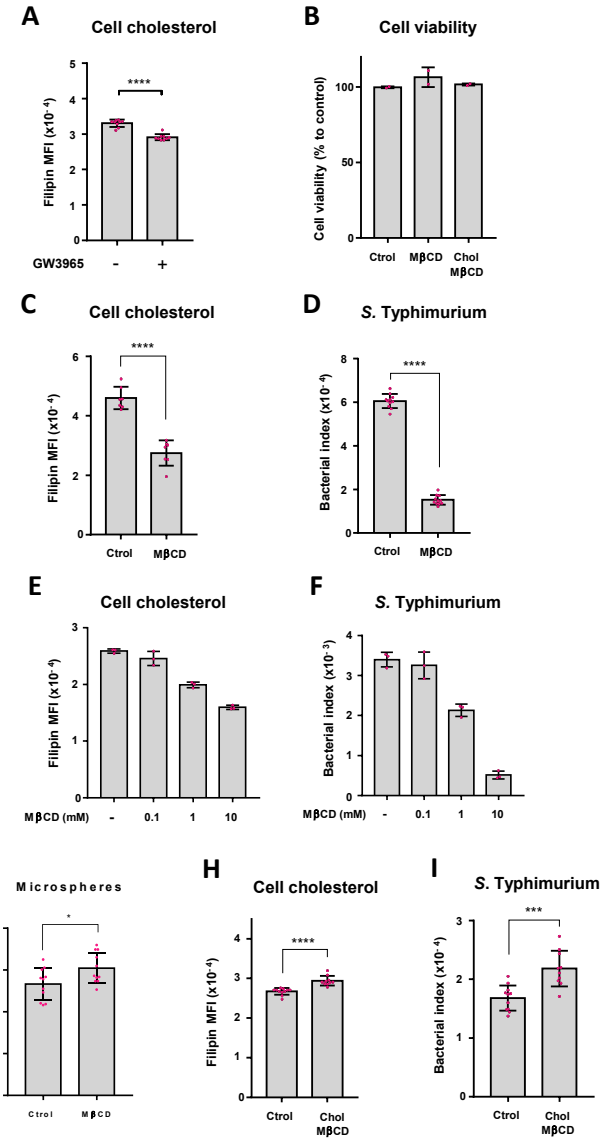

Figure 41. The modulation of plasma membrane cholesterol impacts *S*. Typhimurium internalisation but not the phagocytosis of latex microspheres. (A) BMDMs were treated with vehicle (DMSO) or an LXR agonist (GW3965, 1 µM) for 24 h. (B-G) Macrophages were treated with methyl-beta cyclodextrin (MβCD, 10mM or the indicated concentrations, 1 h) (B-F) or cholesterol-complexed MβCD (Chol MβCD, 100µM, 2 h) (B, H, I). (B) The cells were stained with the LIVE/DEAD Fixable Near-IR Dead Cell Stain Kit for 633 or 635 nm (Thermo Fisher Scientific). Dead cells were detected by flow cytometry. The proportion of viable cells (non-stained) respect to the vehicle-treated cells is represented. (C-I) Macrophages were exposed to exponentially grown RFP$^+$ *S*. Typhimurium (MOI 3) (C-F, H, I) or Fluoresbrite YG microspheres (Polysciences) (5 beads/macrophage) (G) for 30 min. (A, C, E, H) Cholesterol was was stained on fixed samples using filipin. Cell viability (B), *S*. Typhimurium infection (bacterial index) (D, F, I) and cell cholesterol levels (Filipin MFI) (C, E, H) were measured by flow cytometry. Bacterial index = (% of bacteria-containing cells) x (mean fluorescence intensity of bacteria in bacteria-containing cells). Mean ± SD of n=3 (A, C), n= 1 (B, E, F), n=3 (C), n=5 (D, G), and n=4 (H, I) independent experiments performed with biological duplicates or triplicates. The pink dots indicate the values of each replicate. To make different experiments comparable, in A, C, D, G, and H, the statistical mean of all the conditions was calculated and used to normalise the data by the mean of all the experiments. (A, G) Mann-Whitney U test, (C, D, H, I) T- test. *p < 0.05 ***p < 0.001; ****p < 0.0001.

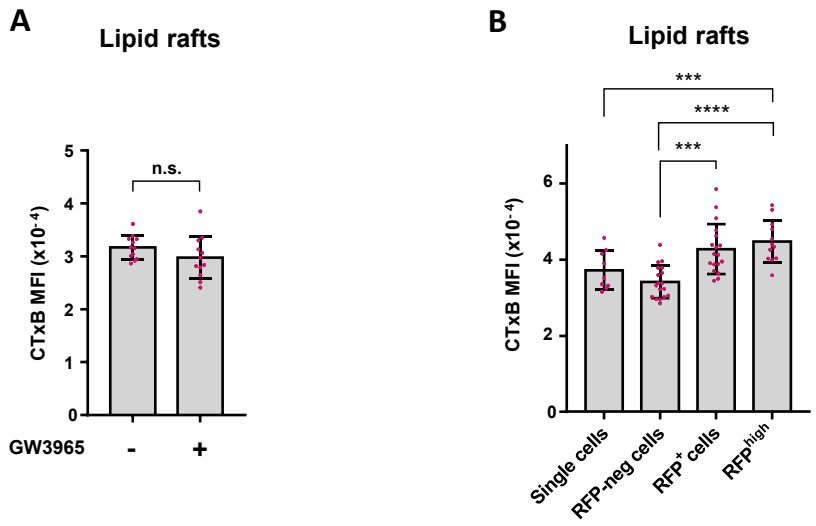

Figure 42. The abundance of lipid rafts may influence bacterial internalisation. (A) BMDMs were treated with vehicle (DMSO) or an LXR agonist (GW3965, 1 µM) for 24 h. (B) Macrophages were exposed to exponentially grown RFP⁺ *S.* Typhimurium for 30 min (MOI 3). (A, B) Lipid rafts were stained in with Cholera Toxin Subunit B, CF633 conjugate (Biotium) (CTxB). Lipid raft staining (A, B) and infection (B) were measured by flow cytometry. (B) The RFP⁺ populations are segregated as described for cholesterol evaluation (see Fig. 40) and the CTxB MFI in each cell population is represented. Mean ± SD of n=4 (A) or n= 3 (B) independent experiments performed with biological triplicates. The pink dots indicate the values of each replicate. To make different experiments comparable, the statistical mean of both treatments (A) or single cells (B) in each experiment was calculated and used to normalise the data by the mean of all the experiments. T test (A) or one-way ANOVA + Tukey's test (B). ***p < 0.001; ****p < 0.0001. n.s.: non-significant statistical differences.

Salmonella and the membrane of macrophages. With that purpose, we obtained a mutant *S.* Typhimurium strain that lacks the invG protein of the T3SS-1 (hereafter named invG bacteria), which results in an inability to assemble the T3SS and secrete effector proteins (Kaniga et al., 1994). Compared to WT bacteria, the internalisation of invG bacteria by macrophages decreased more than 50%, reflecting the great contribution of the T3SS-1 to the bacterial entry (Figure 43). Nevertheless, the activation of LXRs reduced macrophage internalisation by both bacterial strains at similar rates in comparison with vehicle-treated cells. Therefore, we conclude that the T3SS-1 is not responsible for the susceptibility of *Salmonella* to LXR-mediated inhibition. Alternative experimental methods could help to elucidate the impact of LXR activation on the structure or organisation of lipid rafts as well as the potential involvement of lipid rafts in the activation of signalling pathways from phagocytic or other receptors activated by bacteria.

Both phagocytosis and bacteria-induced invasion require the proper coordination of actin-modulating proteins (Popoff, 2014; Rosales and Uribe-Querol, 2017). Rho family of small GTPases are molecular switchers that display key functions during these processes and are targeted by many bacteria to manipulate host cell responses. Based on these facts, we assessed the activity of three major Rho GTPases involved in various internalisation pathways, namely,

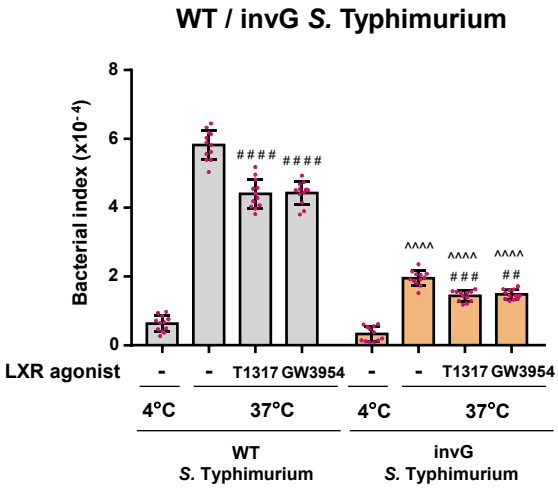

Figure 43. LXR activation does not exert the inhibitory effect on *S.* Typhimurium internalisation by interference with the T3SS-1. BMDMs were treated with vehicle (DMSO) or an LXR agonist (T1317 or GW3965, 1 μM) for 24 h. Macrophages were then exposed to exponentially grown WT or invG mutant (invG) RFP$^+$ *S.* Typhimurium for 30 min (MOI 3). Macrophages incubated at 4°C were used as a control for bacterial adhesion. Infection was detected by flow cytometry. Bacterial index = (% of bacteria-containing cells) x (mean fluorescence intensity of bacteria in bacteria-containing cells). Mean ± SD of n=4 independent experiments performed with biological triplicates. The pink dots indicate the values of each replicate. To make different experiments comparable, the statistical mean of all the conditions with each bacterial strain was calculated and used to normalise data by the mean of all the experiments. Two-way ANOVA + Tukey's test. $^{\#\#}p < 0.01$; $^{\#\#\#}p < 0.001$; $^{\#\#\#\#}p < 0.0001$ *vs* vehicle-treated cells of the same genotype. $^{\wedge\wedge\wedge\wedge}p < 0.0001$ *vs* the same condition in macrophages infected by WT *S.* Typhimurium.

Rac1, Cdc42, and RhoA. The levels of active (GTP-bound) Rac1 increased after 5 min of incubation with *S.* Typhimurium (Figure 44). However, Rac1-GTP levels were not affected by LXR activation. Based on the time interval required to detect Rac1 activation, we measured the activation of the other Rho GTPases at 5 and 10 min post-infection. However, the replicates presented high variability in Cdc42 activity and we did not detect RhoA activity in our cellular model (data not shown). Although we were not able to obtain conclusive results in this set of experiments, exploring the role of Rho GTPases in the modulation of bacterial phagocytosis by LXRs deserves further attention in the future.

We also evaluated whether LXRs alter other intracellular signalling pathways activated by bacteria. The PI3K/AKT pathway is modulated by diverse extracellular stimuli and controls metabolic and immune processes contributing to determine the macrophage phenotype (reviewed in Vergadi et al., 2017). In a time-course experiment measuring the levels of active (phosphorylated) AKT 1 by western blot, we detected a progressive increase of AKT 1 activation after 5, 15, and 30 min of *Salmonella* infection (Figure 45 A). Nevertheless, the treatment of the cells with the LXR agonist GW3965 did not affect AKT 1 activation.

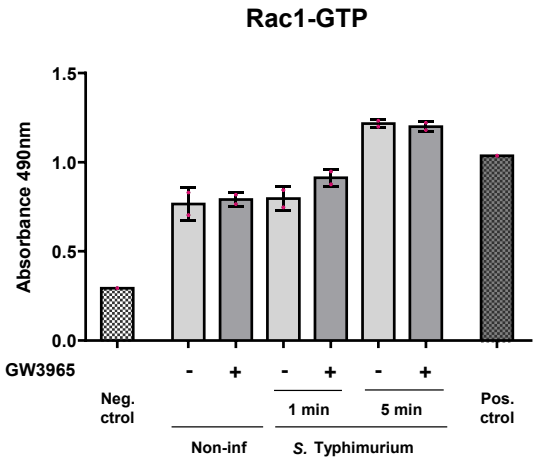

Figure 44. Incubation of macrophages with *S.* Typhimurium activates Rac1 Rho GTPase. BMDMs were treated with vehicle (DMSO) or an LXR agonist (GW3965, 1 µM) in culture medium supplemented with 1% FBS for 24 h. Then, macrophages were exposed to exponentially grown *S.* Typhimurium for 1 or 5 min (MOI 10). The cells were lysed and immediately snap-frozen. The activity of Rac1 was evaluated using the G-LISA® Rac1 Activation Assay Biochem Kit (Cytoskeleton). The data represent the absorbance at 490 nm measured in an Infinite 200 microplate reader (Tecan). Mean ± SD of two biological replicates. The negative (neg. ctrol) and positive (pos. ctrol) controls are the lysis buffer used in the assay and a preparation provided by the manufacturer, respectively. The pink dots indicate the values of each replicate.

On the other hand, the family of MAPKs represents another core signalling platform that also links numerous extracellular signals with intracellular responses (reviewed in Cargnello and Roux, 2011). The most studied MAPKs are ERK 1 and ERK 2, p38 α/β, and JNK 1 and JNK 2. As for AKT detection, we measured the activation (phosphorylation) of these MAPKs in macrophages after the treatment with the vehicle or the LXR agonist for 24 h and the incubation with *S.* Typhimurium for 5, 15, or 30 min. After 5 min of incubation with macrophages, *S.* Typhimurium induced the activation of all these MAPKs, and their activity remained elevated until at least 30 min of incubation (Figure 45 B-D). In macrophages treated with the LXR agonist, the extent of *S.* Typhimurium-induced p38 α/β, ERK 1, and ERK 2 activation by bacteria was equivalent to vehicle-treated cells (Figure 45 B,C). Conversely, the LXR agonist decreased JNK 1 and JNK 2 activation induced by *S.* Typhimurium (Figure 45 D). Consequently, we investigated if the activities of JNK 1 or JNK 2 contributed to the modulation of bacterial internalisation by LXR activation. We obtained BMDM from mice deficient in JNK 1 (JNK $1^{-/-}$) or JNK 2 (JNK $2^{-/-}$) and analysed the infection levels by flow cytometry. Following LXR activation, both JNK $1^{-/-}$ or JNK $2^{-/-}$ macrophages underwent a reduction in infection by *Salmonella* comparable to WT cells, indicating that the restraint activation of JNK does not account for the reduced bacterial internalisation observed in response to the LXR agonist (Figure 46).

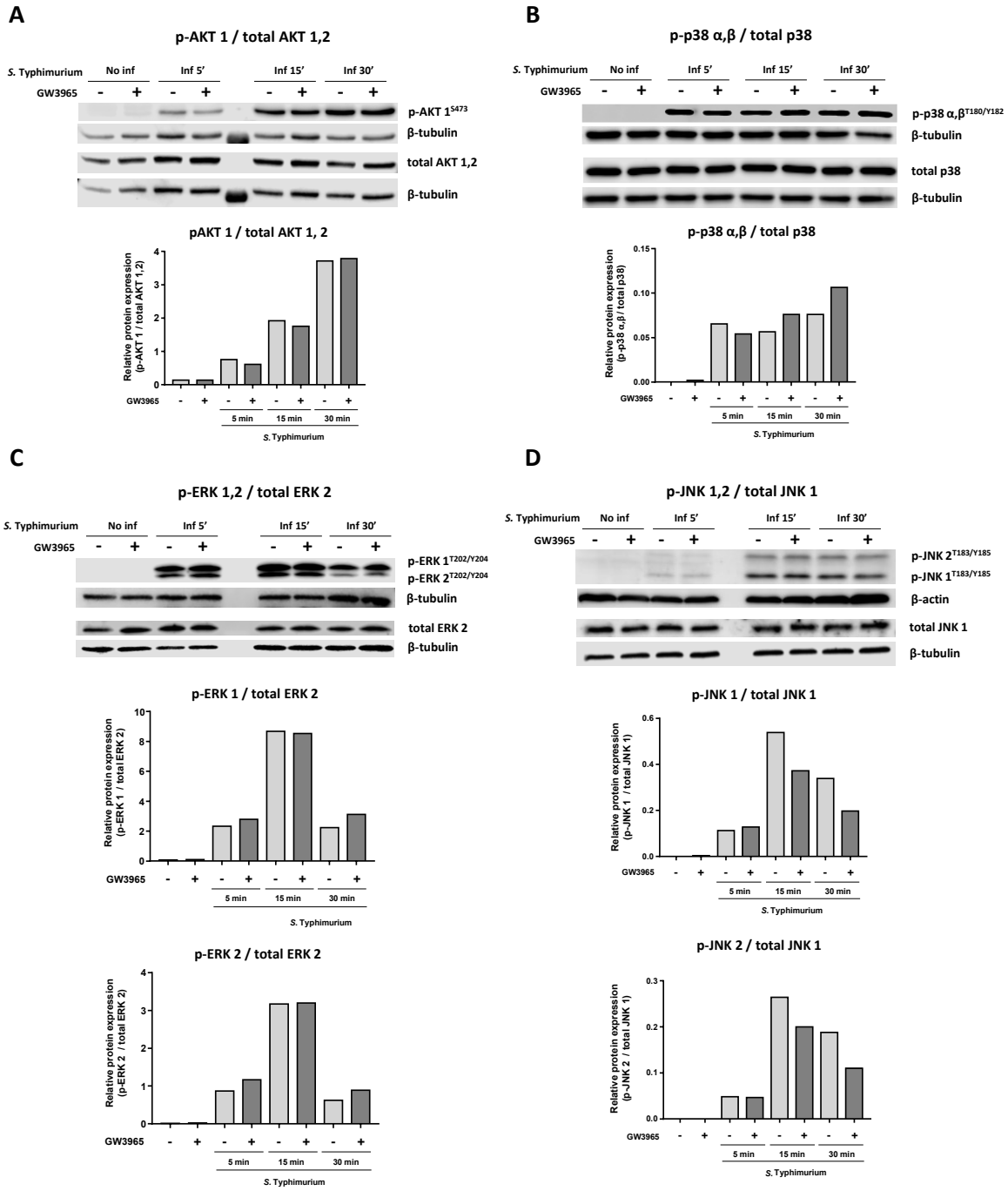

Figure 45. Incubation of macrophages with *S*. Typhimurium stimulates AKT and MAPK signalling pathways and LXRs interfere with JNK 1,2 activation. BMDMs were treated with vehicle (DMSO) or an LXR agonist (GW3965, 1 μM) for 24 h. Then, macrophages were exposed to exponentially grown *S*. Typhimurium for 5, 15, or 30 min (MOI 10) and immediately lysed. The activation (phosphorylation) of proteins belonging to two core signalling platforms was analysed, namely, the PI3K/AKT and MAPK pathways. Phosphorylated (p-AKT 1^{S473}; p-p38 $\alpha,\beta^{T180/Y182}$; p-ERK $1,2^{T202/Y204}$; p-JNK $1,2^{T183/Y185}$) or total (AKT 1,2; p38, ERK 1,2; and JNK 1) protein forms were detected by Western Blot. Two separate immunoblots were performed in parallel using identical conditions and aliquots from the same samples to detect the total and phosphorylated fractions. The differences in protein loading were corrected by a compatible normalising protein: β-tubulin in all the cases except for p-JNK, in which β-actin was used. The data represent the ratio between the normalised phosphorylated and total protein expression. The images and graphs show representative results of n=4 (A, B), n=3 (C), or n=5 (D) independent experiments.

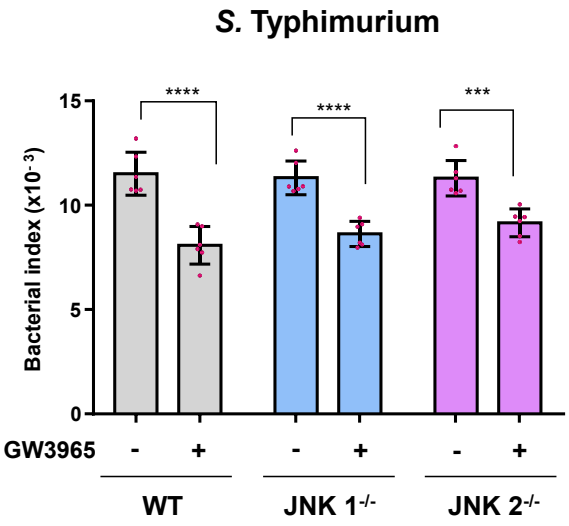

Figure 46. LXR activation reduces macrophage infection by *S.* Typhimurium in the absence of functional JNK 1 or JNK 2. WT, JNK 1-deficient (JNK $1^{-/-}$), or JNK 2-deficient (JNK $2^{-/-}$) BMDMs were treated with vehicle (DMSO) or an LXR agonist (GW3965, 1 µM) for 24 h and exposed to exponentially grown *S.* Typhimurium for 30 min (MOI 3). RFP^{+} *S.* Typhimurium in macrophages was detected by flow cytometry. Bacterial index = (% of bacteria-containing cells) x (mean fluorescence intensity of bacteria in bacteria-containing cells). Mean ± SD of n=2 independent experiments performed with biological triplicates. The pink dots indicate the values of each replicate. To make different experiments comparable, the statistical mean of the infection index in vehicle- and GW3965-treated cells of each genotype was calculated and used to normalise data in each experiment by the mean of all the experiments. Two-way ANOVA + Sidak's test between treatments in each genotype. *** p <0.001; ****p < 0.0001.

3.2 Studies in human macrophages

With the aim to elucidate whether LXRs activation is able to modulate bacterial infection in humans, we established an *in vitro* infection model in human macrophages. We obtained peripheral blood monocytes from healthy human donors and differentiated them to macrophages *in vitro*. Then, we assessed the impact of LXR activation on the internalisation of the bacterial species used in the studies with murine macrophages. The analysis by flow cytometry indicated that LXRs also modulated selectively the entry of bacteria into human macrophages; however, the bacterial species susceptible to this effect did not fully overlap with the ones identified in the studies with murine cells. UPEC caused massive cell death in human macrophages, so we excluded this species of bacteria from the study in human cells. The results obtained with the other bacterial species indicated that the activation of LXRs reduced human macrophage infection by *Salmonella* and *L. monocytogenes*, whereas it did not affect the infection by EIEC and *S. aureus* (Figure 47 A-D). Of note, the outcome of LXR activation was consistent among donors for *Salmonella*, EIEC, and *S. aureus*, whereas the responses diverged

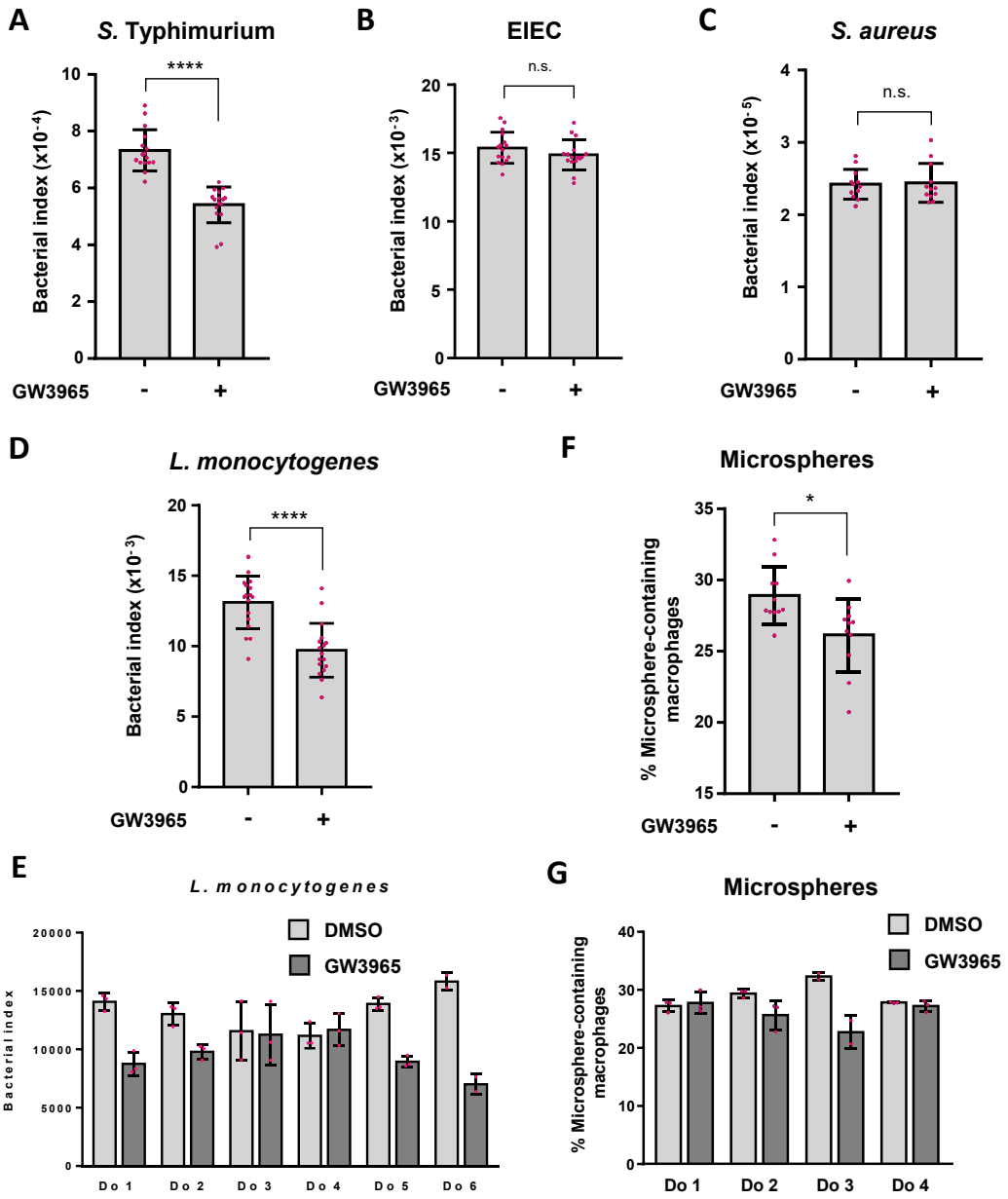

Figure 47. **LXRs selectively reduce bacterial internalisation by human macrophages.** Human primary macrophages were treated with (DMSO) or an LXR agonist (GW3965, 1 µM) for 24 h and exposed for 30 min to the following exponentially grown bacteria (A-E): RFP⁺ *S.* Typhimurium (MOI 3) (A), RFP⁺ EIEC (MOI 15) (B), FITC⁺ *L. monocytogenes* (MOI 8) (D, E), and FITC⁺ *S. aureus* (MOI 5) (C). Some samples were incubated with Fluoresbrite YG microspheres (Polysciences) (5 beads/macrophage) 30 min instead of with bacteria (F, G). The macrophage content of RFP⁺ or FITC⁺ bacteria (A, E) or of microspheres (F, G) was measured by flow cytometry. In A-E, bacterial index: (% of bacteria-containing cells) x (mean fluorescence intensity of bacteria in bacteria-containing cells). (E, G) The bacterial index (E) or the percentage of microsphere-containing macrophages (G) is represented for macrophages from each donor (Do) to show the divergent responses to the LXR agonist. Mean ± SD of n=7 (A), n=6 (B, D), or n=4 (C, F) independent experiments, all performed with biological duplicates or triplicates. The pink dots indicate the values of each replicate. To make different experiments comparable, for each infection setting the statistical mean of both conditions (infected cells in the presence or absence of the LXR agonist) was used to normalise the data in each experiment by the mean of all the experiments. Mann-Whitney U (A, E) or T-test (B-D). *p<0.05; ****p < 0.0001; n.s.: non-significant statistical differences.

for *L. monocytogenes* (Figure 47 E). In this sense, the macrophages from four out of six donors

presented a robust LXR-mediated inhibitory effect on *L. monocytogenes* infection, whereas the cells from the other two donors were unaffected by the LXR agonist (Figure 47 E). We also evaluated the effect of LXR activation on the phagocytosis of latex microspheres (Figure 47 F). Similar to the observations with *L. monocytogenes* infection, of four donors that were evaluated, half of them contained macrophages that exhibited reduced phagocytosis of latex microspheres upon treatment with the LXR agonist, while the macrophages from the other donors did not change the rate of phagocytosis (Figure 47 G).

To know whether the variability among donors was caused by differences in the capability of the LXRs agonist to induce activation, we evaluated the macrophage response to the LXR agonist (GW3965) by quantifying the mRNA expression of two well-established LXR target genes: *ABCA1* and *ABCG1* (reviewed in Calkin and Tontonoz, 2012). All the analysed samples presented a clear induction of *ABCA1* and *ABCG1* expression after the treatment with GW3965, indicating an effective activation of LXRs in macrophages from all the donors in our experimental conditions. The mean values of such induction are presented in Figure 48 (Figure 48 A,B,D,E). Furthermore, the expression of *ABCA1* and *ABCG1* was higher when the combination of RXR and LXR agonists was used (Figure 48 B,E). The induction of the analysed genes required long-term exposure of macrophages to the LXR or RXR agonists, as maximal effects were detected after 14-24 h (Figure 48 A,B). To our surprise, LXR activation did not induce *CD38* expression in this model (Figure 48 G,H). Conversely, the activation of RXRs with the agonist LG268 increased *CD38* expression. As expected, the stimulation of macrophages with LPS drastically increased *CD38* expression (Figure 48 I). However, the combination of LPS with neither the LXR agonist nor the combination of RXR-LXR agonists potentiated the induction of *CD38*. Gene expression analysis of *ABCA1* and *ABCG1* in these conditions confirmed that activated LXRs were capable of activating the transcription of target genes in the presence of LPS (Figure 48 C,F). Interestingly, the expression of *ABCG1* augmented three-fold when combining LPS with the LXR agonist.

Similar results were obtained in the human monocytic cell line THP-1 regarding the effect of LXR activation on *S.* Typhimurium internalisation and on *CD38* expression (Figure 49). In conclusion, in the absence of correlation with increased *CD38* mRNA expression, we interpret that alternative mechanisms might be responsible for the inhibitory effect of the LXR agonist on bacterial entry into human macrophages.

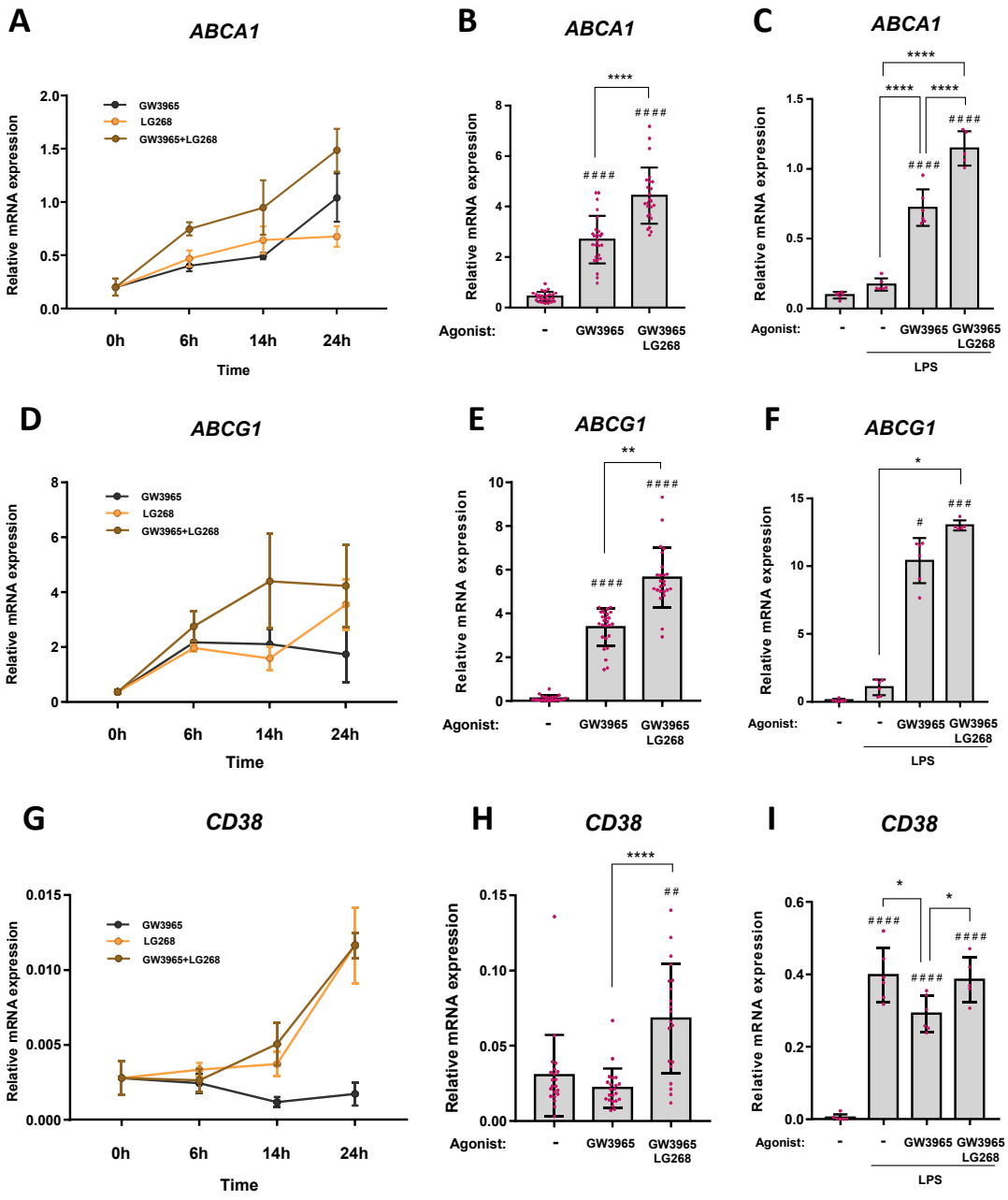

Figure 48. LXR activation does not induce *CD38* expression in human macrophages. Primary human macrophages were treated with vehicle (DMSO), an LXR agonist (GW3965, 1 µM), or the combination of LXR and RXR agonists (GW3965 + LG268, 1 µM). In some cases, the cells were treated with LPS (100ng/ml) and/or LXR/RXR agonists (C, F, I). The cells were treated for 6, 14, and 24 h (A, D, G) or for 24 h (B, C, E, F, H, I). Gene expression was measured by qPCR, and is represented as *ABCA1* (A-C), *ABCG1* (D-F), or *CD38* (E-H) mRNA levels normalised by *GAPDH* expression. Mean ± SD of n=1 (A, D, G), n=14 (B, E), n=11 (H), or n=3 (C, F, I) independent experiments performed with biological duplicates or triplicates. The pink dots indicate the values of each replicate. To make different experiments comparable, the statistical mean of all the conditions was calculated for each experiment and used to normalise the data by the mean of all the experiments. One-way ANOVA + Tukey's test (B, C, I) or Kruskal-Wallis + Dunn's test (E, H, F). *p < 0.05; **p < 0.01; ****p < 0.0001. #p < 0.05; ##p < 0.01; ###p < 0.001; ####p < 0.0001 *vs* the control condition.

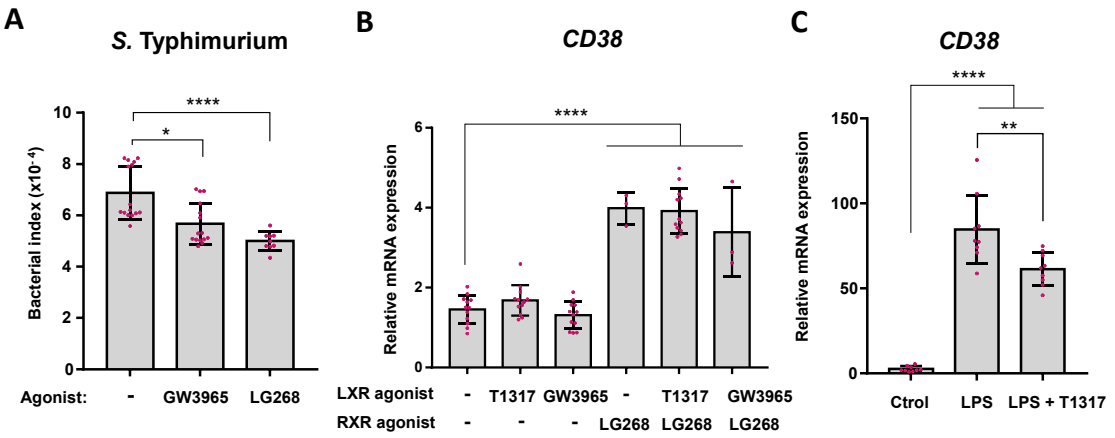

Figure 49. LXR activation reduces *S.* Typhimurium internalisation but does not induce CD38 expression in THP-1 macrophages. Differentiated THP-1 macrophages were treated for 24 h with the following stimuli: (A) vehicle (DMSO), an LXR agonist (GW3965, 1 µM), or an RXR agonist (LG268); (B) vehicle, an LXR agonist (GW3965 or T1317, 1 µM), an RXR agonist (LG268) or the combination of LXR and RXR agonists (GW3965 +LG268, 1µM each); (C) vehicle, LPS (100 ng/ml), or the combination of an LXR agonist (GW3965, 1µM) and LPS (100 ng/ml). (A) THP-1 cells were exposed to exponentially grown RFP⁺ *S.* Typhimurium for 30 min and infection was detected by flow cytometry. Bacterial index: (% of bacteria-containing cells) x (mean fluorescence intensity of bacteria in bacteria-containing cells). (B, C) Gene expression was measured by qPCR, and is represented as *CD38* mRNA levels normalised by *GAPDH* expression. Mean ± SD of n=5 (A), n=1-4 (B), or n=3 (C) independent experiments performed with biological triplicates. The pink dots indicate the values of each replicate. To make different experiments comparable, the statistical mean of all the conditions was calculated for each experiment and used to normalise the data by the mean of all the experiments. Kruskal-Wallis + Dunn's test (A), one-way ANOVA + Dunnet's test (B), or one-way ANOVA + Tukey's test (C). *p < 0.05; **p < 0.01; ****p < 0.0001.

Previous findings in our group indicated that LXR activation interfered with *S.* Typhimurium-induced dorsal actin rearrangements in murine macrophages (Matalonga et al., 2017). During a short-term stay in the laboratory of Dr. Stefan Linder (University Medical Center Hamburg-Eppendorf, Germany), we evaluated whether LXR activation also affected the actin cytoskeleton in human macrophages incubated with *S.* Typhimurium taking advantage of their expertise in the actin cytoskeleton and confocal microscopy techniques. Primary human macrophages were infected with RFP⁺ *S.* Typhimurium as previously described. After macrophage fixation, the F-actin was stained with fluorochrome-conjugated phalloidin and the cell nuclei were stained with Hoechst 33342. We imaged the samples by confocal microscopy and analysed several cellular characteristics using the FIJI software. The results showed that, during incubation with *S.* Typhimurium, LXR activation reduced the size and altered the morphology of host macrophages, making them more elongated (higher aspect ratio) and more irregular (decreased circularity) (Figure 50 A-C). Even if the intensity of F-actin staining at the whole cell level was not different between vehicle- and LXR agonist-treated macrophages (Figure 50 D), the fact that the LXR agonist altered the size and morphology of macrophages suggests that LXRs might affect the distribution of the actin cytoskeleton. Therefore, the actin cytoskeleton may be involved in the

LXR-mediated inhibitory effect on infection in human macrophages as has been previously observed in murine macrophages (Matalonga et al., 2017).

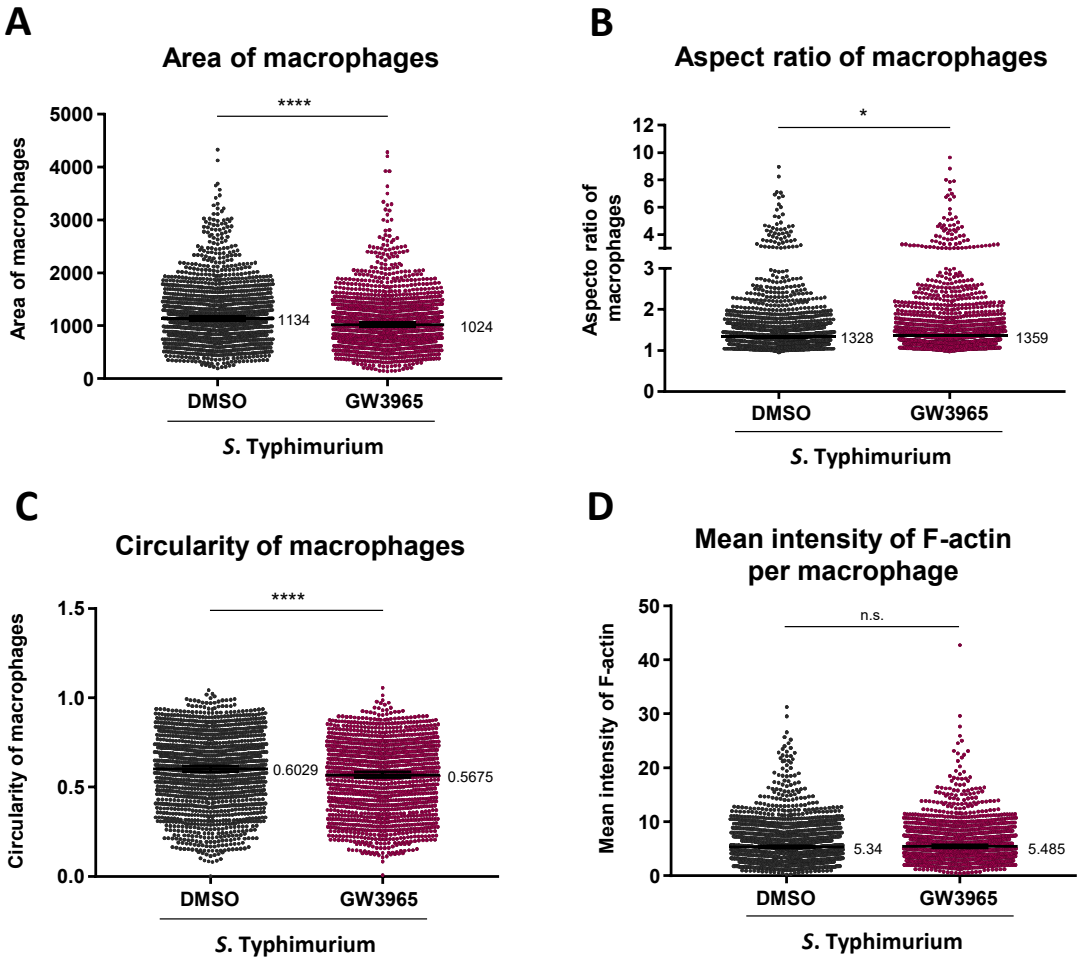

Figure 50. LXR activation alters the size and morphology of human macrophages incubated with *S*. Typhimurium. Human primary macrophages were treated with vehicle (DMSO) (grey dots) or an LXR agonist (GW3965, 1 μM) (pink dots) for 24 h and exposed for 30 min to exponentially grown RFP⁺ *S*. Typhimurium (MOI 10-25). The actin cytoskeleton was stained with Alexa Fluor™ 488 Phalloidin (Thermo Fisher Scientific) and cell nuclei were stained with Hoechst 33342 (Sigma). The images were acquired by confocal microscopy and analysed by the FIJI software as indicated in the "Materials and methods" section. The intensity of F-actin (D) was obtained from images generated through the average intensity Z-projection of all the stacks. The values of F-actin intensity represented for each cell are corrected by the cell area. The cell area (A), aspect ratio (B), circularity (C), and intensity of F-actin (D) are represented. Each dot represents the value of a single cell. The numbers at the right side of each condition in the graphs indicate the median values. Median ± 95% confidence interval from macrophages obtained from 6 donors in two independent experiments. Mann Whitney test, ****p<0.0001, n.s.: non-significant differences.

Since the reduction of plasma membrane free cholesterol resulted in a drastic decrease in bacterial internalisation in murine macrophages, we investigated the consequences of cholesterol depletion also in human macrophages. We used *S.* Typhimurium as a model, as the effects of the LXR agonist were consistent in all the donors. Membrane cholesterol depletion

with MβCD drastically reduced *Salmonella* entry into human macrophages, suggesting that cholesterol levels also condition bacterial infection in these cells (Figure 51).

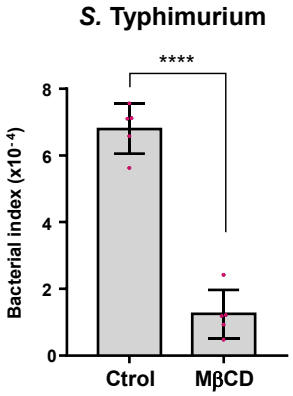

Figure 51. Plasma membrane cholesterol depletion impacts *S.* Typhimurium internalisation by human macrophages. Primary human macrophages were treated with MβCD (10mM, 1 h) and exposed to exponentially grown RFP⁺ *S.* Typhimurium for 30 min (MOI 3). Bacterial index = (% of bacteria-containing cells) x (mean fluorescence intensity of bacteria in bacteria-containing cells). Mean ± SD of n=4 independent experiments. The pink dots indicate the values of each replicate. To make different experiments comparable, the statistical mean of both conditions was calculated and used to normalise the data by the mean of all the experiments. T- test. ****p < 0.0001.

Taken together, the results from human macrophages suggest that LXR activation inhibits selectively the internalisation of target particles, including different types of bacteria and latex microspheres. The consequences of LXR activation in human macrophages were variable among donors and did not fully overlap with the effects detected in murine macrophages. However, some commonalities might exist between the murine and human systems during the interaction with *S.* Typhimurium, as LXRs modified the cell size and shape of macrophages incubated with the bacteria and the depletion of plasma membrane cholesterol reduced the infection in both human and murine macrophages.

DISCUSSION

This work discloses the impact of LXR activation on the interaction of host macrophages with different bacteria, with a special focus on *S.* Typhimurium. Additionally, we unravel a new pathway of transcriptional cooperation between LXRs and inflammatory molecules to promote the expression of *Cd38*, a protein that modulates immune activities against infection (reviewed in Glaría and Valledor, 2020). The initial discoveries about the role of LXRs modulating bacterial infection in murine macrophages and other subsequent results reported in the present thesis have been published (Matalonga et al., 2017).

1. Pharmacological activation of LXRs ameliorates the clinical course of *Salmonella* Typhimurium infection *in vivo*

Although infection by non-typhoidal *Salmonella enterica* serovar Typhimurium generally progresses as self-limiting gastroenteritis in humans, in mice it causes a typhoid-like enteric fever in which bacteria spread systemically (Palmer and Slauch, 2017). To evaluate the impact of pharmacological LXR activation, we used an *in vivo* model of oral infection by *S.* Typhimurium in C57Bl/6J mice, which are highly susceptible to infection due to the natural resistance-associated macrophage protein 1 (NRAMP1) deficiency. In our study, a few days after inoculating a lethal dose of *S.* Typhimurium, mice treated with a synthetic LXR agonist presented a less severe clinical condition and diminished extraintestinal bacterial dissemination. These effects required CD38 expression by bone marrow-derived cells, suggesting that LXRs promote antibacterial functions against *Salmonella* mediated by CD38-expressing immune cells. Indeed, our group described *Cd38* as a new target gene of LXRs in macrophages that is synergistically induced by LXR agonists and pro-inflammatory molecules or bacterial infection (Matalonga et al., 2017). *In vitro*, LXR activation restrained *S.* Typhimurium entry into macrophages, an event that was linked to the induction of CD38 expression. Different studies have shown that CD38 promotes neutrophil chemotaxis through the production of calcium-mobilising second messengers in response to bacteria-derived peptides (Partida-Sanchez et al., 2007; Partida-Sanchez et al., 2004). *In vivo*, CD38 knockout mice present increased susceptibility to *L. monocytogenes* and *Streptococcus pneumoniae* infection, which is associated with deficient neutrophil infiltration to infection sites (Lischke et al., 2013; Partida-Sanchez et al., 2001; Partida-Sanchez et al., 2003). It is possible that LXRs also potentiate *Cd38* expression in neutrophils leading to enhanced chemotaxis as it was recently described for dendritic cells (Beceiro et al., 2018). Therefore, even if we have not completely unravelled the mechanisms leading to protection against *Salmonella* in our *in vivo* model, LXR agonists might act on

macrophages and other immune cells (e.g., neutrophils) to limit bacterial replication and dissemination and to stimulate bacterial killing. In addition, LXRs increased the resistance to *L. monocytogenes* infection *in vivo* through increased macrophage survival mediated by CD5L (Joseph et al., 2004) or to *M. tuberculosis* through stimulation of neutrophil infiltration and Th1 and Th17 responses (Korf et al., 2009). Therefore, we cannot discard that these mechanisms may also contribute to the LXR-mediated amelioration of the clinical severity in our model of infection.

LXRs exert anti-inflammatory effects both in macrophages and *in vivo* (reviewed in Glaría et al., 2020). In our infection model, LXR activation reduced the levels of inflammatory mediators in the spleen and the liver of WT but not of CD38-deficient mice. Since CD38 is not required for the LXR-mediated repression of inflammatory genes in macrophages *in vitro*, we interpret that other factors might be responsible for the reduced capacity of the LXR agonist to inhibit inflammatory gene expression in CD38-deficient mice *in vivo*. On the one hand, in line with the role of CD38 promoting the M1 polarisation of macrophages and dendritic cells (Fedele et al., 2004; Frasca et al., 2006; Lande et al., 2002; Schiavoni et al., 2018; Shu et al., 2018), we observed that CD38-deficient macrophages presented lower inflammatory mediator levels upon incubation with *Salmonella in vitro.* It is feasible that, in CD38-deficient mice, impaired M1 activation of macrophages at the early stages of infection could affect the dynamics of recruitment and activation of other leukocytes and, therefore, alter the response to pharmacological LXR activation. On the other hand, it is probable that the levels of inflammatory gene expression in the spleen and liver reflect the extent of bacterial dissemination to extraintestinal organs. In this sense, the LXR agonist effectively reduced the dissemination of bacteria to the spleen in WT mice, whereas this effect was impaired in CD38-deficient mice.

In conclusion, pharmacological LXR activation rendered promising results for the design of novel host-directed strategies for the treatment of *Salmonella* infection.

2. The transcription factor C/EBPβ mediates the cooperation between LXRs and inflammatory signals in the transcriptional control of *Cd38* expression

From the results described in the previous section and the literature, we can infer that CD38 expression participates in the inflammatory response mediated by immune cells (Glaría and Valledor, 2020). Despite the generally opposing effects of inflammation and LXR activation, our group identified *Cd38* as a non-canonical target gene of LXRs in the sense that its expression was

synergistically induced by the combination of an LXR agonist and inflammatory signals (Matalonga et al., 2017). Subsequent experiments reported here have uncovered some of the mechanisms involved in these cooperative activities. Our study demonstrates that the transcription factor C/EBPβ is required for *Cd38* upregulation by TNFα, IFNγ, and LPS, as well as for their cooperation with the LXR agonist. The upregulation of *Cd38* by any of these inflammatory signals was completely abrogated by C/EBPβ deficiency. This suggests that *Cd38* expression mediated by C/EBPβ cannot be compensated by the functionally similar C/EBPδ isoform as has been described for other LPS-induced genes (reviewed in Tsukada et al., 2011). In line with published data (Amici et al., 2018; Iqbal and Zaidi, 2006; Lee et al., 2012a; Lischke et al., 2013; Musso et al., 2001), the exposure of WT macrophages to TNFα, IFNγ, or LPS increased the expression of C/EBPβ at mRNA and protein levels. In the case of IFNγ, STAT1 contributed to *Cebpb* expression to a large extent. Other studies in various cell types, especially in hepatocytes, have provided mechanisms by which IFN or LPS could mediate *Cebpb* induction, including pathways leading to the activation of the transcription factors STAT, CREB, ATF2, c-Jun, NF-κB, and C/EBPβ itself in an autoregulatory manner (Kravchenko et al., 2003; Lee et al., 2012b; Niehof et al., 2001a; Niehof et al., 2001b; Ruffell et al., 2009; Yokota et al., 2019). Direct binding of NF-κB to regulatory regions of *Cebpb* seems improbable since no functional NF-κB binding sites have been identified (reviewed in Pulido-Salgado et al., 2015). However, in some cases, physically interacting transcription factors can activate gene expression while only one of them is bound to DNA, an event that has been described for NF-κB and C/EBPs (Dooher et al., 2011) and could help explain how NF-κB regulates *Cebpb*.

Aside from transcriptional regulation, the activity of C/EBPβ depends on the relative protein isoform expression and post-translational modifications (reviewed in Pulido-Salgado et al., 2015). As it is common elsewhere, in our experimental setting the most abundant protein isoform induced by inflammatory signals was LAP. The increase in LAP expression was prominent after the incubation of macrophages with TNFα and, especially, with LPS. Instead, IFNγ induced a weak increase in LAP expression. Nevertheless, other authors have reported that the phosphorylation of C/EBPβ by IFNγ-induced ERK or by LPS + IFNγ-induced p38 increases its binding to gene promoters (Hu et al., 2001; Stoffels et al., 2006). Therefore, IFNγ may act on the relatively high basal levels of C/EBPβ in differentiated macrophages (reviewed in Huber et al., 2012) inducing post-translational modifications that enhance its binding to the DNA rather than potently upregulating the protein expression. We also detected an increase in LIP expression induced by inflammatory signals, again most notably by LPS, although its levels were

considerably lower than those of LAP. Most frequently, the LIP isoform opposes the actions of the activator isoforms; consequently, the LIP:LAP ratio has been suggested as a more informative parameter of C/EBPβ functions (reviewed in Pulido-Salgado et al., 2015). Based on this notion, our studies suggest that the main transcriptional activity of C/EBPβ upon stimulation of macrophages with TNFα, IFNγ, or LPS is the positive modulation of target gene expression. In support of this interpretation, transfection experiments using a reporter vector evidenced that the sole overexpression of C/EBPβ induced transcriptional activity on an enhancer region of *Cd38*. Of note, the transcriptional capacity of C/EBPβ was higher in RAW 264.7 macrophages than in COS-7 fibroblasts, which could result from either the absence of some basic transcriptional component(s) in COS-7 cells or the presence of additional factors that contribute to C/EBPβ-induced *Cd38* expression in macrophages. Taken together, these results suggest that inflammatory signals positively modulate the expression of C/EBPβ, whose activity may be further modulated by post-translational modifications. C/EBPβ is subsequently required to induce *Cd38* expression.

Our results suggest that there is a complex interplay between LXRs and C/EBPβ to control the transcription of *Cd38*. C/EBPβ-deficient macrophages presented an altered *Cd38* regulation pattern, as they exhibited higher expression levels of *Cd38* in basal conditions as well as transcriptional inhibition of *Cd38* upon LXR activation. These results suggest that C/EBPβ not only participates in the inflammatory signal-induced activation of *Cd38*, but also represses its basal levels in the absence of stimuli. More experiments are needed to elucidate how C/EBPβ controls *Cd38* expression in each context, but these outcomes are compatible with different possibilities. First, it should be determined whether C/EBPβ directly binds to regulatory regions of *Cd38* and, in case it does, which dimerisation partner(s) are involved. C/EBPβ can form a homodimer or a heterodimer, the latter by binding to another C/EBP isoform or a different bZIP transcription factor such as CREB/ATF, JUN/FOS, or MAF (Grigoryan et al., 2009; Newman and Keating, 2003). The *in silico* analysis of the *Cd38* enhancer region that we cloned predicted eight binding sites for different C/EBP isoforms. However, as the different C/EBP isoforms bind highly conserved consensus sequences, it is unlikely that each binding site can be exclusively occupied by a specific isoform (reviewed in Tsukada et al., 2011). Besides, the *in silico* analysis of the *Cd38* enhancer also predicted binding sites for ATF2, ATF3, and CREB, raising the possibility that interfamily heterodimers control *Cd38* expression. Therefore, in case the C/EBP binding sites on the *Cd38* enhancer are functional, their occupation might depend on the relative expression of C/EBP isoforms and stimulus-dependent modifications. The higher basal levels of *Cd38* in

C/EBPβ-deficient cells may result from the replacement of C/EBPβ by other C/EBP isoforms (or other transcription factors) that exhibit an enhanced transactivation potential on the regulatory regions of *Cd38* under basal conditions. On the other hand, a repressive effect of LXR activation on *Cd38* expression in the absence of C/EBPβ is complicated to explain. We can speculate that C/EBPβ contributes to *Cd38* induction by activated LXRs. In relation to this, a study reported that LXRα and C/EBPβ physically interact on the LXR target gene *Srebp1c* and cooperate in the transcriptional activation induced by insulin (Tian et al., 2016). Notably, in that case, of the two transcription factors only LXRα was bound to the DNA. Although the scenario might be different in our setting, those findings demonstrate that LXRs and C/EBPβ can physically and functionally interact, supporting their cooperation on specific target genes. Additionally, LXRs may act similarly to other ligand-activated nuclear receptors such as the glucocorticoid receptor and PPARγ. These nuclear receptors can bind to response elements that are adjacent to C/EBPβ binding sites and cooperate with C/EBPβ both physically and functionally to induce target gene expression (Lefterova et al., 2008; reviewed in Roos and Nord, 2012). Those studies provide some clues about possible mechanisms underlying the loss of *Cd38* induction by LXR activation in C/EBPβ-deficient macrophages. Perhaps, the lack of C/EBPβ compromises the ability of activated LXRs to recruit co-activator complexes to regulatory regions of the *Cd38* gene. In addition, agonist-activated LXRs may either activate or repress the expression of other genes that modulate *Cd38* levels, resulting in decreased *Cd38* expression in the absence of C/EBPβ.

As mentioned above, a novel finding of this work is the cooperation of inflammatory signal-induced C/EBPβ activity and LXRs in the transcriptional control of *Cd38*. Importantly, a role for LXRs regulating *Cebpb* expression by inflammatory stimuli was discarded for two reasons: first, the incubation of macrophages with an inflammatory molecule and an LXR agonist did not increase *Cebpb* levels above the induction caused by any of the inflammatory molecules alone, and; second, WT and LXR-deficient macrophages induced comparable amounts of *Cebpb* expression in response to the evaluated inflammatory stimuli. On the other hand, we observed that TNFα and LPS but not IFNγ increased *Lxra* mRNA expression; however, the induction of *Lxra* expression was C/EBPβ-independent (data not shown). Therefore, the synergism between C/EBPβ and LXRs is not mediated by one activating each other's expression. Additionally, LXR expression was dispensable for *Cd38* induction by these inflammatory signals. Surprisingly, although the simultaneous stimulation of C/EBPβ-deficient macrophages with TNFα or IFNγ and an LXR agonist did not induce *Cd38* expression, the combination of LPS and an LXR agonist partially rescued their capability to induce *Cd38* expression in the absence of C/EBPβ. These

differences between the inflammatory cytokines and LPS in their ability to cooperate with LXRs to induce *Cd38* in C/EBPβ-deficient macrophages might be caused by the wider effects of LPS in the induction of inflammatory pathways. Indeed, the time-course expression experiments showed that the levels of *Cd38* turned close to basal after 14 h of incubation with TNFα or IFNγ, whereas LPS-stimulated *Cd38* levels remained high at that moment. Of note, the levels of *Cebpb* expression drastically dropped at 12 h of macrophage stimulation with these three inflammatory molecules. Consequently, the expression dynamics of *Cd38* induced by LPS might reflect the sequential activation of various pathways, including C/EBPβ-dependent and C/EBPβ-independent actions, that converge in *Cd38* modulation. In the absence of C/EBPβ, the LXR agonist or LPS alone may not be able to activate the transcriptional machinery required for *Cd38* induction, but the combination of both pathways seems to cooperate to accomplish the transcriptional activation. This would suggest that not only C/EBPβ but also other LPS-activated transcription factors may cooperate with LXRs on *Cd38* induction.

The results obtained from transfection studies support the close collaboration between LXRs and C/EBPβ on regulatory regions of *Cd38*. Specifically, combined C/EBPβ overexpression and LXR activation resulted in an upward tendency in the transcriptional enhancer activity of the *Cd38* enhancer region only when the original LXRE was present, whereas the mutant LXRE prevented this response. These data suggest that direct LXR binding to its response element on at least this enhancer region is required for the cooperation with C/EBPβ. Of note, these experiments were mainly performed overexpressing LXRβ, as LXRα showed a similar but apparently weaker effect. Indeed, a study that characterised the genomic binding landscape of LXRα and LXRβ in murine immortalised macrophages revealed that C/EBP binding sites localised adjacent to DNA regions bound by LXRβ (Ramon-Vazquez et al., 2019). Consequently, we interpret that LXRβ may preferentially mediate the functional cooperation with C/EBPs in physiological conditions.

We also analysed the impact of LXR activation and inflammatory stimuli on the expression of other LXR target genes with immunomodulatory roles, namely, *Mertk* and *Cd5l*. MERTK and CD5L are anti-inflammatory proteins that promote the resolution of inflammation (reviewed in Rothlin et al., 2015; reviewed in Sanjurjo et al., 2015). In line with other LXR target genes (Castrillo et al., 2003; Han et al., 2018; Pascual-Garcia et al., 2013), *Mertk* and *Cd5l* were inversely regulated by inflammatory signals and LXR activation, except for the unaltered *Mertk* expression in the presence of IFNγ, which contrasts with the effects reported by other studies (Grabiec et al., 2018; Thorp et al., 2011). In this sense, in macrophages, a negative effect of LPS or IFNγ on

MERTK has been reported at the level of expression and, for LPS, proteolytic cleavage (Grabiec et al., 2018; Qiao et al., 2016; Thorp et al., 2011). Instead, the expression of CD5L might be more finely tuned, as it was induced by bacterial infections *in vivo* and *in vitro*, but macrophage stimulation with PMA, LPS, or IFNγ *in vitro* did not upregulate CD5L levels (Haruta et al., 2001; Joseph et al., 2004; Kuwata et al., 2003; Miyazaki et al., 1999; Sanjurjo et al., 2013). Therefore, the expression of CD5L may be modulated by various factors in the cellular environment depending on the stage of the inflammatory response. Importantly, the repression of *Mertk* and *Cd5l* by inflammatory signals in our model did not depend on C/EBPβ.

In conclusion, this work has revealed the synergistic cooperation between C/EBPβ and LXRs, preferentially through LXRβ, to control the transcription of *Cd38* in mice. These effects might be relevant in physiological settings in which CD38 upregulation plays a role.

3. The activation of LXRs selectively modulates bacterial entry into macrophages

In this work, we have confirmed the capacity of activated LXRs to inhibit macrophage infection by *S.* Typhimurium. However, important differences have been observed in comparison with previous studies using bacteria at the stationary phase. The unexpected finding that LXR activation inhibited the infection by exponentially grown *Salmonella* independently of CD38 may be related to differences in the metabolic status or in the infective capacity between stationary and exponentially grown bacteria. Using flow cytometry, we detected notably higher infection levels by exponentially grown bacteria at a similar MOI. This outcome was associated with higher numbers of intracellular bacteria per infected macrophage as analysed by fluorescence microscopy (data not shown). Even if we lowered the bacterial MOI, the macrophage infection levels remained high in most of the experiments with exponentially grown *S.* Typhimurium, suggesting that their functional characteristics favoured increased internalisation. Similar observations were also reported in a study that analysed the outcome of incubation of RAW 264.7 macrophages with *S.* Typhimurium that had been grown to either a late exponential phase or to a stationary phase (Drecktrah et al., 2006). Indeed, the authors attributed the entry of exponentially grown bacteria to T3SS-mediated invasion, whereas stationary phase bacterial entry was considered macrophage phagocytosis. Our results using the T3SS mutant invG in the current experimental setting (with exponentially grown bacteria) indicate that the T3SS of *S.* Typhimurium accounts for approximately 65% of bacterial entry into macrophages. However, we do not know to which extent the remaining rate of bacterial entry is mediated by other

mechanisms such as bacteria-induced invasion, macrophage phagocytosis, or other processes involving both. It is possible that the relative contribution of each entry mechanism to total bacterial internalisation changes depending on the growth phase in which bacteria are used. Indeed, in our experiments, the mean rates of LXR-mediated inhibition of infection compared to control cells changed from 50% of inhibition when bacteria were used at the stationary phase, to 20% (ranging between 10%-35%) of inhibition when exponentially grown bacteria were employed. Besides, the high infection levels achieved by exponentially grown bacteria might entail a different macrophage response to subsequent re-infection events, as indicated by a study carried out by Gog and co-workers (Gog et al., 2012). Based on these considerations, we interpret that changes in the mechanisms involved in bacterial internalisation may underlie the differences in the effectiveness of the LXR pathway and its dependence on CD38. Besides, it must be taken into account that we are probably not evaluating the effects in poorly infected cells when assessing the infection by flow cytometry in the current experimental setting.

At this point, we started exploring the dynamics of early bacteria–host macrophage interaction through two different approaches. First, we obtained BMDMs from Lifeact-GFP (green fluorescent protein) transgenic mice, which exhibit fluorescent actin microfilaments (Riedl et al., 2010), and evaluated actin rearrangements during infection by RFP^+ *Salmonella* using spinning disk confocal microscopy. Live cell imaging showed massive actin rearrangements and multiple macrophage contacts with bacteria, but we did not appreciate evident differences in the actin dynamics in response to LXR activation (data not shown). Because the magnification required for a good spatial and temporal resolution limited the field to just a single cell, we decided to broaden our view with a different technique that provided information from a larger number of cells. For this reason, we obtained sequential brightfield microscopy images of live infection to understand the general characteristics of bacteria–macrophage contacts. *Salmonella* was highly motile; it rapidly propelled itself from one macrophage to another, interrupted by more stilled periods during the contact with macrophages (data not shown). Some contacts were short (few seconds), whereas others lasted longer. In some cases, bacteria left after prolonged contact; in others, the video finished while the contact persisted and, due to the limited time that we recorded, we were unable to clearly observe a successful bacterial internalisation event. These experiments were just observational, and we did not make any measurement on the events described above. By contrast, Gog and colleagues (Gog et al., 2012) exhaustively analysed the contacts between *S.* Typhimurium and BMDMs or RAW 264.7 cells at single-cell level. In line with our observations, they reported very frequent bacteria–macrophage contacts that lasted

less than 10 seconds. Upon contact, the estimated probability of infection was lower than 5%. Interestingly, those contacts that lasted more than 10 seconds had a higher probability of leading to bacterial internalisation. The authors also described that macrophage re-infection occurs at a lower frequency than the first infection. Curiously, after 10 min of exposure to bacteria, the mathematical model that best fitted their measurements on internalised bacteria consisted of two macrophage populations with distinct susceptibility to infection, which did not correspond to macrophage M1 and M2 phenotypes. These insights from early infection dynamics added to the visual perception from our microscopy experiments that bacteria were constantly sampling the macrophage surface, prompted us to evaluate plasma membrane components on macrophages that might determine the outcome of macrophage–bacteria interactions.

Increasing pieces of evidence support the crucial role of cholesterol, as well as the cholesterol-enriched lipid rafts, in host–pathogen interactions (reviewed in Bukrinsky et al., 2020). Lipid rafts are dynamic nanoscale assemblies of sphingolipids, cholesterol, and proteins that can coalesce to form membrane signalling platforms (reviewed in Lingwood et al., 2009). This model of compartmentalisation is based on membrane component segregation that leads to the formation of biologically functional complexes. Remarkably, lipid rafts concentrate most signalling proteins and components of the endocytosis machinery present in the plasma membrane, mediating cell interaction with the extracellular "world" (reviewed in Bukrinsky et al., 2020). As a result, lipid rafts arbitrate diverse functional responses to extracellular stimuli but simultaneously represent receptor-enriched entry portals for pathogens. Importantly, LXR activation can alter the membrane lipid composition through the transcriptional regulation of key molecules involved in lipid metabolism, including ABCA1 and ABCG1, which promote cholesterol efflux, and LPCAT3 that promotes long polyunsaturated fatty acid incorporation into phospholipids (reviewed in Wang and Tontonoz, 2018). Indeed, an altered cholesterol content or distribution in membrane lipid rafts by LXR-stimulated ABCA1 expression interfered with intracellular signalling upon TLR engagement in murine macrophages (Ito et al., 2015a). Both LXRα and LXRβ are important for the control of cholesterol homeostasis through ABCA1 and ABCG1 in macrophages (Ramon-Vazquez et al., 2019; Repa et al., 2000b), and both LXR isoforms were involved in the agonist-induced interference with bacterial entry into macrophages observed in our studies. Therefore, these facts support the possibility that LXRs impact bacterial internalisation by macrophages through cholesterol modulation. Actually, LXR activation reduced the free cholesterol levels in murine macrophages, whereas it did not affect the

abundance of the lipid raft marker GM1, findings that correspond with the results reported by Ito *et al.*. Although by only evaluating GM1 expression we cannot state that LXRs alter the characteristics of lipid rafts, it is probable that the cholesterol decrease in our model also affects lipid raft composition. In line with a role for lipid rafts in bacterial internalisation, we discovered that the abundance of GM1 and free cholesterol in macrophages correlated with the infection levels by *Salmonella*. In addition, using cyclodextrins to modulate plasma membrane cholesterol, we corroborated that bacterial infection changed together with the increase or decrease in cholesterol. We should not disregard that cholesterol depletion with MβCD frequently disrupts lipid rafts and could have other effects besides cholesterol reduction (Zidovetzki and Levitan, 2007). Nevertheless, the work presented here supports the idea that the cellular levels of cholesterol affect *Salmonella* infection. Despite these considerations, controversial effects of cholesterol on the T3SS-dependent entry of *Salmonella* into non-phagocytic cells have been reported. In this sense, cholesterol sequestration by MβCD inhibited *Salmonella* entry (Garner, Hayward, & Koronakis, 2002), whereas a cellular model of 24-dehydrocholesterol reductase (DHCR24) deficiency, which is unable to complete the last step of cholesterol biosynthesis and accumulates desmosterol, showed no impact on the internalisation of *S.* Typhimurium (Gilk et al., 2013). Noteworthy, host cell cholesterol might affect other invasive mechanisms of *Salmonella* that could be differentially used for the entry into specific cell types (reviewed in Velge et al., 2012). In addition, macrophages, as phagocytic cells, rely on a diverse set of PRRs to recognise and respond to pathogens, which, in turn, depend on appropriate cholesterol levels and lipid raft integrity for signalling (reviewed in Ruysschaert & Lonez, 2015). Our work indicated that wild type and T3SS-deficient *Salmonella* were similarly susceptible to LXR-mediated inhibition, suggesting that LXRs might affect a common player required for both T3SS-dependent and T3SS-independent internalisation by macrophages. We can speculate that LXR-mediated cholesterol decrease alters critical plasma membrane properties that determine bacterial internalisation in some manner. We consider that candidate LXR target genes that could mediate these effects are *Abca1*, *Abcg1*, *Idol*, *ApoE*, or *Lpcat3* (reviewed in Wang and Tontonoz, 2018). In fact, we attempted to investigate how LXR activation affected *Salmonella* infection in ABCA1- or ABCA1/ABCG1-deficient macrophages through a collaboration with Dr. Miranda van Eck (Leiden University, The Netherlands); however, we had logistical problems due to the Covid-19 pandemic and subsequent lock-downs that impeded the development of these experiments.

We detected that LXRs partially inhibited JNK activation following murine macrophage incubation with *Salmonella*, which contrasted with the inhibition of JNK, ERK, and p38 downstream of TLR4 signalling reported by Ito and co-authors (Ito et al., 2015a). In their study, reduced MyD88 recruitment to LPS-activated receptors led to reduced MAPK activity as well as reduced inflammatory gene expression. Instead, in our model, LXRs interfered exclusively with JNK activation, suggesting that they do not alter general upstream signalling events but rather affect a selective component of the JNK pathway. Therefore, LXR activation might be impacting the expression and/or activity of either a JNK-specific kinase or phosphatase (reviewed in Arthur and Ley, 2013). Nevertheless, the results from JNK 1- or JNK 2-deficient macrophages demonstrated that, at least separately, neither of them prevents the antibacterial effects of LXRs. Consequently, the inhibition of *Salmonella*-induced JNK activity by LXRs might represent a mechanism that contributes to the anti-inflammatory effects of LXRs but does not seem to be responsible for the limitation of bacterial entry.

Many intracellular bacteria have developed strategies to subvert the macrophage microbicidal mechanisms and replicate inside the host cell avoiding extracellular immune attack (reviewed in Mitchell et al., 2016). Importantly, we have demonstrated that not only *Salmonella*, but also other bacterial species are susceptible to the LXR-mediated inhibitory effects on internalisation. These results are intriguing because neither all bacteria are affected by LXR-mediated inhibition, nor their susceptibility is equivalent in the murine and human models, suggesting a high level of complexity in the actions exerted by the LXR pathway during infection. In murine macrophages, the activation of LXRs by a synthetic agonist inhibited the internalisation of *S*. Typhimurium, UPEC, and EIEC, which are Gram-negative species, but not of *L. monocytogenes* and *S. aureus*, which are Gram-positive bacteria. The first impression could be that LXRs selectively interfere with Gram-negative bacteria. However, it would be too ambitious to take this conclusion from only two or three bacterial species of each class. Taking into account the pathogenic and structural features of the bacteria analysed here, we did not identify a common denominator that might help explain such divergent responses. It is also possible that different LXR-mediated activities determine the outcome for each bacterial infection in a rather selective manner. Further research on the inhibitory effects of LXRs will be needed to elucidate the responsible mechanisms involved in these outcomes.

In murine macrophages, the simultaneous incubation with *Salmonella* and latex microspheres affected the phagocytic rates of both types of particles compared to each of them when incubated separately. It is feasible that *Salmonella*-induced membrane ruffling favours contacts

between macrophages and microspheres, subsequently enhancing microsphere phagocytosis. On the other hand, microspheres might compete with bacteria for the molecular machinery or the space required for particle internalisation, thereby hampering the entry of *Salmonella*. These results suggest that macrophages modify their phagocytic activity upon contact with *S.* Typhimurium, but the effects of LXRs selectively inhibit *S.* Typhimurium entry instead of the general internalisation of particles. This outcome points toward a contact-dependent mechanism dictating the selectivity of LXRs. Together, our results and published data picture a highly specific effect of LXRs in the regulation of phagocytosis of each type of particle. In this sense, LXRs promote apoptotic cell efferocytosis, whereas the phagocytosis of IgG-opsonised particles remains unaffected, and non-opsonised bacterial internalisation is selectively modulated (Gonzalez et al., 2009; Matalonga et al., 2017). In conclusion, LXRs seem to finely control macrophage phagocytosis depending on the immunological context.

In human macrophages, LXR activation selectively impaired the internalisation of *Salmonella*, but not of EIEC or *S. aureus*, effects that were uniform in all the donors evaluated. Interestingly, the effects on internalisation of *L. monocytogenes* and latex microspheres varied in a donor-dependent manner, that is, macrophages from only some donors showed reduced engulfment upon LXR activation. Taken together, LXRs exhibited selective effects on particle internalisation by human macrophages but differed in the particle specificity compared to murine cells. These divergent results between species might originate from differences in mechanisms controlling immune responses, in LXR-mediated activities, or in both. For example, LXR activation in murine macrophages consistently induces an anti-inflammatory profile, whereas different studies using LXR agonists in human macrophages reported opposite outcomes on inflammatory gene expression depending on the timing of LXR activation and the inflammatory challenge (reviewed in Waddington et al., 2015). These discrepancies insinuate that human responses might be more diverse and context-specific, while not necessarily corresponding with the murine model. In our study, the variability among donors suggests that host environmental or genetic factors condition the macrophage response to LXR agonists in the context of specific bacterial infections. Taking this variability into account, more donors should be evaluated to get more reliable conclusions from a wider population coverage. Importantly, the LXR agonist induced the expression of the LXR target genes *ABCA1* and *ABCG1* comparably among donors, demonstrating that the differences in the outcome of infection were not caused by unresponsiveness to the agonist in some donors. Regarding the expression of *CD38*, macrophages from none of the donors increased *CD38* levels upon LXR activation. Moreover, macrophage stimulation with LPS

strongly raised *CD38* levels, but its combination with an LXR agonist reduced CD38 expression instead of potentiating it, which is the opposite of what occurs in murine macrophages. These results contrast with the effect of LXR activation in human monocyte-derived dendritic cells described by Beceiro and colleagues (Beceiro et al., 2018). The upregulation of *CD38* upon stimulation of immature dendritic cells with LPS was coincident with our observations, but, in their model, *CD38* expression was further increased by the combination with an LXR agonist. We consider that several differences could explain the discrepancies between both models: the method for the obtention of monocytes from peripheral blood, the acquisition of features during the *ex vivo* differentiation process (e. g. epigenetic and/or transcriptional modifications) to macrophages or dendritic cells, and the involvement of additional factors, such as GM-CSF or IL-4, which were used for dendritic cells but not for macrophage cultures. In conclusion, even if LXRs might be able to stimulate *CD38* production in some contexts, in our experimental model they do not induce *CD38* expression alone nor in combination with LPS. Instead, an RXR agonist did induce *CD38* upregulation in human macrophages, which may occur through homodimerization or heterodimerization with a permissive partner, such as PPARγ (Dawson and Xia, 2012). In fact, the capability of PPARγ to transcriptionally activate *Cd38* expression was demonstrated in murine adipocytes (Song et al., 2012). Taken together, our results suggest that LXR activation in human macrophages can selectively modulate bacterial internalisation depending on host factors other than *CD38*. The detection of changes in the size and shape of human macrophages treated with an LXR agonist and incubated with *S.* Typhimurium, as well as the inhibitory effect of cholesterol depletion on *S.* Typhimurium internalisation raise the possibility that either of these aspects are involved in the modulation of bacterial internalisation by LXR activation.

In summary, our studies demonstrate that the activation of LXRs with a synthetic agonist interferes with the internalisation of specific bacteria by macrophages *in vitro* and results in better control of the infection *in vivo*. The results in murine and human macrophages suggest that the alterations in the lipid composition of the plasma membrane might be involved in the restriction of bacterial entry. In human macrophages, LXRs also reduce the infection by some bacteria, but greater variability is detected among donors, and some of the effects are inconsistent with the murine model. These findings are especially relevant in the context of infection by many intracellular bacteria that can survive within macrophages, as LXRs might represent a way to limit their access to an intracellular niche. We focused on the initial interactions between bacteria and macrophages, but the impact of LXRs on later stages of the

intracellular infection is another pending aspect to study. Additionally, we discovered that the cooperation of LXRs and C/EBPβ is necessary for the transcriptional control of *Cd38* in murine macrophages. Even though the upregulation of CD38 is not involved in the LXR-induced limitation of macrophage infection in the *in vitro* model used in these studies, the consequences of increased expression of CD38 by inflammatory signals and LXR activation *in vivo* deserve further investigation.

In front of the threat represented by the rapidly spreading antibiotic-resistant bacteria, finding new therapies to effectively tackle infections is an urgent matter. Because of their multiple physiological roles and their druggable nature, LXRs appear as promising therapeutic targets for an increasing number of metabolic and inflammatory diseases (reviewed in: Fessler, 2018; Hong and Tontonoz, 2014). Our study has explored to some extent the impact of LXRs in bacterial infections as a potential host-directed therapy that could substitute or complement antibiotic treatment in certain circumstances. Until now, the therapeutic use of LXR agonists in humans has been neglected due to the appearance of adverse effects; however, there is hope that the development of more specific new generation LXR-targeting compounds will overcome these limitations in the future.

CONCLUSIONS

1) In a murine model of infection by *S.* Typhimurium *in vivo*, pharmacological LXR activation attenuates the clinical signs of infection and reduces the bacterial dissemination to the spleen through mechanisms that depend on CD38 expression by bone marrow-derived cells.

2) C/EBPβ is necessary for the induction of *Cd38* expression by the inflammatory mediators TNFα, IFNγ, and LPS in murine macrophages.

3) C/EBPβ cooperates with LXRs for the transcriptional control of *Cd38* in murine macrophages.

4) In murine macrophages, LXR activation selectively diminishes the internalisation of *S.* Typhimurium, UPEC, and EIEC but not of *L. monocytogenes* and *S. aureus*. In addition, LXR activation does not modulate the unspecific phagocytosis of latex microspheres by murine macrophages.

5) CD38 expression is not required for the inhibitory effects of LXRs on the internalisation of exponentially grown *S.* Typhimurium, EIEC, or UPEC by murine macrophages.

6) The activation of LXRs in human macrophages selectively reduces the internalisation of *S.* Typhimurium and *L. monocytogenes* (in some donors) but not of EIEC and *S. aureus*. These effects occur in the absence of increased *CD38* expression.

7) LXRs selectively inhibit JNK activation after the infection of murine macrophage with *S.* Typhimurium. However, the interference with JNK activation does not account for the inhibitory effects of LXRs on *S.* Typhimurium internalisation.

8) The activation of LXRs alters the size and morphology of human macrophages incubated with *S.* Typhimurium.

9) Changes in the cellular cholesterol levels modulate the rate of internalisation of *S.* Typhimurium by murine and human macrophages. In this sense, there is a positive correlation between the bacterial infection rate and the abundance of free cholesterol and lipid rafts.

REFERENCES

Adams, D.O. (1989). Molecular interactions in macrophage activation. Immunol Today *10*, 33-35.

Ahsan, F., Maertzdorf, J., Guhlich-Bornhof, U., Kaufmann, S.H.E., and Moura-Alves, P. (2018). IL-36/LXR axis modulates cholesterol metabolism and immune defense to Mycobacterium tuberculosis. Sci Rep *8*, 1520.

Akira, S., Isshiki, H., Sugita, T., Tanabe, O., Kinoshita, S., Nishio, Y., Nakajima, T., Hirano, T., and Kishimoto, T. (1990). A nuclear factor for IL-6 expression (NF-IL6) is a member of a C/EBP family. EMBO J *9*, 1897-1906.

Amici, S.A., Young, N.A., Narvaez-Miranda, J., Jablonski, K.A., Arcos, J., Rosas, L., Papenfuss, T.L., Torrelles, J.B., Jarjour, W.N., and Guerau-de-Arellano, M. (2018). CD38 Is Robustly Induced in Human Macrophages and Monocytes in Inflammatory Conditions. Front Immunol *9*, 1593.

Arpaia, N., Godec, J., Lau, L., Sivick, K.E., McLaughlin, L.M., Jones, M.B., Dracheva, T., Peterson, S.N., Monack, D.M., and Barton, G.M. (2011). TLR signaling is required for Salmonella typhimurium virulence. Cell *144*, 675-688.

Arthur, J.S., and Ley, S.C. (2013). Mitogen-activated protein kinases in innate immunity. Nat Rev Immunol *13*, 679-692.

Bahri, R., Bollinger, A., Bollinger, T., Orinska, Z., and Bulfone-Paus, S. (2012). Ectonucleotidase CD38 demarcates regulatory, memory-like CD8+ T cells with IFN-gamma-mediated suppressor activities. PLoS One *7*, e45234.

Beceiro, S., Pap, A., Czimmerer, Z., Sallam, T., Guillen, J.A., Gallardo, G., Hong, C., N, A.G., Tabraue, C., Diaz, M.*, et al.* (2018). Liver X Receptor Nuclear Receptors Are Transcriptional Regulators of Dendritic Cell Chemotaxis. Mol Cell Biol *38*.

Beharka, A.A., Crowther, J.E., McCormack, F.X., Denning, G.M., Lees, J., Tibesar, E., and Schlesinger, L.S. (2005). Pulmonary surfactant protein A activates a phosphatidylinositol 3-kinase/calcium signal transduction pathway in human macrophages: participation in the up-regulation of mannose receptor activity. J Immunol *175*, 2227-2236.

Benito, J.M., Zabay, J.M., Gil, J., Bermejo, M., Escudero, A., Sanchez, E., and Fernandez-Cruz, E. (1997). Quantitative alterations of the functionally distinct subsets of CD4 and CD8 T lymphocytes in asymptomatic HIV infection: changes in the expression of CD45RO, CD45RA, CD11b, CD38, HLA-DR, and CD25 antigens. J Acquir Immune Defic Syndr Hum Retrovirol *14*, 128-135.

Bergsbaken, T., Fink, S.L., and Cookson, B.T. (2009). Pyroptosis: host cell death and inflammation. Nat Rev Microbiol *7*, 99-109.

Bhunia, A.K. (2018). Foordborne microbial pathogens: mechanisms and pathogenesis (Springer).

Birmingham, C.L., Smith, A.C., Bakowski, M.A., Yoshimori, T., and Brumell, J.H. (2006). Autophagy controls Salmonella infection in response to damage to the Salmonella-containing vacuole. Journal of Biological Chemistry *281*, 11374-11383.

Biswas, S.K., and Lopez-Collazo, E. (2009). Endotoxin tolerance: new mechanisms, molecules and clinical significance. Trends Immunol *30*, 475-487.

Blaschke, F., Takata, Y., Caglayan, E., Collins, A., Tontonoz, P., Hsueh, W.A., and Tangirala, R.K. (2006). A nuclear receptor corepressor-dependent pathway mediates suppression of cytokine-induced C-reactive protein gene expression by liver X receptor. Circ Res *99*, e88-99.

Bocchetta, S., Maillard, P., Yamamoto, M., Gondeau, C., Douam, F., Lebreton, S., Lagaye, S., Pol, S., Helle, F., Plengpanich, W.*, et al.* (2014). Up-regulation of the ATP-binding cassette transporter A1 inhibits hepatitis C virus infection. PLoS One *9*, e92140.

Bruhn, K.W., Marathe, C., Maretti-Mira, A.C., Nguyen, H., Haskell, J., Tran, T.A., Vanchinathan, V., Gaur, U., Wilson, M.E., Tontonoz, P.*, et al.* (2010). LXR deficiency confers increased protection against visceral Leishmania infection in mice. PLoS Negl Trop Dis *4*, e886.

Bukrinsky, M.I., Mukhamedova, N., and Sviridov, D. (2020). Lipid rafts and pathogens: the art of deception and exploitation: Thematic Review Series: Biology of Lipid Rafts. J Lipid Res *61*, 601-610.

Calkin, A.C., and Tontonoz, P. (2012). Transcriptional integration of metabolism by the nuclear sterol-activated receptors LXR and FXR. Nature reviews Molecular cell biology *13*, 213-224.

Cargnello, M., and Roux, P.P. (2011). Activation and function of the MAPKs and their substrates, the MAPK-activated protein kinases. Microbiol Mol Biol Rev *75*, 50-83.

Castrillo, A., Joseph, S.B., Vaidya, S.A., Haberland, M., Fogelman, A.M., Cheng, G., and Tontonoz, P. (2003). Crosstalk between LXR and toll-like receptor signaling mediates bacterial and viral antagonism of cholesterol metabolism. Mol Cell *12*, 805-816.

Cha, J.Y., and Repa, J.J. (2007). The liver X receptor (LXR) and hepatic lipogenesis. The carbohydrate-response element-binding protein is a target gene of LXR. J Biol Chem *282*, 743-751.

Cockayne, D.A., Muchamuel, T., Grimaldi, J.C., Muller-Steffner, H., Randall, T.D., Lund, F.E., Murray, R., Schuber, F., and Howard, M.C. (1998). Mice deficient for the ecto-nicotinamide adenine dinucleotide glycohydrolase CD38 exhibit altered humoral immune responses. Blood *92*, 1324-1333.

Covarrubias, A.J., Aksoylar, H.I., and Horng, T. (2015). Control of macrophage metabolism and activation by mTOR and Akt signaling. Semin Immunol *27*, 286-296.

Croxen, M.A., and Finlay, B.B. (2010). Molecular mechanisms of Escherichia coli pathogenicity. Nat Rev Microbiol *8*, 26-38.

Curtiss, L.K., and Boisvert, W.A. (2000). Apolipoprotein E and atherosclerosis. Curr Opin Lipidol *11*, 243-251.

Davies, L.C., Jenkins, S.J., Allen, J.E., and Taylor, P.R. (2013). Tissue-resident macrophages. Nat Immunol *14*, 986-995.

Dawson, M.I., and Xia, Z. (2012). The retinoid X receptors and their ligands. Biochim Biophys Acta *1821*, 21-56.

de Oliveira, C.A., and Mantovani, B. (1988). Latrunculin A is a potent inhibitor of phagocytosis by macrophages. Life sciences *43*, 1825-1830.

Deaglio, S., Morra, M., Mallone, R., Ausiello, C.M., Prager, E., Garbarino, G., Dianzani, U., Stockinger, H., and Malavasi, F. (1998). Human CD38 (ADP-ribosyl cyclase) is a counter-receptor of CD31, an Ig superfamily member. J Immunol *160*, 395-402.

Demeure, O., Lecerf, F., Duby, C., Desert, C., Ducheix, S., Guillou, H., and Lagarrigue, S. (2011). Regulation of LPCAT3 by LXR. Gene *470*, 7-11.

Dianzani, U., Bragardo, M., Buonfiglio, D., Redoglia, V., Funaro, A., Portoles, P., Rojo, J., Malavasi, F., and Pileri, A. (1995). Modulation of CD4 lateral interaction with lymphocyte surface molecules induced by HIV-1 gp120. Eur J Immunol *25*, 1306-1311.

Dibble, C.C., and Manning, B.D. (2013). Signal integration by mTORC1 coordinates nutrient input with biosynthetic output. Nat Cell Biol *15*, 555-564.

Diehl, J.A., and Hannink, M. (1994). Identification of a C/EBP-Rel complex in avian lymphoid cells. Mol Cell Biol *14*, 6635-6646.

Dong, C., Yang, D.D., Wysk, M., Whitmarsh, A.J., Davis, R.J., and Flavell, R.A. (1998). Defective T cell differentiation in the absence of Jnk1. Science *282*, 2092-2095.

Dooher, J.E., Paz-Priel, I., Houng, S., Baldwin, A.S., Jr., and Friedman, A.D. (2011). C/EBPalpha, C/EBPalpha oncoproteins, or C/EBPbeta preferentially bind NF-kappaB p50 compared with p65, focusing therapeutic targeting on the C/EBP:p50 interaction. Mol Cancer Res *9*, 1395-1405.

Dos Santos, A.M.P., Ferrari, R.G., and Conte-Junior, C.A. (2019). Virulence Factors in Salmonella Typhimurium: The Sagacity of a Bacterium. Curr Microbiol *76*, 762-773.

Drecktrah, D., Knodler, L.A., Ireland, R., and Steele-Mortimer, O. (2006). The mechanism of Salmonella entry determines the vacuolar environment and intracellular gene expression. Traffic *7*, 39-51.

Endo-Umeda, K., Nakashima, H., Komine-Aizawa, S., Umeda, N., Seki, S., and Makishima, M. (2018). Liver X receptors regulate hepatic F4/80 (+) CD11b(+) Kupffer cells/macrophages and innate immune responses in mice. Sci Rep *8*, 9281.

Ernst, R.K., Guina, T., and Miller, S.I. (2001). Salmonella typhimurium outer membrane remodeling: role in resistance to host innate immunity. Microbes Infect *3*, 1327-1334.

Estrada-Figueroa, L.A., Ramirez-Jimenez, Y., Osorio-Trujillo, C., Shibayama, M., Navarro-Garcia, F., Garcia-Tovar, C., and Talamas-Rohana, P. (2011). Absence of CD38 delays arrival of

neutrophils to the liver and innate immune response development during hepatic amoebiasis by Entamoeba histolytica. Parasite Immunol *33*, 661-668.

Faggioli, L., Costanzo, C., Donadelli, M., and Palmieri, M. (2004). Activation of the Interleukin-6 promoter by a dominant negative mutant of c-Jun. Biochim Biophys Acta *1692*, 17-24.

Fedele, G., Frasca, L., Palazzo, R., Ferrero, E., Malavasi, F., and Ausiello, C.M. (2004). CD38 is expressed on human mature monocyte-derived dendritic cells and is functionally involved in CD83 expression and IL-12 induction. Eur J Immunol *34*, 1342-1350.

Fernandez-Hernando, C., Ackah, E., Yu, J., Suarez, Y., Murata, T., Iwakiri, Y., Prendergast, J., Miao, R.Q., Birnbaum, M.J., and Sessa, W.C. (2007). Loss of Akt1 leads to severe atherosclerosis and occlusive coronary artery disease. Cell Metab *6*, 446-457.

Fessler, M.B. (2018). The challenges and promise of targeting the Liver X Receptors for treatment of inflammatory disease. Pharmacol Ther *181*, 1-12.

Flannagan, R.S., Cosio, G., and Grinstein, S. (2009). Antimicrobial mechanisms of phagocytes and bacterial evasion strategies. Nat Rev Microbiol *7*, 355-366.

Frasca, L., Fedele, G., Deaglio, S., Capuano, C., Palazzo, R., Vaisitti, T., Malavasi, F., and Ausiello, C.M. (2006). CD38 orchestrates migration, survival, and Th1 immune response of human mature dendritic cells. Blood *107*, 2392-2399.

Freeman, S.A., and Grinstein, S. (2014). Phagocytosis: receptors, signal integration, and the cytoskeleton. Immunol Rev *262*, 193-215.

Funaro, A., De Monte, L.B., Dianzani, U., Forni, M., and Malavasi, F. (1993). Human CD38 is associated to distinct molecules which mediate transmembrane signaling in different lineages. Eur J Immunol *23*, 2407-2411.

Ganesan, L.P., Wei, G., Pengal, R.A., Moldovan, L., Moldovan, N., Ostrowski, M.C., and Tridandapani, S. (2004). The serine/threonine kinase Akt Promotes Fc gamma receptor-mediated phagocytosis in murine macrophages through the activation of p70S6 kinase. J Biol Chem *279*, 54416-54425.

Garner, M.J., Hayward, R.D., and Koronakis, V. (2002). The Salmonella pathogenicity island 1 secretion system directs cellular cholesterol redistribution during mammalian cell entry and intracellular trafficking. Cell Microbiol *4*, 153-165.

Ghisletti, S., Huang, W., Jepsen, K., Benner, C., Hardiman, G., Rosenfeld, M.G., and Glass, C.K. (2009). Cooperative NCoR/SMRT interactions establish a corepressor-based strategy for integration of inflammatory and anti-inflammatory signaling pathways. Genes Dev *23*, 681-693.

Ghisletti, S., Huang, W., Ogawa, S., Pascual, G., Lin, M.E., Willson, T.M., Rosenfeld, M.G., and Glass, C.K. (2007). Parallel SUMOylation-dependent pathways mediate gene- and signal-specific transrepression by LXRs and PPARgamma. Mol Cell *25*, 57-70.

Gibbons, H.S., Kalb, S.R., Cotter, R.J., and Raetz, C.R. (2005). Role of Mg2+ and pH in the modification of Salmonella lipid A after endocytosis by macrophage tumour cells. Mol Microbiol *55*, 425-440.

Gilk, S.D., Cockrell, D.C., Luterbach, C., Hansen, B., Knodler, L.A., Ibarra, J.A., Steele-Mortimer, O., and Heinzen, R.A. (2013). Bacterial colonization of host cells in the absence of cholesterol. PLoS Pathog *9*, e1003107.

Giorgi, J.V., Hultin, L.E., McKeating, J.A., Johnson, T.D., Owens, B., Jacobson, L.P., Shih, R., Lewis, J., Wiley, D.J., Phair, J.P.*, et al.* (1999). Shorter survival in advanced human immunodeficiency virus type 1 infection is more closely associated with T lymphocyte activation than with plasma virus burden or virus chemokine coreceptor usage. J Infect Dis *179*, 859-870.

Glaría, E., Letelier, N.A., and Valledor, A.F. (2020). Integrating the roles of liver X receptors in inflammation and infection: Mechanisms and outcomes. Current Opinion in Pharmacology *53*, 55-65.

Glaría, E., Matalonga, J., and Valledor, A.F. (2019). Methods for Assessing the Effects of LXR Agonists on Macrophage Bacterial Infection. In Lipid-Activated Nuclear Receptors G. M., and P.-T. I., eds. (Humana Press, New York, NY), pp. 135-141.

Glaría, E., and Valledor, A.F. (2020). Roles of CD38 in the Immune Response to Infection. Cells *9*, 228.

Glass, C.K., and Ogawa, S. (2006). Combinatorial roles of nuclear receptors in inflammation and immunity. Nat Rev Immunol *6*, 44-55.

Glover, J.N., and Harrison, S.C. (1995). Crystal structure of the heterodimeric bZIP transcription factor c-Fos-c-Jun bound to DNA. Nature *373*, 257-261.

Goethe, R., and Phi-van, L. (1997). Evidence for an enhanced transcription-dependent de novo synthesis of C/EBPbeta in the LPS activation of the chicken lysozyme gene. J Leukoc Biol *61*, 367-374.

Gog, J.R., Murcia, A., Osterman, N., Restif, O., McKinley, T.J., Sheppard, M., Achouri, S., Wei, B., Mastroeni, P., Wood, J.L.*, et al.* (2012). Dynamics of Salmonella infection of macrophages at the single cell level. J R Soc Interface *9*, 2696-2707.

Gogoi, M., Shreenivas, M.M., and Chakravortty, D. (2019). Hoodwinking the Big-Eater to Prosper: The Salmonella-Macrophage Paradigm. J Innate Immun *11*, 289-299.

Goldstein, J.L., DeBose-Boyd, R.A., and Brown, M.S. (2006). Protein sensors for membrane sterols. Cell *124*, 35-46.

Gong, D., Shi, W., Yi, S.J., Chen, H., Groffen, J., and Heisterkamp, N. (2012a). TGFbeta signaling plays a critical role in promoting alternative macrophage activation. BMC Immunol *13*, 31.

Gong, L., Devenish, R.J., and Prescott, M. (2012b). Autophagy as a macrophage response to bacterial infection. IUBMB Life *64*, 740-747.

Gonzalez, N.A., Bensinger, S.J., Hong, C., Beceiro, S., Bradley, M.N., Zelcer, N., Deniz, J., Ramirez, C., Diaz, M., Gallardo, G.*, et al.* (2009). Apoptotic cells promote their own clearance and immune tolerance through activation of the nuclear receptor LXR. Immunity *31*, 245-258.

Gordon, M.A. (2008). Salmonella infections in immunocompromised adults. J Infect *56*, 413-422.

Gorina, R., Font-Nieves, M., Marquez-Kisinousky, L., Santalucia, T., and Planas, A.M. (2011). Astrocyte TLR4 activation induces a proinflammatory environment through the interplay between MyD88-dependent NFkappaB signaling, MAPK, and Jak1/Stat1 pathways. Glia *59*, 242-255.

Grabiec, A.M., Goenka, A., Fife, M.E., Fujimori, T., and Hussell, T. (2018). Axl and MerTK receptor tyrosine kinases maintain human macrophage efferocytic capacity in the presence of viral triggers. Eur J Immunol *48*, 855-860.

Grigoryan, G., Reinke, A.W., and Keating, A.E. (2009). Design of protein-interaction specificity gives selective bZIP-binding peptides. Nature *458*, 859-864.

Hajishengallis, G., and Lambris, J.D. (2011). Microbial manipulation of receptor crosstalk in innate immunity. Nat Rev Immunol *11*, 187-200.

Han, S., Zhuang, H., Shumyak, S., Wu, J., Xie, C., Li, H., Yang, L.J., and Reeves, W.H. (2018). Liver X Receptor Agonist Therapy Prevents Diffuse Alveolar Hemorrhage in Murine Lupus by Repolarizing Macrophages. Front Immunol *9*, 135.

Hanley, T.M., Blay Puryear, W., Gummuluru, S., and Viglianti, G.A. (2010). PPARgamma and LXR signaling inhibit dendritic cell-mediated HIV-1 capture and trans-infection. PLoS Pathog *6*, e1000981.

Haraga, A., Ohlson, M.B., and Miller, S.I. (2008). Salmonellae interplay with host cells. Nat Rev Microbiol *6*, 53-66.

Hartlova, A., Cerveny, L., Hubalek, M., Krocova, Z., and Stulik, J. (2010). Membrane rafts: a potential gateway for bacterial entry into host cells. Microbiology and immunology *54*, 237-245.

Haruta, I., Kato, Y., Hashimoto, E., Minjares, C., Kennedy, S., Uto, H., Yamauchi, K., Kobayashi, M., Yusa, S., Muller, U.*, et al.* (2001). Association of AIM, a novel apoptosis inhibitory factor, with hepatitis via supporting macrophage survival and enhancing phagocytotic function of macrophages. J Biol Chem *276*, 22910-22914.

Hayward, R.D., Cain, R.J., McGhie, E.J., Phillips, N., Garner, M.J., and Koronakis, V. (2005). Cholesterol binding by the bacterial type III translocon is essential for virulence effector delivery into mammalian cells. Mol Microbiol *56*, 590-603.

Heckmann, B.L., and Green, D.R. (2019). Correction: LC3-associated phagocytosis at a glance (doi:10.1242/jcs.222984). J Cell Sci *132*.

Heithoff, D.M., Conner, C.P., Hentschel, U., Govantes, F., Hanna, P.C., and Mahan, M.J. (1999). Coordinate intracellular expression of Salmonella genes induced during infection. J Bacteriol *181*, 799-807.

Henson, P.M., and Hume, D.A. (2006). Apoptotic cell removal in development and tissue homeostasis. Trends Immunol *27*, 244-250.

Hobbie, S., Chen, L.M., Davis, R.J., and Galan, J.E. (1997). Involvement of mitogen-activated protein kinase pathways in the nuclear responses and cytokine production induced by Salmonella typhimurium in cultured intestinal epithelial cells. J Immunol *159*, 5550-5559.

Hogan, K.A., Chini, C.C.S., and Chini, E.N. (2019). The Multi-faceted Ecto-enzyme CD38: Roles in Immunomodulation, Cancer, Aging, and Metabolic Diseases. Front Immunol *10*, 1187.

Holmgren, J. (1973). Comparison of the tissue receptors for Vibrio cholerae and Escherichia coli enterotoxins by means of gangliosides and natural cholera toxoid. Infect Immun *8*, 851-859.

Hong, C., and Tontonoz, P. (2014). Liver X receptors in lipid metabolism: opportunities for drug discovery. Nat Rev Drug Discov *13*, 433-444.

Hong, S., Park, S., and Yu, J.W. (2011). Pyrin domain (PYD)-containing inflammasome in innate immunity. Journal of Bacteriology and Virology *41*, 133-146.

Hotamisligil, G.S. (2006). Inflammation and metabolic disorders. Nature *444*, 860-867.

Hsu, W., Kerppola, T.K., Chen, P.L., Curran, T., and Chen-Kiang, S. (1994). Fos and Jun repress transcription activation by NF-IL6 through association at the basic zipper region. Mol Cell Biol *14*, 268-276.

Hu, J., Roy, S.K., Shapiro, P.S., Rodig, S.R., Reddy, S.P., Platanias, L.C., Schreiber, R.D., and Kalvakolanu, D.V. (2001). ERK1 and ERK2 activate CCAAAT/enhancer-binding protein-beta-dependent gene transcription in response to interferon-gamma. J Biol Chem *276*, 287-297.

Hu, X., and Ivashkiv, L.B. (2009). Cross-regulation of signaling pathways by interferon-gamma: implications for immune responses and autoimmune diseases. Immunity *31*, 539-550.

Hu, X., Li, S., Wu, J., Xia, C., and Lala, D.S. (2003). Liver X receptors interact with corepressors to regulate gene expression. Mol Endocrinol *17*, 1019-1026.

Huber, R., Pietsch, D., Panterodt, T., and Brand, K. (2012). Regulation of C/EBPbeta and resulting functions in cells of the monocytic lineage. Cell Signal *24*, 1287-1296.

Iqbal, J., and Zaidi, M. (2006). TNF regulates cellular NAD+ metabolism in primary macrophages. Biochem Biophys Res Commun *342*, 1312-1318.

Ishibashi, M., Varin, A., Filomenko, R., Lopez, T., Athias, A., Gambert, P., Blache, D., Thomas, C., Gautier, T., Lagrost, L.*, et al.* (2013). Liver x receptor regulates arachidonic acid distribution and eicosanoid release in human macrophages: a key role for lysophosphatidylcholine acyltransferase 3. Arterioscler Thromb Vasc Biol *33*, 1171-1179.

Ito, A., Hong, C., Rong, X., Zhu, X., Tarling, E.J., Hedde, P.N., Gratton, E., Parks, J., and Tontonoz, P. (2015a). LXRs link metabolism to inflammation through Abca1-dependent regulation of membrane composition and TLR signaling. Elife *4*, e08009.

Ito, S., Tanaka, Y., Oshino, R., Aiba, K., Thanasegaran, S., Nishio, N., and Isobe, K. (2015b). GADD34 inhibits activation-induced apoptosis of macrophages through enhancement of autophagy. Sci Rep *5*, 8327.

Jiang, H., Badralmaa, Y., Yang, J., Lempicki, R., Hazen, A., and Natarajan, V. (2012). Retinoic acid and liver X receptor agonist synergistically inhibit HIV infection in CD4+ T cells by up-regulating ABCA1-mediated cholesterol efflux. Lipids Health Dis *11*, 69.

Joseph, S.B., Bradley, M.N., Castrillo, A., Bruhn, K.W., Mak, P.A., Pei, L., Hogenesch, J., O'Connell R, M., Cheng, G., Saez, E.*, et al.* (2004). LXR-dependent gene expression is important for macrophage survival and the innate immune response. Cell *119*, 299-309.

Joseph, S.B., Castrillo, A., Laffitte, B.A., Mangelsdorf, D.J., and Tontonoz, P. (2003). Reciprocal regulation of inflammation and lipid metabolism by liver X receptors. Nat Med *9*, 213-219.

Kagan, J.C., Su, T., Horng, T., Chow, A., Akira, S., and Medzhitov, R. (2008). TRAM couples endocytosis of Toll-like receptor 4 to the induction of interferon-beta. Nat Immunol *9*, 361-368.

Kalliolias, G.D., and Ivashkiv, L.B. (2016). TNF biology, pathogenic mechanisms and emerging therapeutic strategies. Nat Rev Rheumatol *12*, 49-62.

Kang, J., Park, K.H., Kim, J.J., Jo, E.K., Han, M.K., and Kim, U.H. (2012). The role of CD38 in Fcgamma receptor (FcgammaR)-mediated phagocytosis in murine macrophages. J Biol Chem *287*, 14502-14514.

Kang, Y.J., Chen, J., Otsuka, M., Mols, J., Ren, S., Wang, Y., and Han, J. (2008). Macrophage deletion of p38alpha partially impairs lipopolysaccharide-induced cellular activation. J Immunol *180*, 5075-5082.

Kaniga, K., Bossio, J.C., and Galán, J.E. (1994). The Salmonella typhimurium invasion genes invF and invG encode homologues of the AraC and PulD family of proteins. Molecular microbiology *13*, 555-568.

Kim, E.K., and Choi, E.J. (2015). Compromised MAPK signaling in human diseases: an update. Archives of toxicology *89*, 867-882.

Korf, H., Vander Beken, S., Romano, M., Steffensen, K.R., Stijlemans, B., Gustafsson, J.A., Grooten, J., and Huygen, K. (2009). Liver X receptors contribute to the protective immune response against Mycobacterium tuberculosis in mice. J Clin Invest *119*, 1626-1637.

Kravchenko, V.V., Mathison, J.C., Schwamborn, K., Mercurio, F., and Ulevitch, R.J. (2003). IKKi/IKKepsilon plays a key role in integrating signals induced by pro-inflammatory stimuli. J Biol Chem *278*, 26612-26619.

Kuwata, K., Watanabe, H., Jiang, S.Y., Yamamoto, T., Tomiyama-Miyaji, C., Abo, T., Miyazaki, T., and Naito, M. (2003). AIM inhibits apoptosis of T cells and NKT cells in Corynebacterium-induced granuloma formation in mice. Am J Pathol *162*, 837-847.

Lande, R., Urbani, F., Di Carlo, B., Sconocchia, G., Deaglio, S., Funaro, A., Malavasi, F., and Ausiello, C.M. (2002). CD38 ligation plays a direct role in the induction of IL-1beta, IL-6, and IL-10 secretion in resting human monocytes. Cell Immunol *220*, 30-38.

Langer, C., Huang, Y., Cullen, P., Wiesenhutter, B., Mahley, R.W., Assmann, G., and von Eckardstein, A. (2000). Endogenous apolipoprotein E modulates cholesterol efflux and cholesteryl ester hydrolysis mediated by high-density lipoprotein-3 and lipid-free apolipoproteins in mouse peritoneal macrophages. J Mol Med (Berl) *78*, 217-227.

Larson-Casey, J.L., Deshane, J.S., Ryan, A.J., Thannickal, V.J., and Carter, A.B. (2016). Macrophage Akt1 Kinase-Mediated Mitophagy Modulates Apoptosis Resistance and Pulmonary Fibrosis. Immunity *44*, 582-596.

Lee, C.U., Song, E.K., Yoo, C.H., Kwak, Y.K., and Han, M.K. (2012a). Lipopolysaccharide induces CD38 expression and solubilization in J774 macrophage cells. Mol Cells *34*, 573-576.

Lee, J.H., Park, S.M., Kim, O.S., Lee, C.S., Woo, J.H., Park, S.J., Joe, E.H., and Jou, I. (2009). Differential SUMOylation of LXRalpha and LXRbeta mediates transrepression of STAT1 inflammatory signaling in IFN-gamma-stimulated brain astrocytes. Mol Cell *35*, 806-817.

Lee, J.Y., and Parks, J.S. (2005). ATP-binding cassette transporter AI and its role in HDL formation. Curr Opin Lipidol *16*, 19-25.

Lee, K., Na, W., Lee, J.Y., Na, J., Cho, H., Wu, H., Yune, T.Y., Kim, W.S., and Ju, B.G. (2012b). Molecular mechanism of Jmjd3-mediated interleukin-6 gene regulation in endothelial cells underlying spinal cord injury. J Neurochem *122*, 272-282.

Lefterova, M.I., Zhang, Y., Steger, D.J., Schupp, M., Schug, J., Cristancho, A., Feng, D., Zhuo, D., Stoeckert, C.J., Jr., Liu, X.S*., et al.* (2008). PPARgamma and C/EBP factors orchestrate adipocyte biology via adjacent binding on a genome-wide scale. Genes Dev *22*, 2941-2952.

Lingwood, D., Kaiser, H.J., Levental, I., and Simons, K. (2009). Lipid rafts as functional heterogeneity in cell membranes. Biochem Soc Trans *37*, 955-960.

Lischke, T., Heesch, K., Schumacher, V., Schneider, M., Haag, F., Koch-Nolte, F., and Mittrucker, H.W. (2013). CD38 controls the innate immune response against Listeria monocytogenes. Infect Immun *81*, 4091-4099.

Listman, J.A., Wara-aswapati, N., Race, J.E., Blystone, L.W., Walker-Kopp, N., Yang, Z., and Auron, P.E. (2005). Conserved ETS domain arginines mediate DNA binding, nuclear localization, and a novel mode of bZIP interaction. J Biol Chem *280*, 41421-41428.

Liu, Z., Hultin, L.E., Cumberland, W.G., Hultin, P., Schmid, I., Matud, J.L., Detels, R., and Giorgi, J.V. (1996). Elevated relative fluorescence intensity of CD38 antigen expression on CD8+ T cells is a marker of poor prognosis in HIV infection: results of 6 years of follow-up. Cytometry *26*, 1-7.

Lopez-Pelaez, M., Soria-Castro, I., Bosca, L., Fernandez, M., and Alemany, S. (2011). Cot/tpl2 activity is required for TLR-induced activation of the Akt p70 S6k pathway in macrophages: Implications for NO synthase 2 expression. Eur J Immunol *41*, 1733-1741.

Lu, Y.C., Yeh, W.C., and Ohashi, P.S. (2008). LPS/TLR4 signal transduction pathway. Cytokine *42*, 145-151.

Lucke, K., Yan, I., Krohn, S., Volmari, A., Klinge, S., Schmid, J., Schumacher, V., Steinmetz, O.M., Rose-John, S., and Mittrucker, H.W. (2018). Control of Listeria monocytogenes infection requires classical IL-6 signaling in myeloid cells. PLoS One *13*, e0203395.

Majoros, A., Platanitis, E., Kernbauer-Holzl, E., Rosebrock, F., Muller, M., and Decker, T. (2017). Canonical and Non-Canonical Aspects of JAK-STAT Signaling: Lessons from Interferons for Cytokine Responses. Front Immunol *8*, 29.

Malavasi, F., Deaglio, S., Funaro, A., Ferrero, E., Horenstein, A.L., Ortolan, E., Vaisitti, T., and Aydin, S. (2008). Evolution and function of the ADP ribosyl cyclase/CD38 gene family in physiology and pathology. Physiol Rev *88*, 841-886.

Malik-Kale, P., Jolly, C.E., Lathrop, S., Winfree, S., Luterbach, C., and Steele-Mortimer, O. (2011). Salmonella - at home in the host cell. Front Microbiol *2*, 125.

Malini, N., Rajesh, H., Berwal, P., Phukan, S., and Balaji, V.N. (2008). Analysis of crystal structures of LXRbeta in relation to plasticity of the ligand-binding domain upon ligand binding. Chem Biol Drug Des *71*, 140-154.

Mantovani, A., Sica, A., Sozzani, S., Allavena, P., Vecchi, A., and Locati, M. (2004). The chemokine system in diverse forms of macrophage activation and polarization. Trends Immunol *25*, 677-686.

Martinez, F.O., and Gordon, S. (2014). The M1 and M2 paradigm of macrophage activation: time for reassessment. F1000Prime Rep *6*, 13.

Matalonga, J., Glaria, E., Bresque, M., Escande, C., Carbó, J.M., Kiefer, K., Vicente, R., León, T.E., Beceiro, S., Pascual-García, M.*, et al.* (2017). The nuclear receptor LXR limits bacterial infection of host macrophages through a mechanism that impacts cellular NAD metabolism. Cell reports *18*, 1241-1255.

Mazzone, T. (1996). Apolipoprotein E secretion by macrophages: its potential physiological functions. Curr Opin Lipidol *7*, 303-307.

Miao, E.A., Leaf, I.A., Treuting, P.M., Mao, D.P., Dors, M., Sarkar, A., Warren, S.E., Wewers, M.D., and Aderem, A. (2010). Caspase-1-induced pyroptosis is an innate immune effector mechanism against intracellular bacteria. Nat Immunol *11*, 1136-1142.

Miller, M., Shuman, J.D., Sebastian, T., Dauter, Z., and Johnson, P.F. (2003). Structural basis for DNA recognition by the basic region leucine zipper transcription factor CCAAT/enhancer-binding protein alpha. J Biol Chem *278*, 15178-15184.

Mitchell, G., Chen, C., and Portnoy, D.A. (2016). Strategies Used by Bacteria to Grow in Macrophages. Microbiol Spectr *4*.

Miyazaki, T., Hirokami, Y., Matsuhashi, N., Takatsuka, H., and Naito, M. (1999). Increased susceptibility of thymocytes to apoptosis in mice lacking AIM, a novel murine macrophage-derived soluble factor belonging to the scavenger receptor cysteine-rich domain superfamily. J Exp Med *189*, 413-422.

Mocroft, A., Bofill, M., Lipman, M., Medina, E., Borthwick, N., Timms, A., Batista, L., Winter, M., Sabin, C.A., Johnson, M.*, et al.* (1997). CD8+,CD38+ lymphocyte percent: a useful immunological marker for monitoring HIV-1-infected patients. J Acquir Immune Defic Syndr Hum Retrovirol *14*, 158-162.

Morandi, F., Horenstein, A.L., Costa, F., Giuliani, N., Pistoia, V., and Malavasi, F. (2018). CD38: A Target for Immunotherapeutic Approaches in Multiple Myeloma. Front Immunol *9*, 2722.

Morrison, D.K. (2012). MAP kinase pathways. Cold Spring Harb Perspect Biol *4*.

Morrow, M.P., Grant, A., Mujawar, Z., Dubrovsky, L., Pushkarsky, T., Kiselyeva, Y., Jennelle, L., Mukhamedova, N., Remaley, A.T., Kashanchi, F.*, et al.* (2010). Stimulation of the liver X receptor pathway inhibits HIV-1 replication via induction of ATP-binding cassette transporter A1. Mol Pharmacol *78*, 215-225.

Mouthiers, A., Baillet, A., Delomenie, C., Porquet, D., and Mejdoubi-Charef, N. (2005). Peroxisome proliferator-activated receptor alpha physically interacts with CCAAT/enhancer binding protein (C/EBPbeta) to inhibit C/EBPbeta-responsive alpha1-acid glycoprotein gene expression. Mol Endocrinol *19*, 1135-1146.

Mujawar, Z., Rose, H., Morrow, M.P., Pushkarsky, T., Dubrovsky, L., Mukhamedova, N., Fu, Y., Dart, A., Orenstein, J.M., Bobryshev, Y.V.*, et al.* (2006). Human immunodeficiency virus impairs reverse cholesterol transport from macrophages. PLoS Biol *4*, e365.

Murakami, Y., Tian, L., Voss, O.H., Margulies, D.H., Krzewski, K., and Coligan, J.E. (2014). CD300b regulates the phagocytosis of apoptotic cells via phosphatidylserine recognition. Cell Death Differ *21*, 1746-1757.

Murphy, K. (2012). Janeway's Immunobiology, 8 edn (New York, USA: Garland Science).

Murray, P.J., Allen, J.E., Biswas, S.K., Fisher, E.A., Gilroy, D.W., Goerdt, S., Gordon, S., Hamilton, J.A., Ivashkiv, L.B., Lawrence, T.*, et al.* (2014). Macrophage activation and polarization: nomenclature and experimental guidelines. Immunity *41*, 14-20.

Murray, P.J., and Wynn, T.A. (2011). Protective and pathogenic functions of macrophage subsets. Nat Rev Immunol *11*, 723-737.

Musso, T., Deaglio, S., Franco, L., Calosso, L., Badolato, R., Garbarino, G., Dianzani, U., and Malavasi, F. (2001). CD38 expression and functional activities are up-regulated by IFN-gamma on human monocytes and monocytic cell lines. J Leukoc Biol *69*, 605-612.

Naj, X., Hoffmann, A.K., Himmel, M., and Linder, S. (2013). The formins FMNL1 and mDia1 regulate coiling phagocytosis of Borrelia burgdorferi by primary human macrophages. Infect Immun *81*, 1683-1695.

Natsuka, S., Akira, S., Nishio, Y., Hashimoto, S., Sugita, T., Isshiki, H., and Kishimoto, T. (1992). Macrophage differentiation-specific expression of NF-IL6, a transcription factor for interleukin-6. Blood *79*, 460-466.

Newman, J.R., and Keating, A.E. (2003). Comprehensive identification of human bZIP interactions with coiled-coil arrays. Science *300*, 2097-2101.

Niehof, M., Kubicka, S., Zender, L., Manns, M.P., and Trautwein, C. (2001a). Autoregulation enables different pathways to control CCAAT/enhancer binding protein beta (C/EBP beta) transcription. J Mol Biol *309*, 855-868.

Niehof, M., Streetz, K., Rakemann, T., Bischoff, S.C., Manns, M.P., Horn, F., and Trautwein, C. (2001b). Interleukin-6-induced tethering of STAT3 to the LAP/C/EBPbeta promoter suggests a new mechanism of transcriptional regulation by STAT3. J Biol Chem *276*, 9016-9027.

Nunomura, S., Okayama, Y., Matsumoto, K., Hashimoto, N., Endo-Umeda, K., Terui, T., Makishima, M., and Ra, C. (2015). Activation of LXRs using the synthetic agonist GW3965 represses the production of pro-inflammatory cytokines by murine mast cells. Allergol Int *64 Suppl*, S11-17.

O'Keefe, S.J., Mudgett, J.S., Cupo, S., Parsons, J.N., Chartrain, N.A., Fitzgerald, C., Chen, S.L., Lowitz, K., Rasa, C., Visco, D*., et al.* (2007). Chemical genetics define the roles of p38alpha and p38beta in acute and chronic inflammation. J Biol Chem *282*, 34663-34671.

Oram, J.F., Lawn, R.M., Garvin, M.R., and Wade, D.P. (2000). ABCA1 is the cAMP-inducible apolipoprotein receptor that mediates cholesterol secretion from macrophages. J Biol Chem *275*, 34508-34511.

Owen, K.A., Meyer, C.B., Bouton, A.H., and Casanova, J.E. (2014). Activation of focal adhesion kinase by Salmonella suppresses autophagy via an Akt/mTOR signaling pathway and promotes bacterial survival in macrophages. PLoS Pathog *10*, e1004159.

Palmer, A.D., and Slauch, J.M. (2017). Mechanisms of Salmonella pathogenesis in animal models. Hum Ecol Risk Assess *23*, 1877-1892.

Park, H.J., Lee, S.J., Kim, S.H., Han, J., Bae, J., Kim, S.J., Park, C.G., and Chun, T. (2011). IL-10 inhibits the starvation induced autophagy in macrophages via class I phosphatidylinositol 3-kinase (PI3K) pathway. Mol Immunol *48*, 720-727.

Partida-Sanchez, S., Cockayne, D.A., Monard, S., Jacobson, E.L., Oppenheimer, N., Garvy, B., Kusser, K., Goodrich, S., Howard, M., Harmsen, A*., et al.* (2001). Cyclic ADP-ribose production by CD38 regulates intracellular calcium release, extracellular calcium influx and chemotaxis in neutrophils and is required for bacterial clearance in vivo. Nat Med *7*, 1209-1216.

Partida-Sanchez, S., Gasser, A., Fliegert, R., Siebrands, C.C., Dammermann, W., Shi, G., Mousseau, B.J., Sumoza-Toledo, A., Bhagat, H., Walseth, T.F*., et al.* (2007). Chemotaxis of

mouse bone marrow neutrophils and dendritic cells is controlled by adp-ribose, the major product generated by the CD38 enzyme reaction. J Immunol *179*, 7827-7839.

Partida-Sanchez, S., Iribarren, P., Moreno-Garcia, M.E., Gao, J.L., Murphy, P.M., Oppenheimer, N., Wang, J.M., and Lund, F.E. (2004). Chemotaxis and calcium responses of phagocytes to formyl peptide receptor ligands is differentially regulated by cyclic ADP ribose. J Immunol *172*, 1896-1906.

Partida-Sanchez, S., Randall, T.D., and Lund, F.E. (2003). Innate immunity is regulated by CD38, an ecto-enzyme with ADP-ribosyl cyclase activity. Microbes Infect *5*, 49-58.

Pascual-Garcia, M., Rue, L., Leon, T., Julve, J., Carbo, J.M., Matalonga, J., Auer, H., Celada, A., Escola-Gil, J.C., Steffensen, K.R*., et al.* (2013). Reciprocal negative cross-talk between liver X receptors (LXRs) and STAT1: effects on IFN-gamma-induced inflammatory responses and LXR-dependent gene expression. J Immunol *190*, 6520-6532.

Patel, J.C., and Galan, J.E. (2006). Differential activation and function of Rho GTPases during Salmonella-host cell interactions. J Cell Biol *175*, 453-463.

Patton, D.T., Wilson, M.D., Rowan, W.C., Soond, D.R., and Okkenhaug, K. (2011). The PI3K p110delta regulates expression of CD38 on regulatory T cells. PLoS One *6*, e17359.

Peet, D.J., Turley, S.D., Ma, W., Janowski, B.A., Lobaccaro, J.M., Hammer, R.E., and Mangelsdorf, D.J. (1998). Cholesterol and bile acid metabolism are impaired in mice lacking the nuclear oxysterol receptor LXR alpha. Cell *93*, 693-704.

Perissi, V., Aggarwal, A., Glass, C.K., Rose, D.W., and Rosenfeld, M.G. (2004). A corepressor/coactivator exchange complex required for transcriptional activation by nuclear receptors and other regulated transcription factors. Cell *116*, 511-526.

Plotnikov, A., Zehorai, E., Procaccia, S., and Seger, R. (2011). The MAPK cascades: signaling components, nuclear roles and mechanisms of nuclear translocation. Biochim Biophys Acta *1813*, 1619-1633.

Popoff, M.R. (2014). Bacterial factors exploit eukaryotic Rho GTPase signaling cascades to promote invasion and proliferation within their host. Small GTPases *5*.

Pourcet, B., Gage, M.C., Leon, T.E., Waddington, K.E., Pello, O.M., Steffensen, K.R., Castrillo, A., Valledor, A.F., and Pineda-Torra, I. (2016). The nuclear receptor LXR modulates interleukin-18 levels in macrophages through multiple mechanisms. Sci Rep *6*, 25481.

Price, J.V., and Vance, R.E. (2014). The macrophage paradox. Immunity *41*, 685-693.

Pulido-Salgado, M., Vidal-Taboada, J.M., Diaz-Barriga, G.G., Serratosa, J., Valente, T., Castillo, P., Matalonga, J., Straccia, M., Canals, J.M., Valledor, A*., et al.* (2017). Myeloid C/EBPβ deficiency reshapes microglial gene expression and is protective in experimental autoimmune encephalomyelitis. Journal of neuroinflammation *14*, 1-20.

Pulido-Salgado, M., Vidal-Taboada, J.M., and Saura, J. (2015). C/EBPbeta and C/EBPdelta transcription factors: Basic biology and roles in the CNS. Prog Neurobiol *132*, 1-33.

Qian, H., Zhao, X., Cao, P., Lei, J., Yan, N., and Gong, X. (2017). Structure of the Human Lipid Exporter ABCA1. Cell *169*, 1228-1239 e1210.

Qiao, Y., Kang, K., Giannopoulou, E., Fang, C., and Ivashkiv, L.B. (2016). IFN-gamma Induces Histone 3 Lysine 27 Trimethylation in a Small Subset of Promoters to Stably Silence Gene Expression in Human Macrophages. Cell Rep *16*, 3121-3129.

Ramezani, A., Dubrovsky, L., Pushkarsky, T., Sviridov, D., Karandish, S., Raj, D.S., Fitzgerald, M.L., and Bukrinsky, M. (2015). Stimulation of Liver X Receptor Has Potent Anti-HIV Effects in a Humanized Mouse Model of HIV Infection. J Pharmacol Exp Ther *354*, 376-383.

Ramon-Vazquez, A., de la Rosa, J.V., Tabraue, C., Lopez, F., Diaz-Chico, B.N., Bosca, L., Tontonoz, P., Alemany, S., and Castrillo, A. (2019). Common and Differential Transcriptional Actions of Nuclear Receptors Liver X Receptors alpha and beta in Macrophages. Mol Cell Biol *39*.

Repa, J.J., Liang, G., Ou, J., Bashmakov, Y., Lobaccaro, J.M., Shimomura, I., Shan, B., Brown, M.S., Goldstein, J.L., and Mangelsdorf, D.J. (2000a). Regulation of mouse sterol regulatory element-binding protein-1c gene (SREBP-1c) by oxysterol receptors, LXRalpha and LXRbeta. Genes Dev *14*, 2819-2830.

Repa, J.J., Turley, S.D., Lobaccaro, J.A., Medina, J., Li, L., Lustig, K., Shan, B., Heyman, R.A., Dietschy, J.M., and Mangelsdorf, D.J. (2000b). Regulation of absorption and ABC1-mediated efflux of cholesterol by RXR heterodimers. Science *289*, 1524-1529.

Riedl, J., Flynn, K.C., Raducanu, A., Gartner, F., Beck, G., Bosl, M., Bradke, F., Massberg, S., Aszodi, A., Sixt, M.*, et al.* (2010). Lifeact mice for studying F-actin dynamics. Nat Methods *7*, 168-169.

Rocher, C., and Singla, D.K. (2013). SMAD-PI3K-Akt-mTOR pathway mediates BMP-7 polarization of monocytes into M2 macrophages. PLoS One *8*, e84009.

Rong, X., Albert, C.J., Hong, C., Duerr, M.A., Chamberlain, B.T., Tarling, E.J., Ito, A., Gao, J., Wang, B., Edwards, P.A.*, et al.* (2013). LXRs regulate ER stress and inflammation through dynamic modulation of membrane phospholipid composition. Cell Metab *18*, 685-697.

Roos, A.B., and Nord, M. (2012). The emerging role of C/EBPs in glucocorticoid signaling: lessons from the lung. J Endocrinol *212*, 291-305.

Rosales, C., and Uribe-Querol, E. (2017). Phagocytosis: A Fundamental Process in Immunity. Biomed Res Int *2017*, 9042851.

Rothlin, C.V., Carrera-Silva, E.A., Bosurgi, L., and Ghosh, S. (2015). TAM receptor signaling in immune homeostasis. Annual review of immunology *33*, 355-391.

Ruffell, D., Mourkioti, F., Gambardella, A., Kirstetter, P., Lopez, R.G., Rosenthal, N., and Nerlov, C. (2009). A CREB-C/EBPbeta cascade induces M2 macrophage-specific gene expression and promotes muscle injury repair. Proc Natl Acad Sci U S A *106*, 17475-17480.

Ruocco, M.R., Chen, X., Ambrosino, C., Dragonetti, E., Liu, W., Mallardo, M., De Falco, G., Palmieri, C., Franzoso, G., Quinto, I.*, et al.* (1996). Regulation of HIV-1 long terminal repeats by interaction of C/EBP(NF-IL6) and NF-kappaB/Rel transcription factors. J Biol Chem *271*, 22479-22486.

Samanta, D., Mulye, M., Clemente, T.M., Justis, A.V., and Gilk, S.D. (2017). Manipulation of Host Cholesterol by Obligate Intracellular Bacteria. Front Cell Infect Microbiol *7*, 165.

Sanjurjo, L., Amezaga, N., Vilaplana, C., Caceres, N., Marzo, E., Valeri, M., Cardona, P.J., and Sarrias, M.R. (2013). The scavenger protein apoptosis inhibitor of macrophages (AIM) potentiates the antimicrobial response against Mycobacterium tuberculosis by enhancing autophagy. PLoS One *8*, e79670.

Sanjurjo, L., Aran, G., Roher, N., Valledor, A.F., and Sarrias, M.R. (2015). AIM/CD5L: a key protein in the control of immune homeostasis and inflammatory disease. Journal of leukocyte biology *98*, 173-184.

Sarantis, H., and Grinstein, S. (2012). Subversion of phagocytosis for pathogen survival. Cell Host Microbe *12*, 419-431.

Schiavoni, I., Scagnolari, C., Horenstein, A.L., Leone, P., Pierangeli, A., Malavasi, F., Ausiello, C.M., and Fedele, G. (2018). CD38 modulates respiratory syncytial virus-driven proinflammatory processes in human monocyte-derived dendritic cells. Immunology *154*, 122-131.

Schroder, K., Hertzog, P.J., Ravasi, T., and Hume, D.A. (2004). Interferon-gamma: an overview of signals, mechanisms and functions. J Leukoc Biol *75*, 163-189.

Schroeder, G.N., and Hilbi, H. (2008). Molecular pathogenesis of Shigella spp.: controlling host cell signaling, invasion, and death by type III secretion. Clin Microbiol Rev *21*, 134-156.

Schulman, I.G. (2017). Liver X receptors link lipid metabolism and inflammation. FEBS Lett *591*, 2978-2991.

Screpanti, I., Romani, L., Musiani, P., Modesti, A., Fattori, E., Lazzaro, D., Sellitto, C., Scarpa, S., Bellavia, D., and Lattanzio, G. (1995). Lymphoproliferative disorder and imbalanced T-helper response in C/EBP beta-deficient mice. The EMBO journal *14*, 1932-1941.

Shapouri-Moghaddam, A., Mohammadian, S., Vazini, H., Taghadosi, M., Esmaeili, S.A., Mardani, F., Seifi, B., Mohammadi, A., Afshari, J.T., and Sahebkar, A. (2018). Macrophage plasticity, polarization, and function in health and disease. J Cell Physiol *233*, 6425-6440.

Sheng, X.X., Sun, Y.J., Zhan, Y., Qu, Y.R., Wang, H.X., Luo, M., Liao, Y., Qiu, X.S., Ding, C., Fan, H.J.*, et al.* (2016). The LXR ligand GW3965 inhibits Newcastle disease virus infection by affecting cholesterol homeostasis. Arch Virol *161*, 2491-2501.

Shiratsuchi, H., and Basson, M.D. (2007). Akt2, but not Akt1 or Akt3 mediates pressure-stimulated serum-opsonized latex bead phagocytosis through activating mTOR and p70 S6 kinase. J Cell Biochem *102*, 353-367.

Shu, B., Feng, Y., Gui, Y., Lu, Q., Wei, W., Xue, X., Sun, X., He, W., Yang, J., and Dai, C. (2018). Blockade of CD38 diminishes lipopolysaccharide-induced macrophage classical activation and acute kidney injury involving NF-kappaB signaling suppression. Cell Signal *42*, 249-258.

Silva, R.M., Toledo, M.R., and Trabulsi, L.R. (1980). Biochemical and cultural characteristics of invasive Escherichia coli. Journal of Clinical Microbiology *11*, 441-444.

Smith, J.D., Le Goff, W., Settle, M., Brubaker, G., Waelde, C., Horwitz, A., and Oda, M.N. (2004). ABCA1 mediates concurrent cholesterol and phospholipid efflux to apolipoprotein A-I. J Lipid Res *45*, 635-644.

Smoak, K., Madenspacher, J., Jeyaseelan, S., Williams, B., Dixon, D., Poch, K.R., Nick, J.A., Worthen, G.S., and Fessler, M.B. (2008). Effects of liver X receptor agonist treatment on pulmonary inflammation and host defense. J Immunol *180*, 3305-3312.

Soares, M.P., and Hamza, I. (2016). Macrophages and Iron Metabolism. Immunity *44*, 492-504.

Song, E.K., Lee, Y.R., Kim, Y.R., Yeom, J.H., Yoo, C.H., Kim, H.K., Park, H.M., Kang, H.S., Kim, J.S., Kim, U.H*., et al.* (2012). NAADP mediates insulin-stimulated glucose uptake and insulin sensitization by PPARgamma in adipocytes. Cell Rep *2*, 1607-1619.

Song, G., Ouyang, G., and Bao, S. (2005). The activation of Akt/PKB signaling pathway and cell survival. J Cell Mol Med *9*, 59-71.

Sonoki, T., Nagasaki, A., Gotoh, T., Takiguchi, M., Takeya, M., Matsuzaki, H., and Mori, M. (1997). Coinduction of nitric-oxide synthase and arginase I in cultured rat peritoneal macrophages and rat tissues in vivo by lipopolysaccharide. J Biol Chem *272*, 3689-3693.

Spann, N.J., Garmire, L.X., McDonald, J.G., Myers, D.S., Milne, S.B., Shibata, N., Reichart, D., Fox, J.N., Shaked, I., Heudobler, D*., et al.* (2012). Regulated accumulation of desmosterol integrates macrophage lipid metabolism and inflammatory responses. Cell *151*, 138-152.

Stoffels, K., Overbergh, L., Giulietti, A., Verlinden, L., Bouillon, R., and Mathieu, C. (2006). Immune regulation of 25-hydroxyvitamin-D3-1alpha-hydroxylase in human monocytes. J Bone Miner Res *21*, 37-47.

Svensson, S., Ostberg, T., Jacobsson, M., Norstrom, C., Stefansson, K., Hallen, D., Johansson, I.C., Zachrisson, K., Ogg, D., and Jendeberg, L. (2003). Crystal structure of the heterodimeric complex of LXRalpha and RXRbeta ligand-binding domains in a fully agonistic conformation. EMBO J *22*, 4625-4633.

Tahirov, T.H., Sato, K., Ichikawa-Iwata, E., Sasaki, M., Inoue-Bungo, T., Shiina, M., Kimura, K., Takata, S., Fujikawa, A., Morii, H*., et al.* (2002). Mechanism of c-Myb-C/EBP beta cooperation from separated sites on a promoter. Cell *108*, 57-70.

Takeuchi, O., & Akira, S. (2010). Pattern recognition receptors and inflammation. Cell *140*, 137-151.

Tanaka, T., Akira, S., Yoshida, K., Umemoto, M., Yoneda, Y., Shirafuji, N., Fujiwara, H., Suematsu, S., Yoshida, N., and Kishimoto, T. (1995). Targeted disruption of the NF-IL6 gene

discloses its essential role in bacteria killing and tumor cytotoxicity by macrophages. Cell *80*, 353-361.

Tarling, E.J., and Edwards, P.A. (2011). ATP binding cassette transporter G1 (ABCG1) is an intracellular sterol transporter. Proc Natl Acad Sci U S A *108*, 19719-19724.

Tarragó, M.G., Chini, C.C., Kanamori, K.S., Warner, G.M., Caride, A., de Oliveira, G.C., Rud, M., Samani, A., Hein, K.Z., Huang, R.*, et al.* (2018). A potent and specific CD38 inhibitor ameliorates age-related metabolic dysfunction by reversing tissue NAD+ decline. Cell metabolism *27*, 1081-1095.

Tengku-Muhammad, T.S., Hughes, T.R., Ranki, H., Cryer, A., and Ramji, D.P. (2000). Differential regulation of macrophage CCAAT-enhancer binding protein isoforms by lipopolysaccharide and cytokines. Cytokine *12*, 1430-1436.

Terlizzi, M.E., Gribaudo, G., and Maffei, M.E. (2017). UroPathogenic Escherichia coli (UPEC) Infections: Virulence Factors, Bladder Responses, Antibiotic, and Non-antibiotic Antimicrobial Strategies. Front Microbiol *8*, 1566.

Thi, E.P., Lambertz, U., and Reiner, N.E. (2012). Sleeping with the enemy: how intracellular pathogens cope with a macrophage lifestyle. PLoS Pathog *8*, e1002551.

Thorp, E., Vaisar, T., Subramanian, M., Mautner, L., Blobel, C., and Tabas, I. (2011). Shedding of the Mer tyrosine kinase receptor is mediated by ADAM17 protein through a pathway involving reactive oxygen species, protein kinase Cdelta, and p38 mitogen-activated protein kinase (MAPK). J Biol Chem *286*, 33335-33344.

Tian, J., Goldstein, J.L., and Brown, M.S. (2016). Insulin induction of SREBP-1c in rodent liver requires LXRalpha-C/EBPbeta complex. Proc Natl Acad Sci U S A *113*, 8182-8187.

Troutman, T.D., Bazan, J.F., and Pasare, C. (2012). Toll-like receptors, signaling adapters and regulation of the pro-inflammatory response by PI3K. Cell Cycle *11*, 3559-3567.

Tsukada, J., Yoshida, Y., Kominato, Y., and Auron, P.E. (2011). The CCAAT/enhancer (C/EBP) family of basic-leucine zipper (bZIP) transcription factors is a multifaceted highly-regulated system for gene regulation. Cytokine *54*, 6-19.

Valledor, A.F., Comalada, M., Xaus, J., and Celada, A. (2000). The differential time-course of extracellular-regulated kinase activity correlates with the macrophage response toward proliferation or activation. *275*, 7403-7409.

Valledor, A.F., Hsu, L.C., Ogawa, S., Sawka-Verhelle, D., Karin, M., and Glass, C.K. (2004). Activation of liver X receptors and retinoid X receptors prevents bacterial-induced macrophage apoptosis. Proc Natl Acad Sci U S A *101*, 17813-17818.

van der Poll, T., van de Veerdonk, F.L., Scicluna, B.P., and Netea, M.G. (2017). The immunopathology of sepsis and potential therapeutic targets. Nat Rev Immunol *17*, 407-420.

Varshney, P., Yadav, V., and Saini, N. (2016). Lipid rafts in immune signalling: current progress and future perspective. Immunology *149*, 13-24.

Vaure, C., and Liu, Y. (2014). A comparative review of toll-like receptor 4 expression and functionality in different animal species. Front Immunol *5*, 316.

Vegran, F., Berger, H., Boidot, R., Mignot, G., Bruchard, M., Dosset, M., Chalmin, F., Rebe, C., Derangere, V., Ryffel, B.*, et al.* (2014). The transcription factor IRF1 dictates the IL-21-dependent anticancer functions of TH9 cells. Nat Immunol *15*, 758-766.

Velge, P., Wiedemann, A., Rosselin, M., Abed, N., Boumart, Z., Chausse, A.M., Grepinet, O., Namdari, F., Roche, S.M., Rossignol, A.*, et al.* (2012). Multiplicity of Salmonella entry mechanisms, a new paradigm for Salmonella pathogenesis. Microbiologyopen *1*, 243-258.

Venteclef, N., Jakobsson, T., Ehrlund, A., Damdimopoulos, A., Mikkonen, L., Ellis, E., Nilsson, L.M., Parini, P., Janne, O.A., Gustafsson, J.A.*, et al.* (2010). GPS2-dependent corepressor/SUMO pathways govern anti-inflammatory actions of LRH-1 and LXRbeta in the hepatic acute phase response. Genes Dev *24*, 381-395.

Vergadi, E., Ieronymaki, E., Lyroni, K., Vaporidi, K., and Tsatsanis, C. (2017). Akt Signaling Pathway in Macrophage Activation and M1/M2 Polarization. J Immunol *198*, 1006-1014.

Vergadi, E., Ieronymaki, E., Lyroni, K., Vaporidi, K., & Tsatsanis, C. (2017). Akt signaling pathway in macrophage activation and M1/M2 polarization. The Journal of Immunology *198*, 1006-1014.

Viegas, M.S., do Carmo, A., Silva, T., Seco, F., Serra, V., Lacerda, M., and Martins, T.C. (2007). CD38 plays a role in effective containment of mycobacteria within granulomata and polarization of Th1 immune responses against Mycobacterium avium. Microbes Infect *9*, 847-854.

Vignali, D.A., and Kuchroo, V.K. (2012). IL-12 family cytokines: immunological playmakers. Nat Immunol *13*, 722-728.

Vitiello, M., D'Isanto, M., Galdiero, M., Raieta, K., Tortora, A., Rotondo, P., Peluso, L., and Galdiero, M. (2004). Interleukin-8 production by THP-1 cells stimulated by Salmonella enterica serovar Typhimurium porins is mediated by AP-1, NF-kappaB and MAPK pathways. Cytokine *27*, 15-24.

Vivero, A., Baños, R.C., Mariscotti, J.F., Oliveros, J.C., García-del Portillo, F., Juárez, A., and Madrid, C. (2008). Modulation of horizontally acquired genes by the Hha-YdgT proteins in Salmonella enterica serovar Typhimurium. Journal of bacteriology *190*, 1152-1156.

Waddington, K.E., Jury, E.C., and Pineda-Torra, I. (2015). Liver X receptors in immune cell function in humans. Biochem Soc Trans *43*, 752-757.

Wagner, B.L., Valledor, A.F., Shao, G., Daige, C.L., Bischoff, E.D., Petrowski, M., Jepsen, K., Baek, S.H., Heyman, R.A., Rosenfeld, M.G.*, et al.* (2003). Promoter-specific roles for liver X receptor/corepressor complexes in the regulation of ABCA1 and SREBP1 gene expression. Mol Cell Biol *23*, 5780-5789.

Wang, B., and Tontonoz, P. (2018). Liver X receptors in lipid signalling and membrane homeostasis. Nat Rev Endocrinol *14*, 452-463.

Wang, Y., Viscarra, J., Kim, S.J., and Sul, H.S. (2015). Transcriptional regulation of hepatic lipogenesis. Nat Rev Mol Cell Biol *16*, 678-689.

Weisser, S.B., McLarren, K.W., Voglmaier, N., van Netten-Thomas, C.J., Antov, A., Flavell, R.A., and Sly, L.M. (2011). Alternative activation of macrophages by IL-4 requires SHIP degradation. Eur J Immunol *41*, 1742-1753.

Wemyss, M.A., and Pearson, J.S. (2019). Host Cell Death Responses to Non-typhoidal Salmonella Infection. Front Immunol *10*, 1758.

Wynn, T.A., Chawla, A., and Pollard, J.W. (2013). Macrophage biology in development, homeostasis and disease. Nature *496*, 445-455.

Wynn, T.A., and Vannella, K.M. (2016). Macrophages in Tissue Repair, Regeneration, and Fibrosis. Immunity *44*, 450-462.

Yang, D.D., Conze, D., Whitmarsh, A.J., Barrett, T., Davis, R.J., Rincon, M., and Flavell, R.A. (1998). Differentiation of CD4+ T cells to Th1 cells requires MAP kinase JNK2. Immunity *9*, 575-585.

Yokota, A., Hirai, H., Sato, R., Adachi, H., Sato, F., Hayashi, Y., Sato, A., Kamio, N., Miura, Y., Nakano, M.*, et al.* (2019). C/EBPbeta is a critical mediator of IFN-alpha-induced exhaustion of chronic myeloid leukemia stem cells. Blood Adv *3*, 476-488.

Zelcer, N., Hong, C., Boyadjian, R., and Tontonoz, P. (2009). LXR regulates cholesterol uptake through Idol-dependent ubiquitination of the LDL receptor. Science *325*, 100-104.

Zelova, H., and Hosek, J. (2013). TNF-alpha signalling and inflammation: interactions between old acquaintances. Inflamm Res *62*, 641-651.

Zhang, W.Y., Gaynor, P.M., and Kruth, H.S. (1996). Apolipoprotein E produced by human monocyte-derived macrophages mediates cholesterol efflux that occurs in the absence of added cholesterol acceptors. J Biol Chem *271*, 28641-28646.

Zhao, Y.J., Lam, C.M., and Lee, H.C. (2012). The membrane-bound enzyme CD38 exists in two opposing orientations. Sci Signal *5*, ra67.

Zidovetzki, R., and Levitan, I. (2007). Use of cyclodextrins to manipulate plasma membrane cholesterol content: evidence, misconceptions and control strategies. Biochim Biophys Acta *1768*, 1311-1324.

Zilber, M.T., Setterblad, N., Vasselon, T., Doliger, C., Charron, D., Mooney, N., and Gelin, C. (2005). MHC class II/CD38/CD9: a lipid-raft-dependent signaling complex in human monocytes. Blood *106*, 3074-3081.

ANNEXES

Authored publications

1. Matalonga, J., **Glaria, E**., Bresque, M., Escande, C., Carbó, J.M., Kiefer, K., Vicente, R., León, T.E., Beceiro, S., Pascual-García, M.*, et al.* (2017). The nuclear receptor LXR limits bacterial infection of host macrophages through a mechanism that impacts cellular NAD metabolism. Cell reports *18*, 1241-1255.

2. Velasco, E., Wang, S., Sanet, M., Fernandez-Vazquez, J., Jove, D., **Glaria, E**., Valledor, A.F., O'Halloran, T.V., and Balsalobre, C. (2018). A new role for Zinc limitation in bacterial pathogenicity: modulation of alpha-hemolysin from uropathogenic Escherichia coli. Sci Rep *8*, 6535.

3. Huttener, M., Prieto, A., Aznar, S., Bernabeu, M., **Glaria, E**., Valledor, A.F., Paytubi, S., Merino, S., Tomas, J., and Juarez, A. (2019). Expression of a novel class of bacterial Ig-like proteins is required for IncHI plasmid conjugation. PLoS Genet *15*, e1008399.

4. **Glaría, E**., Matalonga, J., and Valledor, A.F. (2019). Methods for Assessing the Effects of LXR Agonists on Macrophage Bacterial Infection. In Lipid-Activated Nuclear Receptors G. M., and P.-T. I., eds. (Humana Press, New York, NY), pp. 135-141.

5. Dorhoi, A., **Glaria, E**., Garcia-Tellez, T., Nieuwenhuizen, N.E., Zelinskyy, G., Favier, B., Singh, A., Ehrchen, J., Gujer, C., Munz, C.*, et al.* (2019). MDSCs in infectious diseases: regulation, roles, and readjustment. Cancer Immunol Immunother *68*, 673-685.

6. **Glaría, E**., Letelier, N.A., and Valledor, A.F. (2020). Integrating the roles of liver X receptors in inflammation and infection: Mechanisms and outcomes. Current Opinion in Pharmacology *53*, 55-65.

7. **Glaría, E**., and Valledor, A.F. (2020). Roles of CD38 in the Immune Response to Infection. Cells *9*, 228.

In the following pages, the full text of the most relevant publications for this thesis is shown. The first page of the other authored publications is also included.

Publication 1

Research article:

The Nuclear Receptor LXR Limits Bacterial Infection of Host Macrophages through a Mechanism that Impacts Cellular NAD Metabolism

Matalonga, J., **Glaria, E.**, Bresque, M., Escande, C., Carbó, J. M., Kiefer, K., Vicente, R., León, T. E., Beceiro, S., Pascual-García, M., Serret, J., Sanjurjo, L., Morón-Ros, S., Riera, A. Paytubi, S., Juarez, A., Sotillo, F., Lindbom, L., Caelles, C., Sarrias, M. R., Sancho, J., Castrillo, A., Chini, E. N. and Valledor, A. F.

January 2017

Cell reports, 18 (5), 1241-1255.

doi: 10.1016/j.celrep.2017.01.007

Impact factor: 8.032

Article

Cell Reports

The Nuclear Receptor LXR Limits Bacterial Infection of Host Macrophages through a Mechanism that Impacts Cellular NAD Metabolism

Graphical Abstract

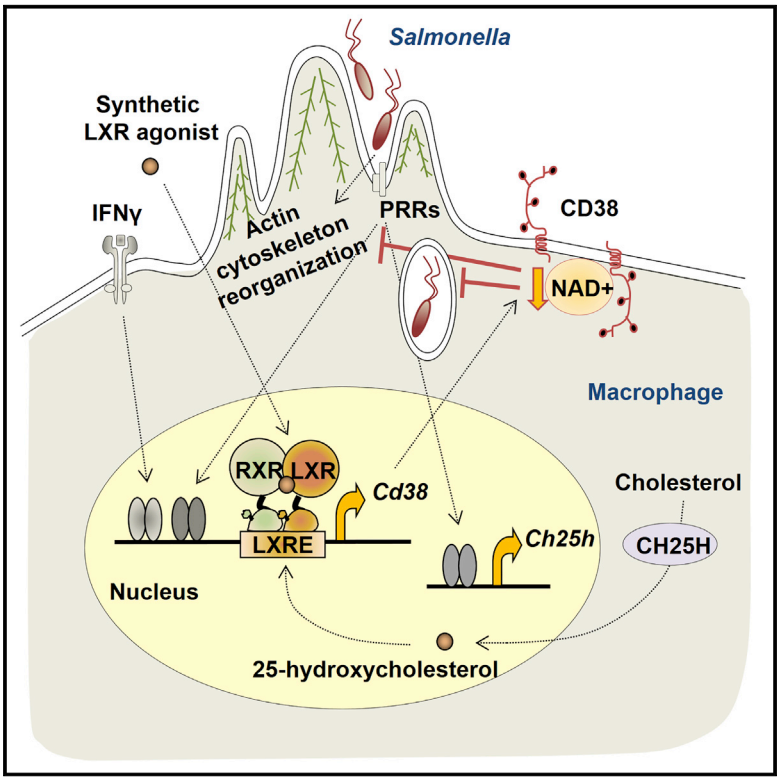

Authors

Jonathan Matalonga, Estibaliz Glaria, Mariana Bresque, ..., Antonio Castrillo, Eduardo N. Chini, Annabel F. Valledor

Correspondence

afernandezvalledor@ub.edu

In Brief

Macrophages constitute a preferential niche for intracellular bacteria to replicate. Matalonga et al. identified an antibacterial circuit mediated by pharmacological targeting of the liver X receptor (LXR) pathway that impacts intracellular NAD metabolism and interferes with macrophage cytoskeletal rearrangements subverted by invasive bacteria.

Highlights

- LXR agonists reduce intracellular NAD levels through induction of CD38
- Activation of LXRs impairs cytoskeletal changes associated with bacterial infection
- The LXR-CD38 circuit protects host macrophages from extensive bacterial infection
- Activation of the LXR-CD38 circuit ameliorates clinical signs of infection in vivo

Matalonga et al., 2017, Cell Reports *18*, 1241–1255
January 31, 2017
http://dx.doi.org/10.1016/j.celrep.2017.01.007

CellPress

Cell Reports
Article

The Nuclear Receptor LXR Limits Bacterial Infection of Host Macrophages through a Mechanism that Impacts Cellular NAD Metabolism

Jonathan Matalonga,[1] Estibaliz Glaria,[1] Mariana Bresque,[2] Carlos Escande,[2] José María Carbó,[1] Kerstin Kiefer,[3] Ruben Vicente,[3] Theresa E. León,[1] Susana Beceiro,[4] Mónica Pascual-García,[1] Joan Serret,[5] Lucía Sanjurjo,[6] Samantha Morón-Ros,[1] Antoni Riera,[7,8] Sonia Paytubi,[9] Antonio Juarez,[9,10] Fernando Sotillo,[7] Lennart Lindbom,[11] Carme Caelles,[12] Maria-Rosa Sarrias,[6] Jaime Sancho,[13] Antonio Castrillo,[4] Eduardo N. Chini,[14] and Annabel F. Valledor[1,15,*]

[1]Nuclear Receptor Group, Department of Cell Biology, Physiology and Immunology, School of Biology, University of Barcelona, Barcelona 08028, Spain
[2]Metabolic Diseases and Aging Laboratory, Institut Pasteur Montevideo, Montevideo 11400, Uruguay
[3]Laboratory of Molecular Physiology and Channelopathies, Department of Experimental and Health Sciences, Universitat Pompeu Fabra, Barcelona 08003, Spain
[4]Instituto de Investigaciones Biomédicas "Alberto Sols" de Madrid and Unidad Asociada de Biomedicina CSIC-Universidad de las Palmas de Gran Canaria (CSIC-ULPGC), Madrid 28029, Spain
[5]Experimental Toxicology and Ecotoxicology Unit, Parc Científic de Barcelona, Barcelona 08028, Spain
[6]Innate Immunity Group, Health Sciences Research Institute Germans Trias i Pujol, Badalona 08916, Spain
[7]Institute for Research in Biomedicine (IRB Barcelona), Barcelona 08028, Spain
[8]Department of Organic Chemistry, School of Chemistry, University of Barcelona, Barcelona 08028, Spain
[9]Department of Microbiology, School of Biology, University of Barcelona, Barcelona 08028, Spain
[10]Institute for Bioengineering of Catalonia (IBEC), Barcelona 08028, Spain
[11]Department of Physiology and Pharmacology, Karolinska Institutet, Stockholm SE-171 77, Sweden
[12]Department of Biochemistry and Molecular Biology, School of Pharmacy, University of Barcelona, Barcelona 08028, Spain
[13]Institute of Parasitology and Biomedicine "López-Neyra" (IPBLN), CSIC, Granada 18016, Spain
[14]Laboratory of Signal Transduction, Department of Anesthesiology and Robert and Arlene Kogod Center on Aging, Mayo Clinic College of Medicine, Rochester, MN 55905, USA
[15]Lead Contact
*Correspondence: afernandezvalledor@ub.edu
http://dx.doi.org/10.1016/j.celrep.2017.01.007

SUMMARY

Macrophages exert potent effector functions against invading microorganisms but constitute, paradoxically, a preferential niche for many bacterial strains to replicate. Using a model of infection by *Salmonella* Typhimurium, we have identified a molecular mechanism regulated by the nuclear receptor LXR that limits infection of host macrophages through transcriptional activation of the multifunctional enzyme CD38. LXR agonists reduced the intracellular levels of NAD^+ in a CD38-dependent manner, counteracting pathogen-induced changes in macrophage morphology and the distribution of the F-actin cytoskeleton and reducing the capability of non-opsonized *Salmonella* to infect macrophages. Remarkably, pharmacological treatment with an LXR agonist ameliorated clinical signs associated with *Salmonella* infection in vivo, and these effects were dependent on CD38 expression in bone-marrow-derived cells. Altogether, this work reveals an unappreciated role for CD38 in bacterial-host cell interaction that can be pharmacologically exploited by activation of the LXR pathway.

INTRODUCTION

Macrophages are essential mediators of the innate immune response. Through phagocytosis, macrophages internalize microbial pathogens, which are subsequently killed and digested in intracellular phagolysosomes (Haas, 2007). Several pathogenic microorganisms have, however, developed strategies to actively invade host cells and evade microbial digestion within the host endosomal system. In fact, despite their repertoire of microbicidal tools, macrophages represent niches in which many pathogens have established themselves for intracellular replication and dissemination (Price and Vance, 2014). For example, *Salmonella enterica* serovar Typhimurium (*S.* Typhimurium) fosters its own uptake by non-phagocytic epithelial cells and phagocytic cells, and infection and intracellular survival in macrophages is required for full virulence and dissemination (Haraga et al., 2008). Invasive *Salmonellae* strains can enter macrophages by several endocytic processes, including macropinocytosis induced by factors secreted by the type III secretion system (T3SS). Within infected host cells, the bacterium first

uses a second T3SS to transform the phagosome into a *Salmonella*-containing vacuole that supports bacterial replication and then induces macrophage pyroptosis for dissemination (Guiney and Lesnick, 2005).

Nuclear receptors are a family of ligand-activated transcription factors with diverse functions in physiology. Liver X receptors (LXRs) are nuclear receptors that can be pharmacologically activated by high-affinity agonists to subsequently regulate the expression of genes involved in lipid homeostasis. Two LXR isoforms have been identified, namely LXRα and LXRβ, both of which heterodimerize with retinoid X receptors (RXRs) to positively modulate target gene expression (Hong and Tontonoz, 2014). Apart from their metabolic functions, LXRs play important roles in the regulation of immune responses. Through different mechanisms, LXRs repress a subset of pro-inflammatory genes induced by pattern recognition receptor engagement (Ghisletti et al., 2007; Ito et al., 2015) or by interferon gamma (IFN-γ) (Pascual-García et al., 2013; Lee et al., 2009). On the other hand, the LXR pathway is involved in the acquisition of a macrophage deactivated phenotype (A-Gonzalez et al., 2009).

Based on the anti-inflammatory actions of LXR agonists, initial predictions anticipated that LXR activation could negatively impact the capability of immune cells to establish an aggressive response against pathogens. However, increased susceptibility to infection by *Mycobacterium tuberculosis* or *Listeria monocytogenes* has been observed in LXR-deficient mice (Joseph et al., 2004; Korf et al., 2009), and LXR activation prevented macrophage apoptosis induced by virulent bacteria, including *Bacillus anthracis* and *S.* Typhimurium (Valledor et al., 2004), which suggests that the LXR pathway exerts complex regulatory actions that affect microbe-host cell interaction. In this work, we have further investigated the involvement of LXR activity in immune cell function during infection by *S.* Typhimurium. Interestingly, the results reported here identify a molecular mechanism regulated by LXRs that serves to limit infection of host macrophages through modulation of cellular NAD metabolism.

RESULTS

LXR Activity Limits Macrophage Infection by *S.* Typhimurium

To investigate the role of the LXR pathway in host-pathogen interaction, we treated primary bone-marrow-derived macrophages with synthetic high-affinity LXR agonists (either TO901317 (T1317) or GW3965) and then infected the cells with *S.* Typhimurium strain SV5015 harboring the plasmid pBR.RFP.1, which encodes red fluorescent protein. Confocal fluorescence microscopy studies indicated that LXR agonists reduce the amount of intracellular bacteria and the percentage of infected macrophages after 30 min of infection (Figures 1A, S1, and S2A). Reduced bacteria burden was corroborated with flow cytometry studies (Figures 1B and S2B) and by determination of viable bacterial colony-forming units (CFUs) after macrophage cell lysis (Figure 1C). The agonists did not inhibit infection of cells deficient in LXRα and LXRβ ($LXR^{-/-}$) (Figures 1A, 1B, and S2B), indicating that the effects of these compounds were LXR dependent and LXR specific. Interestingly, the rate of intracellular bacterial replication during the first 5 hr post-infection was not altered upon LXR activation, as the differences between agonist- and vehicle-treated cells over a time-course of 5 hr were equivalent to the differences observed at 30 min of infection (Figure 1D). These results suggested that LXR activation interferes with early events during bacterial cell interaction with host macrophages. On the other hand, a time-course assay revealed that prolonged treatment with the LXR agonist is required for effective inhibition of macrophage infection (Figure 1E).

Pharmacological treatment with T1317 in vivo also reduced intracellular macrophage infection by *S.* Typhimurium in an intraperitoneal model of infection (Figure 1F). Importantly, the effects of T1317 were not indirectly mediated by any substantial decrease in the ratio of resident macrophages versus neutrophils before the infection (Figure S2C). Interestingly, the LXR agonist did not influence phagocytosis of immunoglobulin G (IgG)-opsonized *Salmonella* cells (Figure 1G), suggesting that LXR activation induces a mechanism that protects macrophages from infection by this microorganism in the absence of opsonizing antibodies.

We next determined whether LXR activation affects the internalization of other bacterial pathogens. These studies revealed that LXR activity inhibits macrophage infection by an enteroinvasive strain of *Escherichia coli* (EIEC 0124:H30) without affecting phagocytosis of non-invasive *E. coli* (Figure S2D) or internalization of Fluoresbright yellow green microspheres (Figure S2E), thus suggesting that LXR activity selectively affects invasive mechanisms induced by pathogenic bacteria.

Morphological studies using fluorescent phalloidin to stain filamentous actin (F-actin) showed that macrophages incubated with *S.* Typhimurium acquire a round pancake-like shape within minutes after bacterial exposure (Figure 1H), a morphological feature previously associated to inflammatory macrophage polarization (McWhorter et al., 2013). Remarkably, pretreatment with an LXR agonist strongly inhibited the changes in macrophage morphology induced upon *S.* Typhimurium infection without altering the morphology of resting cells (Figure 1H, see quantification in Figure 2E). Moreover, LXR activation also reduced the expression of several pro-inflammatory mediators in infected macrophages (Figure S2F).

Interestingly, expression profiling experiments revealed that interference with bacterial internalization was not mediated by repression of membrane receptors traditionally involved in recognition and/or phagocytosis of bacterial products (Figure S3).

A recent study demonstrated a role for cytosolic nicotinamide adenine dinucleotide (NAD^+) in the control of the organization of the actin cytoskeleton required for the spreading performance and the formation of actin-rich membrane protrusions in activated macrophages (Venter et al., 2014). Based on these observations, we evaluated whether altering NAD^+ levels affects the capability of LXRs to interfere with macrophage morphology and/or internalization of *S.* Typhimurium. In mammalian cells, nicotinamide phosphoribosyltransferase (NAMPT) is the rate-limiting enzyme in the biosynthesis of NAD^+ through the salvage pathway. Incubation with FK866, a specific NAMPT inhibitor, resulted in partial inhibition of the capability of macrophages to internalize *S.* Typhimurium (Figure 2A). Interestingly, activation of the LXR pathway significantly reduced the intracellular levels of NAD^+ (Figure 2B), and addition of exogenous NAD^+

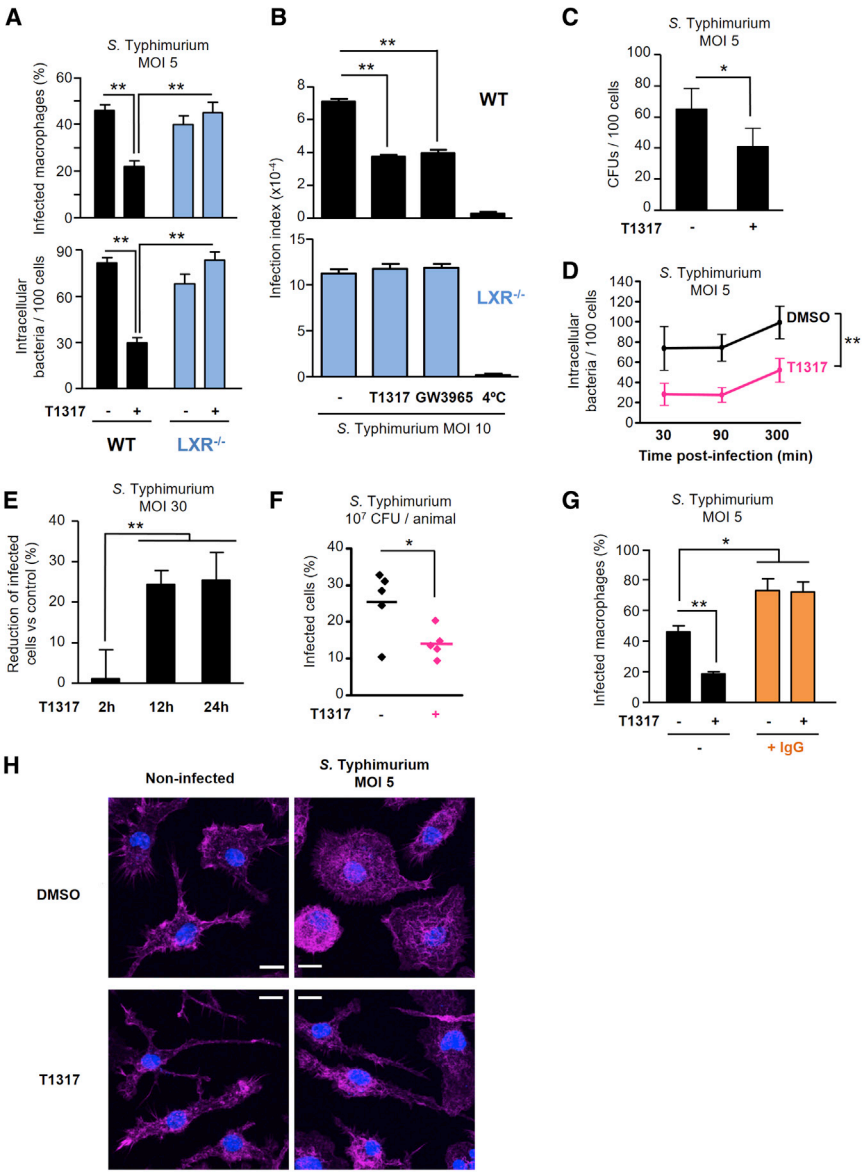

Figure 1. LXR Activation Limits Macrophage Infection by Non-opsonized *S.* Typhimurium

(A) Macrophages from WT (n = 5) or LXR$^{-/-}$ (n = 4) mice treated with the LXR agonist T1317 (1 μM, 24 hr) or DMSO and infected with *S.* Typhimurium (30 min). Analysis of the percentage of infected macrophages (top) and the amount of intracellular bacteria (bottom) by confocal fluorescence microscopy. Data represent mean ± SEM (two-way ANOVA Bonferroni). The dataset in WT cells includes data from Figure 2C.

(B) Analysis of macrophage infection by flow cytometry after incubation with the LXR agonists T1317 or GW3965 (1 μM, 24 hr). Macrophages were infected with *S.* Typhimurium for 30 min at 37°C. As a control, bacterial cell attachment to macrophages (without internalization) was also assessed by carrying out the infection at 4°C. Each experiment was performed in triplicate. Shown is a representative experiment from each genotype (mean ± SD) from n = 5 (WT) or n = 4 (LXR$^{-/-}$) independent experiments (ANOVA Bonferroni).

(C) Quantification of intracellular *S.* Typhimurium burden. The cells were infected for 30 min. Serial dilutions of cell lysates were plated on agar and allowed to grow at 37°C. Bacterial CFUs were counted 24 hr later. Data represent mean ± SEM from n = 3 independent experiments (each including biological duplicates or triplicates) (paired t test).

(D) Confocal fluorescence microscopy evaluating the effects of T1317 on intracellular bacterial burden over time. Data represent mean ± SEM; n = 5 (30 min), n = 7 (90 min), or n = 9 (300 min) (paired t test for each time post-infection).

(E) Macrophages were treated with T1317 for the indicated periods of time, and the inhibitory effects on macrophage infection were evaluated by flow cytometry. Data are expressed as percent reduction in the number of infected cells (versus infection in the absence of T1317) (mean ± SD; n = 5; Kruskal-Wallis Dunn. Similar results were obtained in an independent experiment performed in triplicates.

(F) In vivo infected cells analyzed by confocal microscopy. C57BL/6 male mice were first subjected to an i.p. injection of T1317 (10 mg/kg animal; 24 hr) or vehicle (DMSO in PBS; 24 hr) and then infected i.p. with *S.* Typhimurium (10^7 CFU per animal; 30 min); n = 5 animals/group. Mean bars are indicated (t test).

(G) Bacterial uptake in the presence or absence of opsonizing anti-*Salmonella* LPS IgG. Data represent mean ± SEM (n = 3; Kruskal-Wallis Dunn).

(H) Representative images of infected macrophages stained with phalloidin (F-actin, purple) and DAPI (nuclei, blue) (n = 4). Scale bars, 10 μm.

See also Figures S1 and S2. *p < 0.05, **p < 0.01.

counteracted the ability of the LXR agonist to reduce macrophage infection (Figure 2C), with no effect on the levels of infection in control macrophages (not exposed to LXR agonists). These effects correlated with the observation that in the presence of exogenous NAD$^+$, activation of the LXR pathway did not inhibit morphological changes associated with host cell-pathogen interaction (Figures 2D and 2E). In activated macrophages, changes in macrophage morphology are accompanied by an increase in F-actin-rich dorsal membrane ruffling, with curved or circular protrusions directed upright that precede macropinocytosis (Luo et al., 2014). Interestingly, the LXR agonist interfered with dorsal F-actin accumulation in *Salmonella*-infected cells, and addition of exogenous NAD$^+$ counteracted these effects. Altogether, these observations prompted us to consider whether LXR activation modulates the expression of factors that contribute to NAD$^+$ metabolism as a mechanism protecting macrophages from excessive bacterial internalization.

LXR Agonists Induce the Expression of the NAD Glycohydrolase CD38

In general, NAD$^+$ and its phosphorylated and reduced forms participate as coenzymes in oxidation-reduction reactions

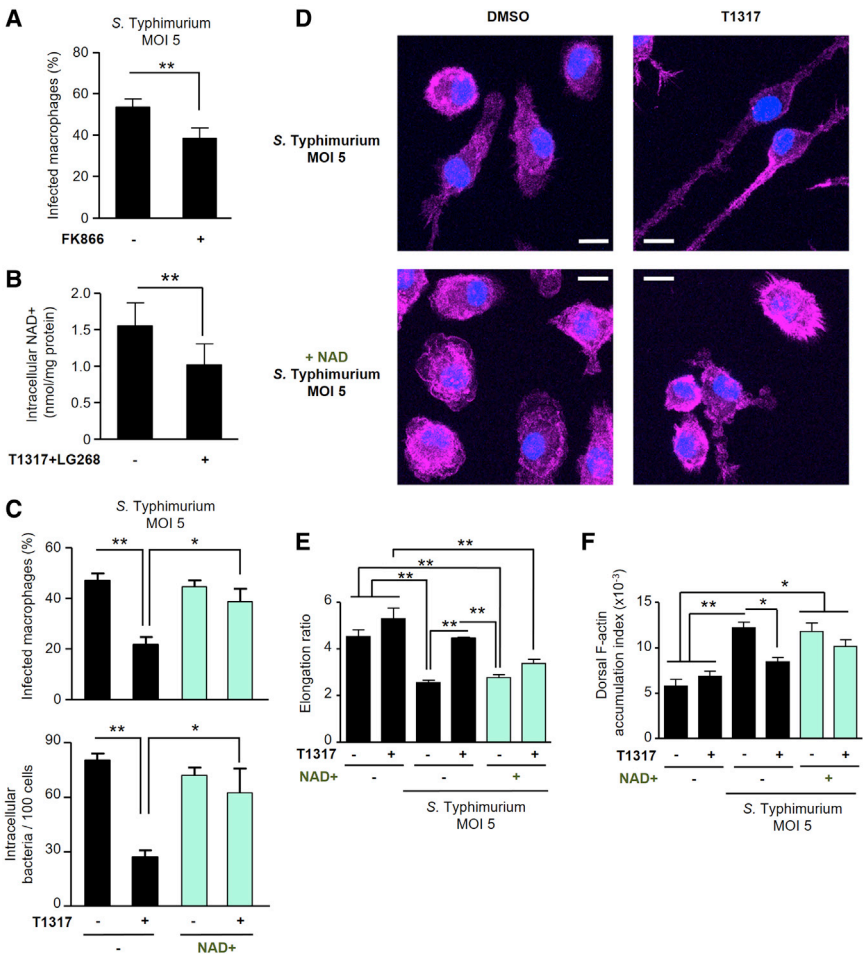

Figure 2. NAD$^+$ Addition Suppresses the Effects of LXR Activation on Macrophage Infection

(A) Confocal fluorescence microscopy analysis of the amount of infected macrophages after treatment with the NAMPT inhibitor FK866 (10 nM) or vehicle for 24 hr. Data represent mean ± SEM (n = 4; paired t test).

(B) Analysis of intracellular NAD$^+$ levels with a NAD cycling assay. The cells were pre-treated with agonists for the LXR-RXR heterodimer, T1317 and LG268 (1 μM each), or vehicle (DMSO) for 24 hr. Data represent mean ± SEM (n = 6; paired t test).

(C) Effects of exogenous addition of NAD$^+$ on macrophage infection. The cells were pretreated with T1317 (1 μM, 24 hr) or DMSO and then incubated with NAD (1 mM) for 2 hr before the infection. Results of confocal microscopy studies are shown. Data represent mean ± SEM (n = 4; two-way ANOVA Bonferroni). The data from WT cells are also included as part of the WT dataset in Figure 1A.

(D) Effects of NAD$^+$ on *S.* Typhimurium-induced changes in macrophage morphology; scale bars, 10 μm. Representative images; n = 4.

(E and F) Cell elongation ratio (E) and dorsal F-actin accumulation index (F). Data represent mean ± SEM (n = 4; ANOVA Bonferroni).

*p < 0.05, **p < 0.01.

without net consumption of intracellular NAD. In contrast, NAD$^+$ is consumed as a substrate by enzymatic activities that mediate protein lysine deacylation and ADP-ribose transfer or synthesis (Belenky et al., 2007). To assess if LXR activation modulates the expression of enzymes that participate in NAD$^+$ biosynthesis or consumption, we analyzed expression-profiling data obtained from macrophages stimulated with an LXR agonist (Figure 3A). The expression of most of the genes evaluated, including *Nampt*, was not altered upon LXR activation. However, selective induction of *Cd38* was observed in cells treated with the LXR agonist. CD38 is a type II transmembrane glycoprotein that catalyzes the conversion of NAD$^+$ into nicotinamide, adenosine diphosphate-ribose (ADPR), and cyclic ADPR (cADPR) (Chini, 2009) and is thus a major regulator of cellular levels of NAD$^+$ (Aksoy et al., 2006). Induction of CD38 upon LXR activation was confirmed by qPCR (Figures 3B and 3C) and western blotting (Figure 3D). It is noteworthy that the basal levels of *Cd38* expression were not significantly reduced in LXR-deficient cells, as it is the case for previously identified LXR target genes (e.g., *Abca1*, *Abcg1*, and *Srebp1c*; Wagner et al., 2003); however, *Cd38* induction by the LXR agonist was LXR dependent and LXR specific (Figure 3B). *Cd38* expression was also upregulated in response to a synthetic agonist for RXR, LG268 (Figure 3B), and combined treatment with agonists for LXR and RXR synergistically upregulated CD38 mRNA and protein expression (Figures 3B, 3E, and 3F) in an LXR-dependent manner, with both LXRα and LXRβ contributing to *Cd38* induction (Figure 3F). Moreover, these effects translated into increased CD38 protein levels at the cell surface (Figure 3G) and augmented cellular NADase activity (Figures 3H–3J). The changes in NADase activity were completely abolished in either LXR$^{-/-}$ or CD38$^{-/-}$ macrophages (Figures 3I and 3J), which correlated with the fact that LXR/RXR agonists significantly downregulate intracellular NAD$^+$ levels in wild-type (WT) cells (Figure 2B), but not in CD38-deficient cells (Figure 3K). Taken together, these results indicate that CD38 mediates the increase in NADase activity and the reduction in intracellular NAD levels upon pharmacological activation of the LXR pathway.

A putative LXR response element (LXRE) was identified in an enhancer ~2 kb upstream of the transcription initiation site, which is fully conserved at least in mouse and rat. A fragment containing the potential LXRE, hereafter named *Cd38* enhancer (*Cd38*enh), was cloned in a pGL3-promoter vector (pGL3-*Cd38*enh), and its activity was characterized in COS-7 cells. Co-transfection of LXRα and RXRα resulted in maximal induction of promoter activity in response to a combination of LXR and RXR agonists (Figure S4). Significant loss of activity was observed after mutation of the potential LXRE in the *Cd38*enh region, which suggests that the site identified here represents a bona fide LXRE (Figure 3L).

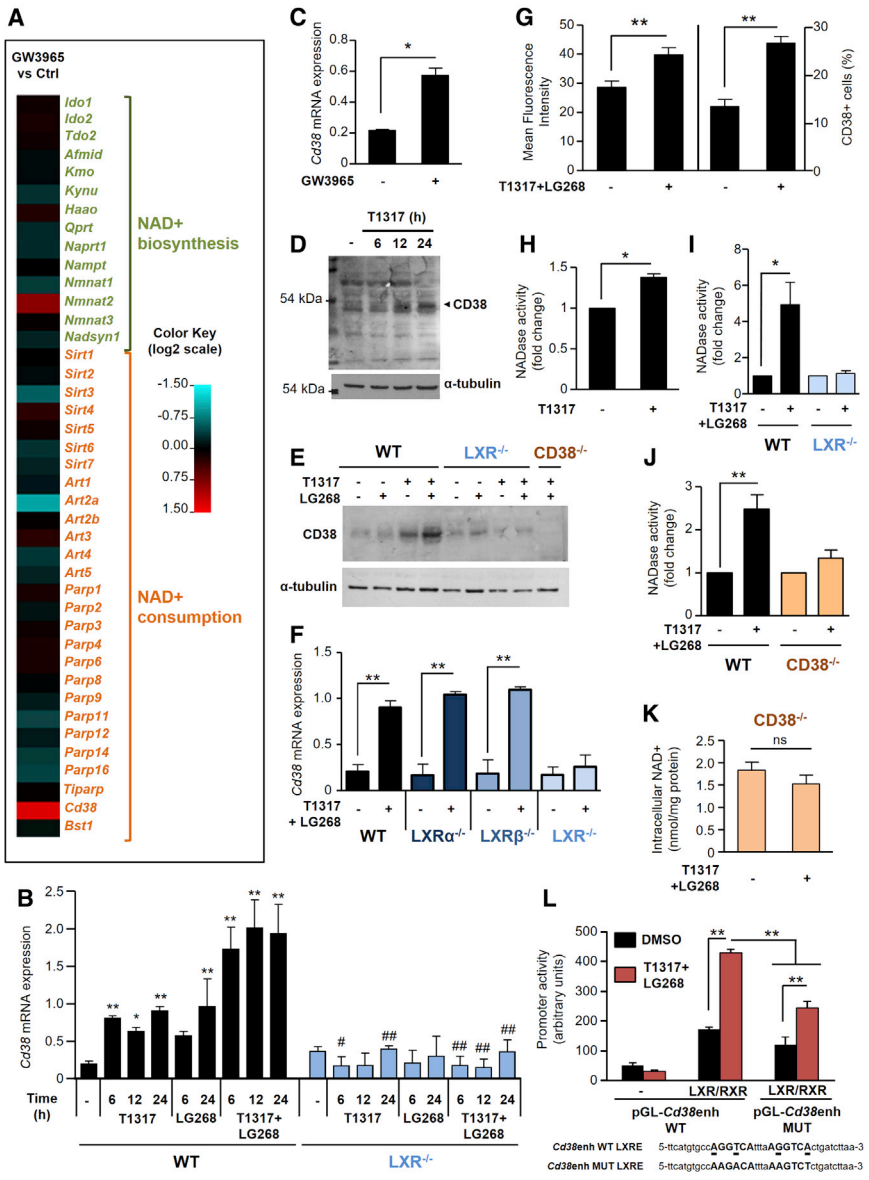

Figure 3. LXR Activation Induces the Expression of the Multifunctional Enzyme CD38

(A) Expression profiling from macrophages treated with GW3965 (2 μM) or DMSO for 18 hr. Heatmap representing average fold expression values (log2 scale) of genes involved in net NAD^+ synthesis or consumption in GW3965-treated cells over DMSO-treated cells (n = 2).

(B and C) qPCR analysis of *Cd38* expression in WT and LXR-deficient macrophages stimulated with LXR agonists T1317 or GW3965 and/or the RXR agonist LG268 (1 μM each). Data represent mean ± SEM (n = 4 with two-way ANOVA Bonferroni in B; n = 3 with t test [with Welch's correction] in C). In (B), *p < 0.05, **p < 0.01 vs control cells from the same genotype; #p < 0.05, ##p < 0.01 vs the same treatment in WT cells.

(D and E) Western blot analysis of CD38 protein expression in WT (D and E) and LXR-deficient and CD38-deficient macrophages (E).

(F) qPCR analysis in macrophages WT or deficient in LXRα ($LXR\alpha^{-/-}$), LXRβ ($LXR\beta^{-/-}$), or both isoforms ($LXR^{-/-}$). Data represent mean ± SEM (n = 4; t test for each genotype).

(G) Flow cytometry analysis of the surface expression of CD38. Data represent mean ± SEM (n = 6; t test).

(H–J) Fluorimetric determination of intracellular NADase activity in WT (H–J), LXR-deficient (I), and CD38-deficient macrophages (J). Data represent mean ± SEM (n = 4 in H, n = 3 in I, and n = 5 in J; Mann-Whitney *U* Wilcoxon test for each genotype).

(K) Intracellular NAD^+ levels in CD38-deficient macrophages. Data represent mean ± SEM (n = 6; paired t test).

(L) Luciferase reporter studies in COS7 cells co-transfected with a WT *Cd38* enhancer-luciferase construct (pGL-*Cd38*enh WT) or a construct containing a mutated LXRE (pGL-*Cd38*enh MUT), as well as plasmids overexpressing LXRα and RXRα or an empty vector. Transfected cells were stimulated for 18 hr with either vehicle (DMSO) or LXR-RXR agonists. Data represent mean ± SEM (n = 3, left; n = 6, middle; and n = 4, right; ANOVA Bonferroni comparing transfections with LXR/RXR coexpression).

See also Figure S4. *p < 0.05, **p < 0.01.

Cooperative Effects of LXRs and Inflammatory Signals on CD38 Expression and NADase Activity

Interestingly, infection by *S.* Typhimurium strongly induced macrophage expression of *Cd38* (Figure 4A). In agreement with previous observations (Musso et al., 2001; Iqbal and Zaidi, 2006; Lee et al., 2012), increased expression of *Cd38* was observed upon prolonged stimulation with IFN-γ, lipopolysaccharide (LPS), or tumor necrosis factor alpha (TNF-α) (Figures 4B and S5A–S5C). In contrast, *Cd38* was not upregulated in macrophages alternatively activated by interleukin 4 (IL-4), IL-10, or transforming growth factor beta (TGF-β) (Figure 4C), despite the fact that these cytokines did induce specific target genes in macrophages (Figures S5D–S5F). In line with increased *Cd38* expression in classically activated macrophages, inflammatory mediators reduced intracellular NAD^+ levels in a CD38-dependent manner (Figure 4D). However, despite the ability of CD38 to alter intracellular NAD^+ levels, early ROS production in response to inflammatory signaling was CD38 independent (Figure 4E).

These studies also led to the unexpected observation that functional LXR expression was required for full induction of *Cd38* by inflammatory signals and that combined activation of inflammatory signaling and the LXR pathway cooperated synergistically to upregulate *Cd38* expression (Figures 4A, 4B, and S5A–S5C) and NADase activity (Figures 4F and S5G). Sequence analysis of the *Cd38*enh region containing the LXRE revealed the presence of two nuclear factor κB (NF-κB) binding sites, an interferon-stimulated response element (ISRE), and an AP-1 site in the proximity of the LXRE. Raw264.7 macrophages that stably express human LXRα were cotransfected with the *Cd38*enh-luciferase reporter and a plasmid overexpressing RXRα. In these studies,

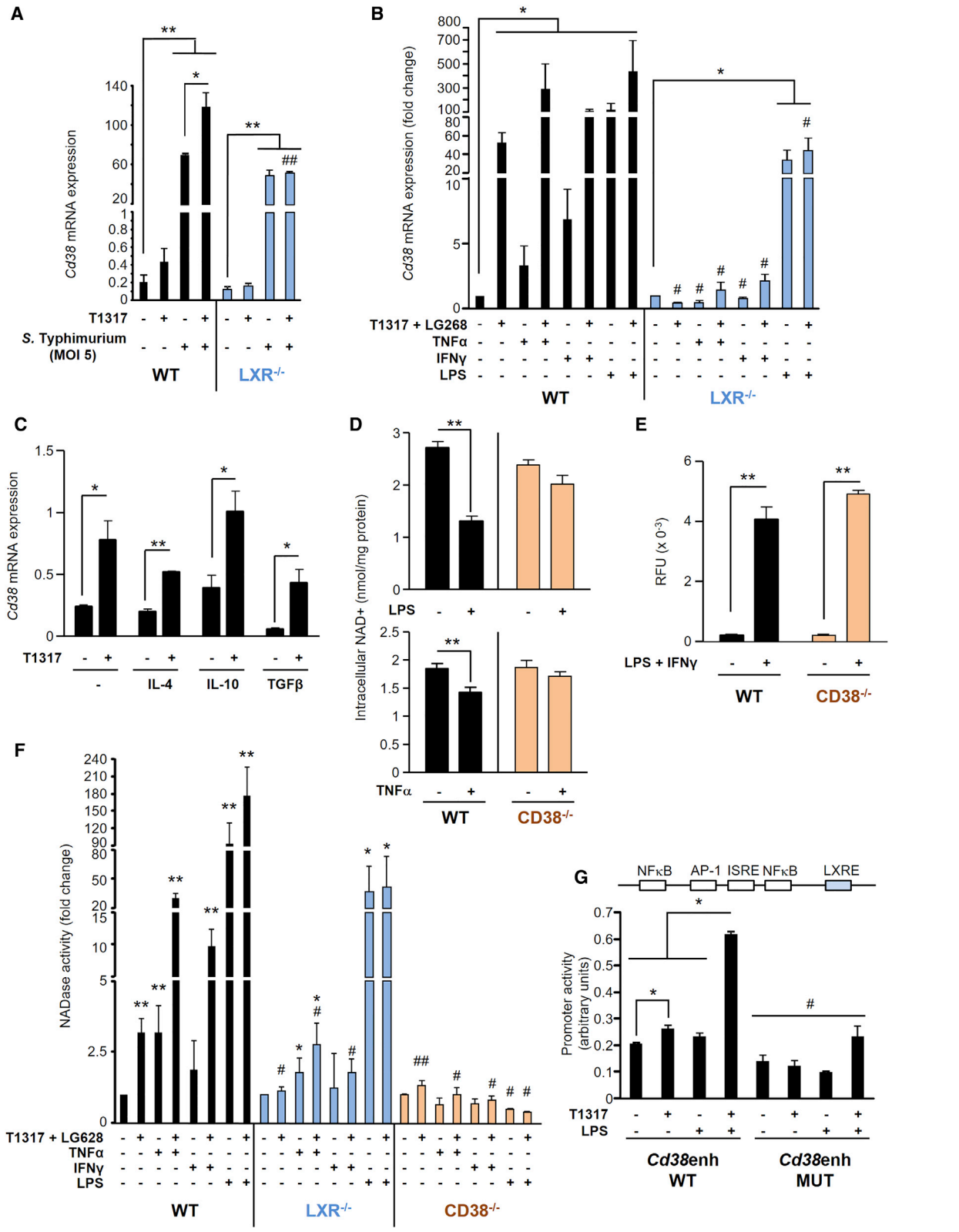

(legend on next page)

cooperation of the LXR pathway with LPS signaling occurred at the transcriptional level, and these effects were abolished when the cells were transfected with the mutant LXRE (Figure 4G).

CD38 Mediates the Protective Effects of LXR Agonists on Macrophage Infection

We next compared the capability of an LXR agonist to protect WT and CD38-deficient macrophages from infection by *S.* Typhimurium. Importantly, the lack of functional expression of CD38 inhibited the capability of the LXR agonist to reduce the amount of infected macrophages and intracellular bacteria (Figure 5A), effects that were similar to those obtained upon addition of exogenous NAD^+ in WT cells (Figure 2C). Moreover, activation of macrophages by IFN-γ has been shown to regulate negatively their capability to internalize non-opsonized bacteria in certain models of infection (Wang et al., 2014; Sun and Metzger, 2008). Interestingly, in our studies, prolonged stimulation with IFN-γ resulted in decreased infection by non-opsonized *Salmonella* cells in a CD38-dependent manner (Figure 5B). Taken together, these results suggest that induction of macrophage CD38 expression represents a strategy to limit infection of macrophages by live *Salmonella* cells.

We also determined the inflammatory response to infection in CD38-deficient macrophages (Figure 5C). To our surprise, the levels of induction of several cytokines were significantly lower in CD38-deficient cells as compared to WT cells. However, for most of the genes examined, LXR agonists were able to repress inflammatory gene expression in cells lacking functional CD38. These data suggest that CD38 selectively facilitates protection against invasive bacterial cell entry but does not contribute broadly to the LXR-mediated anti-inflammatory response in vitro.

Intrinsic to its NADase activity, CD38 mediates the synthesis of ADPR, cADPR, and nicotinic acid adenine dinucleotide phosphate (NAADP), which are Ca^{2+} mobilizing compounds (Musso et al., 2001). Video microscopic measurements from fura-2-AM-loaded cells showed higher basal levels of cytosolic Ca^{2+} in WT macrophages than in LXR-deficient cells (Figure 5D, top). However, Ca^{2+} storage in the endoplasmic reticulum (ER) was not depleted by prolonged treatment with the LXR agonist or by addition of exogenous NAD^+, as shown in experiments in which the cells were acutely stimulated with the sarco-ER Ca^{2+} ATPase inhibitor thapsigargin (Figure 5D, bottom). Altogether, these results suggest that induction of the LXR-CD38 circuit has no substantial long-term impact on Ca^{2+} depletion from the ER in macrophages. In addition, incubation of WT cells with *S.* Typhimurium did not lead to significant cytosolic Ca^{2+} changes in either the presence or absence of an LXR agonist (Figure 5E), and treatment with 8-bromo-cADPR, an analog of cADPR that blocks Ca^{2+} release mediated by ryanodine-receptor-gated stores, did not affect the capability of LXRs to inhibit macrophage infection (Figure 5F). Based on all of these observations, we conclude it is the CD38-dependent reduction in NAD^+ levels (a consequence of its strong NADase activity) and not the concomitant generation of potential Ca^{2+}-mobilizing second messengers that best explains the protective effects on macrophage infection induced by the LXR-CD38 axis. Importantly, lack of functional CD38 expression counteracted the capability of an LXR agonist to inhibit changes in F-actin redistribution and cell morphology associated with bacterial infection (Figures 5G–5I).

An Endogenous Pathway Can Activate the LXR-CD38 Axis during *Salmonella* Infection

Endogenous LXR ligands are generated enzymatically from intermediates of the cholesterol biosynthetic pathway or by oxidation of cholesterol by sterol hydroxylases (Spann et al., 2012). Interestingly, infection of macrophages with *S.* Typhimurium resulted in reduced expression of several enzymes involved in cholesterol biosynthesis but a selective prominent increase in the expression of cholesterol 25-hydroxylase (*Ch25h*), which mediates cholesterol oxidation to 25-hydroxycholesterol (25-HC) (Figure 6A). 25-HC is a relatively weak LXR activator that is able to induce LXR-mediated transcriptional activity at high doses (Lala et al., 1997; Janowski et al., 1999). In our studies, micromolar doses of 25-HC induced the expression of *Cd38*, either alone or in synergy with IFN-γ (Figure 6B), and reduced macrophage infection in an LXR- and CD38-dependent manner (Figures 6C and 6D). 25-HC can modulate inflammatory responses both positively and negatively in different settings (Reboldi et al., 2014; Gold et al., 2014). In macrophages infected with *Salmonella*, 25-HC exerted dose-dependent repression of inflammatory genes (Figure 6E). However, these actions were independent of the LXR-CD38 pathway (Figure 6E), in contrast to

Figure 4. Synergistic Induction of *Cd38* by Inflammatory Signals and LXR Activation

(A–C) qPCR analysis of *Cd38* expression in WT (A–C) or LXR-deficient macrophages (A and B) in response to one or more stimuli: *S.* Typhimurium (MOI 5, 8 hr), LXR agonist T1317 (1 μM, 8 hr in A or 24 hr in B), RXR agonist LG268 (1 μM, 24 hr), TNF-α (20 ng/mL, 24 hr), IFN-γ (5 ng/mL, 24 hr), LPS (100 ng/mL, 24 hr), IL-4 (20 ng/mL, 18 hr), IL-10 (10 ng/mL, 18 hr), and TGF-β (2 ng/mL, 18 hr). Data represent mean ± SEM (n = 3). In (A) and (B), #p < 0.05, ##p < 0.01 versus the same treatment in WT cells. Statistical analysis was performed with a two-way ANOVA Bonferroni (A), Kruskal Wallis followed by Mann-Whitney *U* test for paired comparisons (B), or t test (C).

(D) Intracellular NAD^+ levels in WT and CD38-deficient macrophages stimulated or not with LPS (100 ng/mL) (top) or TNF-α (20 ng/mL) (bottom) for 24 hr. Data represent mean ± SEM; n = 7 (WT, top), n = 3 ($CD38^{-/-}$, top), n = 10 (WT, bottom), and n = 6 ($CD38^{-/-}$, bottom) (t test).

(E) Fluorimetric analysis of intracellular ROS production in response to LPS (100 ng/mL) and IFN-γ (5 ng/mL) (6 hr) in WT and CD38-deficient cells. Data represent mean ± SD (representative experiment of n = 4, with each experiment using biologically distinct triplicates).

(F) Intracellular NADase activity. Data represent mean ± SEM; n = 5 (WT) and n = 3 ($LXR^{-/-}$, $CD38^{-/-}$) (each experiment performed with cells pooled from at least two mice). Statistical analysis was performed using a Kruskal-Wallis test. *p < 0.05, **p < 0.01 vs control cells from the same genotype; #p < 0.05, ##p < 0.01 vs same treatment in WT cells.

(G) Luciferase reporter studies in Raw264.7 macrophages stably transfected with LXRα and transiently cotransfected with a reporter plasmid containing the *Cd38* enhancer with WT LXRE (*Cd38*enh WT) or with mutated LXRE (*Cd38*enh MUT), as well as a plasmid overexpressing RXRα. Transfected cells were stimulated for 24 hr with vehicle (DMSO), T1317 (1 μM), LPS (100 ng/mL), or a combination of both. Data represent mean ± SEM (n = 4). #p < 0.05 versus the same treatment in cells transfected with the WT construct (Kruskal-Wallis).

See also Figure S5. *p < 0.05, **p < 0.01.

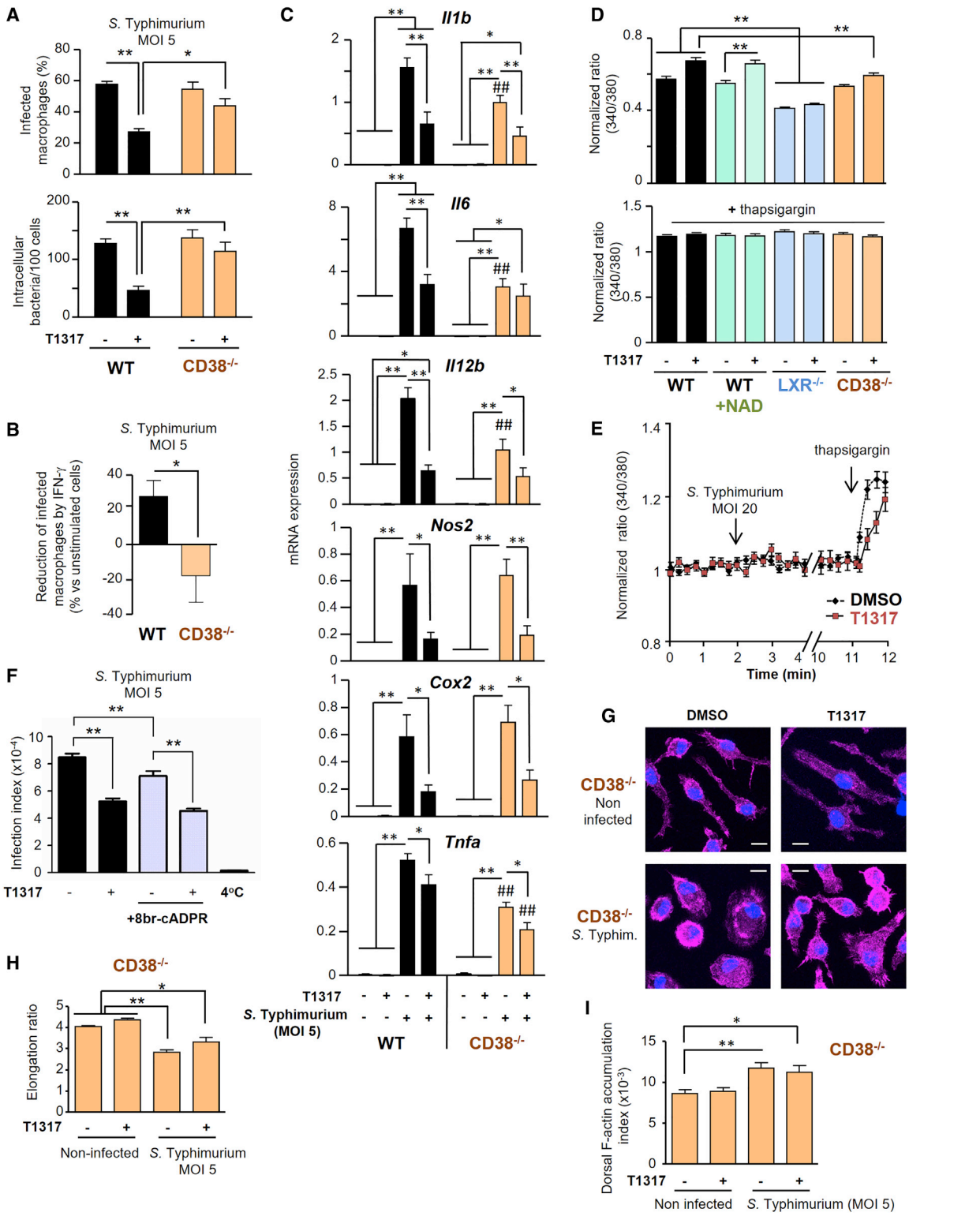

Figure 5. CD38 Mediates the Protective Effects of LXR Agonists on Macrophage Infection

(A) Effects of the LXR agonist T1317 on the percentage of infected cells (top) and the amount of intracellular bacteria (bottom) in WT and CD38-deficient macrophages, as assessed by confocal fluorescence microscopy. Data represent mean ± SEM (n = 4; two-way ANOVA Bonferroni).

(legend continued on next page)

the role in macrophage bacterial infection. Altogether, these observations suggest that induction of CH25H during the host innate response against *Salmonella* may provide local endogenous LXR agonists that limit subsequent macrophage infection through the LXR-CD38 circuit and, in parallel, activate mechanisms that are independent of LXRs to further keep inflammatory responses under control.

Pharmacological Treatment with a Synthetic LXR Agonist Ameliorates the Clinical Signs Associated with Bacterial Infection In Vivo

Based on the findings described throughout this work, we next analyzed whether pharmacological treatment with a synthetic agonist has protective effects on *Salmonella* infection in vivo. Mice were administered either vehicle or the LXR agonist T1317 daily during the course of a lethal infection with *S.* Thyphimurium and monitored for the first 5 days post-infection. Remarkably, pharmacological LXR activation resulted in a significant decrease in body mass loss and in the severity of the clinical score during the course of infection (Figures 7A and 7B). The ameliorating effects of the agonist were abolished in animals deficient in LXRs (Figures 7C and 7D) or CD38 (Figures 7E and 7F). In LXR$^{-/-}$ mice, in fact, treatment with T1317 accelerated the loss of weight associated to infection. Moreover, in WT mice, but not in CD38$^{-/-}$ mice, the agonist decreased the infection index of splenocytes 4 days after the start of infection (Figures 7G and 7H) as well as the expression of several markers of inflammation in the liver and spleen (Figure S6), suggesting that pharmacological activation of LXRs inhibited the capability of orally administered *Salmonella* to disseminate and infect distant organs.

To evaluate the specific contribution of bone-marrow-derived CD38-expressing cells, we analyzed the response to infection in mice that had been sub-lethally irradiated and transplanted with either WT or CD38-deficient bone marrow. Interestingly, activation of the LXR pathway did not reduce the loss of body weight and other clinical signs associated with infection in mice reconstituted with CD38$^{-/-}$ bone marrow, in contrast to the ameliorating effects observed in mice transplanted with WT bone marrow (Figures 7I–7J). In correlation with these observations, treatment with the LXR agonist significantly inhibited the infection index of splenocytes (Figure 7K) and the expression of several inflammatory genes in WT, but not CD38-deficient, bone marrow recipients (Figure S7). Collectively, these results suggest that CD38 induction in bone-marrow-derived cells is an important mediator of the ameliorating actions of the LXR pathway in *Salmonella* infection.

DISCUSSION

In this study, we have identified a previously unappreciated strategy to inhibit the potential of *S.* Typhimurium to infect host macrophages based on pharmacological targeting of the LXR pathway. A key finding of our work is the mechanism that accounts for these protective effects, which involves transcriptional upregulation of the multifunctional enzyme CD38. Interestingly, LXR activation did not interfere with phagocytosis of IgG-opsonized bacteria, suggesting that the protective effects of LXR agonists do not interfere with bacterial clearance through Fcγ receptors once the adaptive immune system has generated opsonizing antibodies against the pathogen.

A role for CD38 in the host response against bacteria has been previously proposed based on increased susceptibility of CD38-deficient mice to other bacterial strains, in correlation with defects in immune cell infiltration to sites of infection (Partida-Sánchez et al., 2001; Lischke et al., 2013) or with defective polarization of Th1 immune responses (Viegas et al., 2007). In this work, we describe a previously unrecognized function of CD38 in mediating macrophage protection from invasive bacterial infection. The major enzymatic activity of CD38 is considered to be its NADase activity, as it hydrolyzes 100 molecules of NAD^+ to generate 1 molecule of cADPR (Aksoy et al., 2006). In the model we propose here, LXR activation reduces NAD^+ levels as a consequence of elevated CD38 expression, resulting in cytoskeletal changes that interfere with membrane ruffling and/or other mechanisms subverted by invasive bacterial strains. Consistent with this model, addition of NAD^+ reverted the changes in cell morphology and dorsal F-actin accumulation in macrophages and rescued the capability of *S.* Typhimurium to infect macrophages in the presence of an LXR agonist. The virulence of invasive *Salmonella* strains correlates with their capability to induce extensive cell membrane ruffling and macropinocytosis and enter inside macrophages via ''spacious phagosomes'' (Kiama et al., 2006; Alpuche-Aranda et al., 1995). Among the effectors secreted by *S.* Typhimurium, cell invasion protein A increases the actin polymerization rate (Lilic et al., 2003) and Salmonella outer protein E enhances the activity of host cell Rho family GTPases involved

(B) Treatment with IFN-γ (5 ng/mL, 24 hr) reduced the infection in WT, but not CD38-deficient, macrophages, as assessed by confocal microscopy. Data represent mean ± SEM (n = 3; Mann-Whitney Wilcoxon).

(C) Repressive effects of T1317 on proinflammatory gene expression in WT and CD38-deficient macrophages (qPCR analysis). Data represent mean ± SEM (n = 5; two-way ANOVA Bonferroni). ##$p < 0.01$ vs the same treatment in WT cells.

(D and E) Video microscopic analysis of cytosolic Ca^{2+} levels in WT (D and E), LXR-deficient (D), and CD38-deficient (D) macrophages loaded with fura-2 AM. Prior to the analysis, the cells were stimulated with T1317 (1 μM, 24 hr) or vehicle (DMSO) with or without exogenous addition of NAD^+ (1 mM) for the last 2 hr of treatment. In (D, bottom), changes in cytosolic Ca^{2+} levels after inducing Ca^{2+} mobilization from the ER by thapsigargin (1 μM). In (D), data represent mean ± SEM (pooled data from three independent experiments; Kruskal Wallis). (E) Representative experiment showing that infection by *S.* Typhimurium (MOI 20) did not result in changes in cytosolic Ca^{2+} levels in cells previously stimulated or not with T1317. As a control, the response to thapsigargin was also evaluated; data represent mean ± SD (n = 3, each experiment performed in triplicates). Similar results were obtained using MOIs 5–10.

(F) Treatment with 8br-cADPR (20 μM, 2 hr) does not impair the capability of T1317 to inhibit macrophage infection, as assessed by flow cytometry studies of macrophage infection. Data represent mean ± SEM (n = 3; ANOVA Bonferroni).

(G–I) Morphological analysis by confocal fluorescence microscopy of CD38-deficient macrophages. Representative images (scale bars, 10 μm) (G), cell elongation ratio (H), and dorsal F-actin accumulation (I). Data represent mean ± SEM (n = 3; ANOVA Bonferroni).

*$p < 0.05$, **$p < 0.01$.

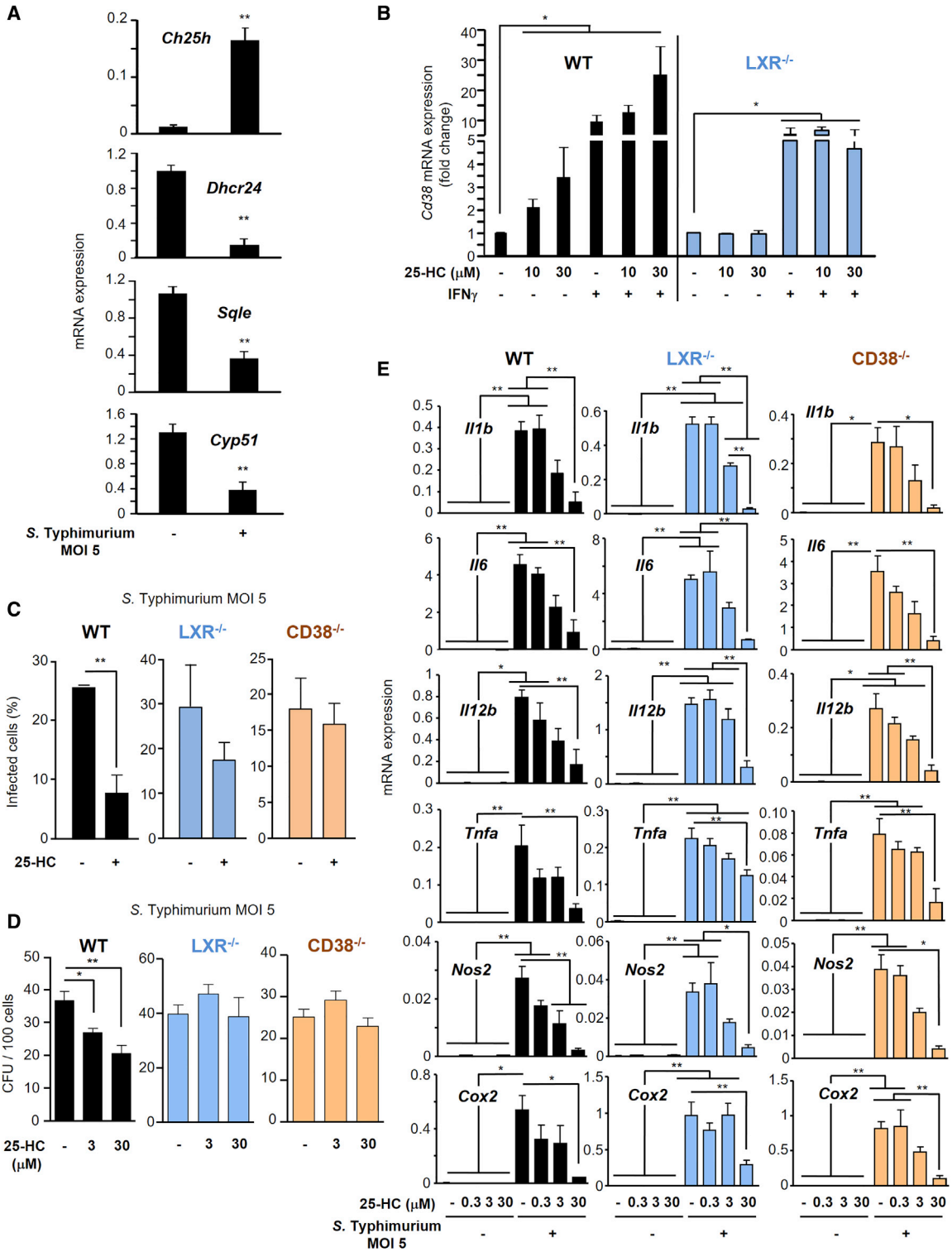

Figure 6. *Salmonella* Infection Induces the Expression of *Ch25h* in Macrophages

(A) Effects of *Salmonella* infection on the relative mRNA levels of several enzymes involved in cholesterol and oxysterol biosynthesis. Macrophages were infected with *S.* Typhimurium for 30 min, and gene expression was evaluated by qPCR 8 hr post-infection. Mean ± SEM (n = 3; t test). *Cyp51*, sterol 14α-demethylase; *Dhcr24*, 24-dehydrocholesterol reductase; *Sqle*, squalene epoxidase.

(legend continued on next page)

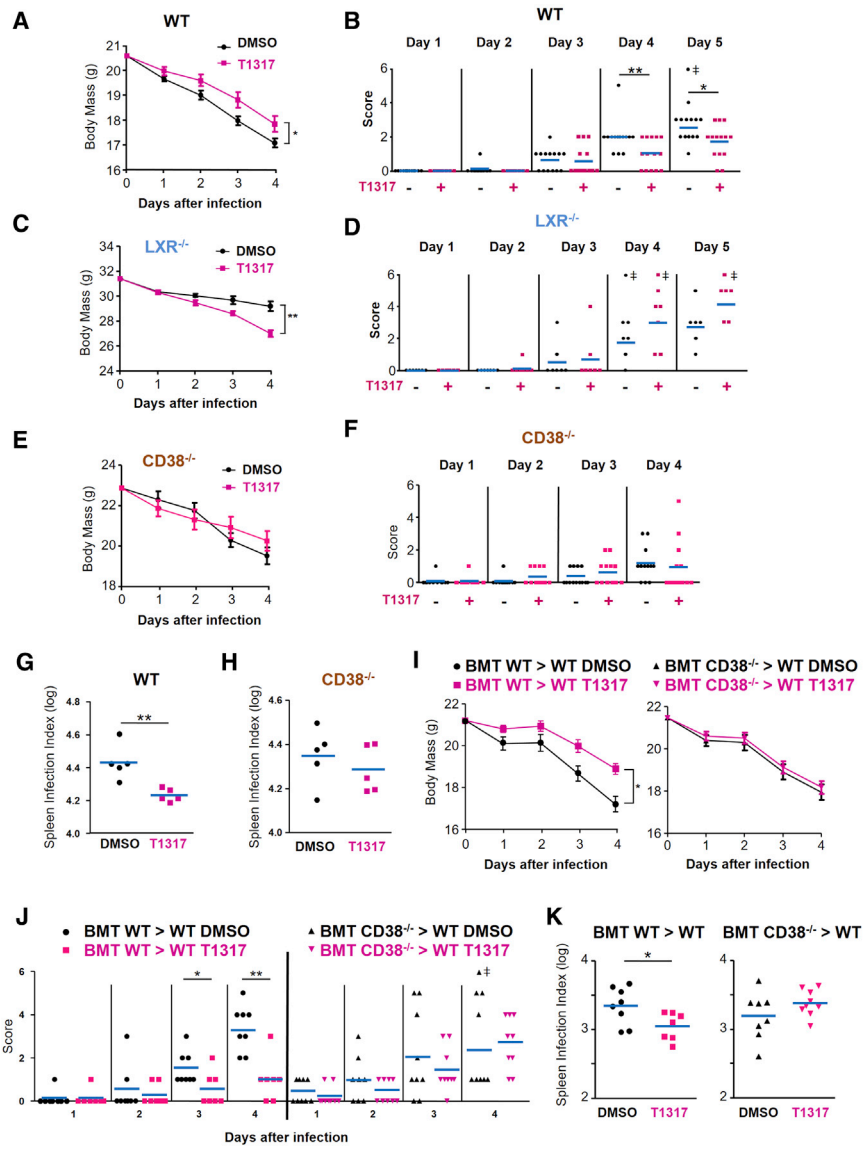

Figure 7. Pharmacological Treatment with a Synthetic LXR Agonist Ameliorates the Clinical Signs Associated with *Salmonella* Infection in a CD38-Dependent Manner

WT (A and B), LXR-deficient (C and D), or CD38-deficient (E and F) female mice were infected by oral gavage with *S.* Typhimurium (10^7 CFU per animal). The animals were daily administered by i.p. injection either vehicle (DMSO in physiologic saline, black circles) or the LXR ligand T1317 (15 mg/kg animal dissolved in physiologic saline, magenta squares), starting 24 hr before the infection; n = 14 (WT), n = 7 ($LXR^{-/-}$), and n = 13 ($CD38^{-/-}$) mice per group.

(A, C, and E) The weight of each mouse was measured daily before and after the infection. The graphics represent estimated marginal means of mass (±SEM) during the first 4 days post-infection. Statistical analysis was performed using repeated-measures two-way ANCOVA after adjusting for mass at the time of infection.

(B, D, and F) Development of clinical signs during the first few days of infection. For each mouse, a score was calculated based on the presence of clinical signs (one point for each sign): >15% weight loss, severe hunched position, ruffled fur, watery eyes, or slow movement. Dead animals (ǂ) were assigned a score of 6. Horizontal bars represent mean values in the live population (Mann-Whitney *U*).

(G and H) WT (G) or CD38-deficient (H) female mice were orally infected with RFP-expressing *S.* Typhimurium (10^7 CFU per animal) and treated with vehicle or an LXR agonist as described above. The infection index in splenocytes after 4 days of infection was determined by flow cytometry (log values); n = 5 mice per group (t test).

(I–K) Sub-lethally irradiated WT female mice were subjected to bone marrow transplantation (3 × 10^6 bone marrow cells per animal) from either WT (BMT WT > WT) or CD38-deficient female donors (BMT $CD38^{-/-}$ > WT). Two months after transplantation, the animals were infected with RFP-expressing *S.* Typhimurium (10^7 CFU). Bacterial infection and administration of LXR agonist or vehicle was performed as described above. Body weight (I) and severity score (J) were registered during 4 days post-infection. The infection index in splenocytes was evaluated by flow cytometry (K); n = 7–9 mice per group. Estimated marginal means of mass (± SEM) and repeated-measures two-way ANCOVA after adjusting for mass at the time of infection (I), Mann-Whitney *U* (J), or t test (K). In (J)–(K), blue horizontal bars indicate mean values.

See also Figures S6 and S7. *p < 0.05, **p < 0.01.

in the regulation of the cytoskeleton (Hardt et al., 1998). Moreover, NAD^+ is used as a cofactor to sustain the glycolytic activity in macrophages and generate ATP for polymerization of F-actin filaments and may also modulate actin dynamics through several other mechanisms (Yin et al., 2012; Venter et al., 2014).

(B) *Cd38* mRNA expression was evaluated by qPCR upon treatment of WT or LXR-deficient macrophages with the indicated doses of 25-HC in the presence or absence of IFN-γ (5 ng/mL). Mean ± SEM (n = 3; Kruskal-Wallis).

(C) Confocal microscopy studies indicating that incubation with 25-HC (30 μM) reduced infection by *S.* Typhimurium in WT, but not LXR- or CD38-deficient, macrophages. Data represent mean ± SEM (n = 3; t test).

(D) Quantification of viable intracellular *S.* Typhimurium. Macrophages from WT (left), LXR-deficient (middle), or CD38-deficient (right) were treated with 25-HC (3–30 μM) or vehicle (ethanol) for 18 hr and then infected with *S.* Typhimurium for 30 min. Quantification of intracellular bacterial CFUs after plating serial dilutions of cell lysates on agar. Data represent mean ± SEM (n = 6; ANOVA Bonferroni).

(E) 25-HC modulates inflammatory gene expression independently of LXR and CD38. Macrophages were treated with 25-HC (0.3–30 μM) 18 hr before infection with *S.* Typhimurium. Inflammatory gene expression was determined by qPCR 6 hr post-infection. Data represent mean ± SEM (n = 4; ANOVA Bonferroni).

*p < 0.05, **p < 0.01.

We have identified a functional LXRE that conferred LXR/RXR agonist responsiveness to a *Cd38* enhancer-directed luciferase construct. Interestingly, CD38 expression can be also induced by other members of the nuclear receptor family, including retinoic acid receptor alpha (Drach et al., 1994) and peroxisome proliferator-activated receptor gamma (Song et al., 2012). Although we cannot discard possible cooperation between other RXR heterodimeric partners and LXRs, the induction of macrophage CD38 by LXR/RXR agonists and the protective mechanism uncovered here depends on functional LXR expression, suggesting that these effects are mediated directly by LXR-RXR heterodimers.

Another major insight from this report is that cooperative actions between LXRs and inflammatory signals translate into synergistic induction of CD38 expression and its NADase activity. Our reporter studies suggest that these effects occur through combined actions at the transcriptional level, which contrasts with general mutually repressive activities between LXRs and LPS or IFN-γ (Castrillo et al., 2003; Ghisletti et al., 2007; Pascual-García et al., 2013). Our results support the notion that such cooperative regulation of macrophage CD38-dependent NADase activity represents a protective mechanism to control excessive internalization of live bacterial cells. This mechanism may be induced endogenously to some extent through induction of CH25H during infection and subsequent production of the oxysterol 25-HC. Micromolar doses of 25-HC resulted in CD38 upregulation and protection from macrophage infection in an LXR- and CD38-dependent manner, raising the possibility that, within infected tissues, intracellular or locally secreted 25-HC levels that reach the threshold to activate the LXR pathway, in combination with inflammatory mediators, contribute to limit intracellular macrophage infection.

Importantly, pharmacological treatment with a high-affinity LXR agonist ameliorated the levels of infection in the spleen and the clinical signs of disease after oral administration of *S.* Typhimurium in a CD38-dependent manner. Once they have infected intestinal epithelial cells, *Salmonella* cells continue to disseminate to other organs and their intracellular life within macrophages is essential for dissemination. We therefore hypothesize that pharmacological activation of the LXR-CD38 circuit, most probably enhanced by mediators in the inflammatory milieu, protects uninfected macrophages from posterior infection, therefore restraining the capability of *Salmonella* cells to disseminate throughout the body. Moreover, the LXR agonist also exerts anti-inflammatory actions that contribute to amelioration of the severity score of disease. Interestingly, despite the fact that LXR agonists repress macrophage inflammatory gene expression independently of CD38 in vitro, the induction of a number of inflammatory mediators in both the spleen and the liver of *Salmonella*-infected animals was downregulated by the LXR agonist in WT, but not CD38-deficient, mice. We interpret that two mechanisms affecting the extent of inflammation may be operating simultaneously in vivo: on one hand, LXR may repress the inflammatory response independently of CD38, and, on the other hand, the LXR-CD38 axis protects macrophages from infection, thus reducing bacterial dissemination to other organs and indirectly contributing to downregulated inflammation. Beyond these considerations, we cannot discard the contribution of other mechanisms regulated by LXRs, such as induction of SPα/AIM, a protein that protects macrophages from bacterial-induced cell death (Joseph et al., 2004; Valledor et al., 2004) and regulates autophagy during mycobacterial infection (Sanjurjo et al., 2015). Importantly, our bone marrow transplantation studies provide evidence that the expression of CD38 specifically in bone-marrow-derived cells is important for the LXR-mediated effects described here, including the reduction in the levels of splenocyte infection, the extent of inflammation, and other clinical signs associated with *Salmonella* infection. Our studies, however, do not exclude that CD38 expression in bone-marrow-derived cells other than macrophages (e.g., neutrophils) contributes to the observed effects of the LXR agonist in vivo. Indeed, the concerted activities of CD38 seem to favor the extracellular permanence of invasive bacterial strains, as suggested here, and the chemotaxis of neutrophils to sites of infection (Partida-Sánchez et al., 2001), which may, in parallel, promote extracellular bacterial killing and limit macrophage-mediated dissemination. In consideration of evolving antimicrobial resistance in certain parts of the world, this work strengthens the relevance of LXR agonists or drugs that potentiate CD38 NADase activity as potential therapeutic strategies in host-directed therapy against infections that use the macrophage as a niche for replication.

EXPERIMENTAL PROCEDURES

See Supplemental Experimental Procedures for more information.

Animal Strains

All the protocols requiring animal manipulation have been approved by the ethical committee from Parc Científic de Barcelona, University of Barcelona, Mayo Clinic and Institut Pasteur in Montevideo.

Cell Cultures

Bone-marrow-derived macrophages were obtained from bone marrow precursors differentiated for 6–7 days in DMEM (PAA Laboratories) supplemented with 20% heat-inactivated fetal bovine serum (FBS) (PAA) and 30% L-cell conditioned medium. Both female and male mice were used indistinctively for generation of primary macrophages. Raw264.7 macrophages and COS-7 (ATCC) cells were grown in DMEM 10% heat-inactivated FBS.

In Vitro Infection

Macrophages were plated in cell culture plates containing DMEM 10% FBS and infected with *S.* Typhimurium or *E. coli* for 30 or 60 min at different MOIs (5–20). Non-internalized bacterial cells were eliminated by three washes with PBS. In some experiments, macrophages were then incubated for 1 hr in complete medium containing 100 μg/mL gentamicin (Sigma-Aldrich) to kill extracellular bacteria and then switched to complete medium with a lower dose of gentamicin (10 μg/mL) and processed at different times post-infection. In some experiments, *S.* Typhimurium was opsonized with anti-*Salmonella* LPS IgG (Santa Cruz Biotechnology) for 2 hr at 4°C.

Determination of Macrophage Infection by Flow Cytometry

Infected cells were fixed in PBS 4% paraformaldehyde, and cells containing fluorescent bacteria (RFP+) were counted using a FacsAria I SORP sorter (Becton Dickinson). In each experiment, non-infected cells were used as internal controls of macrophage auto-fluorescence, and cells infected at 4°C were used to distinguish attached versus internalized bacteria. For more detailed information, see Supplemental Experimental Procedures.

Confocal Fluorescence Microscopy

Infected macrophages were washed with PBS and fixed with 4% paraformaldehyde for 10 min. After two additional washes with PBS, the cells were

incubated with wheat germ agglutinin (WGA)-Alexa 488 (2.5 μg/mL, 10 min) or Bodipy-fluorescein isothiocyanate (FITC) (4 μg/mL, 30 min) (Life Technologies) to stain cell membranes. In some experiments, F-actin filaments were stained with phalloidin-Alexa 633 (Life Technologies) (10 μg/mL) for 30 min at 37°C. Cell nuclei were stained with DAPI (1 μg/mL) for 5 min, whereas intracellular bacteria were detected by RFP emission. The cells were mounted in Vectashield (Vector Laboratories). Confocal images and z stack sections were acquired using Leica TCS SP2 and SP5 confocal microscopes (Leica Microsystems) and processed with ImageJ software. Five random fields per coverslip were recorded and, in each experiment, at least triplicate coverslips were generated for each condition.

In Vivo Infection

In experiments evaluating the clinical signs of infection, adult (3–5 months old) WT, LXR-deficient, or CD38-deficient female mice were pretreated with 10% sodium bicarbonate for 10 min and then infected by oral gavage with *S.* Typhimurium (10^7 CFU in 200 μL saline solution per animal). To evaluate the effects of LXR activation on morbidity, the animals were daily administered by intraperitoneal (i.p.) injection either vehicle (DMSO) or the LXR ligand T1317 (15 mg/kg animal) dissolved in physiologic saline, starting 24 hr prior to infection. Each animal was daily monitored for weight changes and other parameters associated with infection-induced morbidity, and a clinical scoring system was defined according to the development of any of the following clinical signs (one point for each sign): >15% weight loss, severe hunched position, ruffled fur, watery eyes, or slow movement. In some experiments, the mice were sacrificed at day 4 post-infection, and the infection index in the spleen was determined. In these assays, the spleens were disaggregated through a 100-μm cell strainer, and the erythrocytes were lysed using 1X Pharm Lyse lysing solution (BD Biosciences). The splenocytes were fixed in PBS 5% paraformaldehyde, and the percentage of infected cells (containing RFP+ bacteria) was analyzed by flow cytometry. An infection index was calculated for each animal by using the following formula: infection index = (percentage of RFP+ splenocytes) × (mean fluorescence intensity in the RFP+ population). Spleen samples from non-infected mice were used as negative controls.

Irradiation and Bone Marrow Transfer

Eight-week-old C57BL/6 females were sub-lethally irradiated with two sessions of 4.5 Gy separated by 4 hr. The animals were then injected with 3×10^6 bone marrow cells from either WT or CD38-deficient female donors. These procedures were carried out at the animal facility of *Parc de Recerca Biomèdica Barcelona* (PRBB). Two months after the bone marrow transfer, the mice were treated with an LXR agonist or vehicle and infected with *S.* Typhimurium as indicated above. Blood, spleen, and bone marrow specimens from non-infected mice were used to analyze the efficiency of replacement of the hematopoietic system. In these assays, surface CD38 expression was analyzed through flow cytometry. See Supplemental Experimental Procedures for more information.

RNA Extraction and Quantitative Real-Time PCR Determination

Total RNA was extracted using TRIzol Reagent (Life Technologies) as recommended by the manufacturer. More information on cDNA synthesis and quantitative real-time PCR (real-time qPCR) can be found in Supplemental Experimental Procedures. Primers used for measuring specific gene expression are described in Table S1.

Protein Extraction and Western Blot Analysis

Cells were washed in cold PBS and lysed on ice in RIPA buffer (25 mM Tris-HCl [pH 7.6], 150 mM NaCl, 1% NP-40, 1% sodium deoxycholate, and 0.1% SDS) supplemented with protease inhibitors. The samples were processed as described in Supplemental Experimental Procedures.

NAD Cycling Activity

To determine intracellular NAD^+ levels, 3×10^6 macrophages were lysed in 10% trichloroacetic acid (TCA) (Sigma-Aldrich) by sonication. Sonicated samples were centrifuged at 12,000 rpm for 2 min. The supernatants were collected, and the pellets were resuspended in 0.2 N NaOH for protein determination. TCA extraction was performed on the supernatants by adding 2 vol 1,1,2-trichloro-1,2,2-trifluroethane and 3 vol trioctylamine. After phase separation, the top aqueous layer containing NAD^+ was recovered, and its pH was adjusted to 8.0. In a 96-well plate, 100 μL of each sample diluted in water was mixed with 100 μL of a cycling reagent solution (100 mM NaH_2PO_4 [pH 8], 0.76% ethanol, 4 μM riboflavin 5′-monophosphate, 27.2 U/mL alcohol dehydrogenase, 0.24 U/mL diaphorase, and 8 μM resazurin) and incubated for 20 min in the dark. The samples were monitored every min for 60 min in a fluorescence plate reader (excitation wavelength = 544 nm; emission wavelength = 590 nm). A standard curve with known concentrations of NAD^+ was used to determine the amount of NAD^+ in the processed samples. The data were normalized by the amount of protein in each sample.

NADase Activity

NADase activity was measured using a fluorescence-based assay. In each sample, 5×10^6 macrophages were lysed by sonication in Sucrose-Tris buffer (0.25 M sucrose, 40 mM Tris [pH 7.4], and protease inhibitors). The samples were excited at 300 nm and the fluorescence was measured at 410 nm. After the baseline was recorded, 80 μM of $1,N^6$-etheno-adenine dinucleotide was added to start the reaction. The emission of fluorescence was followed at 37°C every min for 1 hr in a Gemini XPS fluorescence microplate reader (Molecular Devices). NADase activity was calculated as the slope of the linear portion of the fluorescence-time curve, corrected by the amount of protein in each sample. The final results are expressed as NADase activity (df/dt) per milligram protein. For each experimental condition, duplicate samples were processed.

Statistical Analysis

Statistical analyses were performed with SPSS software (IBM). For data with normal distribution, an ANOVA Bonferroni test or a Student's t test was used to determine statistical differences between multiple or paired comparisons, respectively. Instead, a Kruskal-Wallis Dunn's test or a Mann-Whitney *U* Wilcoxon test was used for data without normal distribution. In experiments evaluating changes of body weight along the course of infection, a repeated-measures two-way ANCOVA was used, adjusting for weight at day 0 of infection. Differences were considered significant when $p < 0.05$.

To make different experiments comparable in Figures 1A and 2C, the data were normalized using the following procedure. The intensity of each experiment (i_e) was calculated by determining the mean value of infection between the vehicle-treated control and the T1317-treated WT cells. The intensities of separate experiments were normalized by the mean intensity value of all the experiments (i_m) and, for each experiment, the resulting normalization factor (i_m/i_e) was multiplied with the percentage of infected cells of all the samples in that experiment. Similar calculations were applied to Figures 3G, 3L, 4D, and 4G.

The accession number for the microarray datasets reanalyzed in this work is MIAMExpress: E-MEXP-3871 (Pascual-García et al., 2013).

SUPPLEMENTAL INFORMATION

Supplemental Information includes Supplemental Experimental Procedures, seven figures, and one table and can be found with this article online at http://dx.doi.org/10.1016/j.celrep.2017.01.007.

AUTHOR CONTRIBUTIONS

Conceptualization, J.M., E.N.C., and A.F.V.; Methodology, J.M., F.S., S.P., L.S., S.M.-R., J. Serret, K.K., R.V., and A.F.V.; Formal Analysis, J.M., E.G., R.V., and A.F.V.; Investigation, J.M., E.G., M.B., C.E., J.M.C., K.K., R.V., T.L., M.P.-G., L.S., and A.F.V.; Validation, S.B. and A.C.; Resources, A.R., A.J., L.L., C.C., and J. Sancho; Writing–Original Draft, J.M., A.C., E.N.C., and A.F.V.; Writing–Review & Editing, C.E., M.R.S., and A.F.V.; Visualization, J.M., E.G., and A.F.V.; Supervision, E.N.C. and A.F.V.; Project Administration, A.F.V.; Funding Acquisition, C.E., R.V., C.C., and A.F.V.

ACKNOWLEDGMENTS

We thank D. Mangelsdorf for the LXR-deficient mice, J.H. Brumell for the pBR.RFP.1 plasmid, M. Sorribas and M. García for technical assistance, and A. Kupz, A. Dorhoi, and J.M. Caballero for protocols and scientific discussion. This work was supported by grants from the Spanish MICINN to A.F.V. (SAF2010-14989, SAF2011-23402, and SAF2014-57856), R.V. (SAF2010-16725), and the NuRCaMeIn network (SAF2015-71878-REDT); from Fundació la Marató de TV3 to A.F.V. (080930) and R.V. (20134030); and from COST Action BM1404 (Mye-EUNITER). M.R.S. is a Miguel Servet II researcher (ISCIII CPII14/00021), and C.E. is supported by a grant from ANII (INNOVA II, FCE_1_2014_1_104002, Uruguay). J.M. received fellowships from the Spanish MICINN (FPI, BES-2009-014828) and from the Institut Pasteur-Pierre Ledoux Jeunesse Internationale Foundation, M.P. received fellowships from the Spanish MEC (FPU, AP 2007-00821), J.M.C. received fellowships from the UB (APIF), and M.B. received fellowships from ANII (Uruguay).

Received: January 29, 2016
Revised: November 11, 2016
Accepted: January 5, 2017
Published: January 31, 2017

REFERENCES

A-Gonzalez, N., Bensinger, S.J., Hong, C., Beceiro, S., Bradley, M.N., Zelcer, N., Deniz, J., Ramirez, C., Díaz, M., Gallardo, G., et al. (2009). Apoptotic cells promote their own clearance and immune tolerance through activation of the nuclear receptor LXR. Immunity *31*, 245–258.

Aksoy, P., White, T.A., Thompson, M., and Chini, E.N. (2006). Regulation of intracellular levels of NAD: a novel role for CD38. Biochem. Biophys. Res. Commun. *345*, 1386–1392.

Alpuche-Aranda, C.M., Berthiaume, E.P., Mock, B., Swanson, J.A., and Miller, S.I. (1995). Spacious phagosome formation within mouse macrophages correlates with Salmonella serotype pathogenicity and host susceptibility. Infect. Immun. *63*, 4456–4462.

Belenky, P., Bogan, K.L., and Brenner, C. (2007). NAD+ metabolism in health and disease. Trends Biochem. Sci. *32*, 12–19.

Castrillo, A., Joseph, S.B., Vaidya, S.A., Haberland, M., Fogelman, A.M., Cheng, G., and Tontonoz, P. (2003). Crosstalk between LXR and toll-like receptor signaling mediates bacterial and viral antagonism of cholesterol metabolism. Mol. Cell *12*, 805–816.

Chini, E.N. (2009). CD38 as a regulator of cellular NAD: a novel potential pharmacological target for metabolic conditions. Curr. Pharm. Des. *15*, 57–63.

Drach, J., McQueen, T., Engel, H., Andreeff, M., Robertson, K.A., Collins, S.J., Malavasi, F., and Mehta, K. (1994). Retinoic acid-induced expression of CD38 antigen in myeloid cells is mediated through retinoic acid receptor-alpha. Cancer Res. *54*, 1746–1752.

Ghisletti, S., Huang, W., Ogawa, S., Pascual, G., Lin, M.-E., Willson, T.M., Rosenfeld, M.G., and Glass, C.K. (2007). Parallel SUMOylation-dependent pathways mediate gene- and signal-specific transrepression by LXRs and PPARgamma. Mol. Cell *25*, 57–70.

Gold, E.S., Diercks, A.H., Podolsky, I., Podyminogin, R.L., Askovich, P.S., Treuting, P.M., and Aderem, A. (2014). 25-Hydroxycholesterol acts as an amplifier of inflammatory signaling. Proc. Natl. Acad. Sci. USA *111*, 10666–10671.

Guiney, D.G., and Lesnick, M. (2005). Targeting of the actin cytoskeleton during infection by Salmonella strains. Clin. Immunol. *114*, 248–255.

Haas, A. (2007). The phagosome: compartment with a license to kill. Traffic *8*, 311–330.

Haraga, A., Ohlson, M.B., and Miller, S.I. (2008). Salmonellae interplay with host cells. Nat. Rev. Microbiol. *6*, 53–66.

Hardt, W.D., Chen, L.M., Schuebel, K.E., Bustelo, X.R., and Galán, J.E. (1998). S. typhimurium encodes an activator of Rho GTPases that induces membrane ruffling and nuclear responses in host cells. Cell *93*, 815–826.

Hong, C., and Tontonoz, P. (2014). Liver X receptors in lipid metabolism: opportunities for drug discovery. Nat. Rev. Drug Discov. *13*, 433–444.

Iqbal, J., and Zaidi, M. (2006). TNF regulates cellular NAD+ metabolism in primary macrophages. Biochem. Biophys. Res. Commun. *342*, 1312–1318.

Ito, A., Hong, C., Rong, X., Zhu, X., Tarling, E.J., Hedde, P.N., Gratton, E., Parks, J., and Tontonoz, P. (2015). LXRs link metabolism to inflammation through Abca1-dependent regulation of membrane composition and TLR signaling. eLife *4*, e08009.

Janowski, B.A., Grogan, M.J., Jones, S.A., Wisely, G.B., Kliewer, S.A., Corey, E.J., and Mangelsdorf, D.J. (1999). Structural requirements of ligands for the oxysterol liver X receptors LXRalpha and LXRbeta. Proc. Natl. Acad. Sci. USA *96*, 266–271.

Joseph, S.B., Bradley, M.N., Castrillo, A., Bruhn, K.W., Mak, P.A., Pei, L., Hogenesch, J., O'connell, R.M., Cheng, G., Saez, E., et al. (2004). LXR-dependent gene expression is important for macrophage survival and the innate immune response. Cell *119*, 299–309.

Kiama, S.G., Dreher, D., Cochand, L., Kok, M., Obregon, C., Nicod, L., and Gehr, P. (2006). Host cell responses of Salmonella typhimurium infected human dendritic cells. Immunol. Cell Biol. *84*, 475–481.

Korf, H., Vander Beken, S., Romano, M., Steffensen, K.R., Stijlemans, B., Gustafsson, J.-Å., Grooten, J., and Huygen, K. (2009). Liver X receptors contribute to the protective immune response against Mycobacterium tuberculosis in mice. J. Clin. Invest. *119*, 1626–1637.

Lala, D.S., Syka, P.M., Lazarchik, S.B., Mangelsdorf, D.J., Parker, K.L., and Heyman, R.A. (1997). Activation of the orphan nuclear receptor steroidogenic factor 1 by oxysterols. Proc. Natl. Acad. Sci. USA *94*, 4895–4900.

Lee, J.H., Park, S.M., Kim, O.S., Lee, C.S., Woo, J.H., Park, S.J., Joe, E.H., and Jou, I. (2009). Differential SUMOylation of LXRalpha and LXRbeta mediates transrepression of STAT1 inflammatory signaling in IFN-gamma-stimulated brain astrocytes. Mol. Cell *35*, 806–817.

Lee, C.-U., Song, E.-K., Yoo, C.-H., Kwak, Y.-K., and Han, M.-K. (2012). Lipopolysaccharide induces CD38 expression and solubilization in J774 macrophage cells. Mol. Cells *34*, 573–576.

Lilic, M., Galkin, V.E., Orlova, A., VanLoock, M.S., Egelman, E.H., and Stebbins, C.E. (2003). Salmonella SipA polymerizes actin by stapling filaments with nonglobular protein arms. Science *301*, 1918–1921.

Lischke, T., Heesch, K., Schumacher, V., Schneider, M., Haag, F., Koch-Nolte, F., and Mittrücker, H.-W. (2013). CD38 controls the innate immune response against Listeria monocytogenes. Infect. Immun. *81*, 4091–4099.

Luo, L., Wall, A.A., Yeo, J.C., Condon, N.D., Norwood, S.J., Schoenwaelder, S., Chen, K.W., Jackson, S., Jenkins, B.J., Hartland, E.L., et al. (2014). Rab8a interacts directly with PI3Kγ to modulate TLR4-driven PI3K and mTOR signalling. Nat. Commun. *5*, 4407.

McWhorter, F.Y., Wang, T., Nguyen, P., Chung, T., and Liu, W.F. (2013). Modulation of macrophage phenotype by cell shape. Proc. Natl. Acad. Sci. USA *110*, 17253–17258.

Musso, T., Deaglio, S., Franco, L., Calosso, L., Badolato, R., Garbarino, G., Dianzani, U., and Malavasi, F. (2001). CD38 expression and functional activities are up-regulated by IFN-gamma on human monocytes and monocytic cell lines. J. Leukoc. Biol. *69*, 605–612.

Partida-Sánchez, S., Cockayne, D.A., Monard, S., Jacobson, E.L., Oppenheimer, N., Garvy, B., Kusser, K., Goodrich, S., Howard, M., Harmsen, A., et al. (2001). Cyclic ADP-ribose production by CD38 regulates intracellular calcium release, extracellular calcium influx and chemotaxis in neutrophils and is required for bacterial clearance in vivo. Nat. Med. *7*, 1209–1216.

Pascual-García, M., Rué, L., León, T., Julve, J., Carbó, J.M., Matalonga, J., Auer, H., Celada, A., Escolà-Gil, J.C., Steffensen, K.R., et al. (2013). Reciprocal negative cross-talk between liver X receptors (LXRs) and STAT1: effects on IFN-γ-induced inflammatory responses and LXR-dependent gene expression. J. Immunol. *190*, 6520–6532.

Price, J.V., and Vance, R.E. (2014). The macrophage paradox. Immunity *41*, 685–693.

Reboldi, A., Dang, E.V., McDonald, J.G., Liang, G., Russell, D.W., and Cyster, J.G. (2014). Inflammation. 25-Hydroxycholesterol suppresses interleukin-1-driven inflammation downstream of type I interferon. Science *345*, 679–684.

Sanjurjo, L., Amézaga, N., Aran, G., Naranjo-Gómez, M., Arias, L., Armengol, C., Borràs, F.E., and Sarrias, M.-R. (2015). The human CD5L/AIM-CD36 axis: a novel autophagy inducer in macrophages that modulates inflammatory responses. Autophagy *11*, 487–502.

Song, E.-K., Lee, Y.-R., Kim, Y.-R., Yeom, J.-H., Yoo, C.-H., Kim, H.-K., Park, H.-M., Kang, H.-S., Kim, J.-S., Kim, U.-H., and Han, M.K. (2012). NAADP mediates insulin-stimulated glucose uptake and insulin sensitization by PPARγ in adipocytes. Cell Rep. *2*, 1607–1619.

Spann, N.J., Garmire, L.X., McDonald, J.G., Myers, D.S., Milne, S.B., Shibata, N., Reichart, D., Fox, J.N., Shaked, I., Heudobler, D., et al. (2012). Regulated accumulation of desmosterol integrates macrophage lipid metabolism and inflammatory responses. Cell *151*, 138–152.

Sun, K., and Metzger, D.W. (2008). Inhibition of pulmonary antibacterial defense by interferon-gamma during recovery from influenza infection. Nat. Med. *14*, 558–564.

Valledor, A.F., Hsu, L.-C., Ogawa, S., Sawka-Verhelle, D., Karin, M., and Glass, C.K. (2004). Activation of liver X receptors and retinoid X receptors prevents bacterial-induced macrophage apoptosis. Proc. Natl. Acad. Sci. USA *101*, 17813–17818.

Venter, G., Oerlemans, F.T.J.J., Willemse, M., Wijers, M., Fransen, J.A.M., and Wieringa, B. (2014). NAMPT-mediated salvage synthesis of NAD+ controls morphofunctional changes of macrophages. PLoS ONE *9*, e97378.

Viegas, M.S., do Carmo, A., Silva, T., Seco, F., Serra, V., Lacerda, M., and Martins, T.C. (2007). CD38 plays a role in effective containment of mycobacteria within granulomata and polarization of Th1 immune responses against Mycobacterium avium. Microbes Infect. *9*, 847–854.

Wagner, B.L., Valledor, A.F., Shao, G., Daige, C.L., Bischoff, E.D., Petrowski, M., Jepsen, K., Baek, S.H., Heyman, R.A., Rosenfeld, M.G., et al. (2003). Promoter-specific roles for liver X receptor/corepressor complexes in the regulation of ABCA1 and SREBP1 gene expression. Mol. Cell. Biol. *23*, 5780–5789.

Wang, Z., Zhou, S., Sun, C., Lei, T., Peng, J., Li, W., Ding, P., Lu, J., and Zhao, Y. (2014). Interferon-γ inhibits nonopsonized phagocytosis of macrophages via an mTORC1-c/EBPβ pathway. J. Innate Immun. *7*, 165–176.

Yin, H., van der Veer, E., Frontini, M.J., Thibert, V., O'Neil, C., Watson, A., Szasz, P., Chu, M.W.A., and Pickering, J.G. (2012). Intrinsic directionality of migrating vascular smooth muscle cells is regulated by NAD(+) biosynthesis. J. Cell Sci. *125*, 5770–5780.

Publication 2

Research article:

A new role for Zinc limitation in bacterial pathogenicity: Modulation of α-hemolysin from uropathogenic Escherichia coli

Velasco E, Wang S, Sanet M, Fernández-Vázquez J, Jové D, **Glaría E**, Valledor A. F., O'Halloran TV, and Balsalobre C.

April 2018

Scientific Reports, 8(1), 6535.

doi: 10.1038/s41598-018-24964-1

Impact factor: 4.011

SCIENTIFIC REPORTS

OPEN

A new role for Zinc limitation in bacterial pathogenicity: modulation of α-hemolysin from uropathogenic *Escherichia coli*

Received: 21 September 2017
Accepted: 9 April 2018
Published online: 25 April 2018

Elsa Velasco[1], Suning Wang[2], Marianna Sanet[1], Jorge Fernández-Vázquez[1], Daniel Jové[1], Estibaliz Glaría[3], Annabel F. Valledor[3], Thomas V. O'Halloran[2] & Carlos Balsalobre[1]

Metal limitation is a common situation during infection and can have profound effects on the pathogen's success. In this report, we examine the role of zinc limitation in the expression of a virulence factor in uropathogenic *Escherichia coli*. The pyelonephritis isolate J96 carries two *hlyCABD* operons that encode the RTX toxin α-hemolysin. While the coding regions of both operons are largely conserved, the upstream sequences, including the promoters, are unrelated. We show here that the two *hlyCABD* operons are differently regulated. The hly_{II} operon is efficiently silenced in the presence of zinc and highly expressed when zinc is limited. In contrast, the hly_{I} operon does not respond to zinc limitation. Genetic studies reveal that zinc-responsive regulation of the hly_{II} operon is controlled by the Zur metalloregulatory protein. A Zur binding site was identified in the promoter sequence of the hly_{II} operon, and we observe direct binding of Zur to this promoter region. Moreover, we find that Zur regulation of the hly_{II} operon modulates the ability of *E. coli* J96 to induce a cytotoxic response in host cell lines in culture. Our report constitutes the first description of the involvement of the zinc-sensing protein Zur in directly modulating the expression of a virulence factor in bacteria.

During infection, pathogens often encounter metal limitation. Alterations in the concentrations of certain metal ions have a great impact in cell physiology and gene expression. For instance, changes in the concentration of iron regulate the expression of virulence factors through metalloregulatory proteins such as Fur, the ferric uptake regulator, and the closely related PerR, the peroxide-stress regulator[1,2]. Recent studies revealed that another metal ion, zinc, also has an effect on bacterial physiology during infection[3,4]. Zinc is an essential element as a catalytic or structural cofactor of key enzymes and proteins involved in many processes such as DNA replication and protein synthesis and turnover[5,6]. Conversely, zinc can be toxic to bacteria when present in excess and so intracellular levels must be tightly controlled[5,7]. Zinc release from host tissue has been proposed to be an important innate defense mechanism[7]. In the case of *S. pneumoniae* infection in mice, elevated total zinc concentrations have been reported in host tissue and serum samples. The authors propose that the ability of zinc excess to inhibit pathogen growth arises from zinc competition with Mn uptake[7]. Zinc concentration in host fluids can rise in response to bacterial infection and inflammation by its release from damaged or apoptotic cells, and from sequestering proteins such as metallothionein[7].

Studies in both *E. coli* and *B. subtilis* have shown that, in response to variations in zinc concentration, cells regulate gene expression using the metalloregulatory protein Zur (zinc uptake regulator) as a sensor. Zur forms a dimeric complex with zinc acquiring the ability to bind DNA and to repress gene expression[8]. Characterized Zur regulons mainly consist of genes coding for proteins involved in zinc homeostasis and paralogs of ribosomal proteins which, under zinc limitation conditions, replace ribosomal proteins that contain zinc[9]. Although most known Zur-regulated genes are involved in zinc uptake and adaptation to low concentrations of the metal[8–10], a number of questions about how Zur impacts overall cell physiology and pathogenesis remain unanswered.

[1]Department of Genetics, Microbiology and Statistics, School of Biology, Universitat de Barcelona, Avda. Diagonal 643, Barcelona, 08028, Spain. [2]Chemistry of Life Process Institute, and Department of Chemistry, Northwestern University, Evanston, Illinois, 60208-3113, United States of America. [3]Nuclear Receptor Group, Department of Cell Biology, Physiology and Immunology, School of Biology, Universitat de Barcelona, Avda. Diagonal 643, Barcelona, 08028, Spain. Correspondence and requests for materials should be addressed to C.B. (email: cbalsalobre@ub.edu)

Publication 3

Research article:

Expression of a novel class of bacterial Ig-like proteins is required for IncHI plasmid conjugation

Hüttener M, Prieto A, Aznar S, Bernabeu M, **Glaría E**, Valledor A. F., Paytubi S, Merino S, Tomás J, and Juárez A.

September 2018

PLoS Genetics, 15(9), e1008399.

doi: 10.1371/journal.pgen.1008399

Impact factor: 5.224

PLOS GENETICS

RESEARCH ARTICLE

Expression of a novel class of bacterial Ig-like proteins is required for IncHI plasmid conjugation

Mário Hüttener[1], Alejandro Prieto[1], Sonia Aznar[1], Manuel Bernabeu[1], Estibaliz Glaría[2], Annabel F. Valledor[2], Sonia Paytubi[1], Susana Merino[1], Joan Tomás[1], Antonio Juárez[1,3]*

1 Department of Genetics, Microbiology and Statistics, University of Barcelona, Barcelona, Spain, **2** Department of Cell Biology, Physiology and Immunology, University of Barcelona, Barcelona, Spain, **3** Institute for Bioengineering of Catalonia, The Barcelona Institute of Science and Technology, Barcelona, Spain

* ajuarez@ub.edu

Citation: Hüttener M, Prieto A, Aznar S, Bernabeu M, Glaría E, Valledor AF, et al. (2019) Expression of a novel class of bacterial Ig-like proteins is required for IncHI plasmid conjugation. PLoS Genet 15(9): e1008399. https://doi.org/10.1371/journal.pgen.1008399

Editor: Diarmaid Hughes, Uppsala University, SWEDEN

Received: June 14, 2019

Accepted: September 4, 2019

Published: September 17, 2019

Data Availability Statement: All relevant data are within the manuscript and its Supporting Information files.

Funding: A.P. was the recipient of a FPU fellowship from the Ministerio de Educación, Cultura y Deporte. M.B. was the recipient of a FI Fellowship from the Generalitat de Catalunya. E.G. received a fellowship from the University of Barcelona (APIF). This work was supported by grants CSD2008-00013 from Ministerio de Ciencia y Tecnología, BIO2016-76412-C2-1-R (AEI/FEDER, UE) from

Abstract

Antimicrobial resistance (AMR) is currently one of the most important challenges to the treatment of bacterial infections. A critical issue to combat AMR is to restrict its spread. In several instances, bacterial plasmids are involved in the global spread of AMR. Plasmids belonging to the incompatibility group (Inc)HI are widespread in *Enterobacteriaceae* and most of them express multiple antibiotic resistance determinants. They play a relevant role in the recent spread of colistin resistance. We present in this report novel findings regarding IncHI plasmid conjugation. Conjugative transfer in liquid medium of an IncHI plasmid requires expression of a plasmid-encoded, large-molecular-mass protein that contains an Ig-like domain. The protein, termed RSP, is encoded by a gene (ORF *R0009*) that maps in the Tra2 region of the IncHI1 R27 plasmid. The RSP protein is exported outside the cell by using the plasmid-encoded type IV secretion system that is also used for its transmission to new cells. Expression of the protein reduces cell motility and enables plasmid conjugation. Flagella are one of the cellular targets of the RSP protein. The RSP protein is required for a high rate of plasmid transfer in both flagellated and nonflagellated *Salmonella* cells. This effect suggests that RSP interacts with other cellular structures as well as with flagella. These unidentified interactions must facilitate mating pair formation and, hence, facilitate IncHI plasmid conjugation. Due to its location on the outer surfaces of the bacterial cell, targeting the RSP protein could be a means of controlling IncHI plasmid conjugation in natural environments or of combatting infections caused by AMR enterobacteria that harbor IncHI plasmids.

Author summary

Dissemination of antimicrobial resistance (AMR) among different bacterial populations occurs due to mainly the presence of plasmids that encode AMR determinants. IncHI

Publication 4

Book chapter:

Methods for assessing the effects of LXR agonists on macrophage bacterial infection

Glaría, E., Matalonga, J., and Valledor, A. F.

March 2019

Methods in Molecular Biology, vol 1951, 135-141.

doi: 10.1007/978-1-4939-9130-3_10

Chapter 10

Methods for Assessing the Effects of LXR Agonists on Macrophage Bacterial Infection

Estibaliz Glaría, Jonathan Matalonga, and Annabel F. Valledor

Abstract

Macrophages are phagocytic cells that actively engulf and kill microorganisms within a specialized phagolysosomal system. Several pathogenic bacteria, however, actively co-opt host mechanisms and escape from microbial digestion to establish intracellular replication within macrophages. This chapter highlights detailed protocols to measure the effects of the LXR pathway on bacterial infection of murine bone marrow-derived macrophages.

Key words LXR, Macrophage, Bacteria, Infection

1 Introduction

Macrophages play essential roles in the immune response against pathogens. Upon recognition of pathogen-associated molecular patterns and/or opsonins, they internalize microorganisms, including bacterial cells, through phagocytosis. After engulfment, macrophages kill and digest the internalized material within the phagolysosomal system [1]. Although a wide range of microorganisms are successfully eliminated by phagocytes, several pathogenic bacteria have developed strategies, including the capability to actively invade host cells and escape from microbial digestion within phagolysosomes, to survive within the host. Paradoxically, despite harboring an arsenal of microbicidal tools, macrophages represent a cellular compartment in which many pathogens establish for intracellular replication and subsequent dissemination [2]. As an example, *Salmonella enterica* serovar Typhimurium (*S.* Typhimurium) actively promotes its own uptake by macropinocytosis through the use of a type III secretion system that allows the bacterium to inject effectors that target the host cell cytoskeleton [3]. Later on, the bacterium is able to modify the phagosome transforming it into a *Salmonella*-containing vacuole that supports

Matthew C. Gage and Inés Pineda-Torra (eds.), *Lipid-Activated Nuclear Receptors: Methods and Protocols*, Methods in Molecular Biology, vol. 1951, https://doi.org/10.1007/978-1-4939-9130-3_10,

bacterial cell survival and replication. Infection and intracellular survival in macrophages is required for full virulence of *S.* Typhimurium in vivo [4].

Nuclear receptors are a family of ligand-activated transcription factors that control many aspects of physiology. Within this family, liver X receptors (LXRs) are activated by specific oxidized forms of cholesterol (oxysterols) and intermediaries of cholesterol biosynthesis to subsequently regulate the expression of genes involved in lipid and glucose homeostasis and in immune responses [5, 6]. Two LXR isoforms have been described (LXRα and β), and each of them forms heterodimers with retinoid X receptors (RXRs) to positively modulate target gene expression. Recent work from our group has identified a molecular mechanism by which LXR agonists interfere with the capability of *S.* Typhimurium to infect murine macrophages [7]. This mechanism involves transcriptional activation of the NADase CD38, which translates in reduced intracellular NAD+ levels and interferes with pathogen-induced changes in the F-actin cytoskeleton, limiting the capability of non-opsonized *Salmonella* to infect macrophages.

In this chapter we describe in detail protocols based on the use of flow cytometry and confocal microscopy to measure the effects of the LXR pathway on infection of murine bone marrow-derived macrophages by an invasive *S.* Typhimurium strain.

2 Materials

All the materials must be sterile and endotoxin-free.

1. LXR agonists: T0901317, GW3965, and 25-hydroxycholesterol.
2. RXR agonist: LG100268.
3. Dimethyl sulfoxide (DMSO).
4. High-glucose DMEM with L-glutamine and without sodium pyruvate.
5. Fetal bovine serum (FBS).
6. Phosphate-buffered saline (PBS) without calcium/magnesium.
7. Bacterial liquid growth medium 2xYT: 1.6% Bacto tryptone, 1% Bacto yeast extract, 0.5% NaCl, pH 7.
8. Bacterial liquid growth medium Super Optimal Broth (SOB): 2% Bacto tryptone, 0.5% Bacto yeast extract, 10 mM NaCl, 2.5 mM KCl, 10 mM $MgCl_2$, 10 mM $MgSO_4$, pH 7.
9. Ampicillin.

10. Transformation buffer 1: 0.1 M RbCl, 50 mM $MnCl_2{\cdot}4H_2O$, 30 mM KAc, 10 mM $CaCl_2{\cdot}2H_2O$, 10% glycerol, pH 5.8.
11. Transformation buffer 2: 0.2 M MOPS, 10 mM RbCl, 75 mM $CaCl_2{\cdot}2H_2O$, 12% glycerol, pH 6.8.
12. 100 mL and 1 L Erlenmeyer flasks.
13. Tissue culture plates (6-well and 24-well).
14. Cell scrapper.
15. 50 mL polypropylene tubes.
16. 1.5 mL polypropylene microtubes.
17. Centrifuge.
18. Hemacytometer.
19. Liquid bath.
20. Incubator at 37 °C.
21. Humidified incubator at 37 °C, 5% CO_2.
22. Horizontal shaker.
23. Petri dishes containing solid LB agar.
24. Bunsen burner.
25. L-Shaped glass spreader.
26. 75% ethanol.
27. Spectrophotometer.
28. Paraformaldehyde (PFA) 1% and 4% in PBS, prepared fresh.
29. Wheat germ agglutinin (WGA) conjugated to Alexa Fluor 488.
30. DAPI (1 μg/mL).
31. Mounting medium.
32. Microscopy slides and coverslips.
33. Milli-Q H_2O.
34. Flow cytometer (equipped with an excitation red laser (561 nm) and fluorescence detector at 610/20 nm).
35. Confocal microscope (equipped with lasers exciting at 405 nm, 488 nm, and 561 nm wavelengths).

3 Methods

All the steps before sample processing must be carried out under sterile conditions.

3.1 Macrophage Plating and Culture

1. Murine bone marrow-derived macrophages should be generated as described [8].
2. Plate macrophages using the following indications:

3.1.1 For Flow Cytometry

1. Plate 1.5×10^6 macrophages per well in 6-well plates with 2 mL of DMEM-10% FBS, and allow them to attach for 2 h in a humidified incubator at 37 °C, 5% CO_2.

3.1.2 For Confocal Microscopy

1. Plate 2×10^5 macrophages per well in 24-well plates containing UV-sterilized coverslips. Cover the cells with 1 mL of DMEM-10% FBS, and allow them to attach for 2 h in a humidified incubator at 37 °C, 5% CO_2.

3.2 Treatment with LXR/RXR Agonists

1. Prepare a stock solution of LXR (or RXR) agonist (1–10 mM in DMSO). Store stock at −80 °C.
2. Once the cells have attached to the plates, add LXR/RXR agonists at 1 μM each for the desired period of time (*see* **Note 1**). Culture cells in a humidified incubator at 37 °C, 5% CO_2. For control samples, incubate the cells with DMSO (vehicle) at the same dilution than the one in the samples treated with ligands.

3.3 Obtention of Bacterial Cells Expressing Red Fluorescent Protein (RFP)

This protocol shows steps used for the generation of fluorescent *S.* Typhimurium strain SL1344. To avoid contamination by other microorganisms, perform all the steps next to a Bunsen burner or inside a biological safety cabinet with laminar flow.

3.3.1 Prepare Competent Bacterial Cells for Heat Shock Transformation

1. Inoculate a bacterial colony in a 100 mL Erlenmeyer flask containing 30 mL of SOB.
2. Grow bacteria overnight at 37 °C with horizontal shaking at 250 rpm.
3. Subculture the cells in a 1 L Erlenmeyer flask using a 1:50 dilution in 100 mL of SOB.
4. Grow bacteria at 37 °C with horizontal shaking at 250 rpm until the optical density of the culture at 600 nm (OD_{600}) reaches 0.45 (mid-log phase).
5. Distribute the volume to four 50 mL Falcon tubes and keep them on ice for 15 min.
6. Centrifuge for 15 min at 3000 × *g*, 4 °C to pellet the bacterial cells.
7. Remove supernatants, and resuspend bacterial cell pellets in 10 mL of transformation buffer 1.
8. Centrifuge for 15 min at 3000 × *g*, 4 °C.
9. Remove supernatants and resuspend in 4 mL of transformation buffer 2.
10. Prepare 500 μL aliquots and freeze at −80 °C.

3.3.2 Transform S. *Typhimurium Strain SL1344 with pBR.RFP.1 Plasmid Encoding Red Fluorescent Protein (RFP) [9] (See* **Note 2***) by Heat Shock*

1. Mix 100 µL of competent bacteria with 1–10 ng of supercoiled plasmid DNA. For the negative control, use H_2O instead of plasmid DNA.
2. Keep on ice for 30 min.
3. Perform the heat shock at 42 °C for 1.5 min (in a liquid bath).
4. Put the cells on ice for 5 min.
5. Add 2xYT medium up to 1 mL, and grow the transformed bacterial cells in a 1.5 mL microtube for 1 h at 37 °C with horizontal shaking at 250 rpm.
6. Plate 50 µL bacterial growth onto LB agar plates supplemented with 100 µg/mL ampicillin, and allow the colonies to grow for 15 h at 37 °C.

3.4 Bacterial Cell Growth

1. Pick a bacterial colony with a sterile pipette tip, and transfer it to a 50 mL tube containing 10 mL 2xYT medium supplemented with 100 µg/mL ampicillin. To obtain a saturated culture, let the bacteria grow for at least 16 h at 37 °C with horizontal shaking at 250 rpm.
2. Once at saturation ($OD_{600} = 2$), dilute the bacterial cell culture 1:100 by transferring 100 µL to a new 50 mL tube with 10 mL 2xYT, and culture it at 37 °C, 250 rpm for 2–3 h (at this time bacterial growth would be in log phase, and bacterial cells would express optimal levels of effectors for invasion).
3. Measure the OD_{600} of the bacterial cell culture using a spectrophotometer, and estimate the bacterial cell concentration using a standard curve (*see* **Note 3**).

3.5 Macrophage Infection

1. Add bacteria to the macrophage culture at the desired multiplicity of infection (MOI) (*see* **Note 4**). Let the infection occur for 30 min in an incubator at 37 °C, 5% CO_2. Also include two types of controls: (a) negative control (noninfected cells) and (b) control for attachment without engulfment (macrophages are incubated with the bacteria for 30 min at 4 °C).
2. Place the plates on ice to stop infection and bacterial replication. Remove culture media, and wash the cells three times with 2 mL of ice-cold PBS to remove non-internalized bacteria.

3.6 Process the Cells for the Analysis of Infection

3.6.1 Analysis by Flow Cytometry

1. Scrape cells in 1 mL PBS and transfer them to 1.5 mL microtubes.
2. Centrifuge for 5 min at 200 × *g*, 4 °C to pellet the cells.
3. Remove supernatant, and fix the cells in 150 µL 1% PFA for 30 min at room temperature.
4. To measure infection, analyze RFP fluorescence in macrophages by flow cytometry using a 561 nm laser for excitation and a 610/20 nm filter for the detection of emission. Check

bacterial cell fluorescence by comparing it to a negative control (bacterial cells not transformed with an RFP encoding plasmid).

3.6.2 Analysis by Confocal Microscopy

1. Fix cells on coverslips (inside the cell culture plates) with 300 µL 4% PFA for 30 min at room temperature.
2. Wash cells with 1 mL PBS.
3. Stain cell membranes with 2.5 µg/mL fluorescent WGA for 30 min at room temperature.
4. Stain nuclei with 1 µg/mL DAPI for 5 min at room temperature.
5. Wash cells twice for 5 min with 1 mL PBS.
6. Wash cells with 1 mL mQ H_2O.
7. Plate coverslips on microscopy slides with a drop of mounting medium (follow recommendations for the specific mounting medium).
8. Store samples in the dark at 4 °C until subsequent analysis by confocal microscopy (*see* **Note 5**).
9. For each fluorochrome, collect serial 1 µm *z*-axis optical images from whole cells using a 63× objective. Use the following lasers: 405 nm (DAPI, nuclei), 488 nm (WGA-Alexa Fluor 488, membranes), and 561 nm (RFP, bacteria).

3.7 Estimation of MOI After the Infection

1. Make dilutions of bacterial culture in 1.5 mL microtubes with 2xYT (*see* **Note 6**).
2. Dispense 100 µL of each dilution on LB agar plates (in duplicates), and incubate overnight at 37 °C.
3. Count colonies to calculate the exact MOI used in the experiment.

4 Notes

1. LXRs form heterodimers with RXRs to activate transcription of their target genes. Agonists for both nuclear receptors can be used (1 µM each) to obtain synergistic effects on induction of gene expression.
2. Transformation with a plasmid which, in addition to fluorescence, confers antibiotic resistance enables the selection of bacteria of interest and avoids contamination by other bacteria. When using antibiotic-resistant colonies, antibiotics should be added to the solid LB agar plates and to the bacterial growth medium.

3. To obtain a standard curve, make serial dilutions of a saturated bacterial cell culture ranging from the original concentration to 1:100 dilution (e.g., 1:2, 1:4, 1:10, 1:100). Measure OD_{600} and dispense 100 μL of each dilution on solid LB agar plates. Incubate the plates with bacteria overnight at 37 °C. Then count colonies to calculate the bacterial cell concentration, and generate the standard curve by plotting cell concentration vs absorbance.
4. At MOI 5–10, invasive *Salmonella* will infect 10–40% macrophages within 30 min, and a reduction of infection by LXR agonists can be detected.
5. For optimal results, analysis of infection by confocal microscopy should be performed no longer than 2 weeks after sample preparation.
6. Despite the fact that an estimation of the bacterial MOI is performed before the infection based on the OD_{600} of the bacterial growth, it is recommended to calculate the exact MOI used in each experiment by plating bacterial cell dilutions on LB agar plates. Usually, dilutions 10^{-6} to 10^{-7} work best for subsequent counting of viable bacterial colonies on plates.

Acknowledgments

This work was supported by a grant from the Spanish Ministry of Economy and Competitivity (SAF2017-89510-R) to A.F. Valledor. Estibaliz Glaría is supported by a fellowship from the University of Barcelona (Ajuts de Personal Investigador predoctoral en Formació, APIF).

References

1. Flannagan RS, Cosío G, Grinstein S (2009) Antimicrobial mechanisms of phagocytes and bacterial evasion strategies. Nat Rev Microbiol 7:355–366
2. Price JV, Vance RE (2014) The Macrophage Paradox. Immunity 41:685–693
3. Guiney DG, Lesnick M (2005) Targeting of the actin cytoskeleton during infection by Salmonella strains. Clin Immunol 114:248–255
4. Haraga A, Ohlson MB, Miller SI (2008) Salmonellae interplay with host cells. Nat Rev Microbiol 6:53–66
5. Hong C, Tontonoz P (2014) Liver X receptors in lipid metabolism: opportunities for drug discovery. Nat Rev Drug Discov 13:433–444
6. Pascual-García M, Valledor AF (2012) Biological roles of liver x receptors in immune cells. Arch Immunol Ther Exp 60:235–249
7. Matalonga J, Glaria E, Bresque M et al (2017) The Nuclear Receptor LXR Limits Bacterial Infection of Host Macrophages through a Mechanism that Impacts Cellular NAD Metabolism. Cell Rep 18:1241–1255
8. Valledor AF, Comalada M, Xaus J et al (2000) The differential time-course of extracellular-regulated kinase activity correlates with the macrophage response toward proliferation or activation. J Biol Chem 275:7403–7409
9. Birmingham CL, Smith AC, Bakowski MA et al (2006) Autophagy controls Salmonella infection in response to damage to the Salmonella-containing vacuole. J Biol Chem 281:11374–11383

Publication 5

Review article:

MDSCs in infectious diseases: regulation, roles, and readjustment

Dorhoi A, **Glaría E**, Garcia-Tellez T, Nieuwenhuizen NE, Zelinskyy G, Favier B, Singh A, Ehrchen J, Gujer C, Münz C, Saraiva M, Sohrabi Y, Sousa AE, Delputte P, Müller-Trutwin M, and Valledor A. F.

April 2019

Cancer Immunology, Immunotherapy, 68(4), 673–685.

doi: 10.1007/s00262-018-2277-y

Impact factor: 5.442

Cancer Immunology, Immunotherapy (2019) 68:673–685
https://doi.org/10.1007/s00262-018-2277-y

SYMPOSIUM-IN-WRITING PAPER

MDSCs in infectious diseases: regulation, roles, and readjustment

Anca Dorhoi[1,2,3] · Estibaliz Glaría[4,5] · Thalia Garcia-Tellez[6] · Natalie E. Nieuwenhuizen[3] · Gennadiy Zelinskyy[7] · Benoit Favier[8] · Anurag Singh[9] · Jan Ehrchen[10] · Cornelia Gujer[11] · Christian Münz[11] · Margarida Saraiva[12,13] · Yahya Sohrabi[14,15] · Ana E. Sousa[16] · Peter Delputte[17] · Michaela Müller-Trutwin[6] · Annabel F. Valledor[4,5]

Received: 20 February 2018 / Accepted: 29 October 2018 / Published online: 19 December 2018

Abstract

Many pathogens, ranging from viruses to multicellular parasites, promote expansion of MDSCs, which are myeloid cells that exhibit immunosuppressive features. The roles of MDSCs in infection depend on the class and virulence mechanisms of the pathogen, the stage of the disease, and the pathology associated with the infection. This work compiles evidence supported by functional assays on the roles of different subsets of MDSCs in acute and chronic infections, including pathogen-associated malignancies, and discusses strategies to modulate MDSC dynamics to benefit the host.

Keywords Myeloid regulatory cells · MDSC · Infection · Immunosuppression · Oncogenic viruses · Mye-EUNITER

Abbreviations

Arg	Arginase
Arm	Armstrong
ATRA	All-trans retinoic acid
B. fragilis	*Bacteroides fragilis*
C. albicans	*Candida albicans*
C13	Clone 13
CCR	C-C Chemokine receptor
COST	European Cooperation in Science and Technology
EBV	Epstein Barr virus
ETBF	Enterotoxigenic *Bacteroides fragilis*
FV	Friend virus
H. felis	*Helicobacter felis*
H. polygyrus	*Heligmosomoides polygyrus*
HbsAg	HBV surface antigen
HDT	Host-directed therapy
IAV	Influenza A virus
iNKT	Invariant NK T
JEV	Japanese encephalitis virus
K. pneumoniae	*Klebsiella pneumoniae*
L. major	*Leishmania major*
LCMV	Lymphocytic choriomeningitis virus
LOX	Lipoxygenase
Mφ	Macrophage
M-MDSC	Monocytic MDSC
M. tuberculosis	*Mycobacterium tuberculosis*
MR	Mannose receptor
MRC	Myeloid regulatory cell
mTOR	Mammalian target of rapamycin
NADPH	Nicotinamide adenine dinucleotide phosphate
NOS	NO synthase
P. aeruginosa	*Pseudomonas aeruginosa*
PcP	*Pneumocystis* pneumonia
PDE	Phosphodiesterase
PGE2	Prostaglandin E2
PMN-MDSC	Neutrophil-like MDSC
ROS	Reactive oxygen species
S. aureus	*Staphylococcus aureus*
SIV	Simian immunodeficiency virus
T. crassiceps	*Taenia crassiceps*
T. cruzi	*Trypanosoma cruzi*
T. gondii	*Toxoplasma gondii*
TB	Tuberculosis
Tfh	T Follicular helper

Electronic supplementary material The online version of this article (https://doi.org/10.1007/s00262-018-2277-y) contains supplementary material, which is available to authorized users.

✉ Anca Dorhoi
anca.dorhoi@fli.de

✉ Annabel F. Valledor
afernandezvalledor@ub.edu

Extended author information available on the last page of the article

Publication 6

Review article:

Roles of CD38 in the Immune Response to Infection

Glaría E and Valledor A. F.

January 2020

Cells, 9(1), 228.

doi: 10.3390/cells9010228

Impact factor: 4.829

cells

MDPI

Review

Roles of CD38 in the Immune Response to Infection

Estibaliz Glaría and Annabel F. Valledor *

Department of Cell Biology, Physiology and Immunology, School of Biology, University of Barcelona, and Institute of Biomedicine of the University of Barcelona (IBUB), 08028 Barcelona, Spain; estiglari@gmail.com

* Correspondence: afernandezvalledor@ub.edu; Tel.: +34-93-4039384

Received: 26 November 2019; Accepted: 14 January 2020; Published: 16 January 2020

Abstract: CD38 is a multifunctional protein widely expressed in cells from the immune system and as a soluble form in biological fluids. CD38 expression is up-regulated by an array of inflammatory mediators, and it is frequently used as a cell activation marker. Studies in animal models indicate that CD38 functional expression confers protection against infection by several bacterial and parasitic pathogens. In addition, infectious complications are associated with anti-CD38 immunotherapy. Although CD38 displays receptor and enzymatic activities that contribute to the establishment of an effective immune response, recent work raises the possibility that CD38 might also enhance the immunosuppressive potential of regulatory leukocytes. This review integrates the current knowledge on the diversity of functions mediated by CD38 in the host defense to infection.

Keywords: CD38; CD157; immune response; infection

1. Introduction

The immune system is composed of a tightly regulated network of cells and molecules that cooperate to protect the organism from a diversity of dangerous agents. Compartmentalization of the immune system guarantees constant monitoring of tissues and controlled activation of the immune response to eliminate pathogens and other harmful agents and return to homeostasis. The innate immune system is essential for the initial containment of pathogens. Professional phagocytes such as macrophages and neutrophils are recruited toward the infection site to engulf and kill microorganisms. Dendritic cells internalize exogenous agents and migrate to the lymph nodes to trigger activation of the adaptive immune system. Upon activation by antigen presentation through major histocompatibility complexes (MHC), T cells either execute cytolysis on target infected cells (cytolytic T cells) or secrete cytokines to further modulate the type of immune response (helper T cells, Th). In addition, B cells can detect antigens on pathogens and differentiate to antibody-producing plasma cells [1].

CD38 is a multifunctional transmembrane protein that is widely expressed in immune cells. In lymphocytes, monocytes, macrophages, dendritic cells, granulocytes, and natural killer (NK) cells, the expression levels of CD38 on the cell surface depend on the stage of maturation and/or activation of the cell (reviewed in [2]). Since its discovery almost four decades ago [3], accumulated evidence indicates that CD38 plays important roles in various cell types in both physiological and pathological contexts. Early studies suggested that human CD38 can establish lateral associations with various membrane proteins/complexes, such as CD16 (in NK cells), the T cell receptor (TCR)/CD3 complex and CD4 (in T cells), membrane immunoglobulin (Ig) and the B cell co-receptor complex (CD19/CD81) (in B lymphocytes), and class II MHC (in monocytes) [4–6]. On the basis of such interactions, CD38 was proposed to potentially contribute to cell signaling from these complexes. In agreement with this notion, and despite the fact that CD38 contains a short cytoplasmic domain without signaling motifs, CD38 relocalized at the immunologic synapse in T cells upon TCR engagement, contributing to modulation of antigen-mediated T-cell responses [7]. In the same line, CD38 crosslinking decreased

the threshold for B cell activation via the B-cell receptor (BCR) [8], suggesting its participation in BCR signaling. Human CD38 was also shown to bind a specific nonsubstrate ligand, CD31/PECAM-1, a member of the Ig superfamily that is highly expressed on the surface of different cell types, including endothelial cells [9]. Interference with CD38–CD31 interaction inhibited lymphocyte adhesion to endothelial cells.

In addition to receptor or co-receptor functions, CD38 also plays multiple roles derived from intrinsic enzymatic activities. At neutral pH, CD38 converts nicotinamide adenine dinucleotide (NAD) into ADP ribose (ADPR), cyclic ADPR (cADPR) and nicotinamide, whereas at acidic pH, CD38 uses NAD phosphate (NADP) to generate nicotinic acid adenine dinucleotide phosphate [10,11]. The enzymatic products of these reactions are calcium-mobilizing second messengers with relevant signaling consequences in diverse cellular contexts. Because the generation of ADPR and cADPR requires large consumption of NAD, CD38 is considered the major NAD glycohydrolase (NADase) in mammalian tissues [12]. In addition, CD38 can also catabolize the extracellular NAD^+ precursors nicotinamide mononucleotide and nicotinamide riboside before they are transported into the cell for NAD^+ biosynthesis [13].

The consequences of CD38 expression depend also on the ultrastructural configuration of the molecule and its location within the cell (reviewed in [14]). CD38 has been shown to exist as either monomeric [15], dimeric or even multimeric type II forms [16,17], displaying the catalytic site outside of the cell, and as a type III form with the catalytic site facing the cytoplasm [18]. Moreover, an intracellular pool of CD38 has been shown to be associated to mitochondrial and nuclear membranes (reviewed in [19]). In these configurations, CD38 could have access to both extracellular and intracellular NAD^+. In addition, CD38 also exists as a soluble form, which is detectable in biological fluids [20].

Because of its abundant expression in immune cells, several studies have focused on the roles of CD38 in the immune response to infection. Both in vivo and in vitro models have been used in combination with CD38 deficiency, ligating/blocking antibodies or agonists/antagonists of CD38 activities in order to decipher the effects of CD38 in different cell types and infection settings. The aim of the present review is to provide an updated overview on the diversity of functions mediated by CD38 in the context of the host defense to infection.

2. CD38 Deficiency Results in Increased Susceptibility to Several Pathogens

Pathogenic bacteria are causative agents for a wide spectrum of infectious diseases. Bacterial infection causes tissue damage through different mechanisms, including the killing of infected host cells, the secretion of toxins and the induction of an exacerbated inflammatory response [21]. In vivo studies demonstrated that CD38 deficiency in mice conferred increased susceptibility to infection by several bacteria, namely *Listeria monocytogenes* (*L. monocytogenes*) [22], *Mycobacterium avium* (*M. avium*) [23] and *Streptococcus pneumoniae* (*S. pneumoniae*) [24,25], and the parasite *Entamoeba histolytica* (*E. histolytica*) [26].

In addition, CD38 was recently shown to be a transcriptional target of the nuclear receptor liver X receptor (LXR), which is activated by derivatives of cholesterol metabolism [27,28]. Pharmacological treatment with a synthetic LXR agonist ameliorated the clinical severity of *Salmonella* Typhimurium (*S.* Typhimurium)-infected mice and reduced the dissemination of the bacteria to the spleen in a CD38-dependent manner. Of note, the expression of CD38 in bone marrow-derived cells was required for the ameliorating effects of the LXR agonist [27].

Altogether, the observations in animal models indicate the importance of CD38 in the control of infection, raising its potential interest as a target for host-directed therapy against infection. An overview of mechanisms associated with the multifaceted nature of CD38 that modulate the establishment of an effective immune response is provided in the following sections.

3. CD38 Contributes to Pro-Inflammatory Phenotypes in Innate Immune Cells

Pathogens that overcome natural barriers of the body can be subsequently recognized by innate immune cells. Macrophages, neutrophils and dendritic cells detect pathogen-associated molecular

patterns (PAMPs) through specialized receptors and initiate signaling cascades that lead to phagocytosis and production of inflammatory mediators [1].

Pro-inflammatory cytokines produced by the host, such as tumor necrosis factor alpha and interferon gamma (IFNγ), or the bacterial component lipopolysaccharide (LPS) induced the expression of CD38 in murine and human macrophages [22,27,29–32] and during maturation of dendritic cells [28,33]. Reciprocally, accumulated evidence suggests that CD38 helps sustain classical activation of macrophages and dendritic cells (Figure 1). In this sense, CD38 signaling upon ligation by monoclonal antibodies induced cytokine secretion in resting human monocytes [34] and enhanced interleukin (IL)-12 production in synergy with IFNγ in human dendritic cells [33]. The effects on monocytes were also observed upon CD38 interaction with CD31 [34]. Furthermore, the lack of functional CD38 expression or the selective interference with its receptor or enzymatic activities in myeloid cells resulted in reduced production of pro-inflammatory mediators in response to LPS [35,36] or to bacterial [27] or viral infection [37]. In macrophages, these effects correlated with inhibition of the activation of the NFκB signaling pathway [36].

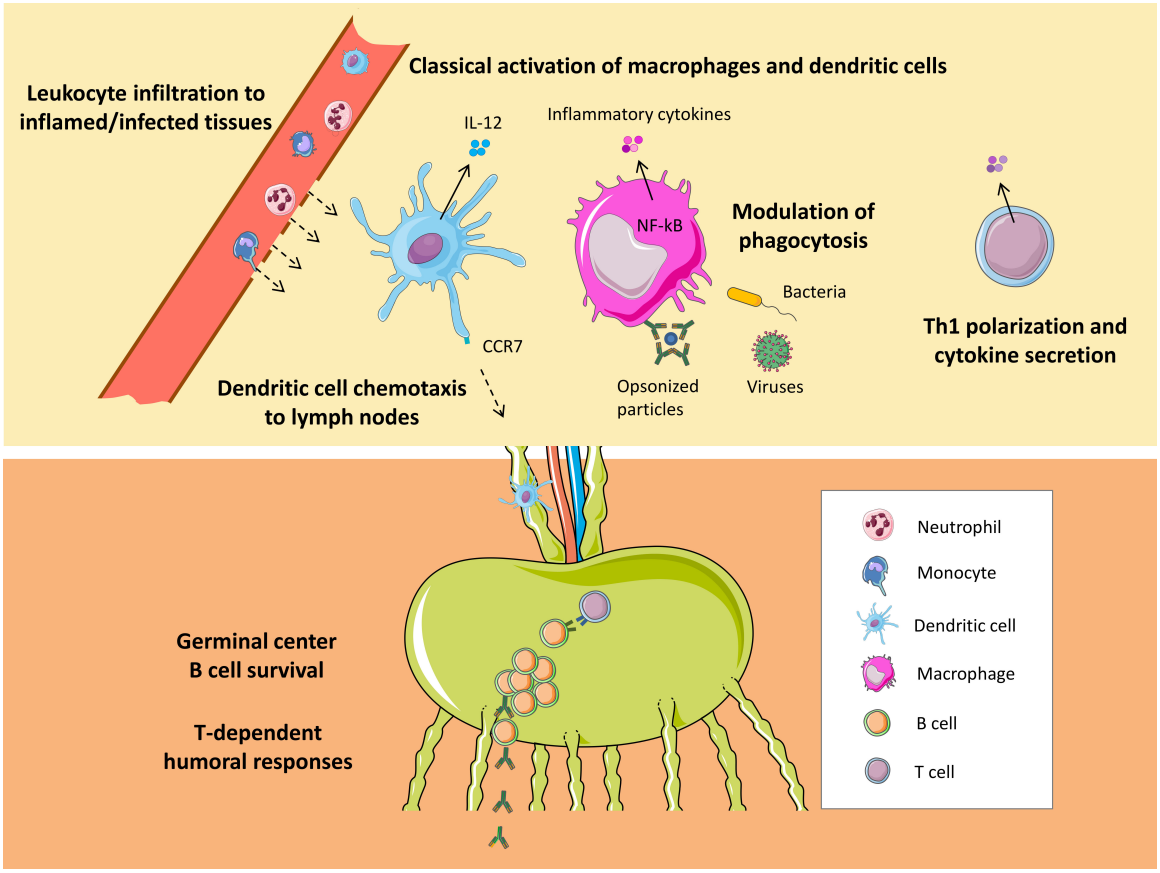

Figure 1. Summary of immunological roles of CD38 in the response to infection. Steps of the immune response to pathogens for which there are solid data involving the participation of CD38. Some elements in the image have been obtained from Smart Servier Medical Art.

4. CD38 Enzymatic Activities Regulate Leukocyte Infiltration to Infected/Inflamed Tissues

Several inflammatory mediators, including cytokines and chemokines, increase vascular permeability to facilitate sequential recruitment of immune cell types toward the site of infection [38]. Furthermore, molecules released by infectious agents are also recognized as chemoattractant signals for a number of infiltrating cells [39].

In addition to a direct role of CD38 signaling on pro-inflammatory myeloid cell activation, the enzymatic activities of CD38 and the subsequent generation of calcium-mobilizing second

messengers are important for the recruitment of different leukocytes toward a number of chemotactic signals produced at the site of infection [24,40,41] (Figure 1). A decrease in neutrophil accumulation in *S. pneumoniae*-infected lungs was reported in mice lacking functional CD38 expression, in correlation with reduced in vitro migration of CD38-deficient neutrophils to the chemoattractant formylmethionyl-leucyl-phenylalanine [24,25]. Likewise, CD38 deficiency resulted in lower infiltration of innate leukocytes in the liver and spleen of *Listeria*-infected mice [22] and in delayed recruitment of neutrophils to livers infected with the parasite *E. histolytica* [26]. The intracellular calcium rise and the chemotactic response of murine neutrophils to formyl peptide receptor ligands was inhibited by the cADPR and ADPR antagonists 8-Br-cADPR and 8-Br-ADPR, respectively [40]. Similar results were obtained upon treatment with a NAD^+ analog, $N(8Br\text{-}A)D^+$, which can be converted to 8-Br-cADPR by the ADP-ribosyl cyclase activity of CD38. Furthermore, antagonistic analogs of cADPR and ADPR also blocked the chemotaxis of other leukocytes of human and murine origin to multiple chemoattractant signals, including inflammatory chemokines [40,41].

5. Multifaceted Roles of CD38 in Phagocytosis

Within infected tissues, phagocytosis is a major mechanism used by professional phagocytes to eliminate pathogens and dead cells [42]. Internalized bacteria are then killed and digested in specialized phagolysosomes.

CD38-deficient macrophages displayed impaired capability to phagocytose *L. monocytogenes* in vitro [22]. In experiments in which mice were first infected with *L. monocytogenes* and then injected with fluorescent latex beads, $CD38^+$ inflammatory monocytes and neutrophils recovered from the liver had taken up more beads than their $CD38^-$ counterparts [43], suggesting that CD38 activities could also facilitate unspecific engulfment.

CD38 also positively regulated phagocytosis of latex beads coated with IgG in the absence of PAMPs [44], a mechanism that is mediated by Fcγ receptors. CD38 was shown to be recruited to the forming phagosomes during internalization of IgG-opsonized particles by macrophages, with the catalytic domain oriented to the lumen and correlating with an increase in intracellular cADPR and calcium mobilization. The use of an antagonistic analog of cADPR or peritoneal macrophages from CD38-deficient mice impaired the phagocytosis of IgG-coated latex beads. Noteworthy, the environment usually found during the primary response to infection includes the presence of PAMPs and an inflammatory milieu that might be complemented later with antigen-specific antibodies if the adaptive immune system becomes activated. Thus, the role of CD38 in mediating phagocytosis of IgG-opsonized material might be of particular relevance once the adaptive immune response has generated antibodies against the pathogen (Figure 1).

In contrast with CD38 facilitating the internalization of *L. monocytogenes* and latex beads, treatment of macrophages with an LXR agonist limited the internalization of *S.* Thyphimurium, an effect that was largely dependent on functional CD38 expression [27]. Macrophages sensing *Salmonella* infection underwent both extensive dorsal accumulation of F-actin cytoskeletal structures and morphological changes that might facilitate the entry of invasive bacteria. Once inside, *Salmonella* uses the macrophage as a niche for replication and dissemination (reviewed in [45]). Interestingly, the inhibitory actions of LXR agonists on the internalization of *S.* Thyphimurium were counteracted by abundant NAD^+ levels, but a cADPR antagonist had no significant impact, suggesting that LXR-induced CD38 might contribute to control *Salmonella* infection in macrophages mostly by reducing the levels of NAD^+. In line with this notion, treatment with FK866, a highly specific inhibitor of nicotinamide phosphoribosyltransferase that impacts NAD^+ biosynthesis, resulted in decreased macrophage infection.

6. The Chemotactic Response of Dendritic Cells Is Modulated by CD38 Activity

Myeloid dendritic cells play an important role at the crosstalk between innate and adaptive immune responses. Upon pathogen recognition, they undergo maturation and migrate to draining lymph nodes in order to present antigens and trigger specific T-cell activation [1]. Mature dendritic

cells express a C-C chemokine receptor (CCR)7, which directs migration to lymph nodes following a gradient of the chemokines C-C chemokine ligand (CCL)19 and CCL21 (reviewed in [46]).

Several studies propose the participation of CD38 in dendritic cell chemotaxis mediated by CCR7 (Figure 1), although different mechanisms have been reported in murine and human cells. In this regard, CD38-deficient mice displayed defective migration of dendritic cells to draining lymph nodes and impaired T cell-dependent humoral responses [47]. In vitro, CD38-deficient dendritic cells had an intrinsic inability to mobilize calcium and migrate in response to CCL19 and CCL21, and cADPR antagonism impaired the chemotactic response of dendritic cells to such ligands [28,47]. Interestingly, agonists that activate LXRs enhanced the chemotactic activity of murine dendritic cells toward CCL19, and this activity was largely dependent on functional CD38 expression and cADPR production [28].

In human dendritic cells, CD38 up-regulated chemotaxis to CCR7 ligands in vitro, but this effect was not abrogated by a cADPR antagonist [35]. Although the role of additional CD38-produced calcium-mobilizing second messengers was not tested, antibodies that block CD38–CD31 interaction impaired human dendritic cell chemotaxis. Moreover, in that work, CD38 was shown to co-localize with CCR7, CD83 and CD11b in membrane microdomains known as lipid rafts, suggesting that lateral associations between these proteins could contribute to the migratory activity of human dendritic cells.

7. CD38 Activities in the Adaptive Immune System

An effective adaptive immune response is initiated through antigen recognition and clonal expansion of T and B lymphocytes in secondary lymphoid organs. Mature B cells that are stimulated by antigens and T cell-derived signals proliferate within germinal centers and then differentiate toward either antibody-secreting plasma cells or memory B cells [1]. Because human CD38 is highly expressed on both germinal center B cells and plasma cells, it has been extensively used as a marker of B cell activation (reviewed in [48]). CD38 ligation prevented apoptosis of human germinal center B cells [49], suggesting that CD38 signaling could play a role in the selection of B cells within the germinal center. Interestingly, localization within lipid rafts and association with the CD19 complex were required for CD38-mediated signaling in human B cells [50].

Noteworthy, contrary to the observations in the human system, CD38 was down-regulated in murine germinal center B cells and mature plasma B cells [49]. Despite these discrepancies, CD38-deficient mice showed an impaired humoral response to T-dependent antigens after primary and secondary immunizations [51] (Figure 1). Although defects in innate immune activation and in leukocyte migration could lead to the observed phenotype, several studies have shown that CD38 engagement directly affects B cell responses also in mice. For example, in mature B cells, CD38 crosslinking induced tyrosine phosphorylation-mediated signal transduction, resulting in B cell proliferation and IgM secretion [52]. Moreover, CD38 provided a strong costimulatory proliferative signal to LPS-activated B cells and enhanced the expression of CD86, suggesting that CD38 might also facilitate costimulatory interaction between activated B and helper T cells [53].

Antigenic activation results in the generation of effector T cells that will recirculate from secondary lymphoid organs to sites of infection. Although the receptorial function of CD38 toward CD31 was shown to facilitate human T cell adhesion to endothelial cells [9], and it could be responsible for weak leukocyte binding to the endothelium [54], a role for CD38 in recruitment of effector T cells to sites of infection remains elusive. Evidence suggests, however, that CD38 could modulate inflammatory gene expression in helper T cells as is the case with innate immune cells. In this sense, CD38 ligation in human T lymphocytes in vitro resulted in the secretion of several cytokines, including IFNγ, IL-6, granulocyte-macrophage colony-stimulating factor, and IL-10 [55]. In addition, splenocytes from CD38-deficient mice infected with *M. avium* secreted lower amounts of IFNγ and displayed Th2 polarization, in correlation with their compromised ability to limit mycobacterial burden within granulomata [23].

The involvement of lymphocyte CD38 in the host defense against viruses has been mostly studied in the context of human immunodeficiency virus (HIV) infection. Interestingly, the levels

of CD38 expression associated with prognosis differ depending on the population analyzed (adults *versus* children) (reviewed in [56]). Overexpression of CD38 on lymphocytes is, in fact, a strong predictor of $CD4^+$ T cell depletion in adult HIV-infected individuals (reviewed in [57]). Early after HIV infection, the expression of CD38 increased in $CD4^+$ and $CD8^+$ T lymphocytes [58–60], and high proportions of the $CD8^+CD38^+$ subpopulation were associated with progression to acquired immune deficiency syndrome in adults [61,62]. In cross-sectional studies, a marked decline in the abundance of $CD8^+$ T cells expressing CD38 was detected in patients on stable antiretroviral treatment [63]. Moreover, high levels of CD38 expression on $CD4^+$ T cells was also a marker of poor prognosis in adult HIV-infected individuals [64,65]. In contrast to the evidences in adults, high frequencies of $CD8^+CD38^+$ or $CD4^+CD38^+$ T cells in children were associated with favorable prognoses [66,67].

Several studies have tried to understand the functional role of CD38 in HIV infection. In different human $CD4^+$ T cell lines, the levels of CD38 expression correlated negatively with viral loads and HIV-1-induced cell death [68,69]. In addition, nicotinamide, a major product of CD38 activity, reduced the rates of HIV-1-induced cell death in $CD38^{low}CD4^+$ T cell lines. Together, these studies suggested that CD38 expression could inhibit lymphocyte susceptibility to HIV-1 infection and that its enzymatic activity could be involved in enhancing the survival of infected $CD4^+$ T cells. It was proposed that increased expression of CD38 could mediate recycling of nucleotides and protect from cell death induced by nucleotide depletion [56]. In addition, HIV-1 envelope glycoprotein gp120 enhanced the lateral association between CD38 and CD4 at the cell membrane [4]. Interestingly, human CD38 was shown to inhibit the binding of either purified gp120 or HIV-1 with $CD4^+$ cells [68] by displaying a sequence homologous to the V3 loop of gp120 [70]. These observations suggested that CD38 could play an inhibitory role on HIV-1 attachment to cells by interfering with gp120–CD4 interaction. However, while such a protective role would help explain the association between high CD38 expression levels and favorable prognoses in HIV-infected children, it may not offer an advantage for the control of infection in adults. Indeed, an interesting speculation was provided in [56] by proposing that because T cells displaying high levels of CD38 in adults are mostly activated cells that express chemokine receptors frequently used for viral attachment and entry, the effects of CD38-mediated protection of viral binding to these cells would have a minor impact.

Another aspect to take into account is the fact that gp120 was also shown to promote the dynamic binding of human $CD4^+$ T cells to endothelial cells in vitro, through a mechanism potentially involving CD38–CD31 interaction [71]. In those studies, gp120 increased the homing of a murine T cell line expressing $CD4^+$ into the spleen and intestine and mesenteric lymph nodes, raising the possibility that CD38 could be involved in mediating T cell homing during HIV infection. Nevertheless, despite CD38 overexpression representing a marker of activation and of poor prognosis in HIV infection, whether CD38 enzymatic activities play a role in the pathogenicity of HIV infection in adults remains an open question [57].

Interestingly, in a controlled *Plasmodium falciparum* (*P. falciparum*) infection study in humans, an expansion of $CD38^+CD4^+$ T cells was also detected in the peripheral blood of infected individuals and their frequency inversely correlated with parasite burden [72]. These cells exhibited cytolytic potential and impaired production of IFN-γ, although it was not determined whether CD38 provides an advantage to these cells in the control of *P. falciparum* infection.

8. CD38 in Sepsis

In some cases, the host response to an invading pathogen leads to the development of sepsis, a pathological syndrome with a hyperreactive phase in which exacerbated inflammation causes organ dysfunction followed by immunosuppression [73]. A role for CD38 in LPS-induced acute kidney injury [36] was suggested using quercetin, a dietary flavonoid that inhibits the NADase activity of CD38 [74,75]. Quercetin reduced the infiltration of neutrophils and macrophages in the liver. In line with the role of CD38 in maintenance of a pro-inflammatory phenotype, macrophages that had recovered from quercetin-treated mice had lower levels of NF-kB signaling and inflammatory markers

as compared to macrophages from vehicle-treated mice [36]. Flavonoids, however, may also use protective mechanisms that are independent of CD38 inhibition, as the contributing role of CD38 in tissue damage was not confirmed in CD38-deficient mice [76]. CD38 deficiency aggravated kidney injury upon LPS-induced sepsis, in correlation with increased expression of Toll-like receptor (TLR)4 in the kidney and pro-inflammatory cytokine production. In a separate model of sepsis, induced by cecal ligation in rats, CD38 expression and cADPR production increased in the central nervous system [77]. Blocking this pathway through lentiviral-mediated CD38 knockdown or cADPR antagonism protected the hippocampus from apoptosis, oxidative stress and morphological damages associated with sepsis. Taking these contrasting observations into consideration, additional studies are required in order to assess whether interference with selective CD38 activities represents a strategy for the amelioration of immunopathology induced by excessive inflammation.

An aspect to consider is that regulatory T cells play key roles in limiting excessive immune responses. In mice and humans, regulatory $CD8^+$ T cells displaying immunosuppressive actions on $CD4^+$ effector T cell proliferation expressed high levels of CD38 [78]. In vivo, $CD8^+CD38^{high}$, but not $CD8^+CD38^-$, T cells ameliorated the clinical severity of murine experimental autoimmune encephalomyelitis, suggesting that $CD8^+CD38^{high}$ T cells are potential inhibitors of excessive immune responses. Likewise, high levels of CD38 expression on $CD4^+$ regulatory T cells also correlated with superior suppressive activity [79]. These results raise interest in exploring whether any of the activities mediated by CD38 exert a direct role on the mechanisms for immunosuppression used by these cells. Moreover, regulatory T cells are also highly responsible for the immunosuppression phase associated with sepsis. Patients undergoing the hyporesponsive phase of sepsis fail to eradicate invading pathogens and become highly susceptible to opportunistic infections. Therefore, the role of CD38 in the immunosuppressive phase of sepsis should also be investigated.

9. CD157, a CD38 Paralogue, Is Important for the Host Response to *Mycobacterium tuberculosis*

CD157/bone marrow stromal cell antigen 1 (BST1) is a CD38 paralogue that can be found as a glycosylphosphatidylinositol (GPI)-anchored protein on the membrane or as a soluble form. Human CD157 is highly expressed on neutrophils, monocytes/macrophages, plasmacytoid and follicular dendritic cells, and many other cell types. CD157 exerts NADase activity, which leads to the production of ADPR. In humans, CD157, in contrast to CD38, has very limited ADPR cyclase activity, whereas in mice, this activity may be biologically important. In addition, an alternatively spliced form of CD157 exists with no detectable NADase activity (reviewed in [80]).

CD157 locates primarily within lipid rafts in the cell membrane. Despite not containing intracellular domains, CD157 was able to interact with integrins CD18 and CD29 on human neutrophils and monocytes, forming supramolecular complexes that activated signaling pathways to modulate transendothelial migration and adhesion to extracellular matrix components [81,82]. A number of extracellular matrix proteins containing heparin-binding domains were indeed shown to be high affinity non-substrate ligands for CD157, including fibronectin and fibrinogen [81,83].

Although limited information is available on the role of CD157 in the host response to infection, recent studies indicated that CD157 is important for conferring host resistance to *Mycobacterium tuberculosis* (*M. tuberculosis*) [84]. The activity of macrophages at the infection site is indeed critical for the host defense against *M. tuberculosis*. Importantly, CD157 expression was selectively up-regulated in circulating monocytes and in lungs from patients with tuberculosis and decreased after effective antituberculosis chemotherapy. CD157 contributed to the macrophage bactericidal activity by facilitating TLR2-dependent production of reactive oxygen species, an important mechanism used for bacterial killing. Interestingly, the levels of soluble CD157 correlated with human monocyte-derived macrophage bactericidal activity and exogenous administration of this form restored the bactericidal capacity of CD157-deficient macrophages, which raises the possibility that soluble CD157 might have a potential use in host-directed therapy against tuberculosis.

CD157 deficiency also resulted in alterations in the development of specific B cell subclasses, along with partial impairment of either the systemic humoral response after immunization with

thymus-independent antigens or the mucosa-associated humoral response upon immunization with cholera toxin, a thymus-dependent antigen [85].

10. Increased Risk of Infections in Immunotherapies Using Anti-CD38 Antibodies

Because of its high expression in plasma cells, CD38 has emerged as a suitable target for immunotherapy of multiple myeloma [86]. Daratumumab is an approved anti-CD38 monoclonal antibody used for the treatment of multiple myeloma. The mechanism of action of daratumumab is based on the elimination of tumor cells expressing high levels of CD38 through antibody-dependent cellular cytotoxicity and complement-dependent cytotoxicity. Recent studies have reported an increased risk of infection in multiple myeloma patients undergoing treatment with daratumumab, either as monotherapy or as combined therapy with other drugs, with some cases resulting in lethal sepsis [87–93]. Infections reported as drug-related adverse effects include opportunistic bacterial infections of the respiratory or urinary tracts (e.g., *S. pneumoniae*, *Pseudomonas aeruginosa*, *Staphylococcus aureus*, *Escherichia coli* and *Haemophilus influenzae*), exogenous viral infections (e.g., acute respiratory syncytial virus, human metapneumovirus and influenza A and B viruses) and viral reactivations (e.g., cytomegalovirus, herpes simplex virus and varicella-zoster virus). Furthermore, increased risk of infection was also observed in a study exploring the effects of daratumumab in patients with systemic light-chain amyloidosis [94] and in clinical trials using isatuximab, a separate anti-CD38 monoclonal antibody, for multiple myeloma [95,96]. Of note, many patients undergoing anti-CD38-based immunotherapy are in relapsed or refractory phases of the disease and have been heavily treated, which implies that immunosuppression derived from previous lines of treatment could influence the risk of infection. Nevertheless, adverse effects associated with infection were also reported in patients with newly diagnosed multiple myeloma who were ineligible for autologous stem cell transplantation and received daratumumab as treatment [97].

Infectious complications may derive from anti-CD38 immunotherapy also targeting CD38-positive immune subpopulations different from tumor plasma cells. In fact, daratumumab treatment was shown to reduce the numbers of NK cells and other CD38-expressing immune cells [91,98]. Therefore, although additional studies are required to further understand the basis of daratumumab-induced immunosuppression in some patients, the accumulated data show the importance of cells expressing CD38 in the defense against pathogens in humans, which is consistent with the different activities of CD38 in the control of infection described earlier in this review.

11. Emerging Perspectives

The rapid development of antimicrobial resistances across the world is a major threat to public health, which is why efforts are addressed toward the discovery of novel approaches based on host-directed therapy to fight drug-resistant pathogens [99]. Lessons learned from anti-CD38 antibody therapy suggest that depletion of subpopulations of immune cells expressing CD38 increase the susceptibility to infection. However, whether manipulation of specific CD38 activities represents an adequate strategy for host-directed therapy against infections requires further investigation. In this sense, many studies support the importance of CD38 in maintaining pro-inflammatory profiles in innate immune cells. However, recent work has raised the possibility that CD38 might also enhance the immunosuppressive potential of regulatory lymphocytes. Therefore, the relative contribution of such opposing actions needs to be carefully examined. To date, the impact of the absence of functional CD38 in the host response to infection has been studied using systemic CD38-deficient mice. However, to better understand the different roles of CD38 in the immune system, approaches using conditional knockout models are required.

In addition, most attempts at dissecting the involvement of different activities associated with the multifunctional nature of CD38 have been accomplished using either blocking or agonistic antibodies or chemical inhibitors. Whereas such approaches have provided valuable information, more sophisticated models incorporating genetic modifications that interfere with selective CD38-mediated activities

(whether receptorial or enzymatic) might help gain perspective on the relative importance of each of these functions in the immune response.

Among the varied consequences of increased CD38 expression, the implications of a substantial decline in NAD^+ levels on the inflammatory response and the outcome on the course of infection offer an open area for exploration. Different studies have indeed generated discrepancies in regard to the effects of NAD^+ depletion on inflammatory pathways. For example, a decrease in intracellular NAD^+ through different mechanisms correlated with activation of the inflammasome in murine macrophages and the administration of exogenous NAD^+ counteracted these effects [100]. In contrast, decreasing the levels of cellular NAD^+ in human monocytes by using FK866 resulted in reduced TLR4 signal transduction and the inflammatory response to LPS [101]. Group A *Streptococcus* bacteria benefit, in fact, from the use of a molecule with NADase activity that inhibits inflammasome-dependent interleukin 1β release from infected macrophages [102]. Moreover, many bacteria use exogenous NAD to maintain their NAD turnover and limit the use of energy for NAD biosynthesis. The most drastic example is provided by the genus *Haemophilus*, which includes several pathogenic bacterial species that completely depend on exogenous NAD^+ because they are not able to synthesize or recycle this molecule (reviewed in [19]). Therefore, the role of CD38 NADase activity in host cells as a protective mechanism against this type of pathogen deserves attention.

Apart from its cell surface and soluble forms, CD38 has also been identified within exosomes derived from HIV-1-infected lymphocytes [103]. Exosomes are extracellular vesicles that are secreted by the cellular endosomal compartment, and their cargos can change markedly during infection [104]. Exosomal cargos have been shown to influence different aspects of the host response, including the immune response to infection and the pathogenesis of sepsis [104,105]. Despite the fact that exosomal CD38 retains enzymatic activity [106], its role in extracellular NAD^+ depletion and exosomal-mediated intercellular communication has not been characterized.

In conclusion, despite considerable knowledge existing on the diverse roles of CD38 in the immune response, new (and more sophisticated) approaches are required in order to determine the consequences of targeting specific CD38-mediated activities during the host response to infection.

Funding: This work was supported by the Spanish Ministry of Economy and Competitivity (MINECO) grant SAF2017-89510-R (to A.F.V). E.G. received a fellowship from the University of Barcelona (APIF).

Conflicts of Interest: The authors declare no conflict of interest. The funders had no role in the collection of information or interpretation of data, in the writing of the manuscript, or in the decision to publish the results.

References

1. Murphy, K.; Weaver, C. *Janeway's Immunobiology*, 9th ed.; Garland Science/Taylor & Francis Group, LLC: New York, NY, USA, 2017; ISBN 9780815345053.
2. Malavasi, F.; Deaglio, S.; Funaro, A.; Ferrero, E.; Horenstein, A.L.; Ortolan, E.; Vaisitti, T.; Aydin, S. Evolution and function of the ADP ribosyl cyclase/CD38 gene family in physiology and pathology. *Physiol. Rev.* **2008**, *88*, 841–886. [CrossRef] [PubMed]
3. Reinherz, E.L.; Kung, P.C.; Goldstein, G.; Levey, R.H.; Schlossman, S.F. Discrete stages of human intrathymic differentiation: Analysis of normal thymocytes and leukemic lymphoblasts of T-cell lineage. *Proc. Natl. Acad. Sci. USA* **1980**, *77*, 1588–1592. [CrossRef] [PubMed]
4. Dianzani, U.; Bragardo, M.; Buonfiglio, D.; Redoglia, V.; Funaro, A.; Portoles, P.; Rojo, J.; Malavasi, F.; Pileri, A. Modulation of CD4 lateral interaction with lymphocyte surface molecules induced by HIV-1 gp120. *Eur. J. Immunol.* **1995**, *25*, 1306–1311. [CrossRef] [PubMed]
5. Funaro, A.; De Monte, L.B.; Dianzani, U.; Forni, M.; Malavasi, F. Human CD38 is associated to distinct molecules which mediate transmembrane signaling in different lineages. *Eur. J. Immunol.* **1993**, *23*, 2407–2411. [CrossRef] [PubMed]
6. Zilber, M.T.; Setterblad, N.; Vasselon, T.; Doliger, C.; Charron, D.; Mooney, N.; Gelin, C. MHC class II/CD38/CD9: A lipid-raft-dependent signaling complex in human monocytes. *Blood* **2005**, *106*, 3074–3081. [CrossRef] [PubMed]

7. Muñoz, P.; Mittelbrunn, M.; De La Fuente, H.; Perez-Martinez, M.; Garcfa-Perez, A.; Ariza-Veguillas, A.; Malavasi, F.; Zubiaur, M.; Sanchez-Madrid, F.; Sancho, J. Antigen-induced clustering of surface CD38 and recruitment of intracellular CD38 to the immunologic synapse. *Blood* **2008**, *111*, 3653–3664. [CrossRef] [PubMed]
8. Lund, F.E.; Yu, N.; Kim, K.M.; Reth, M.; Howard, M.C. Signaling through CD38 augments B cell antigen receptor (BCR) responses and is dependent on BCR expression. *J. Immunol.* **1996**, *157*, 1455–1467.
9. Deaglio, S.; Morra, M.; Mallone, R.; Ausiello, C.M.; Prager, E.; Garbarino, G.; Dianzani, U.; Stockinger, H.; Malavasi, F. Human CD38 (ADP-ribosyl cyclase) is a counter-receptor of CD31, an Ig superfamily member. *J. Immunol.* **1998**, *160*, 395–402.
10. Aarhus, R.; Graeff, R.M.; Dickey, D.M.; Walseth, T.F.; Lee, H.C. ADP-ribosyl cyclase and CD38 catalyze the synthesis of a calcium-mobilizing metabolite from NADP. *J. Biol. Chem.* **1995**, *270*, 30327–30333. [CrossRef]
11. Gelman, L.; Deterre, P.; Gouy, H.; Boumsell, L.; Debré, P.; Bismuth, G. The lymphocyte surface antigen CD38 acts as a nicotinamide adenine dinucleotide glycohydrolase in human T lymphocytes. *Eur. J. Immunol.* **1993**, *23*, 3361–3364. [CrossRef]
12. Aksoy, P.; White, T.A.; Thompson, M.; Chini, E.N. Regulation of intracellular levels of NAD: A novel role for CD38. *Biochem. Biophys. Res. Commun.* **2006**, *345*, 1386–1392. [CrossRef] [PubMed]
13. Camacho-Pereira, J.; Tarragó, M.G.; Chini, C.C.S.; Nin, V.; Escande, C.; Warner, G.M.; Puranik, A.S.; Schoon, R.A.; Reid, J.M.; Galina, A.; et al. CD38 Dictates Age-Related NAD Decline and Mitochondrial Dysfunction through an SIRT3-Dependent Mechanism. *Cell Metab.* **2016**, *23*, 1127–1139. [CrossRef] [PubMed]
14. Quarona, V.; Zaccarello, G.; Chillemi, A.; Brunetti, E.; Singh, V.K.; Ferrero, E.; Funaro, A.; Horenstein, A.L.; Malavasi, F. CD38 and CD157: A long journey from activation markers to multifunctional molecules. *Cytom. B Clin. Cytom.* **2013**, *84*, 207–217. [CrossRef] [PubMed]
15. Terhorst, C.; van Agthoven, A.; Leclair, K.; Snow, P.; Reinherz, E.; Schlossman, S. Biochemical studies of the human thymocyte cell-surface antigens T6, T9 and T10. *Cell* **1981**, *23*, 771–780. [CrossRef]
16. Bruzzone, S.; Guida, L.; Franco, L.; Zocchi, E.; Corte, G.; De Flora, A. Dimeric and tetrameric forms of catalytically active transmembrane CD38 in transfected HeLa cells. *FEBS Lett.* **1998**, *433*, 275–278. [CrossRef]
17. Hara-Yokoyama, M.; Kukimoto-Niino, M.; Terasawa, K.; Harumiya, S.; Podyma-Inoue, K.A.; Hino, N.; Sakamoto, K.; Itoh, S.; Hashii, N.; Hiruta, Y.; et al. Tetrameric interaction of the ectoenzyme CD38 on the cell surface enables its catalytic and raft-association activities. *Structure* **2012**, *20*, 1585–1595. [CrossRef] [PubMed]
18. Zhao, Y.J.; Lam, C.M.C.; Lee, H.C. The membrane-bound enzyme CD38 exists in two opposing orientations. *Sci. Signal.* **2012**, *5*, ra67. [CrossRef]
19. Hogan, K.A.; Chini, C.C.S.; Chini, E.N. The Multi-faceted Ecto-enzyme CD38: Roles in immunomodulation, cancer, aging, and metabolic diseases. *Front. Immunol.* **2019**, *10*, 1187. [CrossRef]
20. Funaro, A.; Horenstein, A.L.; Calosso, L.; Morra, M.; Tarocco, R.P.; Franco, L.; De Flora, A.; Malavasi, F. Identification and characterization of an active soluble form of human CD38 in normal and pathological fluids. *Int. Immunol.* **1996**, *8*, 1643–1650. [CrossRef]
21. Ginsburg, I.; Korem, M.; Koren, E.; Varani, J. Pro-inflammatory agents released by pathogens, dying host cells, and neutrophils act synergistically to destroy host tissues: A working hypothesis. *J. Inflamm. Res.* **2019**, *12*, 35–47. [CrossRef]
22. Lischke, T.; Heesch, K.; Schumacher, V.; Schneider, M.; Haag, F.; Koch-Nolte, F.; Mittrücker, H.-W. CD38 controls the innate immune response against Listeria monocytogenes. *Infect. Immun.* **2013**, *81*, 4091–4099. [CrossRef] [PubMed]
23. Viegas, M.S.; do Carmo, A.; Silva, T.; Seco, F.; Serra, V.; Lacerda, M.; Martins, T.C. CD38 plays a role in effective containment of mycobacteria within granulomata and polarization of Th1 immune responses against Mycobacterium avium. *Microbes Infect.* **2007**, *9*, 847–854. [CrossRef] [PubMed]
24. Partida-Sánchez, S.; Cockayne, D.A.; Monard, S.; Jacobson, E.L.; Oppenheimer, N.; Garvy, B.; Kusser, K.; Goodrich, S.; Howard, M.; Harmsen, A.; et al. Cyclic ADP-ribose production by CD38 regulates intracellular calcium release, extracellular calcium influx and chemotaxis in neutrophils and is required for bacterial clearance in vivo. *Nat. Med.* **2001**, *7*, 1209–1216. [CrossRef] [PubMed]
25. Partida-Sánchez, S.; Randall, T.D.; Lund, F.E. Innate immunity is regulated by CD38, an ecto-enzyme with ADP-ribosyl cyclase activity. *Microbes Infect.* **2003**, *5*, 49–58. [CrossRef]

26. Estrada-Figueroa, L.A.; Ramírez-Jiménez, Y.; Osorio-Trujillo, C.; Shibayama, M.; Navarro-García, F.; García-Tovar, C.; Talamás-Rohana, P. Absence of CD38 delays arrival of neutrophils to the liver and innate immune response development during hepatic amoebiasis by Entamoeba histolytica. *Parasite Immunol.* **2011**, *33*, 661–668. [CrossRef]
27. Matalonga, J.; Glaria, E.; Bresque, M.; Escande, C.; Carbó, J.M.; Kiefer, K.; Vicente, R.; León, T.E.; Beceiro, S.; Pascual-García, M.; et al. The Nuclear Receptor LXR Limits Bacterial Infection of Host Macrophages through a Mechanism that Impacts Cellular NAD Metabolism. *Cell Rep.* **2017**, *18*, 1241–1255. [CrossRef]
28. Beceiro, S.; Pap, A.; Czimmerer, Z.; Sallam, T.; Guillén, J.A.; Gallardo, G.; Hong, C.; A-Gonzalez, N.; Tabraue, C.; Diaz, M.; et al. Liver X receptor nuclear receptors are transcriptional regulators of dendritic cell chemotaxis. *Mol. Cell. Biol.* **2018**, *38*, e00534-17. [CrossRef]
29. Amici, S.A.; Young, N.A.; Narvaez-Miranda, J.; Jablonski, K.A.; Arcos, J.; Rosas, L.; Papenfuss, T.L.; Torrelles, J.B.; Jarjour, W.N.; Guerau-de-Arellano, M. CD38 Is Robustly Induced in Human Macrophages and Monocytes in Inflammatory Conditions. *Front. Immunol.* **2018**, *9*, 1593. [CrossRef]
30. Iqbal, J.; Zaidi, M. TNF regulates cellular NAD+ metabolism in primary macrophages. *Biochem. Biophys. Res. Commun.* **2006**, *342*, 1312–1318. [CrossRef]
31. Lee, C.-U.; Song, E.-K.; Yoo, C.-H.; Kwak, Y.-K.; Han, M.-K. Lipopolysaccharide induces CD38 expression and solubilization in J774 macrophage cells. *Mol. Cells* **2012**, *34*, 573–576. [CrossRef]
32. Musso, T.; Deaglio, S.; Franco, L.; Calosso, L.; Badolato, R.; Garbarino, G.; Dianzani, U.; Malavasi, F. CD38 expression and functional activities are up-regulated by IFN-gamma on human monocytes and monocytic cell lines. *J. Leukoc. Biol.* **2001**, *69*, 605–612. [PubMed]
33. Fedele, G.; Frasca, L.; Palazzo, R.; Ferrero, E.; Malavasi, F.; Ausiello, C. CD38 is expressed on human mature monocyte-derived dendritic cells and is functionally involved in CD83 expression and IL-12 induction. *Eur. J. Immunol.* **2004**, *34*, 1342–1350. [CrossRef] [PubMed]
34. Lande, R.; Urbani, F.; Di Carlo, B.; Sconocchia, G.; Deaglio, S.; Funaro, A.; Malavasi, F.; Ausiello, C.M. CD38 ligation plays a direct role in the induction of IL-1β, IL-6, and IL-10 secretion in resting human monocytes. *Cell. Immunol.* **2002**, *220*, 30–38. [CrossRef]
35. Frasca, L.; Fedele, G.; Deaglio, S.; Capuano, C.; Palazzo, R.; Vaisitti, T.; Malavasi, F.; Ausiello, C.M. CD38 orchestrates migration, survival, and Th1 immune response of human mature dendritic cells. *Blood* **2006**, *107*, 2392–2399. [CrossRef] [PubMed]
36. Shu, B.; Feng, Y.; Gui, Y.; Lu, Q.; Wei, W.; Xue, X.; Sun, X.; He, W.; Yang, J.; Dai, C. Blockade of CD38 diminishes lipopolysaccharide-induced macrophage classical activation and acute kidney injury involving NF-κB signaling suppression. *Cell. Signal.* **2018**, *42*, 249–258. [CrossRef] [PubMed]
37. Schiavoni, I.; Scagnolari, C.; Horenstein, A.L.; Leone, P.; Pierangeli, A.; Malavasi, F.; Ausiello, C.M.; Fedele, G. CD38 modulates respiratory syncytial virus-driven proinflammatory processes in human monocyte-derived dendritic cells. *Immunology* **2018**, *154*, 122–131. [CrossRef]
38. Schimmel, L.; Heemskerk, N.; van Buul, J.D. Leukocyte transendothelial migration: A local affair. *Small GTPases* **2017**, *8*, 1–15. [CrossRef]
39. David, B.A.; Kubes, P. Exploring the complex role of chemokines and chemoattractants in vivo on leukocyte dynamics. *Immunol. Rev.* **2019**, *289*, 9–30. [CrossRef]
40. Partida-Sanchez, S.; Gasser, A.; Fliegert, R.; Siebrands, C.C.; Dammermann, W.; Shi, G.; Mousseau, B.J.; Sumoza-Toledo, A.; Bhagat, H.; Walseth, T.F.; et al. Chemotaxis of Mouse Bone Marrow Neutrophils and Dendritic Cells Is Controlled by ADP-Ribose, the Major Product Generated by the CD38 Enzyme Reaction. *J. Immunol.* **2007**, *179*, 7827–7839. [CrossRef]
41. Partida-Sánchez, S.; Iribarren, P.; Moreno-García, M.E.; Gao, J.-L.; Murphy, P.M.; Oppenheimer, N.; Wang, J.M.; Lund, F.E. Chemotaxis and Calcium Responses of Phagocytes to Formyl Peptide Receptor Ligands Is Differentially Regulated by Cyclic ADP Ribose. *J. Immunol.* **2004**, *172*, 1896–1906. [CrossRef]
42. Rosales, C.; Uribe-Querol, E. Phagocytosis: A Fundamental Process in Immunity. *BioMed Res. Int.* **2017**, *2017*, 9042851. [CrossRef] [PubMed]
43. Lücke, K.; Yan, I.; Krohn, S.; Volmari, A.; Klinge, S.; Schmid, J.; Schumacher, V.; Steinmetz, O.M.; Rose-John, S.; Mittrücker, H.-W. Control of Listeria monocytogenes infection requires classical IL-6 signaling in myeloid cells. *PLoS ONE* **2018**, *13*, e0203395. [CrossRef] [PubMed]

44. Kang, J.; Park, K.-H.; Kim, J.-J.; Jo, E.-K.; Han, M.-K.; Kim, U.-H. The role of CD38 in Fcγ receptor (FcγR)-mediated phagocytosis in murine macrophages. *J. Biol. Chem.* **2012**, *287*, 14502–14514. [CrossRef] [PubMed]
45. Price, J.V.; Vance, R.E. The Macrophage Paradox. *Immunity* **2014**, *41*, 685–693. [CrossRef]
46. Schineis, P.; Runge, P.; Halin, C. Cellular traffic through afferent lymphatic vessels. *Vascul. Pharmacol.* **2019**, *112*, 31–41. [CrossRef]
47. Partida-Sánchez, S.; Goodrich, S.; Kusser, K.; Oppenheimer, N.; Randall, T.D.; Lund, F.E. Regulation of dendritic cell trafficking by the ADP-ribosyl cyclase CD38: Impact on the development of humoral immunity. *Immunity* **2004**, *20*, 279–291. [CrossRef]
48. Vences-Catalán, F.; Santos-Argumedo, L. CD38 through the life of a murine B lymphocyte. *IUBMB Life* **2011**, *63*, 840–846. [CrossRef]
49. Zupo, S.; Rugari, E.; Dono, M.; Taborelli, G.; Malavasi, F.; Ferrarini, M. CD38 signaling by agonistic monoclonal antibody prevents apoptosis of human germinal center B cells. *Eur. J. Immunol.* **1994**, *24*, 1218–1222. [CrossRef]
50. Deaglio, S.; Vaisitti, T.; Billington, R.; Bergui, L.; Omede', P.; Genazzani, A.A.; Malavasi, F. CD38/CD19: A lipid raft-dependent signaling complex in human B cells. *Blood* **2007**, *109*, 5390–5398. [CrossRef]
51. Cockayne, D.A.; Muchamuel, T.; Grimaldi, J.C.; Muller-Steffner, H.; Randall, T.D.; Lund, F.E.; Murray, R.; Schuber, F.; Howard, M.C. Mice deficient for the ecto-nicotinamide adenine dinucleotide glycohydrolase CD38 exhibit altered humoral immune responses. *Blood* **1998**, *92*, 1324–1333. [CrossRef]
52. Kikuchi, Y.; Yasue, T.; Miyake, K.; Kimoto, M.; Takatsu, K. CD38 ligation induces tyrosine phosphorylation of Bruton tyrosine kinase and enhanced expression of interleukin 5-receptor α chain: Synergistic effects with interleukin 5. *Proc. Natl. Acad. Sci. USA* **1995**, *92*, 11814–11818. [CrossRef] [PubMed]
53. Manjarrez-Orduño, N.; Moreno-García, M.E.; Fink, K.; Santos-Argumedo, L. CD38 cross-linking enhances TLR-induced B cell proliferation but decreases IgM plasma cell differentiation. *Eur. J. Immunol.* **2007**, *37*, 358–367. [CrossRef] [PubMed]
54. Dianzani, U.; Funaro, A.; DiFranco, D.; Garbarino, G.; Bragardo, M.; Redoglia, V.; Buonfiglio, D.; De Monte, L.B.; Pileri, A.; Malavasi, F. Interaction between endothelium and CD4+CD45RA+ lymphocytes. Role of the human CD38 molecule. *J. Immunol.* **1994**, *153*, 952–959. [PubMed]
55. Ausiello, C.M.; la Sala, A.; Ramoni, C.; Urbani, F.; Funaro, A.; Malavasi, F. Secretion of IFN-gamma, IL-6, granulocyte-macrophage colony-stimulating factor and IL-10 cytokines after activation of human purified T lymphocytes upon CD38 ligation. *Cell. Immunol.* **1996**, *173*, 192–197. [CrossRef]
56. Savarino, A.; Bottarel, F.; Malavasi, F.; Dianzani, U. Role of CD38 in HIV-1 infection: An epiphenomenon of T-cell activation or an active player in virus/host interactions? *AIDS* **2000**, *14*, 1079–1089. [CrossRef]
57. Rodríguez-Alba, J.C.; Abrego-Peredo, A.; Gallardo-Hernández, C.; Pérez-Lara, J.; Santiago-Cruz, W.; Jiang, W.; Espinosa, E. HIV Disease Progression: Overexpression of the Ectoenzyme CD38 as a Contributory Factor? *BioEssays* **2018**, *41*, 1800128. [CrossRef]
58. Kestens, L.; Vanham, G.; Gigase, P.; Young, G.; Hannet, I.; Vanlangendonck, F.; Hulstaert, F.; Bach, B.A. Expression of activation antigens, HLA-DR and CD38, on CD8 lymphocytes during HIV-1 infection. *AIDS* **1992**, *6*, 793–797. [CrossRef]
59. Yagi, M.J.; Chu, F.N.; Jiang, J.D.; Wallace, J.; Mason, P.; Liu, Y.; Carafa, J.; Bekesi, J.G. Increases in soluble CD8 antigen in plasma, and CD8+ and CD8+CD38+ cells in human immunodeficiency virus type-1 infection. *Clin. Immunol. Immunopathol.* **1992**, *63*, 126–134. [CrossRef]
60. Zaunders, J.J.; Munier, M.L.; Kaufmann, D.E.; Ip, S.; Grey, P.; Smith, D.; Ramacciotti, T.; Quan, D.; Finlayson, R.; Kaldor, J.; et al. Early proliferation of CCR5(+) CD38(+++) antigen-specific CD4(+) Th1 effector cells during primary HIV-1 infection. *Blood* **2005**, *106*, 1660–1667. [CrossRef]
61. Mocroft, A.; Bofill, M.; Lipman, M.; Medina, E.; Borthwick, N.; Timms, A.; Batista, L.; Winter, M.; Sabin, C.A.; Johnson, M.; et al. CD8+, CD38+ lymphocyte percent: A useful immunological marker for monitoring HIV-1-infected patients. *J. Acquir. Immune Defic. Syndr. Hum. Retrovirology* **1997**, *14*, 158–162. [CrossRef]
62. Liu, Z.; Hultin, L.E.; Cumberland, W.G.; Hultin, P.; Schmid, I.; Matud, J.L.; Detels, R.; Giorgi, J. V Elevated relative fluorescence intensity of CD38 antigen expression on CD8+ T cells is a marker of poor prognosis in HIV infection: Results of 6 years of follow-up. *Cytometry* **1996**, *26*, 1–7. [CrossRef]

63. Bürgisser, P.; Hammann, C.; Kaufmann, D.; Battegay, M.; Rutschmann, O.T. Expression of CD28 and CD38 by CD8+ T lymphocytes in HIV-1 infection correlates with markers of disease severity and changes towards normalization under treatment. The Swiss HIV Cohort Study. *Clin. Exp. Immunol.* **1999**, *115*, 458–463. [CrossRef] [PubMed]
64. Benito, J.M.; Zabay, J.M.; Gil, J.; Bermejo, M.; Escudero, A.; Sánchez, E.; Fernández-Cruz, E. Quantitative alterations of the functionally distinct subsets of CD4 and CD8 T lymphocytes in asymptomatic HIV infection: Changes in the expression of CD45RO, CD45RA, CD11b, CD38, HLA-DR, and CD25 antigens. *J. Acquir. Immune Defic. Syndr. Hum. Retrovirology* **1997**, *14*, 128–135. [CrossRef] [PubMed]
65. Giorgi, J.V.; Hultin, L.E.; McKeating, J.A.; Johnson, T.D.; Owens, B.; Jacobson, L.P.; Shih, R.; Lewis, J.; Wiley, D.J.; Phair, J.P.; et al. Shorter Survival in Advanced Human Immunodeficiency Virus Type 1 Infection Is More Closely Associated with T Lymphocyte Activation than with Plasma Virus Burden or Virus Chemokine Coreceptor Usage. *J. Infect. Dis.* **1999**, *179*, 859–870. [CrossRef]
66. De Martino, M.; Rossi, M.E.; Azzari, C.; Gelli, M.G.; Galli, L.; Vierucci, A. Different meaning of CD38 molecule expression on CD4 + and CD8 + cells of children perinatally infected with human immunodeficiency virus type 1 infection surviving longer than five years. *Pediatr. Res.* **1998**, *43*, 752–758. [CrossRef]
67. Schlesinger, M.; Peters, V.; Jiang, J.D.; Roboz, J.P.; Bekesi, J.G. Increased expression of activation markers on CD8 lymphocytes in children with human immunodeficiency virus-1 infection. *Pediatr. Res.* **1995**, *38*, 390–396. [CrossRef]
68. Savarino, A.; Bottarel, F.; Calosso, L.; Feito, M.J.; Bensi, T.; Bragardo, M.; Rojo, J.M.; Pugliese, A.; Abbate, I.; Capobianchi, M.R.; et al. Effects of the human cd38 glycoprotein on the early stages of the HIV-1 replication cycle. *FASEB J.* **1999**, *13*, 2265–2276. [CrossRef]
69. Savarino, A.; Pugliese, A.; Martini, C.; Pich, P.G.; Pescarmona, G.P.; Malavasi, F. Investigation of the potential role of membrane CD38 in protection against cell death induced by HIV-1. *J. Biol. Regul. Homeost. Agents* **1996**, *10*, 13–18.
70. Savarino, A.; Bensi, T.; Chiocchetti, A.; Bottarel, F.; Mesturini, R.; Ferrero, E.; Calosso, L.; Deaglio, S.; Ortolan, E.; Buttò, S.; et al. Human CD38 interferes with HIV-1 fusion through a sequence homologous to the V3 loop of the viral envelope glycoprotein gp120. *FASEB J.* **2003**, *17*, 461–463. [CrossRef]
71. Bragardo, M.; Buonfiglio, D.; Feito, M.J.; Bonissoni, S.; Redoglia, V.; Rojo, J.M.; Ballester, S.; Portoles, P.; Garbarino, G.; Malavasi, F.; et al. Modulation of lymphocyte interaction with endothelium and homing by HIV-1 gp120. *J. Immunol.* **1997**, *159*, 1619–1627.
72. Burel, J.G.; Apte, S.H.; Groves, P.L.; Klein, K.; McCarthy, J.S.; Doolan, D.L. Reduced Plasmodium Parasite Burden Associates with CD38+ CD4+ T Cells Displaying Cytolytic Potential and Impaired IFN-γ Production. *PLoS Pathog.* **2016**, *12*, e1005839. [CrossRef] [PubMed]
73. Van Der Poll, T.; Van De Veerdonk, F.L.; Scicluna, B.P.; Netea, M.G. The immunopathology of sepsis and potential therapeutic targets. *Nat. Rev. Immunol.* **2017**, *17*, 407–420. [CrossRef] [PubMed]
74. Escande, C.; Nin, V.; Price, N.L.; Capellini, V.; Gomes, A.P.; Barbosa, M.T.; O'Neil, L.; White, T.A.; Sinclair, D.A.; Chini, E.N. Flavonoid apigenin is an inhibitor of the NAD+ase CD38: Implications for cellular NAD+ metabolism, protein acetylation, and treatment of metabolic syndrome. *Diabetes* **2013**, *62*, 1084–1093. [CrossRef] [PubMed]
75. Kellenberger, E.; Kuhn, I.; Schuber, F.; Muller-Steffner, H. Flavonoids as inhibitors of human CD38. *Bioorganic Med. Chem. Lett.* **2011**, *21*, 3939–3942. [CrossRef] [PubMed]
76. Li, Q.; Wu, C.; Liu, Z.; Zhang, H.; Du, Y.; Liu, Y.; Song, K.; Shi, Q.; Li, R. Increased TLR4 Expression Aggravates Sepsis by Promoting IFN-γ Expression in CD38 -/- Mice. *J. Immunol. Res.* **2019**, *2019*, 3737890. [CrossRef] [PubMed]
77. Peng, Q.-Y.; Wang, Y.-M.; Chen, C.-X.; Zou, Y.; Zhang, L.-N.; Deng, S.-Y.; Ai, Y.-H. Inhibiting the CD38/cADPR pathway protected rats against sepsis associated brain injury. *Brain Res.* **2018**, *1678*, 56–63. [CrossRef]
78. Bahri, R.; Bollinger, A.; Bollinger, T.; Orinska, Z.; Bulfone-Paus, S. Ectonucleotidase CD38 Demarcates Regulatory, Memory-Like CD8+ T Cells with IFN-γ-Mediated Suppressor Activities. *PLoS ONE* **2012**, *7*, 45234. [CrossRef]
79. Patton, D.T.; Wilson, M.D.; Rowan, W.C.; Soond, D.R.; Okkenhaug, K. The PI3K p110δ regulates expression of CD38 on regulatory T cells. *PLoS ONE* **2011**, *6*, 17359. [CrossRef]
80. Ortolan, E.; Augeri, S.; Fissolo, G.; Musso, I.; Funaro, A. CD157: From immunoregulatory protein to potential therapeutic target. *Immunol. Lett.* **2019**, *205*, 59–64. [CrossRef]

81. Lo Buono, N.; Parrotta, R.; Morone, S.; Bovino, P.; Nacci, G.; Ortolan, E.; Horenstein, A.L.; Inzhutova, A.; Ferrero, E.; Funaro, A. The CD157-integrin partnership controls transendothelial migration and adhesion of human monocytes. *J. Biol. Chem.* **2011**, *286*, 18681–18691. [CrossRef]
82. Lavagno, L.; Ferrero, E.; Ortolan, E.; Malavasi, F.; Funaro, A. CD157 is part of a supramolecular complex with CD11b/CD18 on the human neutrophil cell surface. *J. Biol. Regul. Homeost. Agents* **2007**, *21*, 5–11. [PubMed]
83. Morone, S.; Augeri, S.; Cuccioloni, M.; Mozzicafreddo, M.; Angeletti, M.; Lo Buono, N.; Giacomino, A.; Ortolan, E.; Funaro, A. Binding of CD157 protein to fibronectin regulates cell adhesion and spreading. *J. Biol. Chem.* **2014**, *289*, 15588–15601. [CrossRef] [PubMed]
84. Yang, Q.; Liao, M.; Wang, W.; Zhang, M.; Chen, Q.; Guo, J.; Peng, B.; Huang, J.; Liu, H.; Yahagi, A.; et al. CD157 Confers Host Resistance to Mycobacterium tuberculosis via TLR2-CD157-PKCzeta-Induced Reactive Oxygen Species Production. *MBio* **2019**, *10*, e01949-19. [CrossRef] [PubMed]
85. Itoh, M.; Ishihara, K.; Hiroi, T.; Lee, B.O.; Maeda, H.; Iijima, H.; Yanagita, M.; Kiyono, H.; Hirano, T. Deletion of bone marrow stromal cell antigen-1 (CD157) gene impaired systemic thymus independent-2 antigen-induced IgG3 and mucosal TD antigen-elicited IgA responses. *J. Immunol.* **1998**, *161*, 3974–3983.
86. Morandi, F.; Horenstein, A.L.; Costa, F.; Giuliani, N.; Pistoia, V.; Malavasi, F. CD38: A target for immunotherapeutic approaches in multiple myeloma. *Front. Immunol.* **2018**, *9*, 2722. [CrossRef]
87. Mateos, M.-V.; Cavo, M.; Blade, J.; Dimopoulos, M.A.; Suzuki, K.; Jakubowiak, A.; Knop, S.; Doyen, C.; Lucio, P.; Nagy, Z.; et al. Overall survival with daratumumab, bortezomib, melphalan, and prednisone in newly diagnosed multiple myeloma (ALCYONE): A randomised, open-label, phase 3 trial. *Lancet* **2019**. [CrossRef]
88. Usmani, S.Z.; Nahi, H.; Mateos, M.V.; van de Donk, N.W.C.J.; Chari, A.; Kaufman, J.L.; Moreau, P.; Oriol, A.; Plesner, T.; Benboubker, L.; et al. Subcutaneous delivery of daratumumab in relapsed or refractory multiple myeloma. *Blood* **2019**, *134*, 668–677. [CrossRef]
89. Nakagawa, R.; Onishi, Y.; Kawajiri, A.; Onodera, K.; Furukawa, E.; Sano, S.; Saito, K.; Ichikawa, S.; Fujiwara, T.; Fukuhara, N.; et al. Preemptive therapy for cytomegalovirus reactivation after daratumumab-containing treatment in patients with relapsed and refractory multiple myeloma. *Ann. Hematol.* **2019**, *98*, 1999–2001. [CrossRef]
90. Xu, W.; Li, D.F.; Sun, Y.; Ran, X.; Wang, B.; Wu, W.; Sheng, Z.; Liu, L. Daratumumab added to standard of care in patients with newly diagnosed multiple myeloma: A network meta-analysis. *Eur. J. Haematol.* **2019**, *103*, 542–551. [CrossRef]
91. Nahi, H.; Chrobok, M.; Gran, C.; Lund, J.; Gruber, A.; Gahrton, G.; Ljungman, P.; Wagner, A.K.; Alici, E. Infectious complications and NK cell depletion following daratumumab treatment of multiple myeloma. *PLoS ONE* **2019**, *14*, e0211927. [CrossRef]
92. Chari, A.; Lonial, S.; Mark, T.M.; Krishnan, A.Y.; Stockerl-Goldstein, K.E.; Usmani, S.Z.; Londhe, A.; Etheredge, D.; Fleming, S.; Liu, B.; et al. Results of an early access treatment protocol of daratumumab in United States patients with relapsed or refractory multiple myeloma. *Cancer* **2018**, *124*, 4342–4349. [CrossRef] [PubMed]
93. Park, S.S.; Eom, H.S.; Kim, J.S.; Koh, Y.; Choi, C.W.; Lee, J.J.; Kim, K.; Suh, C.; Lee, J.H.; Min, C.K. Brief report: Clinical experiences after emergency use of daratumumab monotherapy for relapsed or refractory multiple myeloma in real practice. *Jpn. J. Clin. Oncol.* **2019**, *49*, 92–95. [CrossRef] [PubMed]
94. Van de Wyngaert, Z.; Carpentier, B.; Pascal, L.; Lionne-Huyghe, P.; Leduc, I.; Srour, M.; Vasseur, M.; Demarquette, H.; Terriou, L.; Herbaux, C.; et al. Daratumumab is effective in the relapsed or refractory systemic light-chain amyloidosis but associated with high infection burden in a frail real-life population. *Br. J. Haematol.* **2019**. [CrossRef] [PubMed]
95. Mikhael, J.; Richardson, P.; Usmani, S.Z.; Raje, N.; Bensinger, W.; Karanes, C.; Campana, F.; Kanagavel, D.; Dubin, F.; Liu, Q.; et al. A phase 1b study of isatuximab plus pomalidomide/dexamethasone in relapsed/refractory multiple myeloma. *Blood* **2019**, *134*, 123–133. [CrossRef] [PubMed]
96. Attal, M.; Richardson, P.G.; Rajkumar, S.V.; San-Miguel, J.; Beksac, M.; Spicka, I.; Leleu, X.; Schjesvold, F.; Moreau, P.; Dimopoulos, M.A.; et al. Isatuximab plus pomalidomide and low-dose dexamethasone versus pomalidomide and low-dose dexamethasone in patients with relapsed and refractory multiple myeloma (ICARIA-MM): A randomised, multicentre, open-label, phase 3 study. *Lancet* **2019**, *394*, 2096–2107. [CrossRef]
97. Syed, Y.Y. Daratumumab: A Review in Combination Therapy for Transplant-Ineligible Newly Diagnosed Multiple Myeloma. *Drugs* **2019**, *79*, 447–454. [CrossRef]

98. Krejcik, J.; Casneuf, T.; Nijhof, I.S.; Verbist, B.; Bald, J.; Plesner, T.; Syed, K.; Liu, K.; Van De Donk, N.W.C.J.; Weiss, B.M.; et al. Daratumumab depletes CD38+ immune regulatory cells, promotes T-cell expansion, and skews T-cell repertoire in multiple myeloma. *Blood* **2016**, *128*, 384–394. [CrossRef]
99. Kaufmann, S.H.E.; Dorhoi, A.; Hotchkiss, R.S.; Bartenschlager, R. Host-directed therapies for bacterial and viral infections. *Nat. Rev. Drug Discov.* **2018**, *17*, 35–56. [CrossRef]
100. Misawa, T.; Takahama, M.; Kozaki, T.; Lee, H.; Zou, J.; Saitoh, T.; Akira, S. Microtubule-driven spatial arrangement of mitochondria promotes activation of the NLRP3 inflammasome. *Nat. Immunol.* **2013**, *14*, 454–460. [CrossRef]
101. Yang, K.; Lauritzen, K.H.; Olsen, M.B.; Dahl, T.B.; Ranheim, T.; Ahmed, M.S.; Attramadal, H.; Aukrust, P.; Halvorsen, B.; Nyman, T.A.; et al. Low Cellular NAD + Compromises Lipopolysaccharide-Induced Inflammatory Responses via Inhibiting TLR4 Signal Transduction in Human Monocytes. *J. Immunol.* **2019**, *203*, 1598–1608. [CrossRef]
102. Hancz, D.; Westerlund, E.; Bastiat-Sempe, B.; Sharma, O.; Valfridsson, C.; Meyer, L.; Love, J.F.; O'Seaghdha, M.; Wessels, M.R.; Perssona, J.J. Inhibition of inflammasome-dependent interleukin 1β production by streptococcal NAD+-glycohydrolase: Evidence for extracellular activity. *MBio* **2017**, *8*, e00756-17. [CrossRef] [PubMed]
103. Li, M.; Aliotta, J.M.; Asara, J.M.; Tucker, L.; Quesenberry, P.; Lally, M.; Ramratnam, B. Quantitative proteomic analysis of exosomes from HIV-1-infected lymphocytic cells. *Proteomics* **2012**, *12*, 2203–2211. [CrossRef] [PubMed]
104. Alenquer, M.; Amorim, M.J. Exosome biogenesis, regulation, and function in viral infection. *Viruses* **2015**, *7*, 5066–5083. [CrossRef] [PubMed]
105. Park, E.J.; Appiah, M.G.; Myint, P.K.; Gaowa, A.; Kawamoto, E.; Shimaoka, M. Exosomes in Sepsis and Inflammatory Tissue Injury. *Curr. Pharm. Des.* **2019**. [CrossRef]
106. Zumaquero, E.; Muñoz, P.; Cobo, M.; Lucena, G.; Pavón, E.J.; Martín, A.; Navarro, P.; García-Pérez, A.; Ariza-Veguillas, A.; Malavasi, F.; et al. Exosomes from human lymphoblastoid B cells express enzymatically active CD38 that is associated with signaling complexes containing CD81, Hsc-70 and Lyn. *Exp. Cell Res.* **2010**, *316*, 2692–2706. [CrossRef]

Publication 7

Review article:

Integrating the roles of liver X receptors in inflammation and infection: mechanisms and outcomes

Glaría E, Letelier NA, and Valledor A. F.

August 2020

Current Opinion in Pharmacology, 53, 55–65.

doi: 10.1016/j.coph.2020.05.001

Impact factor: 4.807

Available online at www.sciencedirect.com

ScienceDirect

Current Opinion in Pharmacology

Integrating the roles of liver X receptors in inflammation and infection: mechanisms and outcomes

Estibaliz Glaría[1,2], Nicole A Letelier[1,2] and Annabel F Valledor[1,2]

Liver X receptors (LXRs) are transcription factors from the nuclear receptor family that can be pharmacologically activated by high-affinity agonists. LXR activation exerts a combination of metabolic and anti-inflammatory actions that result in the modulation of immune responses and in the amelioration of inflammatory disorders. In addition, LXR agonists modulate the metabolism of infected cells and limit the infectivity and/or growth of several pathogens. This review gives an overview of the recent advances in understanding the complexity of the mechanisms through which the LXR pathway controls inflammation and host–cell pathogen interaction.

Addresses

[1] Department of Cell Biology, Physiology and Immunology, School of Biology, University of Barcelona, 08028?Barcelona, Spain

[2] Institute of Biomedicine of the University of Barcelona (IBUB), 08028? Barcelona, Spain

Corresponding author: Valledor, Annabel F (afernandezvalledor@ub.edu)

Current Opinion in Pharmacology 2020, **53**:55–65

This review comes from a themed issue on **Immunomodulation**

Edited by **Tamás Röszer**

For a complete overview see the Issue and the Editorial

Available online 28th June 2020

https://doi.org/10.1016/j.coph.2020.05.001

Introduction

Liver X receptors (LXRs), namely, NR1H3 (LXRα) and NR1H2 (LXRβ), are transcription factors from the nuclear receptor family (reviewed in Ref. [1]). LXRβ is ubiquitously expressed, whereas LXRα expression is more predominant in tissues that are highly involved in lipid metabolism. Within the immune system, macrophages, dendritic cells, and neutrophils express both isoforms, B lymphocytes express mainly LXRβ, and T cell populations have been reported to express either LXRβ or both isoforms [2–5,6•]. LXRs can be activated by endogenous agonists, including specific oxysterols and intermediates of cholesterol biosynthesis, and by specific high-affinity agonists that are frequently used *in vivo* to explore the consequences of pharmacological LXR activation.

LXRs form heterodimers with retinoid X receptors (RXRs) on LXR response elements and, once activated by agonists, they positively regulate the expression of target genes. Recent studies have proposed three possible modes of action for LXRα-mediated transcriptional activation [7•]. Two mechanisms are based on the canonical induction of target gene expression by RXR-LXR heterodimers in a pharmacologically responsive-manner. In the absence of agonistic activation, the target genes are repressed by LXR/RXR heterodimers, which may lead to de-repression in the absence of functional LXRs [8]. A third mechanism was proposed, by which the expression of a number of transcripts depends on the presence of LXRs, but these transcripts are not upregulated upon pharmacological LXR activation [7•].

Most of the targets that are positively induced in response to LXR agonists play key roles in lipid and glucose metabolism (reviewed in Ref. [1]). These include (but are not restricted to) several sterol transporters from the ATP binding cassette (ABC) family, for example, ABCA1 and ABCG1; transcription factors sterol regulatory element-binding protein 1c (SREBP1c) and carbohydrate regulatory element-binding protein with important lipogenic roles; the E3 ubiquitin ligase inducible degrader of the low-density lipoprotein receptor (IDOL); and several apolipoproteins involved in lipid transport.

The use of immortalized murine macrophages that express equivalent levels of FLAG-tagged LXRα or LXRβ in an LXR-deficient background has contributed in defining the specific roles of LXR isoforms in gene regulation. In addition to a signature simultaneously regulated by both isoforms, LXRα selectively regulates the expression of genes linked to the control of apoptosis and leukocyte migration, whereas LXRβ-specific functions are associated with lymphocyte differentiation and selection [7•].

In addition to their positive effects on gene transcription, LXRs can negatively affect the expression of inflammatory mediators through a plethora of mechanisms, which will be further revised in the following section. Agonist-bound LXRs undergo conjugation to small ubiquitin-related modifier (SUMO), a process known as SUMOylation, which is required for some of the repressive actions of these proteins [9]. Moreover, a study in astrocytes proposed different SUMOylation pathways for agonist-bound LXRα and LXRβ, mediated by separate members of the SUMO E3 ligase family [10].

In a complex scenario combining metabolic and anti-inflammatory actions, LXRs are able to modulate immune responses. These actions are particularly relevant in the management of an infection, as a number of pathogens are able to hijack host metabolic pathways for their own benefit. This review integrates the recent conceptual advances in understanding the complexity of mechanisms used by the LXR pathway to control inflammation and the response of the host to infection.

LXRs as attenuators of inflammatory disorders

Accumulated evidence indicates the importance of the LXR pathway in the negative control of inflammatory conditions. For example, pharmacological activation of LXRs reduced the extent of the inflammatory response in murine models of dermatitis [11,12], neuroinflammation [13,14], lupus [15], arthritis [16], and atherosclerosis [12], consistent with the fact that LXR-deficient mice develop an age-related lupus-like autoimmune disease [17]. Furthermore, several polymorphisms affecting the promoter region of the gene encoding LXRα were associated with susceptibility to systemic lupus erythematosus in a Korean cohort [18].

To explain the anti-inflammatory actions of pharmacologically activated LXRs, many studies have focused on the capability of high-affinity agonists to repress pro-inflammatory gene expression in macrophages and other cell types activated by the engagement of toll-like receptors (TLRs) or by endogenous inflammatory cytokines [9,12,14,19,20]. The LXR pathway impairs the transcriptional activity of nuclear factor kappa B (NF-κB) [12] and the recruitment of signal transducer and activator of transcription (STAT)1 to target gene promoters [10,14]. Putting together the pieces of evidence reported by different groups, it is apparent that several mechanisms contribute to the antagonizing actions of the LXR pathway on pro-inflammatory signaling (Figure 1). First, agonist-bound LXRs underwent SUMOylation and exerted transrepression by inhibiting the removal of nuclear receptor co-repressor (NCoR) complexes from pro-inflammatory gene promoters in response to lipopolysaccharide (LPS) [9,21,22]. In macrophages, this process involves the interaction of SUMOylated LXRs with the actin-binding protein CORONIN 2A (CORO2A). This interaction prevented actin recruitment to inflammatory gene promoters [21], in line with more recent evidence on the important roles of nuclear actin in the transcriptional control of macrophage activation [23]. In the hepatic acute phase response in mice, the anti-inflammatory effects were selectively mediated by SUMOylated LXRβ and its interaction with the corepressor complex subunit G protein pathway suppressor 2 (GPS2) [22]. LXRβ also attenuated inflammatory cytokine production in murine mast cells stimulated with LPS or FcεRI crosslinking [24]. By contrast, both SUMOylated LXRα and LXRβ contributed in inhibiting the transcriptional response of murine macrophages and astrocytes to interferon (IFN)-γ through interference with STAT1 [10,14], which supports the notion that the relative contribution of each isoform depends on the cell type and the inflammatory trigger.

Direct repressive actions have also been proposed involving the binding of LXRs to specific sites within macrophage inflammatory gene enhancer elements and potential chromatin closure, although additional studies are required to better define this mechanism. Gene signatures affected by this repressive activity are associated with leukocyte cell–cell adhesion and neutrophil chemotaxis, in line with the inhibitory effects of LXR agonists on neutrophil infiltration in a model of zymosan-induced peritonitis in mice [25].

Other mechanisms contributing to the repression of inflammation imply the increased transcription of LXR targets in macrophages (Figure 1). First, the cholesterol and phospholipid transporter ABCA1, whose upregulation results in changes in membrane cholesterol homeostasis that are able to disrupt the recruitment of key adaptor molecules to lipid rafts, thereby antagonizing TLR signaling [20]. Second, several enzymes involved in the synthesis of fatty acids (fatty acid synthase) and in their conversion to derivatives with anti-inflammatory properties (predominantly mediated by stearoyl-CoA desaturase-2 (SCD2) and its products 9Z palmitoleic acid and oleic acid). The induction of these enzymes is exerted directly by LXRs or indirectly through the upregulation of the transcription factor SREBP1c, depending on the type of agonist mediating LXR activation [26]. Third, MER, a receptor tyrosine kinase that recognizes the plasma protein growth arrest-specific 6 (GAS6) bound to phosphatidylserine (PtdSer) on the surface of apoptotic bodies and contributes to apoptotic cell clearance. The upregulation of MER has been proposed as a mechanism coupling the engulfment of apoptotic cells (efferocytosis) with the suppression of inflammatory pathways. Indeed, LXR deficiency resulted in an aberrant pro-inflammatory response of macrophages to apoptotic cells and in the development of autoimmune disease in mice [17]. Fourth, interferon regulatory factor (IRF)8, a transcription factor with multiple roles in myeloid cells. Through the upregulation of IRF8, the LXR pathway indirectly induced the expression of interleukin (IL)-18 binding protein (IL18BP) in the murine and human systems. IL18BP is a potent endogenous inhibitor of the pro-inflammatory cytokine IL-18 [27]. In parallel, LXR agonists also repressed IL18 transcription and blocked the processing of pro-IL-18 to its bioactive form by interfering with pro-caspase 1 expression and activation, indicating that the LXR pathway uses a combination of mechanisms to inhibit IL-18 production [27]. In addition, increased expression of IRF8 in murine macrophages overexpressing LXRα resulted in the upregulation of the anti-inflammatory enzyme arginase 1 [28].

Figure 1

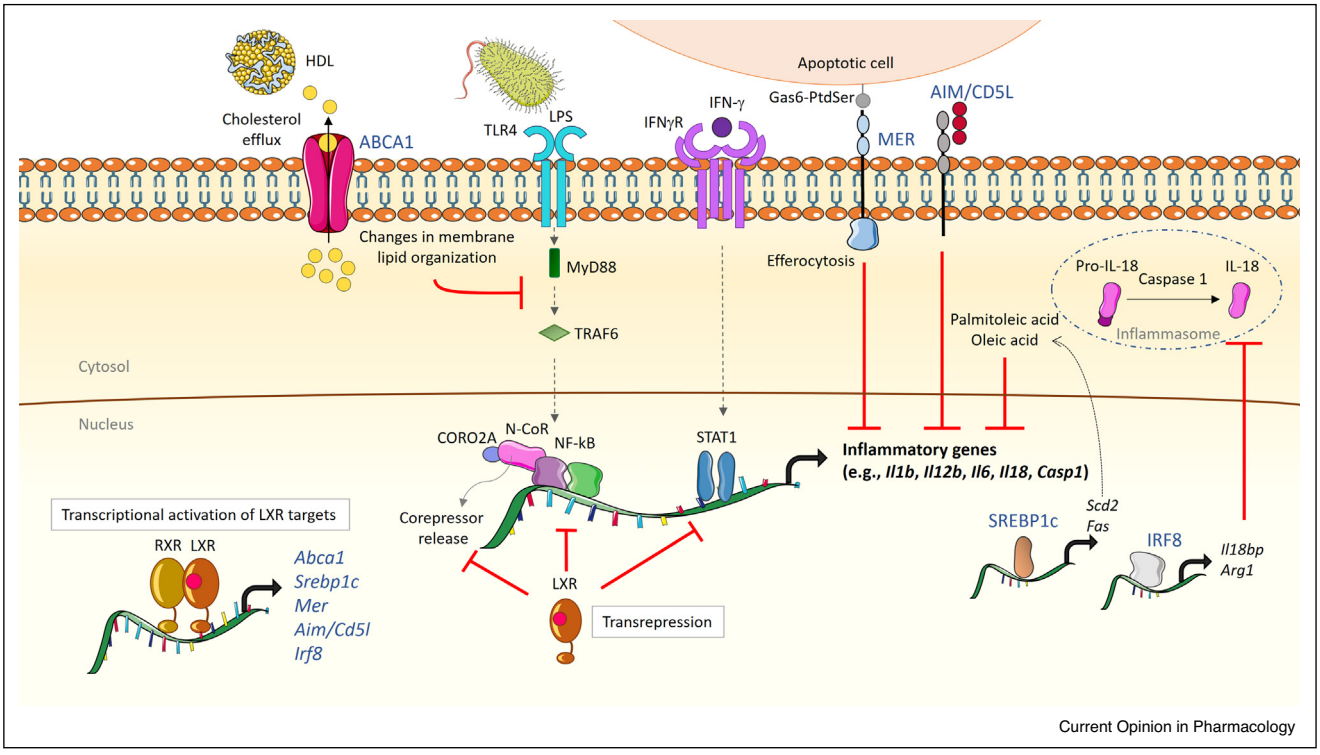

LXRs inhibit the inflammatory response in macrophages through multiple mechanisms.
TLR signaling or IFN-γ stimulation induce inflammatory gene expression. Agonist-bound LXRs mediate mechanisms of transrepression, which interfere with the release of corepressors or with the activity/recruitment of transcription factors (NF-κB, STAT1) required for inflammatory gene expression. In addition, LXRs inhibit inflammation indirectly through the transcriptional activation of LXR targets (in blue) involved in the modulation of metabolic and/or immune responses. The cholesterol efflux mediated by ABCA1 results in changes in the lipid composition of the membrane, which interferes with TLR signaling. SREBP1c induces the expresion of enzymes involved in the generation of lipids with anti-inflammatory properties. MER couples efferocytosis with the suppression of the inflammatory response. AIM/CD5L enhances the expression of molecules involved in the resolution of inflammation and promotes an anti-inflammatory profile. IRF8 induces the expression of IL18BP, which binds to secreted IL-18 and inhibits its biological actions. Some elements in this image have been downloaded from SMART – Servier Medical ART. *Arg1*, arginase 1; *Casp1*, caspase 1; *Fas*, fatty acid synthase; HDL, high-density lipoprotein; IFNγR, IFN-γ receptor; *Il1b*, interleukin 1β; *Il12b*, interleukin 12?subunit b; *Il6*, interleukin 6; MyD88, myeloid differentiation primary response 88; TRAF6, tumor necrosis factor receptor associated factor 6.

Aside from the mechanisms described above, LXR agonists also induce the expression of apoptosis inhibitory factor secreted by macrophages (AIM)/CD5L [29,30]. In the murine system, this effect is mediated specifically by LXRα [7•,30]. AIM/CD5L is a soluble scavenger receptor that can also act as a pattern-recognition receptor [31]. The endogenous production of human AIM/CD5L enhanced the expression of molecules involved in the resolution of inflammation, namely, MER and CD163, increased autophagy, and promoted an anti-inflammatory profile in human monocytes, resembling the actions of IL-10 [32•], which suggests the possibility that AIM might also be involved in facilitating the resolution of inflammation in response to LXR agonists.

In contrast to predominant anti-inflammatory activities of LXR agonists in macrophages, both pro-inflammatory and anti-inflammatory actions have been reported in dendritic cells. In this regard, LXR activation downregulated the expression of the actin-bundling protein fascin in human myeloid dendritic cells, suppressing T cell stimulation due to inefficient immunological synapse formation [33]. However, prolonged NF-κB activation was detected in a different study, which translated into increased pro-inflammatory and T cell stimulatory activities [34]. Moreover, LXR agonism increased the chemotaxis of murine dendritic cells to signals generated in inflammatory settings, such as chemokine (C–C motif) ligand (CCL)19 and CCL21. This action was mediated through transcriptional activation of the ectoenzyme CD38, which is capable of converting nicotinamide adenine dinucleotide (NAD) into cyclic adenosine diphosphoribose (cADPR), an important second messenger in leukocyte trafficking [6•]. These contrasting observations raise the question as to whether the effects of the LXR pathway are influenced by additional factors involved in dendritic cell maturation, which requires further exploration.

In addition to the actions in myeloid cells, LXR agonists inhibited the differentiation of murine and human helper T (Th)17 cells [35], which are a subset of $CD4^+$ T cells that secrete IL-17 and contribute to the pathogeny of inflammatory diseases [36]. An indirect mechanisms was proposed, by which LXR-induced SREBP1 negatively interfered with the activity of the transcription factor aryl hydrocarbon receptor on the *Il17* promoter. The differentiation of other $CD4^+$ T cell populations was also inhibited by LXR agonists [37], consistent with the anti-proliferative actions of LXRβ in murine T cells mediated by the upregulation of ABCG1 and subsequent changes in sterol homeostasis [3]. Moreover, LXR activation induced regulatory T cell (Treg) expansion. Although a molecular mechanism was not defined, the oral administration of an LXR agonist in mice increased the abundance of gut-associated Treg with high suppressive capacity [38], which may provide additional explanation to the protective effects of the LXR pathway against the development of autoimmune diseases.

The interplay between the metabolic actions of LXRs and their role in the modulation of adaptive immune responses was further illustrated by the observation that excessive lipid accumulation in LXRβ-deficient antigen presenting cells induced the expression of B cell activating factor (BAFF) and a proliferation inducing ligand (APRIL) that support B cell survival and differentiation [39]. This scenario triggered the expansion of auto-reactive B cells and contributed to the development of autoimmune disease. In addition, despite the fact that B cells mostly express the LXRβ isoform, the activation of LXRα repressed BAFF production in human B cell lines through interference with NF-κB, STAT1 and mothers against decapentaplegic homolog 3 (SMAD3) signaling [40].

Beyond the anti-inflammatory actions in immune cells, transcriptional activation by LXRs impairs inflammatory responses in the liver in the context of metabolic disease. In particular, lysophosphatidylcholine acyltransferase 3 (LPCAT3) is highly induced by LXR agonists in hepatic cells, where it drives the incorporation of unsaturated fatty acids into phospholipids [41]. The activity of LPCAT3 resulted in reduced membrane lipid saturation, thus inhibiting pro-inflammatory c-Src kinase activation, and in decreased availability of saturated lipids for the synthesis of inflammatory mediators.

Impact of metabolic and anti-inflammatory actions of LXRs on host cell–pathogen interaction

Despite contributing to immunopathology, inflammatory responses are crucial for the establishment of an effective immune response against infection. Based on the anti-inflammatory actions of the LXR pathway, one could expect that LXR agonism would lead to deficient immune responses against infection. However, as will be discussed in this section, several studies have shown otherwise. Notably, a number of pathogens have developed mechanisms to hijack the host immune response and establish intracellular infection, particularly in phagocytic cells, even under adverse inflammatory conditions. Metabolic reprogramming of host cells or adaptation to their metabolic status are indeed common strategies used by intracellular pathogens for survival and replication [42].

Interestingly, many studies have shown increased expression and/or activity of LXR isoforms in leukocytes infected by intracellular pathogens [30,43•,44–46]. Although the signaling pathway/s leading to increased LXR expression during infection have not been fully characterized, muramyl dipeptide, a ligand of nucleotide-binding oligomerization domain-containing protein 2 (NOD2) that is present in many bacteria, was able to induce LXRα expression in murine macrophages [30]. In addition, type I and II IFNs and IL-36, which are produced during the immune response to infection, as well as LPS from Gram-negative bacteria, upregulated the expression of enzymes that transform free cholesterol into endogenous LXR agonists, such as 25-hydroxycholesterol (25-HC) [14,43•,47,48]. However, the involvement of LXRs in the physiological actions of 25-HC is still unclear [49]. Sterile acute inflammation also increased LXR expression and activity through a mechanism requiring functional MER signaling [50], in line with the observation that efferocytosis via MER activates the LXR pathway [17].

By contrast, LXRα expression was inhibited in experimental models of sepsis [51,52] and the transcriptional control of LXR target genes was compromised in several infection/inflammatory settings [14,15,53]. In this regard, TLR3/4 ligands and IFN-γ interfered with the LXR-mediated control of cholesterol metabolism through activation of IRF3 and STAT1, respectively [14,53]. Competition for the coactivator p300/CREB-binding protein (CBP) was proposed as a mechanism for IRF3 and STAT1 to inhibit the transcriptional activity of LXRs on specific target genes.

Such divergent consequences of infection/inflammation on LXR signaling have fueled the need to explore the roles of this pathway in host–pathogen interaction (Figure 2). Initial studies in mice defined the general role for LXRs in promoting macrophage survival after infection by different bacteria, namely *Listeria monocytogenes*, *Bacillus anthracis*, *Escherichia coli*, and *Salmonella enterica* serovar Typhimurium (*S.* Typhimurium), which correlated with the upregulated expression of the anti-apoptotic molecule AIM/CD5L, a specific target of LXRα, and with the downregulation of pro-apoptotic factors [29,30]. Deficient LXR expression, particularly in bone marrow-derived cells, resulted in a higher susceptibility to

Figure 2

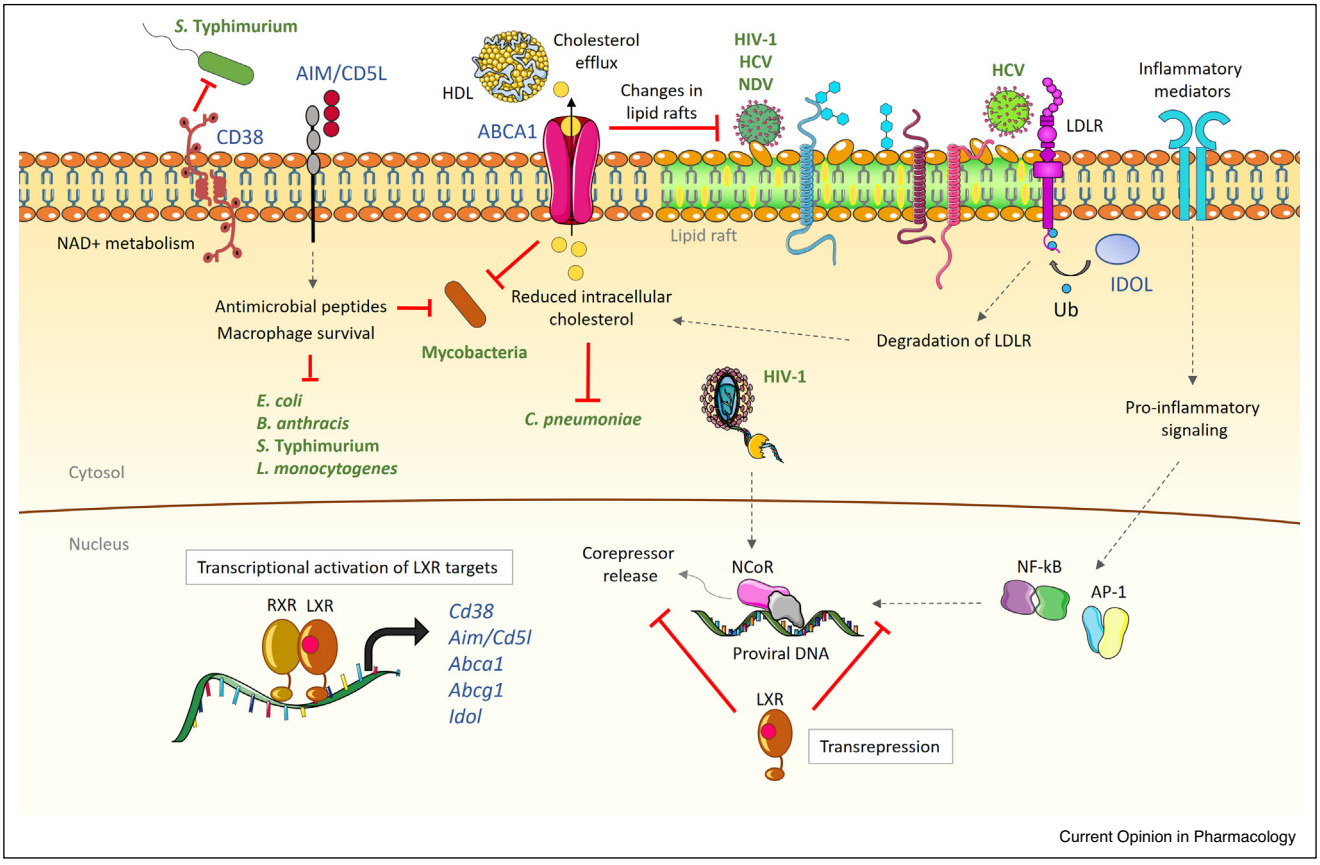

LXR activation induces protective mechanisms that limit viral and bacterial infection.
LXR agonists upregulate the expression of LXR targets (in blue) that contribute in reducing the infection by several pathogens (names of pathogens in green). AIM/CD5L confers resistance to apoptosis and induces the synthesis of antimicrobial peptides. CD38 reduces intracellular NAD + levels and the infection by *S.* Typhimurium, ABCA1 promotes cholesterol efflux. As a consequence, reduced intracellular cholesterol limits the growth of mycobacteria and, potentially, of other bacterial strains that depend on intracellular cholesterol. In addition, changes in the cholesterol levels within lipid rafts may interfere with the entry of several viruses into host cells. IDOL, by virtue of its role in controling the turnover of the LDLR, inhibits the capability of HCV to infect host cells. LXRs can also affect the intracellular replication of HIV-1 through mechanisms of transrepression, which affect corepressor release or transcription factor recruitment to the proviral DNA. Ub, ubiquitin. Some elements in this image have been downloaded from SMART – Servier Medical ART.

infection by *L. monocytogenes*, with increased bacterial burden and neutrophilic abscesses in the liver and a lower survival rate [30]. In studies comparing the relative contribution of LXR isoforms, the lack of expression of LXRα was responsible for the increased susceptibility to *L. monocytogenes*.

Later on, a solid amount of evidence supported the involvement of LXRs in the control of the infection by *Mycobacterium tuberculosis*. In human macrophages and in a murine model of mycobacterial infection, LXR agonists reduced the intracellular bacterial burden [43•,44,45]. In line with these observations, LXR-deficient mice had higher bacterial burdens and increased granulomatous lesions in the lungs and underwent more rapid progression to systemic infection than their wild-type counterparts [45]. The increased susceptibility of LXR-deficient mice was associated with the impaired activities of the innate and adaptive immune systems, including the infiltration of neutrophils to the lungs and the establishment of local Th1 and Th17 responses. These observations are in contrast with the general anti-inflammatory roles of the LXR pathway in non-infectious inflammatory diseases described in the previous section. Interestingly, whereas both LXRα and LXRβ participated in limiting mycobacterial infection in human macrophages *in vitro* [43•], LXRα was specifically required to control the course of infection in mice [45], mirroring the selective contribution of this isoform in the protection against *L. monocytogenes* [30].

In addition, LXR agonists increased the production of antimicrobial peptides in *M. tuberculosis*-infected macrophages [43•], consistent with the capability of the LXRα

target AIM/CD5L to enhance this mechanism of defense and to contribute to mycobacterial clearance [54]. Therefore, it is plausible that activities regulated by AIM/CD5L beyond the control of apoptotic cell death also contribute to the protective effects of LXR agonists against bacterial infection. On the other hand, in contrast to the pro-survival actions described above, LXR agonists promoted apoptosis in human macrophages infected with *M. tuberculosis*, which may represent a mycobactericidal strategy [44]. Although the mechanisms leading to increased cell death were not determined, further investigation is required to better understand the implications of the LXR-AIM axis in different types of infection and how this pathway integrates with the other transcriptional effects of LXR agonists.

In this regard, the upregulation of the LXR targets ABCA1 and ABCG1, which mediate intracellular cholesterol efflux, may also represent an important host mechanism for inhibiting mycobacterial growth [44]. Indeed, interference with ABCA1 expression facilitated the growth of the vaccine strain Bacille Calmette–Guérin in human macrophages [55], probably because mycobacteria have a preference for intracellular fatty acids and cholesterol as carbon sources (reviewed in [56]). The obligate intracellular bacterium *Chlamydia pneumoniae* also relies heavily on intracellular cholesterol and uses the TIR domain-containing adapter inducing IFN-β (TRIF)-IRF3 signaling pathway to promote the conversion of infected macrophages into cholesterol-loaded foam cells [57]. Although this study did not evaluate the effects on cholesterol transporters, the results are consistent with the capability of IRF3 to inhibit ABCA1 expression [53]. Interestingly, LXR activation interfered with IRF3 activity and inhibited foam cell formation during *C. pneumoniae* infection [57]. Therefore, it is possible that LXR agonists use cooperative mechanisms based on the induction of ABCA1/G1 and the repressive actions on IRF3 to limit the accumulation of cholesterol and control the infection by bacterial species that benefit from intracellular lipid storages.

Accumulated data support that alterations in the membrane cholesterol as a consequence of increased ABCA1 expression may also affect other critical steps in the infection cycle of several pathogens. Lipid rafts are membrane microdomains enriched in cholesterol and glycosphingolipids that concentrate molecules specifically targeted by a number of microorganisms for host cell binding, invasion, or dissemination, as well as receptors that initiate signaling pathways in host cells in response to environmental stimuli [58]. Indeed, a number of pathogens disrupt cellular cholesterol homeostasis either to promote lipid raft formation and gain entry into host cells or to hijack host cell signaling pathways that facilitate intracellular survival/replication [59]. For example, human immunodeficiency virus (HIV)-1, via its protein Nef, diminished cholesterol efflux from macrophages by modulating the post-transcriptional expression of ABCA1 and its redistribution, thus facilitating viral infectivity [60]. Reciprocally, the activation of the LXR-ABCA1 axis resulted in antiviral effects against HIV-1, including inhibitory effects on viral entry into human $CD4^+$ T cells [61], on virus production and the fusion activity of the virions [62], and on the capability of human dendritic cells to capture HIV-1 and trans-infect T cells [63]. Furthermore, pharmacological treatment with an LXR agonist reduced the viral load in humanized models of HIV infection in mice [62,64]. The antiviral effects were not exclusive for HIV infection, as the control of cholesterol homeostasis by the LXR-ABCA1 pathway also impacted the capability of hepatitis C virus (HCV) to establish virus-host cell fusions and consequently enter the liver cells [65], as well as both the entry and replication capacity of Newcastle disease virus (NDV) [66].

In addition to mechanisms for cholesterol efflux, LXRs control cholesterol uptake through the transcriptional upregulation of IDOL, an E3 ubiquitin ligase that triggers the ubiquitination and degradation of several members of the low-density lipoprotein receptor (LDLR) family [67]. Therefore, the role of IDOL in lowering intracellular cholesterol could help, in combination with the activity of ABCA1/G1, reduce the infectivity and/or growth of some pathogens. Moreover, HCV associates with lipoproteins and benefits from the surface expression of the LDLR to infect hepatocytes (reviewed in [68]). As the overexpression of IDOL inhibited the infection of human hepatocytes with HCV [69], it is plausible that a reduction in the LDLR levels represents an additional mechanism mediating the inhibitory actions of LXR agonists on HCV entry into host cells.

Most studies exploring the role of synthetic LXR agonists in viral infection have not addressed the exact contribution of LXR isoforms. However, the expression of at least LXRα (in the absence of pharmacological treatment) was required to restrict the reactivation of gammaherpesvirus in chronically infected mice [70]. LXRα-deficiency resulted in viral reactivation in peritoneal cells, but not in splenocytes, despite intact virus-specific T cell responses.

The recent discovery of the multifunctional protein CD38 as an additional LXR transcriptional target provided new insights to the way LXR agonists control bacterial infection [6•,71•]. Indeed, CD38 exerts multiple roles in the regulation of the immune response to pathogens [72]. Its expression in cells originating at the bone marrow was required for LXR agonists to ameliorate the clinical severity of *S.* Typhimurium infection in mice [71•]. These effects were consistent with the reduced internalization of *S.* Typhimurium by macrophages [71•] and may be influenced by an enhanced migratory potential of

dendritic cells [6•] upon activation of the LXR-CD38 axis. CD38 displays strong NADase activity, being able to modulate cellular NAD^+ homeostasis while generating calcium-mobilizing second messengers [73]. It also exerts important receptorial and accessory functions in immune cells. Interestingly, the effects of LXR agonists on bacterial cell internalization were overcome with exogenous supplementation of NAD^+ [71•], highlighting the potential significance of intracellular NAD^+ levels in host cell–pathogen interaction. Whether the effects in NAD^+ metabolism cooperate with other LXR-mediated metabolic changes in the control of infection has not been determined. In addition, the contribution of the LXR-CD38 axis in controlling the progression of other types of infection requires investigation.

The LXR pathway can also impact the course of infection through mechanisms based on transcriptional repression. As an example, LXR agonists repressed the basal transcription of HIV-1 in infected macrophages and counteracted HIV-1 replication in response to TLR signaling. These effects were mediated by preventing the release of the corepressor NCoR and inhibiting the recruitment of NF-κB, AP1 components, and CBP to the proviral DNA [74]. Additionally, the repression of pro-inflammatory genes was also proposed as a potential mechanism to downregulate the activation of HIV-1 expression in infected cells.

In line with anti-inflammatory effects in the context of endotoxemia [75], LXR agonists reduced organ dysfunction and mortality associated with sepsis in rodent models [51,52]. The functional expression of silent mating type information regulation 2 homolog (SIRT)-1 was required for the protective effects of LXR agonists on myocardial function in septic mice, which coincided with a reduction in NF-κB activity, oxidative stress, and myocardial cell apoptosis, although the mechanism leading to increased SIRT-1 transcription/activation was not defined [51]. In addition, evidence was provided for a selective role of LXRα, but not of LXRβ, in the protection against liver injury during sepsis [52], which contrasts with the role of LXRβ in ameliorating the hepatic acute response [22]. In general, these observations argue that the LXR pathway plays a role in limiting exacerbated tissue damage due to infection. However, in a different study, LXR agonism increased sepsis-induced mortality in mice due to an impairment of neutrophil infiltration to the infection site [5], raising the possibility that the outcome of LXR activation in sepsis depends on additional factors, which warrants further investigation.

In contrast to the predominant protective effects of the LXR pathway on bacterial and viral infections, the anti-inflammatory environment potentiated by LXR agonists may be a favorable scenario for certain pathogens. In this regard, LXR deficiency conferred resistance to the parasite *Leishmania chagasi/infantum* [76], despite the fact that *Leishmania* spp. are NAD^+ auxotrophs and highly sensitive to the host cell membrane cholesterol for infection [77]. Resistance to infection was associated with increased production of nitric oxide and IL-1β and augmented parasite killing by LXR-deficient macrophages [76]. Similarly, LXR agonists enhanced mortality during *Klebsiella pneumoniae* infection in mice, which correlated with the changes in the course of infiltration of neutrophils to the infected lungs [78]. The inhibition of chemokine-induced RhoA activation was proposed as a potential underlying mechanism.

Putting together all of the pieces of evidence obtained from the different models of infection, the modulation of inflammatory and metabolic responses by LXRs has different consequences depending on the pathogen. Therefore, targeting the LXR pathway as a strategy against infection must take into account the multiple mechanisms contributing to the effects of LXRs in host cell–pathogen interaction.

Conclusions and future perspectives

Because of the emergence of antimicrobial resistances and the absence of effective vaccines for a large number of pathogens, one of the major necessities in public health is the development of innovative host-directed therapies (HDTs) against infection. LXRs, by virtue of their condition as druggable targets and their multiple roles at the intersection between metabolism and inflammation, are promising candidates for HDT.

As summarized in this review, LXR activation exerts a protective role in many pre-clinical models of viral and bacterial infection. Different studies have focused on at least one molecular mechanism to explain these protective effects, but it is likely that several mechanisms cooperate simultaneously to reduce the capacity of infection of pathogens and the inflammatory response. As discussed here, some commonalities exist in relation to the metabolic resources hijacked by different pathogens. Accumulated evidence points toward the LXR pathway as part of the host response to modulate the metabolism of the infected cell and limit the infectivity and/or growth of intracellular pathogens, a role that can be boosted upon pharmacological LXR activation. In this regard, cholesterol metabolism is targeted by LXR agonists in a manner that is beneficial to limiting the infection, at least in animal and *in vitro* studies. Reciprocally, pathogens that are able to interfere with the capacity of LXRs to alter the host cell metabolism may benefit from a more favorable environment. In fact, there is significant evidence of the LXR pathway itself being modulated at the level of both expression and activity by signals derived from pathogen recognition or from cytokines produced at the infection site.

Table 1

Specific contributions of LXR isoforms to the control of inflammation and infection

Disease/cellular model	Trigger	Species	LXR isoform	Effects	Ref.
Macrophages (*in vitro*)	LPS; IFN-γ	Mouse	LXRα/LXRβ	Repression of inflammatory genes	[12,14]
Astrocytes (*in vitro*)	IFN-γ	Mouse	LXRα/LXRβ	Repression of inflammatory genes	[10]
Lupus-like autoimmunity (*in vivo*)	Aging	Mouse	LXRα/LXRβ	Protection from autoimmunity	[17]
Hepatic acute phase response (*in vivo*)	LPS	Mouse	LXRβ	Repression of acute phase response	[22]
Ear inflammation (*in vivo*)	TPA	Mouse	LXRβ	Inhibition of inflammation	[11]
Mast cells (*in vitro*)	LPS; FcεRI crosslinking	Mouse	LXRβ	Repression of inflammatory cytokine production	[24]
T cells (*in vivo*; *in vitro*)	Aging; mitogens	Mouse	LXRβ	Inhibition of proliferation	[3]
Antigen presenting cells (*in vivo*)	Cholesterol accumulation	Mouse	LXRβ	Limitation of B cell expansion	[39]
B cell lines (*in vitro*)	Basal conditions	Human	LXRα	Repression of BAFF production	[40]
Macrophages (*in vitro*)	*M. tuberculosis*	Human	LXRα/LXRβ	Limitation of mycobacterial infection	[43•]
M. tuberculosis infection *in vivo*	*M. tuberculosis*	Mouse	LXRα	Increased resistance to infection	[45]
L. monocytogenes infection *in vivo*	*L. monocytogenes*	Mouse	LXRα	Increased resistance to infection	[30]
GHV infection *in vivo*	GHV	Mouse	LXRα	Restriction of viral reactivation in peritoneal cells	[70]
Cecal ligation and puncture (*in vivo*)	Sepsis	Mouse	LXRα	Protection against liver injury	[52]

Ref., reference. TPA, phorbol 12-myristate-13-acetate.

In addition, excessive tissue damage due to an exacerbated immune response is a common feature in infection and in inflammatory disorders. Beyond its role in limiting the extent of infection, activated LXRs trigger mechanisms to keep the inflammatory response under control and to avoid excessive organ injury in pre-clinical studies.

Given their role at the intersection of lipid metabolism and immune responses, the effects of LXR activation in the context of infection have been studied in depth in macrophages. Indeed, despite their relevance in microbial killing and in the recruitment of immune cells to the site of infection, macrophages are commonly targeted by intracellular pathogens for their replication and dissemination [79]. Therefore, LXRs limit the extent of infection and restrict excessive inflammatory responses in a cell type that represents a selective niche for intracellular infection and, at the same time, is crucial for the preservation of tissue integrity. Despite the importance of LXRs in macrophage biology, this review also integrates data showing the beneficial effects of LXR agonists in other host cells that are targets of the infection, especially in the context of viral infection.

A major limitation in the use of LXR agonists is their adverse effects in pre-clinical models of disease due to the activation of a lipogenic program [80]. Based on hepatic LXRα as the main isoform involved in agonist-induced lipogenesis, attempts have been made to develop LXRβ-specific ligands to circumvent this problem (reviewed in Ref. [1]). However, this kind of approach would probably have limitations as a HDT against infection. Whereas the anti-inflammatory effects of LXR agonists depend on LXRβ in a number of disease models in mice, LXRα activity is essential for the development of protective immune responses against several types of infection (Table 1). Therefore, the development of more sophisticated agonists that are capable of promoting selective LXR functions while inhibiting specific targets [81••] and/or new routes of administration targeting specific immune compartments [82•] deserves further attention in the context of infection.

Conflict of interest statement

Nothing declared.

CRediT authorship contribution statement

Estibaliz Glaría: Conceptualization, Writing - original draft, Writing - review & editing. **Nicole A Letelier:** Conceptualization, Writing - original draft, Writing - review & editing. **Annabel F Valledor:** Conceptualization, Writing - original draft, Supervision, Funding acquisition, Writing - review & editing.

Acknowledgements

This work was supported by grants from the Spanish Ministry of Economy and Competitivity (MINECO) to AFV (SAF2017-89510-R) and to the NuRCaMeIn network (SAF2017-90604REDT), and from Fundació La Marató de TV3 to AFV (201605-31). EG received a fellowship from the University of Barcelona (APIF). NAL received a fellowship from CONICYT (Comisión Nacional de Investigación Científica y Tecnología) (PFCHA/DOCTORADO BECAS CHILE/2016-72170639), Chilean Ministry of Education.

References and recommended reading

Papers of particular interest, published within the period of review, have been highlighted as:

- • of special interest
- •• of outstanding interest

1. Schulman IG: **Liver X receptors link lipid metabolism and inflammation**. *FEBS Lett* 2017, **591**:2978-2991.

2. Walcher D, Kümmel A, Kehrle B, Bach H, Grüb M, Durst R, Hombach V, Marx N: **LXR activation reduces proinflammatory cytokine expression in human CD4-positive lymphocytes**. *Arterioscler Thromb Vasc Biol* 2006, **26**:1022-1028.

3. Bensinger SJ, Bradley MN, Joseph SB, Zelcer N, Janssen EM, Hausner MA, Shih R, Parks JS, Edwards PA, Jamieson BD *et al.*: **LXR signaling couples sterol metabolism to proliferation in the acquired immune response**. *Cell* 2008, **134**:97-111.

4. Diehl CJ, Barish GD, Downes M, Chou MY, Heinz S, Glass CK, Evans RM, Witztum JL: **Research resource: comparative nuclear receptor atlas: basal and activated peritoneal B-1 and B-2 cells**. *Mol Endocrinol* 2011, **25**:529-545.

5. Souto FO, Castanheira FVS, Trevelin SC, Lima BHF, Cebinelli GCM, Turato WM, Auxiliadora-Martins M, Basile-Filho A, Alves-Filho JC, Cunha FQ: **Liver X receptor activation impairs neutrophil functions and aggravates sepsis**. *J Infect Dis* 2020, **221**:1542-1553.

6. • Beceiro S, Pap A, Czimmerer Z, Sallam T, Guillén JA, Gallardo G, Hong C, A-Gonzalez N, Tabraue C, Diaz M *et al.*: **Liver X receptor nuclear receptors are transcriptional regulators of dendritic cell chemotaxis**. *Mol Cell Biol* 2018, **38** e00534-17.

Using gain- and loss-of-function models, this work shows that dendritic cells depend on functional LXRs to migrate *in vivo*. The study also defines CD38 as the molecular mechanism by which LXR agonists enhance dendritic cell chemotaxis.

7. • Ramón-Vázquez A, de la Rosa JV, Tabraue C, Lopez F, Díaz-Chico BN, Bosca L, Tontonoz P, Alemany S, Castrillo A: **Common and differential transcriptional actions of nuclear receptors liver X receptors α and β in macrophages**. *Mol Cell Biol* 2019, **39** e00376-18.

Through the design of immortalized macrophages expressing equivalent amounts of tagged LXRα and LXRβ in an LXR-deficient background, the authors characterize the genomic distribution and transcriptional capacity of each isoform. The study shows that LXRα and LXRβ control the transcription of receptor-exclusive sets of genes.

8. Wagner BL, Valledor AF, Shao G, Daige CL, Bischoff ED, Petrowski M, Jepsen K, Baek SH, Heyman RA, Rosenfeld MG *et al.*: **Promoter-specific roles for liver X receptor/corepressor complexes in the regulation of ABCA1 and SREBP1 gene expression**. *Mol Cell Biol* 2003, **23**:5780-5789.

9. Ghisletti S, Huang W, Ogawa S, Pascual G, Lin M-E, Willson TM, Rosenfeld MG, Glass CK: **Parallel SUMOylation-dependent pathways mediate gene- and signal-specific transrepression by LXRs and PPARgamma**. *Mol Cell* 2007, **25**:57-70.

10. Lee JH, Park SM, Kim OS, Lee CS, Woo JH, Park SJ, Joe E, Jou I: **Differential SUMOylation of LXRalpha and LXRbeta mediates transrepression of STAT1 inflammatory signaling in IFN-gamma-stimulated brain astrocytes**. *Mol Cell* 2009, **35**:806-817.

11. Fowler AJ, Sheu MY, Schmuth M, Kao J, Fluhr JW, Rhein L, Collins JL, Willson TM, Mangelsdorf DJ, Elias PM *et al.*: **Liver X receptor activators display anti-inflammatory activity in irritant and allergic contact dermatitis models: liver-X-receptor-specific inhibition of inflammation and primary cytokine production**. *J Invest Dermatol* 2003, **120**:246-255.

12. Joseph SB, Castrillo A, Laffitte BA, Mangelsdorf DJ, Tontonoz P: **Reciprocal regulation of inflammation and lipid metabolism by liver X receptors**. *Nat Med* 2003, **9**:213-219.

13. Hindinger C, Hinton DR, Kirwin SJ, Atkinson RD, Burnett ME, Bergmann CC, Stohlman SA: **Liver X receptor activation decreases the severity of experimental autoimmune encephalomyelitis**. *J Neurosci Res* 2006, **1234**:1225-1234.

14. Pascual-García M, Rué L, León T, Julve J, Carbó JM, Matalonga J, Auer H, Celada A, Escolà-Gil JC, Steffensen KR *et al.*: **Reciprocal negative cross-talk between liver X receptors (LXRs) and STAT1: effects on IFN-γ–induced inflammatory responses and LXR-dependent gene expression**. *J Immunol* 2013, **190**:6520-6532.

15. Han S, Zhuang H, Shumyak S, Wu J, Xie C, Li H, Yang LJ, Reeves WH: **Liver X receptor agonist therapy prevents diffuse alveolar hemorrhage in murine lupus by repolarizing macrophages**. *Front Immunol* 2018, **9**:135.

16. Park M-C, Kwon Y-J, Chung S-J, Park Y-B, Lee S-K: **Liver X receptor agonist prevents the evolution of collagen-induced arthritis in mice**. *Rheumatology (Oxford)* 2010, **49**:882-890.

17. A-Gonzalez N, Bensinger SJ, Hong C, Beceiro S, Bradley MN, Zelcer N, Deniz J, Ramirez C, Díaz M, Gallardo G *et al.*: **Apoptotic cells promote their own clearance and immune tolerance through activation of the nuclear receptor LXR**. *Immunity* 2009, **31**:245-258.

18. Jeon JY, Nam JY, Kim HA, Park YB, Bae SC, Suh CH: **Liver X receptors alpha gene (NR1H3) promoter polymorphisms are associated with systemic lupus erythematosus in Koreans**. *Arthritis Res Ther* 2014, **16**:R112.

19. Endo-Umeda K, Nakashima H, Komine-Aizawa S, Umeda N, Seki S, Makishima M: **Liver X receptors regulate hepatic F4/80 + CD11b+ kupffer cells/macrophages and innate immune responses in mice**. *Sci Rep* 2018, **8**:9281.

20. Ito A, Hong C, Rong X, Zhu X, Tarling EJ, Hedde PN, Gratton E, Parks J, Tontonoz P: **LXRs link metabolism to inflammation through Abca1-dependent regulation of membrane composition and TLR signaling**. *eLife* 2015, **4**:e08009.

21. Huang W, Ghisletti S, Saijo K, Gandhi M, Aouadi M, Tesz GJ, Zhang DX, Yao J, Czech MP, Goode BL *et al.*: **Coronin 2A mediates actin-dependent de-repression of inflammatory response genes**. *Nature* 2011, **470**:414-418.

22. Venteclef N, Jakobsson T, Ehrlund A, Damdimopoulos A, Mikkonen L, Ellis E, Nilsson L-M, Parini P, Jänne OA, Gustafsson J-A *et al.*: **GPS2-dependent corepressor/SUMO pathways govern anti-inflammatory actions of LRH-1 and LXRbeta in the hepatic acute phase response**. *Genes Dev* 2010, **24**:381-395.

23. Misu S, Takebayashi M, Miyamoto K: **Nuclear actin in development and transcriptional reprogramming**. *Front Genet* 2017, **8**:27.

24. Nunomura S, Okayama Y, Matsumoto K, Hashimoto N, Endo-Umeda K, Terui T, Makishima M, Ra C: **Activation of LXRs using the synthetic agonist GW3965 represses the production of pro-inflammatory cytokines by murine mast cells**. *Allergol Int* 2015, **64(Suppl)**:S11-S17.

25. Thomas DG, Doran AC, Fotakis P, Westerterp M, Antonson P, Jiang H, Jiang XC, Gustafsson JÅ, Tabas I, Tall AR: **LXR suppresses inflammatory gene expression and neutrophil migration through cis-repression and cholesterol efflux**. *Cell Rep* 2018, **25**:3774-3785.e4.

26. Spann NJ, Garmire LX, McDonald JG, Myers DS, Milne SB, Shibata N, Reichart D, Fox JN, Shaked I, Heudobler D *et al.*: **Regulated accumulation of desmosterol integrates macrophage lipid metabolism and inflammatory responses**. *Cell* 2012, **151**:138-152.

27. Pourcet B, Gage MC, Leon TE, Waddington KE, Pello OM, Steffensen KR, Castrillo A, Valledor AF, Pineda-Torra I: **The nuclear receptor LXR modulates interleukin-18 levels in macrophages through multiple mechanisms**. *Sci Rep* 2016, **6**:25481.

28. Pourcet B, Feig JE, Vengrenyuk Y, Hobbs A, Kepka-Lenhart D, Garabedian M, Morris SM, Fisher EA, Pineda-Torra I: **LXRα regulates macrophage arginase 1 through PU.1 and interferon regulatory factor 8**. *Circ Res* 2011, **109**:492-501.

29. Valledor AF, Hsu LC, Ogawa S, Sawka-Verhelle D, Karin M, Glass CK: **Activation of liver X receptors and retinoid X receptors prevents bacterial-induced macrophage apoptosis**. *Proc Natl Acad Sci U S A* 2004, **101**:17813-17818.

30. Joseph SB, Bradley MN, Castrillo A, Bruhn KW, Mak PA, Pei L, Hogenesch J, O'connell RM, Cheng G, Saez E *et al.*: **LXR-dependent gene expression is important for macrophage survival and the innate immune response**. *Cell* 2004, **119**:299-309.

31. Sarrias MR, Roselló S, Sánchez-Barbero F, Sierra JM, Vila J, Yélamos J, Vives J, Casals C, Lozano F: **A role for human SPα as a pattern recognition receptor**. *J Biol Chem* 2005, **280**:35391-35398.

32. • Sanjurjo L, Aran G, Téllez É, Amézaga N, Armengol C, López D, Prats C, Sarrias MR: **CD5L promotes M2 macrophage polarization through autophagy-mediated upregulation of ID3**. *Front Immunol* 2018, **9**:480.

This paper establishes the relevance of CD5L as a potential target in therapeutic strategies aiming at modulating human macrophage polarization.

33. Geyeregger R, Zeyda M, Bauer W, Kriehuber E, Säemann MD, Zlabinger GJ, Maurer D, Stulnig TM: **Liver X receptors regulate dendritic cell phenotype and function through blocked induction of the actin-bundling protein fascin**. *Blood* 2007, **109**:4288-4295.

34. Töröcsik D, Baráth M, Benko S, Széles L, Dezso B, Póliska S, Hegyi Z, Homolya L, Szatmári I, Lányi A *et al.*: **Activation of liver X receptor sensitizes human dendritic cells to inflammatory stimuli**. *J Immunol* 2010, **184**:5456-5465.

35. Cui G, Qin X, Wu L, Zhang Y, Sheng X, Yu Q, Sheng H, Xi B, Zhang JZ, Zang YQ: **Liver X receptor (LXR) mediates negative regulation of mouse and human Th17 differentiation**. *J Clin Invest* 2011, **121**:658-670.

36. Yasuda K, Takeuchi Y, Hirota K: **The pathogenicity of Th17 cells in autoimmune diseases**. *Semin Immunopathol* 2019, **41**:283-297.

37. Solt LA, Kamenecka TM, Burris TP: **LXR-mediated inhibition of CD4+ T helper cells**. *PLoS One* 2012, **7**:e46615.

38. Herold M, Breuer J, Hucke S, Knolle P, Schwab N, Wiendl H, Klotz L: **Liver X receptor activation promotes differentiation of regulatory T cells**. *PLoS One* 2017, **12**:e0184985.

39. Ito A, Hong C, Oka K, Salazar JV, Diehl C, Witztum JL, Diaz M, Castrillo A, Bensinger SJ, Chan L *et al.*: **Cholesterol accumulation in CD11c+ immune cells is a causal and targetable factor in autoimmune disease**. *Immunity* 2016, **45**:1311-1326.

40. Huang Y, Fu X, Lyu X, Xu Z, He Z, Zhang Y, Zeng Y, He F, Huang G: **Activation of LXR attenuates collagen-induced arthritis via suppressing BLyS production**. *Clin Immunol* 2015, **161**:339-347.

41. Rong X, Albert CJ, Hong C, Duerr MA, Chamberlain BT, Tarling EJ, Ito A, Gao J, Wang B, Edwards PA *et al.*: **LXRs regulate ER stress and inflammation through dynamic modulation of membrane phospholipid composition**. *Cell Metab* 2013, **18**:685-697.

42. Eisenreich W, Rudel T, Heesemann J, Goebel W: **How viral and intracellular bacterial pathogens reprogram the metabolism of host cells to allow their intracellular replication**. *Front Cell Infect Microbiol* 2019, **9**:42.

43. • Ahsan F, Maertzdorf J, Guhlich-Bornhof U, Kaufmann SHE, Moura-Alves P: **IL-36/LXR axis modulates cholesterol metabolism and immune defense to *Mycobacterium tuberculosis***. *Sci Rep* 2018, **8**:1520.

This work describes a novel mechanism of crosstalk by which coordinated IL-36 and LXR signaling limit mycobacterial growth in human macrophages. The conclusions from this study may also have implications in other infection settings.

44. Bouttier M, Laperriere D, Memari B, Mangiapane J, Fiore A, Mitchell E, Verway M, Behr MA, Sladek R, Barreiro LB *et al.*: **Alu repeats as transcriptional regulatory platforms in macrophage responses to *M. tuberculosis* infection**. *Nucleic Acids Res* 2016, **44**:10571-10587.

45. Korf H, Vander Beken S, Romano M, Steffensen KR, Stijlemans B, Gustafsson J-Å, Grooten J, Huygen K: **Liver X receptors contribute to the protective immune response against *Mycobacterium tuberculosis* in mice**. *J Clin Invest* 2009, **119**:1626-1637.

46. Lange PT, Schorl C, Sahoo D, Tarakanova VL: **Liver X receptors suppress activity of cholesterol and fatty acid synthesis pathways to oppose gammaherpesvirus replication**. *mBio* 2018, **9**:e01115-18.

47. Dang EV, McDonald JG, Russell DW, Cyster JG: **Oxysterol restraint of cholesterol synthesis prevents AIM2 inflammasome activation**. *Cell* 2017, **171**:1057-1071.e11.

48. Park K, Scott AL: **Cholesterol 25-hydroxylase production by dendritic cells and macrophages is regulated by type I interferons**. *J Leukoc Biol* 2010, **88**:1081-1087.

49. Cyster JG, Dang EV, Reboldi A, Yi T: **25-Hydroxycholesterols in innate and adaptive immunity**. *Nat Rev Immunol* 2014, **14**:731-743.

50. Choi JY, Seo JY, Yoon YS, Lee YJ, Kim HS, Kang JL: **Mer signaling increases the abundance of the transcription factor LXR to promote the resolution of acute sterile inflammation**. *Sci Signal* 2015, **8**:ra21.

51. Han D, Li X, Li S, Su T, Fan L, Fan W-S, Qiao H-Y, Chen J-W, Fan M-M, Li X-J *et al.*: **Reduced silent information regulator 1 signaling exacerbates sepsis-induced myocardial injury and mitigates the protective effect of a liver X receptor agonist**. *Free Radic Biol Med* 2017, **113**:291-303.

52. Wang YY, Ryg U, Dahle MK, Steffensen KR, Thiemermann C, Chaudry IH, Reinholt FP, Collins JL, Nebb HI, Aasen AO *et al.*: **Liver X receptor protects against liver injury in sepsis caused by rodent cecal ligation and puncture**. *Surg Infect (Larchmt)* 2011, **12**:283-289.

53. Castrillo A, Joseph SB, Vaidya SA, Haberland M, Fogelman AM, Cheng G, Tontonoz P: **Crosstalk between LXR and toll-like receptor signaling mediates bacterial and viral antagonism of cholesterol metabolism**. *Mol Cell* 2003, **12**:805-816.

54. Sanjurjo L, Amézaga N, Vilaplana C, Cáceres N, Marzo E, Valeri M, Cardona PJ, Sarrias MR: **The scavenger protein apoptosis inhibitor of macrophages (AIM) potentiates the antimicrobial response against *Mycobacterium tuberculosis* by enhancing autophagy**. *PLoS One* 2013, **8**:e79670.

55. Long J, Roy RB, Zhang YJ, Antrobus R, Du Y, Smith DL, Weekes MP, Javid B: **Plasma membrane profiling reveals upregulation of ABCA1 by infected macrophages leading to restriction of mycobacterial growth**. *Front Microbiol* 2016, **7**:1086.

56. Huang L, Nazarova EV, Russell DG: ***Mycobacterium tuberculosis*: bacterial fitness within the host macrophage**. *Microbiol Spectr* 2019, **7**.

57. Chen S, Sorrentino R, Shimada K, Bulut Y, Doherty TM, Crother TR, Arditi M: ***Chlamydia pneumoniae* -induced foam cell formation requires MyD88-dependent and -independent signaling and is reciprocally modulated by liver X receptor activation**. *J Immunol* 2008, **181**:7186-7193.

58. Bukrinsky MI, Mukhamedova N, Sviridov D: **Lipid rafts and pathogens: the art of deception and exploitation**. *J Lipid Res* 2019, **61**:601-610.

59. Samanta D, Mulye M, Clemente TM, Justis AV, Gilk SD: **Manipulation of host cholesterol by obligate intracellular bacteria**. *Front Cell Infect Microbiol* 2017, **7**:165.

60. Mujawar Z, Rose H, Morrow MP, Pushkarsky T, Dubrovsky L, Mukhamedova N, Fu Y, Dart A, Orenstein JM, Bobryshev YV *et al.*: **Human immunodeficiency virus impairs reverse cholesterol transport from macrophages**. *PLoS Biol* 2006, **4**:e365.

61. Jiang H, Badralmaa Y, Yang J, Lempicki R, Hazen A, Natarajan V: **Retinoic acid and liver X receptor agonist synergistically inhibit HIV infection in CD4+ T cells by up-regulating ABCA1-mediated cholesterol efflux**. *Lipids Health Dis* 2012, **11**:69.

62. Morrow MP, Grant A, Mujawar Z, Dubrovsky L, Pushkarsky T, Kiselyeva Y, Jennelle L, Mukhamedova N, Remaley AT, Kashanchi F *et al.*: **Stimulation of the liver X receptor pathway inhibits HIV-1 replication via induction of ATP-binding cassette transporter A1**. *Mol Pharmacol* 2010, **78**:215-225.

63. Hanley TM, Blay Puryear W, Gummuluru S, Viglianti GA: **PPARgamma and LXR signaling inhibit dendritic cell-**

mediated HIV-1 capture and trans-infection. *PLoS Pathog* 2010, **6**:e1000981.

64. Ramezani A, Dubrovsky L, Pushkarsky T, Sviridov D, Karandish S, Raj DS, Fitzgerald ML, Bukrinsky M: **Stimulation of liver X receptor has potent anti-HIV effects in a humanized mouse model of HIV infection**. *J Pharmacol Exp Ther* 2015, **354**:376-383.

65. Bocchetta S, Maillard P, Yamamoto M, Gondeau C, Douam F, Lebreton S, Lagaye S, Pol S, Helle F, Plengpanich W *et al.*: **Up-regulation of the ATP-binding cassette transporter A1 inhibits hepatitis C virus infection**. *PLoS One* 2014, **9**:e92140.

66. Sheng Xiang-Xiang, Sun Ying-Jie, Zhan Yuan, Qu Yu-Rong, Wang Hua-Xia, Luo Miao, Liao Ying, Qiu Xu-Sheng, Ding Chan, Fan Hong-Jie *et al.*: **The LXR ligand GW3965 inhibits Newcastle disease virus infection by affecting cholesterol homeostasis**. *Arch Virol* 2016, **161**:2491-2501.

67. Zelcer N, Hong C, Boyadjian R, Tontonoz P: **LXR regulates cholesterol uptake through Idol-dependent ubiquitination of the LDL receptor**. *Science* 2009, **325**:100-104.

68. Grassi G, Di Caprio G, Fimia GM, Ippolito G, Tripodi M, Alonzi T: **Hepatitis C virus relies on lipoproteins for its life cycle**. *World J Gastroenterol* 2016, **22**:1953-1965.

69. Zeng J, Wu Y, Liao Q, Li L, Chen X, Chen X: **Liver X receptors agonists impede hepatitis C virus infection in an Idol-dependent manner**. *Antiviral Res* 2012, **95**:245-256.

70. Lange PT, Jondle CN, Darrah EJ, Johnson KE, Tarakanova VL: **LXR alpha restricts gammaherpesvirus reactivation from latently infected peritoneal cells**. *J Virol* 2019, **93** e02071-18.

71. • Matalonga J, Glaria E, Bresque M, Escande C, Carbó JM, Kiefer K, Vicente R, León TE, Beceiro S, Pascual-García M *et al.*: **The nuclear receptor LXR limits bacterial infection of host macrophages through a mechanism that impacts cellular NAD metabolism**. *Cell Rep* 2017, **18**:1241-1255.

This report described for the first time that the multifunctional enzyme CD38 is a transcriptional target of LXR. Through upregulation of this enzyme, LXR agonists modulated the levels of intracellular NAD+, which might have physiological implications beyond the management of infection.

72. Glaría E, Valledor AF: **Roles of CD38 in the immune response to infection**. *Cells* 2020, **9**:228.

73. Chini EN, Chini CCS, Espindola Netto JM, de Oliveira GC, van Schooten W: **The pharmacology of CD38/NADase: an emerging target in cancer and diseases of aging**. *Trends Pharmacol Sci* 2018, **39**:424-436.

74. Hanley TM, Viglianti GA: **Nuclear receptor signaling inhibits HIV-1 replication in macrophages through multiple trans-repression mechanisms**. *J Virol* 2011, **85**:10834-10850.

75. Wang YY, Dahle MK, Steffensen KR, Reinholt FP, Collins JL, Thiemermann C, Aasen AO, Gustafsson JÅ, Wang JE: **Liver x receptor agonist GW3965 dose-dependently regulates lps-mediated liver injury and modulates posttranscriptional TNF-α production and p38 mitogen-activated protein kinase activation in liver macrophages**. *Shock* 2009, **32**:548-553.

76. Bruhn KW, Marathe C, Maretti-Mira AC, Nguyen H, Haskell J, Tran TA, Vanchinathan V, Gaur U, Wilson ME, Tontonoz P *et al.*: **LXR deficiency confers increased protection against visceral Leishmania infection in mice**. *PLoS Negl Trop Dis* 2010, **4**:e886.

77. Kumar GA, Jafurulla M, Chattopadhyay A: **The membrane as the gatekeeper of infection: cholesterol in host–pathogen interaction**. *Chem Phys Lipids* 2016, **199**:179-185.

78. Smoak K, Madenspacher J, Jeyaseelan S, Williams B, Dixon D, Poch KR, Nick JA, Worthen GS, Fessler MB: **Effects of liver X receptor agonist treatment on pulmonary inflammation and host defense**. *J Immunol* 2008, **180**:3305-3312.

79. Price JV, Vance RE: **The macrophage paradox**. *Immunity* 2014, **41**:685-693.

80. Schultz JR, Tu H, Luk A, Repa JJ, Medina JC, Li L, Schwendner S, Wang S, Thoolen M, Mangelsdorf DJ *et al.*: **Role of LXRs in control of lipogenesis**. *Genes Dev* 2000, **14**:2831-2838.

81. •• Muse ED, Yu S, Edillor CR, Tao J, Spann NJ, Troutman TD, Seidman JS, Henke A, Roland JT, Ozeki KA *et al.*: **Cell-specific discrimination of desmosterol and desmosterol mimetics confers selective regulation of LXR and SREBP in macrophages**. *Proc Natl Acad Sci U S A* 2018, **115**:E4680-E4689.

This study reveals the capacity of certain endogenous LXR ligands to dissociate LXR functions in a cell-specific manner, which is important for the development of new agonists with diminished adverse effects.

82. • Cao E, Lindgren A, Martinsson S, Hu L, Lindfors L, Sigfridsson K, Skantze U, Michaëlsson E, Trevaskis NL, Porter CJH: **Promoting intestinal lymphatic transport targets a liver-X receptor (LXR) agonist (WAY-252,623) to lymphocytes and enhances immunomodulation**. *J Control Release* 2019, **296**:29-39.

This paper reports a new delivery route for an LXR agonist, in combination with a lymph-directing long chain lipid-based formulation, which targets the agonist specifically to lymphocytes. This type of approach may facilitate the modulation of immune responses while avoiding the adverse lipogenic effects of conventional LXR agonist administration.